Development of Sindbis Virus as an Oncolytic Agent

Gray Kueberuwa

University College

University of Oxford

A thesis submitted for the degree of Doctor of Philosophy

to the Department of Oncology, University of Oxford

Trinity Term 2012

Supervisor: Professor Leonard Seymour

Development of Sindbis virus as an oncolytic agent

Gray Kueberuwa, University College, University of Oxford

A thesis submitted for the degree of Doctor of Philosophy to the Department of Oncology, University of Oxford, Trinity Term 2012

Abstract

The poor stability of most therapeutic viruses in the human bloodstream is a major obstacle in the field of cancer virotherapy, preventing systemic intravenous delivery to treat tumour metastases. Delivery is typically limited by inactivation of virus particles by blood components and rapid scavenging by hepatic phagocytes. Members of the *Alphavirus* family are exposed to blood during natural infections; as such, we hypothesised that evolutionary pressure may have led to blood stability and clearance kinetics superior to those of other viruses currently in development for use as oncolytic agents.

Sindbis virus is a member of the *Alphavirus* family that has shown promising anti-cancer activity in pre-clinical models. A concern for the clinical use of Sindbis virus as an anticancer agent is its pathology in humans, known as Pogosta disease. The symptoms of Pogosta disease may be a result of Sindbis virus replication in neuronal, muscle or haematopoietic tissues. Inhibiting virus replication in these tissues could, therefore, alleviate such potential side effects of virotherapy treatment. Introduction of microRNA response elements, perfectly complementary to microRNAs specifically expressed in liver (miR122), neuronal (miR124), muscle (miR133 and miR206) and haematopoietic (miR142-3p) cells, successfully attenuated SV replication in these tissues.

In contrast to all other viruses studied, data presented in this thesis show that Sindbis virus infectivity *in vitro* is not significantly inhibited by incubation with neat, whole naïve human blood. Despite full infectivity in naïve mouse blood, virus particles were rapidly cleared from the circulation of mice *in vivo* by the liver. An attempt to decrease the clearance rate by depletion of Kupffer cells through pre-treatment of mice with clodronate liposomes was ineffective. We also explored the use of Sindbis virus packaged in mosquito cells to more closely mimic virus particles exposed to blood in the wild during mosquito mediated transmission, but this also failed to improve virus circulation kinetics in mice. Despite rapid clearance from the circulation, intravenous administration of Sindbis virus had significant anti-cancer efficacy in C57BL/6 mice bearing syngeneic B16F10 metastatic melanomas.

Overall, data presented support our proposed use of Sindbis virus as a systemically delivered oncolytic agent and suggest decreasing the rate of clearance by the liver could dramatically enhance therapeutic outcomes. In addition it is shown that microRNA targeting of Sindbis virus provides a means of alleviating potential side effects of the administration of large virus doses.

Declaration of Authentication

All the work presented in this thesis was performed by me and in no way forms part of any other thesis in this or any other university. Where contributions have been made by others, this is acknowledged. The work was performed under the supervision of Professor Leonard Seymour, Department of Oncology, Division of Medical Sciences, University of Oxford.

Gray Kueberuwa

Oxford, September 2012

Acknowledgements

I would like to thank my parents. Their sacrifice and struggle has given me the opportunity to be here.

I would like to thank Professor Seymour for his guidance and advice during the writing of this thesis. I am also grateful for the freedom and independence I have had throughout the course of this project which has allowed me to develop as a scientist.

I would also like to thank my co-supervisor Dr Tedcastle, as well as Professor Seymour, Dr Carlisle, and Dr Cawood for their thoughtful scientific discussions which have influenced the way in which I have interpreted results and approached technical hurdles.

The great atmosphere in the Seymour lab is down to its members; their attitude to their work and each other. Working within it has been a pleasure.

Most of all I would like to thank Nichola, who is a continual inspiration.

Table of Contents

Development of Sindbis Virus as an Oncolytic Agent 1

Abstract 2

Declaration of Authentication 3

Acknowledgements 4

Table of Contents 5

List of Figures 11

List of Tables 15

List of Abbreviations 16

1 Introduction 22

1.1 Virotherapy 23

1.1.1 Oncolytic Viruses with Natural Cancer Selectivity 24

1.1.2 Oncolytic Viruses with Engineered Cancer Cell Selectivity 26

1.1.3 Clinical Investigation of Oncolytic Viruses with Natural Cancer Selectivity 29

1.1.4 Clinical Investigation of Viruses with Genetically Engineered Cancer Selectivity 31

1.1.5 Limitations to Successful Virotherapy 37

1.2 Anticancer Applications of Alphaviruses 44

1.2.1 Alphaviruses as Anti-cancer Vaccines 44

1.2.2 Alphaviruses as Immune Modulating agents 47

1.2.3 Oncolytic Efficacy of Alphaviruses 47

1.3 Sindbis Virus 51

1.3.1 Transmission 51

1.3.2 SV Structure and Cell Entry 53

1.3.3 SV Replication 56

1.3.4 Underlying Causes of SV Tumour Selectivity 61
1.3.5 Mechanism of SV Oncolytic Activity 63
1.4 MicroRNA 65
1.4.1 Discovery 65
1.4.2 MiRNA Production 66
1.4.3 MiRNA Regulation of Gene Expression 69
1.4.4 Tissue Specific MiRNA Expression 70
1.4.5 Interactions Between Viruses and MiRNAs 71
1.4.5 MicroRNA Control of Viral Vectors 74
1.4.6 MicroRNA Control of Replicating Viruses 75
1.4.7 MicroRNA Controlled Oncolytic Viruses 75
1.5 Thesis Objectives 78
1.5.1 Hypothesis 78
2 Materials and Methods 80
2.1 Production of Heat Shock Competent E.Coli Cells 81
2.2 Bacterial Transformation 81
2.3 DNA Restriction Digests 82
2.4 DNA Ligation 83
2.5 Agarose Gel Electrophoresis 83
2.6 Quantitation of purified DNA and RNA 84
2.7 Polymerase Chain Reaction 84
2.8 *In Vitro* Transcription 85
2.9 Transfection of Sindbis Virus Genomic RNA 86
2.10 Transfection of Pre-miR MicroRNA Precursors 86
2.11 Virus Luciferase *In Vitro* Assay 87
2.12 Protein Assay 87

2.13 Flow Cytometry 88
2.14 MTS Assay 88
2.15 Reverse-Transcription Polymerase Chain Reaction 89
2.16 Reverse Transcription Quantitative Polymerase Chain Reaction 90
2.17 Cell Culture 98
2.18 Differentiation of Myoblasts 100
2.19 Microscopy of Live Cells 100
2.20 Microscopy Primary Tissue Samples 101
2.21 Determination of Viral Titres by $TCID_{50}$ 102
2.22 Isolation of SV Clones by Serial Dilution 103
2.23 Collection and Preparation of Human Blood 104
2.24 Measurement of Complement Activation 104
2.25 Tyrosinase Assay 106
2.26 Animal Experimentation 107
2.27 Statistical Analysis 107
3 Physical and Genetic Stability of SV 109
3.1 Introduction 110
3.1.2 Aims 112
3.2 Results 113
3.2.1. Insertion of Luciferase, eGFP and TurboRFP Genes into Sindbis Virus cDNA Sequence 113
3.2.2. Rescue of Reporter Sindbis Viruses 118
3.2.3 Characterisation of Rescued Viruses 119
3.2.4 Purification 120
3.2.5 Storage Conditions 124
3.2.6 Virus Replication and Transgene Expression 127

3.2.7 Analysis of Sindbis Virus Cell Tropism 130
3.2.8 Possible Mechanisms of Loss of Transgene Expression 133
3.2.9 Analysis of the Mechanism of Loss of Transgene Expression 138
3.2.9 Prevention of Transgene Loss 143
3.2.10 FMDV2A Self Cleavable Transgene System 146
3.2.11 Production of SVGFP 2A 150
3.2.12 Rescue of SVLuc 2A and SVGFP 2A 152
3.2.13 Comparison of SVGFP DSG and SVFGP2A 153
3.2.14 Mechanism of Transgene Loss 155
3.3 Concluding Discussion 159
4 MicroRNA Controlled Sindbis Virus 162
4.1 Introduction 163
4.1.1 Aims 164
4.2 Results 168
4.2.1 Selection of Regulatory MiRs 168
4.2.2 Cloning of SV DSG MiR-T variants 169
4.2.3 Rescue of MiR-T SV Variants 170
4.2.4 Inhibition of SV DSG MiR-T by Ectopically Expressed MiRs 172
4.2.5 Identification of Cell lines Expressing MiRs 176
4.2.6 Inhibition of SV DSG MiR-Ts by Endogenously Expressed miRs 181
4.2.7 Production of MiRNA Targeted SVGFP 2A 183
4.2.8 Inhibition of SV 2A MiR-T by Ectopically Expressed MiRs 185
4.2.9 Inhibition of SV 2A MiR-T by Endogenously Expressed miRs 188
4.2.10 A Special Case for miR124? 193
4.2.11 Ex Vivo Inhibition of SVmiR-T 2A 196
4.3 Concluding Discussion 201

5 Blood Stability 205
5.1 Introduction 206
5.1.1 Aims 208
5.2 Results 209
5.2.1 Behaviour of SV in Human Blood 209
5.2.2 SV May Bind Erythrocytes 212
5.2.3 Effect of Anticoagulant on SV Neutralisation by Whole Human Blood and Plasma 214
5.2.4 Reversing the Neutralising Capacity of Human Serum 218
5.2.5 Complement and SV Infectivity 220
5.2.6 SV Behaviour in Human and Mouse Blood is Comparable 223
5.2.7 SV May Have a Direct Cell-Cell Spread Mechanism 224
5.2.8 Spread of SV in the Presence of Neutralising Antibodies 226
5.2.9 SV Infection of Invertebrate Cells 230
5.2.10 Production of SV from Invertebrate Cells 233
5.2.11 Tropism of Invertebrate and Vertebrate Cell Derived SV 234
5.2.12 VD and ID SV Behaviour in Human Blood In Vitro is Similar 236
5.2.13 The In Vivo Pharmacokinetics of VD and ID SV in Mice are Similar 239
5.2.14 Effect of Clodronate Liposomes on Pharmacokinetics of SV 243
5.2.15 Anticancer Efficacy of SV 246
5.3 Concluding Discussion 251
6 Discussion 256
6.1 Overview of the Main Findings of this Thesis 257
Using SV as an Oncolytic Agent 257
Genetic Stability of SV 257
Tissue Specific Attenuation of SV 258

SV as a Systemically Delivered Oncolytic Agent 260
6.2 Future Directions 263
Genetic Stability of SV 263
Tissue Specific Attenuation of SV 265
SV as a Systemically Delivered Oncolytic Agent 266
7 References 270

List of Figures

Figure 1.1: Clearance of Intravenously Delivered Virus 40

Figure 1.2: SV Virion Structure 55

Figure 1.3: Overview of SV RNA Replication, Translation and Protein Processing 59

Figure 1.4: MiRNA Processing 68

Figure 1.5: Tissue Specific miRNAs in Humans 70

Figure 2.1: RTQPCR Standard Curves for Detection of SV *In Vitro* 92

Figure 2.2: RTQPCR Standard Curves for nsp1 and eGFP 93

Figure 2.3: RTQPCR Standard Curves for Nsp1 Detection in Human Blood Fractions – 94

Figure 2.4 Standard Curve for Detection of VD SV and ID SV *In Vivo* 96

Figure 2.5 Standard Curves for Detection of SV *In Vivo* after Clodronate Liposome Treatment 97

Figure 3.1: RNA species produced by SV DSG 112

Figure 3.2: Insertion of reporter transgenes into pSV DSG 117

Figure 3.3: Confirmation of SV Rescue by Reporter Gene Expression 120

Figure 3.4: Assessment of Virus Quality 122

Figure 3.6: Analysis of SV Uptake, Transgene Expression and Release 130

igure 3.7: Relation of transgene expression to cell killing 133

Figure 3.8: RNA agarose gel electrophoresis of SV RNA 136

Figure 3.9: Luciferase Expression of SVLuc.....139

Figure 3.10: SVLuc.....141

Figure 3.11: Proportion of Luciferase Transgene Encoding SVLuc 143

Figure 3.12: Analysis of Clonal SVLuc DSG Upon Serial Passage.....146

Figure 3.13: Processing of the Structural Polyprotein.....149

Figure 3.14: Production of SV with eGFP or Luciferase Expressed as Part of the Structural Polyprotein.....152

Figure 3.15: Confirmation of SV Rescue by Reporter Gene Expression 153

Figure 3.16: Comparison of the Rate eGFP Loss from SVGFP.....154

Figure 3.17: Chromatogram of Early and Late SVGFP 2A Passages 158

Figure 4.1: Micro RNA processing.....165

Figure 4.2: - Human Tissue miRNA Profile.....167

Figure 4.3: Schematic diagram of miR-T sites.....172

Figure 4.4 Attenuation of SVmiR-T Viruses by Transfected MiRs.....175

Figure 4.5 Increase of Muscle Specific MiR levels Upon C2C12 Cell Differentiation179

Figure 4.7: Attenuation of SVmiR-T DSGs by Endogenously Expressed MiRs 183

Figure 4.8: Schematic Diagram of MiR-T Sites in SVmiR-T 2A Variants.....185

Figure 4.9 Inhibition of SVGFPmiR-T 2A Viruses by Transfected Pre-miRs.....188

Figure 4.10: Attenuation of SVmiR-T 2A by Endogenously Expressed MiRs.....191

Figure 4.11: Attenuation of SVmiR-T 2A replication by Endogenously Expressed MiRs 192

Figure 4.12: Re-Analysis of SVGFP124-T 2A.....195

Figure 4.13: SVLuc DSG Gene Expression *In Vivo*.....197

Figure 4.14: Infection of Human Liver and Tumour –.....200

Figure 5.1: Effect of Blood Components on SV Infectivity.....210

Figure 5.2: Effect of Blood Components on SV Infectivity from a Panel of Donors ..212

Figure 5.3: RTQPCR Detection of SVLuc DSG in Blood Compartments –.....214

Figure 5.4: Lithium Heparin Does Not Directly Enhance SV Infectivity -.....215

Figure 5.5: Anticoagulants and Activated Clotting Factors Present in Blood *in vitro* .217

Figure 5.6: SV Stability in Whole Human Blood and Plasma Collected with Different Anticoagulants 218

Figure 5.7 Anticoagulant Relief of Serum Inhibition of SVLuc DSG Infectivity.....220

Figure 5.8: Complement Active Blood Collected with Hirudin Does Not Neutralize SV 222

Figure 5.9: SV Neutralisation by Human and Mouse Blood.....223

Figure 5.10: Possible Cell-Cell Spread of SV 226

Figure 5.11: Inhibition of SVLuc DSG Infection by Immune Human Serum 227

Figure 5.12: Reduced Neutralising Capacity of "Used" 08PG365.....230

Figure 5.13: Transgene Expression in Mosquito Cells.....231

Figure 5.14: Mosquito Cells Resistant to Killing by SV 232

Figure 5.15 SV Shedding from Persistently Infected Invertebrate Cells.....234

Figure 5.16: Tropism of Invertebrate and Vertebrate Derived SV 235

Figure 5.17: VD and ID SV are Resistant to Human Blood.....238

Figure 5.18: Pharmacokinetics and biodistribution of VD and ID SV.....242

Figure 5.19 SV Pharmacokinetics and Biodistribution after Treatment with Clodronate Liposomes.....245

Figure 5.20: Antitumor Efficacy of Systemically Delivered SV.....250

List of Tables

Table 1.1 : Summary of Oncolytic Viruses Tested in Clinical Trials.....29

Table 2.2: RTQPCR Primer and Probe Sequences.....92

Table 2.2: Details of Cell Lines and Culture Media.....99

Table 4.1: Sequences of Tissue Specific MiRNAs.....169

Table 4.2: Comparison of Levels of SVmiR-T DSG and SVmiR-T 2A Attenuation .201

List of Abbreviations

/	per
+ssRNA	positive sense single stranded RNA
β-gal	β-galactosidase
µ	micro
5' and 3'	5 prime and 3 prime ends of an RNA or DNA molecule
5FU	5'fluorouracil
67LR	67kDa high affinity laminin receptor
AAV	adeno-associated virus
ACD	acid citrate dextrose
Ad2	adenovirus serotype 2
Ad5	adenovirus serotype 5
AGE	agarose gel electrophoresis
Ago2	Argonaute 2
Akt	protein kinase B
ANOVA	analysis of variance
APC	antigen presenting cell
Arbovirus	arthropod borne virus
aSMase	acid sphingomyelin phosphodiesterase
ATCC	American type culture collection
BCA	bicinchoninic acid
BHK	baby hamster kidney fibroblasts
bp	base pairs
CCR4-NOT	RNA de-adenylation complex

CEA	carcinoembryonic antigen
CgA	chromogranin-A
CIAP	calf intestinal alkaline phosphatase
CMV	cytomegalovirus
CPE	cytopathic effect
CSE	conserved sequence element
C_T	Threshold cycle number
CTL	cytotoxic T lymphocyte
DC	dendritic cell
Dcr2	dicer 2
DEPC	di-ethyl pyrocarbonate
DGCR8	Pasha
DIC	differential interference contrast
DMEM	Dulbecco's Modified Eagle Medium
dsRNA	double stranded RNA
ECCAC	European collection of cell cultures
ECM	extracellular matrix
eGFP	enhanced GFP
EGFR	epidermal growth factor receptor
eIF-2α	eukaryotic initiation factor 2 alpha subunit
eIF4E	eukaryotic initiation factor 4E
EMEM	Eagle’s minimum essential medium
EPR	enhanced permeability retention
eRF	eukaryotic translation release factor
Exp5	exportin 5

FCS	foetal calf serum
FMDV2A	Foot and Mouth Disease Virus 2A peptide
GM-CSF	granulocyte macrophage colony stimulating factor
GMP	good manufacturing practice
h	hours
HBS	HEPES buffered saline
HBV	hepatitis B virus
HCC	hepatocellular carcinoma
HCV	hepatitis C virus
HER2	human epidermal growth factor receptor 2
HIF	hypoxia induced factor
HPV	human papilloma virus
HoS	horse serum
HS	heparin sulphate proteoglycan
HSV-1	human herpes simplex virus type 1
HSV-TK	HSV thymidine kinase
hTERT	human telomerase reverse transcriptase gene
IC	intracranial
IC_{50}	virus dose required to kill 50% of cells
ID	invertebrate derived
IFN	interferon
IL-12	interleukin 12
IL-18	interleukin 18
IP	intraperitoneal
IT	intratumoural

IU	international units
IV	intravenous
LB	lysogeny broth
MAGE	melanoma associated antigen
MAPK	mitogen activated protein kinase
MCAM	melanoma cell adhesion molecule
MEK	MAPK kinase
miR	microRNA
miR-T	microRNA targeted
MOI	multiplicity of infection
MOSEC	murine ovarian surface epithelial carcinoma
MRE	microRNA response element
mRNA	messenger RNA
MTD	maximum tolerated dose
NDV	Newcastle disease virus
NK	natural killer cell
NLR	NOD like receptor
NOD	nucleotide-binding oligomerisation domain
nSMase	neutral sphingomyelin phosphodiesterase
OCT	optimal cutting temperature compound
OD	optical density
OV	oncolytic virus
OVA	ovalbumin
PCR	polymerase chain reaction
PFU	plaque forming unit

PI	post-infection
PIL	Home Office personal licence
PK	pharmacokinetic
PKR	protein kinase R
PP1A	protein phosphatase 1A
PPL	Home Office personal project licence
Pre-miR	microRNA precursor
Pri-miRs	primary microRNA
PSA	prostate specific antigen
PSCA	prostate stem cell antigen
PV	poliovirus
Ran	Ras related nuclear protein
RdRp	RNA-dependent RNA polymerase
RES	reticuloendothelial system
RIG-I	retinoic acid inducible gene I
RISC	RNA induced silencing complex
RLR	RIG-I like receptor
RNA pol II	RNA polymerase II
RNAi	RNA interference
RPMI	Roswell park memorial institute
SC	subcutaneous
SCID	severe combined immunodeficient
SEM	standard error of the mean
SFDMEM	serum free DMEM
SFV	Semliki forest virus

STEAP	six transmembrane epithelial antigen
SV	Sindbis virus
SV001	Seneca valley virus strain 001
TAA	tumour associated antigen
TAR	HIV-1 transactivating response
TC	tissue culture
TEM	transmission electron microscopy
TGFβ	transforming growth factor beta
Th1	type 1 helper T cell
TK	thymidine kinase
TLR	toll like receptor
TRBP	TAR RNA-binding protein
TRP-1	tyrosine related protein 1
UV	ultraviolet
VA	Adenovirus non-coding virus associated RNA
VD	vertebrate derived
VEE	Venezuelan equine encephalitis virus
VLP	virus like particle
VP	virus particle
VSV	vesicular stomatitis virus
VSV-G	vesicular stomatitis virus glycoprotein G
WT	wild-type

1 Introduction

1.1 Virotherapy

The concept of virotherapy, utilising viruses for the treatment of cancer, has been a topic of research interest for over 100 years, as a consequence of several independent observations of cancer remissions following viral infections (Kelly and Russell 2007).

Between 1950 and 1980 live attenuated strains of several viruses were tested for their ability to treat cancer. These included adenovirus, influenza virus, mumps virus, Newcastle disease virus (NDV), rabies virus, Sendai Virus and Semliki Forest Virus (Wheelock and Dingle 1964; Asada 1974). However, the results from both anecdotal experimental settings and formal clinical trials failed to clearly establish any reproducible therapeutic effects of these viruses, resulting in a reduction in interest in virotherapy. In recent decades, concurrent improvements in the understanding of the molecular biology of cancer and the interactions between viruses and host cells, as well as technological advances in DNA sequencing and genetic engineering, have led to renewed interest in the field.

Whether the anticancer activity of conventional chemotherapy drugs is a consequence of their toxicity in rapidly dividing cells is a subject of debate (Baguley, Marshall et al. 1995; Mitchison 2011). However, most conventional cancer chemotherapy drugs cause toxicity in off-target tissues; these are typically rapidly proliferating such as gut epithelial, follicular and haematopoietic tissues. As a result, cancer chemotherapy drugs typically have low therapeutic indices due to their effects on normal tissues as well as on target malignancies. Toxicity to non-tumour tissue causes severe side effects, limiting doses that can be administered to patients, usually to below a curative threshold. This can enable the acquisition of chemoresistance by rapidly mutating tumour cells. In

contrast to most conventional chemotherapy agents, instead of targeting all rapidly dividing tissues, oncolytic viruses (OVs) offer high cancer cell specificity at several stages of their infection cycle. In addition, they have the ability to selectively replicate at their site of action, providing substantial amplification of their therapeutic effect. These two factors give virotherapy the potential of therapeutic indices way above those feasible when using conventional chemotherapy drugs (Hesketh 2008; Beljanski and Hiscott 2012; Parato, Breitbach et al. 2012).

In contrast to chemotherapy, virotherapy can instigate a range of death mechanisms including apoptosis, necrosis and necroptosis, the precise mechanism used differs from virus to virus and even between virus strains where genetic modifications are used (Coukos, Makrigiannakis et al. 2000; Varghese and Rabkin 2002). This gives great potential to the use of virotherapy in conjunction with existing modes of treatment. Furthermore, due to distinct modes of action, resistance that is so often acquired by tumours following treatment with existing chemotherapeutics is unlikely to protect target cells against virotherapy. It is also possible that different oncolytic viruses, utilising different modes of cytotoxicity, could be used in combination for the treatment of cancer; thereby reducing the chances of the acquisition of resistance.

1.1.1 Oncolytic Viruses with Natural Cancer Selectivity

Several viruses possess selective infection and/or replication capabilities in human tumour cells compared to non-cancerous human cells. These include vesicular stomatitis virus (VSV), reovirus, NDV and myxoma virus (Barber 2005; Wang, Barrett et al. 2006; Stanford, Barrett et al. 2007; Yap, Brunetto et al. 2008; Mansour, Palese et al. 2011).

The basis of this intrinsic selectivity has been attributed to deficient interferon signalling, resistance to apoptosis and the up-regulation of virus receptor proteins in certain cancer cells. For DNA viruses, the loss of cell cycle check points that leads to continual cell cycling in cancerous cells also contributes to increased permissivity of tumours to infection in comparison to non-transformed tissues (Antonio Chiocca 2002).

It has also been shown that the infection of human cells by myxoma virus only occurs in the presence of constitutively active protein kinase B (Akt) (Wang, Barrett et al. 2006). Akt is a serine/threonine kinase involved in many cellular processes including regulation of glucose uptake, cell cycle progression, apoptosis and has been shown to be capable of relieving cell cycle arrest at the G2/M checkpoint following DNA damage (Kandel, Skeen et al. 2002; Brazil, Yang et al. 2004). Akt is one of the most commonly occurring mutations in tumourigenesis (Testa and Bellacosa 2001), making many cancers susceptible to infection and killing by myxoma virus whilst untransformed cells remain unaffected.

There is significant crossover in interferon (IFN) and apoptotic signalling (Schroder, Hertzog et al. 2004) and it seems that during tumourigenesis, as cancer cells acquire defects in apoptotic signalling pathways, IFN signalling also becomes defective. This may increase susceptibility to infection by viruses that would normally be nullified by the IFN mediated pathways (Stojdl, Lichty et al. 2000; Balachandran and Barber 2004).

A wealth of evidence supports the notion that the immune system targets and eradicates newly emerging tumours (Baldwin 1977; Dunn, Koebel et al. 2006). Those tumours that develop in spite of this must undergo a process known as immune editing, during which they gain mechanisms that allow evasion of immune mediated recognition and/or killing

such as down-regulation of immunogenic epitopes. IFNs have been shown to play a key role in immune mediated tumour suppression (Abril, Mendez et al. 1996; Wong, Krauer et al. 1997; Shimada, Shiota et al. 1998; Dunn, Koebel et al. 2006). Tumours established in immune competent hosts have therefore successfully "escaped" IFN mediated elimination. Mutations in IFN signalling pathways, that may benefit the efficacy of viral therapeutics, are therefore, perhaps, a consequence of cancer cell immune evasion necessary for tumour development.

Once established, many tumours form an immune suppressed environment, largely through over-expression of transforming growth factor beta (TGFβ) (Jarnicki, Lysaght et al. 2006; Alshaker and Matalka 2011; Wilson, El-Jawhari et al. 2011). Within this immune suppressed environment, anti-viral as well as anti-tumour responses may be reduced, producing a haven in which viruses can replicate more freely than in normal tissues, conferring natural tumour selectivity of viruses.

1.1.2 Oncolytic Viruses with Engineered Cancer Cell Selectivity

Virus surface proteins govern their interaction and uptake into cells. Changing the surface proteins of a virus can be used to confer cancer cell selectivity of virus particles through preferential uptake into these cells. This can be achieved through pseudotyping, producing virus particles with foreign surface proteins, or genetic engineering. This has been successful in conferring cancer cell selectivity for many viruses including adenovirus type 5 (Ad5), measles virus, herpes simplex virus 1 (HSV-1) and adeno-associated virus (AAV) by replacing surface proteins with surface protein-antibody chimeric proteins, or single chain variable fragments or proteins known to bind antigens

overexpressed on the surface or cancer cells, or editing endogenous cell receptor binding regions (Girod, Ried et al. 1999; Nakamura and Russell 2004; Belousova, Mikheeva et al. 2008; Manservigi, Argnani et al. 2010; Poulin, Lanthier et al. 2010; Verheije and Rottier 2012). A second way that changing the cell-selectivity of a virus can be achieved is by chemically attaching polymers to existing virus surface proteins. By then attaching a molecule of choice to the attached polymer, such as an antibody, one can bestow binding affinity to cell types of choice (Ohno, Sawai et al. 1997; Morrison, Briggs et al. 2009).

Several viruses have been well studied and, as such, the replication cycles and host interactions of many viruses have been well characterized. Where these viruses do not naturally possess high specificity for replication in tumour cells, it can be conferred. This can be achieved by genetic modification in two ways; by deleting genes that permit efficient infection or replication in normal cells but not in cancer cells, or by replacing viral promoters with tumour specific promoters, so that virus replication is dependent on transcription factors present exclusively, or in abundance in tumour cells. These strategies have been successful in the production of cancer selective adenovirus, vaccinia and HSV-1 (Kirn 2000; Thorne 2009; Carson, Haddad et al.). The use of pseudotyping and genetic modification in combination offers the potential to increase cancer cell selectivity with respect to either approach applied alone, as demonstrated in studies of adenovirus (Stoff-Khalili, Rivera et al. 2007).

Several viruses have displayed anticancer activity in pre-clinical settings and progressed to evaluation in human clinical trials. These fall into the two classifications mentioned above, those with naturally occurring cancer cell selectivity, or those that have been genetically modified to endow them with this phenotype (Table 1.1).

Virus (Strain)	Genetic target in cancers	Genetic modification(s)	Transgene encoded	Reference
Non-engineered viruses				
NDV	Unknown (boosts immune response)	None	None	(Csatary, Eckhardt et al. 1993; Pecora, Rizvi et al.
Reovirus	Defects in tumour PKR/interferon pathways	None	None	(Morris 2002)
Mumps	Unknown	None	None	(Asada 1974)
West Nile	Unknown	None	None	(Southam and Moore 1952)
Adenovirus	Unknown	None	None	(Smith, Huebner et al. 1956)
Vaccinia	Unknown (EGFR pathway driven)	None	None	(Roenigk, Deodhar et al. 1974)
Engineered, non-armed viruses				
Adenovirus (dl1520/ ONYX-015)	p53 pathway defects; late RNA transport defects	E1B-55K (–), E3B (–)	None	(Kirn 2001)
Adenovirus (H101)	p53 pathway defects; late RNA transport defects	E1B-55K (–), E3 (–)	None	(Xia, Chang et al. 2004)
Adenovirus (CG7060)	None (prostate tissue-specific)	PSE1A, E3B (–)	None	(DeWeese, van der Poel et al.
Adenovirus (CG7870)	None (prostate tissue-specific)	PSE1A, PSE1B	None	(Small, Carducci et al. 2006)
HSV (1716)	Defects in tumour PKR/interferon pathways (ICP34.5–); attenuated neurotoxicity	ICP34.5 (–)	None	(Hammill, Conner et al. 2010)
HSV (G207)	Tumour cell complementation of ribonucleotide reductase (ICP6–); Defects in tumour PKR/interferon pathways (ICP34.5–); attenuated	ICP34.5 (–), ICP6 (–)	None	(Markert, Medlock et al. 2000)
Engineered, armed viruses				
Vaccinia (JX-594)	Tumour cell complementation of thymidine kinase deletion; cellular thymidine kinase expression E2F pathway-driven	Thymidine kinase (–)	GM-CSF (immune stimulation)	(Mastrangelo, Maguire et al. 1999; Heo 2012)
Adenovirus (Ad5-CD/Tkrep)	p53 pathway defects; late RNA transport defects	E1B-55K (–), E3B (–), CD/TK expression	CD/TK (prodrug activation)	(Freytag, Khil et al. 2002; Freytag, Stricker et al. 2003)
HSV (OncoVEX GM-CSF)	Defects in tumour PKR/interferon pathways (ICP34.5–)	ICP34.5 (–), ICP47 (–), Us11 up-regulation	GM-CSF (immune stimulation)	(Senzer, Kaufman et al. 2009)
Measles (MV-CEA)	Tumour-selective binding through CD46; CD46 overexpressed in most cancers	None (vaccine strain)	CEA (serum monitoring)	(Galanis, Hartmann et al. 2010)

Table 1.1 : Summary of Oncolytic Viruses Tested in Clinical Trials – CD/TK, gene encoding a fusion protein of cytosine deaminase and herpes virus thymidine kinase; CEA, carcinoembryonic antigen; EGFR, epidermal growth factor receptor; GM-CSF, granulocyte-macrophage colony-stimulating factor; HSV, herpes simplex virus; MV, measles virus vaccine strain; NDV, Newcastle disease virus; NA, not applicable; PKR, protein kinase R (double-stranded RNA activated inhibitor of translation); PSE1A, prostate-specific promoter-driven E1A; PSE1B, prostate-specific promoter-driven E1B. Adapted, with permission, from (Liu, Galanis et al. 2007).

1.1.3 Clinical Investigation of Oncolytic Viruses with Natural Cancer Selectivity

Between 1950 and 1995, there were a number clinical trials and case studies that investigated the therapeutic effects of virotherapy; however, in these studies there was a lack of consistency in the routes of virus administration, doses, dosing schedules and clear definitions of clinical outcomes. Despite this, the concept of virotherapy was validated in treating multiple cancer types with a range of viruses. Oncolytic viruses tested during this period were not modified, but possessed natural cancer cell tropism. Examples of viruses evaluated clinically include adenovirus, reovirus, NDV, mumps virus, vaccinia virus, parvovirus and West Nile virus. Though these viruses were isolated wild type strains, they were somewhat attenuated through repeated serial passage *in vitro* (Liu, Galanis et al. 2007), with the exception of the Egypt 101 strain of West Nile virus that had been passaged in mice or chick embryos only twice after isolation from human serum (Southam and Moore 1952). Examples of larger studies where tumour regression occurred following treatment with viruses include West Nile virus (4/34, (Southam and Moore 1952)), adenovirus (11/40, (Smith, Huebner et al.

1956)), mumps virus (37/90, (Asada 1974)), NDV (8/33, (Csatary, Eckhardt et al. 1993)) and vaccinia virus (8/20 (Wyeth vaccine strain) (Roenigk, Deodhar et al. 1974)). Although tumour shrinkage was associated with mumps virus and adenovirus treatments, it was followed by tumour progression. Some clinically relevant outcomes, however, were observed for other viruses tested. Of the above mentioned cases where tumour shrinkage was reported; for mumps virus 9/37 patients with regression remained in remission for "a long time", for NDV 7/8 survived 2 years compared to 0 in placebo group and for vaccinia virus, survival of patients with metastatic melanoma increased over 8-fold from 4.6 to 37.5 months.

By the 1990s, clinical trial design was much more meticulous and clinical endpoints better defined and consistent between trials. During this decade NDV was re-evaluated in a phase I clinical trial. The PV701 strain, attenuated by repeat tissue culture passage, was administered intravenously to patients with several cancer types, including patients with renal, colorectal pancreatic, breast, nasopharyngeal or non-small cell lung cancers. Only 1/62 patients showed a complete response. This patient, who presented with a 1.5cm diameter pharyngeal tumour, became non-compliant with treatment after 5 months. 2 months after non-compliance a separate tumour was detected in the pharynx by radiography (Pecora, Rizvi et al. 2002). In a subsequent trial the *in vitro* passage attenuated NDV OV 001 strain was used to treat patients with non-responsive glioblastoma multiforme. Multiple intravenous administrations led to a complete response in one patient, however lack of completion of dose regimens by patients in this trial makes data interpretation difficult (Freeman, Gomori et al. 2004).

Reinvestigation of reovirus in a phase I trial of 18 patients treated with intratumoural (IT) injections of superficial tumours of multiple cancer types saw a good safety profile,

with doses up to 1 x 10^{10} PFU, and a complete response was seen in 1/18 patients (Morris 2002).

Seneca valley virus, discovered in 2002, was isolated from cell culture media and seropositivity in pigs suggests they are its natural hosts. Studies of a wild type strain of Seneca valley virus (SV001) showed lack of pre-existing immunity in blood donors (1/120) and stability in human serum (Reddy, Burroughs et al. 2007). Serum samples, however, were heat inactivated in this study therefore it is not clear whether SV001 is inactivated by complement. SV001 has natural oncolytic properties and was tested in a phase I study where it was administered intravenously (IV) to patients with neuroendocrine cancers. Treatment resulted in 1/30 patients demonstrating stable disease (+16 months), but no complete responses were observed (Rudin 2009).

1.1.4 Clinical Investigation of Viruses with Genetically Engineered Cancer Selectivity

OVs with Cancer Specific Deletions

1997 marked the beginning of clinical trials using genetically engineered viruses, the first "wave" of which contained modifications to improve cancer selectivity through deletion of genes necessary for efficient replication in non-cancer cells. Improving the restriction of virus replication to tumours lowers toxicity in non-tumour tissues at any given dose. This has an effect of raising maximum tolerated doses (MTDs), which increases the potential dose of therapeutic virus a tumour can receive during treatment.

The first of these viruses to be tested was a serotype 2/5 hybrid of adenovirus with deletions in the E1B-55K and E3B regions, ONYX-015/dl1520. The product of the E1B-55K gene mediates the binding, functional inhibition and proteasomal degradation of the tumour suppressor protein p53, as well as selective nuclear export of late viral mRNAs (Lober, Lenz-Stoppler et al. 2002). The E3B region encodes genes for the 10.4, 14.5 and 14.7 kDa proteins. At the time this was known to attenuate ONYX-015 compared to wild type Ad5 in normal cells but the underlying mechanisms were not well understood. The p53 tumour suppressor gene is mutated in more than 50% of human tumours. In addition, mutations or aberrant expression of other components of the pathway, namely MDM2, Akt, PTEN and chk2 make up a substantial part of the remainder (Soussi and Wiman 2007). The ONYX-015 virus was designed to be lacking adenovirus proteins necessary for inhibition of p53 mediated apoptosis, making it dependent on replication in tumour cells deficient of functional p53 signalling. Increased tumour selectivity was indeed observed, however, it has since been found through the observation that ONYX-015 can replicate just as well in tumour cells with intact p53 signalling, that the basis of tumour selectivity is reliant on other genetic determinants (McCormick 2000). The E3 deletion in ONYX-015, of genes encoding 10.4/14.5 kDa and 14.7kDa, has also since been shown to attenuate adenovirus replication through loss of inhibition of premature apoptosis induced by TNF, TRAIL or FasL (Efrat, Serreze et al. 2001; Wang, Hallden et al. 2003). Trials assessing the anticancer efficacy of ONYX-015 as a single agent were disappointing with objective responses in only ~14% of patients, however, when tested in combination with conventional chemotherapy significantly higher objective response rates (~36%) and some complete responses (27%) were observed, without overlapping toxicities (Khuri, Nemunaitis et al. 2000; Kirn 2001).

Another adenovirus, H101, was developed that contained the deletions of ONYX-015 and an additional deletion in the E3-ADP region. Phase III clinical trial results showed that combination of H101 with cisplatin and 5'fluorouracil (5FU) approximately doubled tumour response rates from to 39.6% to 78.8% compared to a treatment regimen of cisplatin and 5FU alone (Xia, Chang et al. 2004). The results of this trial led to H101 gaining approval from the Chinese State Food and Drug Administration in 2004, making it the first approved oncolytic virus worldwide.

Utilising the same approach of virus gene deletions to confer increased oncolytic virus cancer cell selectivity, several HSV-1 viruses containing γ34.5 deletions were produced. The presence of intracellular double stranded RNA (dsRNA) of over 30 bp in length is associated with viral infection. Upon binding this RNA, protein kinase R (PKR) is activated by dimerization and autophosphorylation (Lemaire, Anderson et al. 2008). Once activated, PKR phosphorylates several intracellular proteins, one of which is eukaryotic initiation factor 2 alpha (eIF-2α). Phosphorylation inactivates eIF-2α and, as it is required for initiation of translation, viral and host cell synthesis is inhibited; this contributes to intracellular antiviral defence (Dar, Dever et al. 2005). During HSV infection, the virally encoded protein ICP34.5, binds to the cellular serine/threonine protein phosphatase 1A (PP1A) and causes it to dephosphorylate inactivated eIF-2α, relieving the inhibition of protein synthesis by PKR (He, Chou et al. 1997). Deleting the γ34.5 gene, which encodes ICP34.5, therefore renders HSV-1 replication sensitive to PKR mediated inhibition. This has been confirmed by observations of reduced neurovirulence in mice by 10^4 fold (Bolovan, Sawtell et al. 1994). The PKR antiviral defence pathway is suppressed by overactive mitogen activated protein kinase (MAPK)

kinase (MEK) in several cancers. In these cells, HSV-1 strains lacking the ICP34.5 gene can replicate uninhibited (Smith, Mezhir et al. 2006).

Four HSV-1 viruses with γ34.5 amongst other deletions have been evaluated in clinical trials; three of which, G207, 1716 and NV1020 failed to induce any complete responses (Markert, Medlock et al. 2000; Hammill, Conner et al. 2010). Hepatic arterial infusion of NV1020, however, was associated with a one year survival rate of 47.2% in patients with metastatic colorectal cancer with liver metastases in a phase I/II trial (Geevarghese, Geller et al. 2010). Due to the lack of a group receiving chemotherapy alone in this trial, it is unclear as to whether treatment with NV1020 represents a significant improvement on standard therapy, but investigation in a phase II/III trial may be justified.

OVs with Tumour Specific Promoters

A separate approach to improve cancer cell selectivity of oncolytic viruses is to replace viral promoter elements with those responsive to transcriptional promoters selectively up-regulated in cancer cells. Two adenoviruses were designed according to this concept, to express early genes under the control of prostate specific promoter and enhancer elements, and were analysed in clinical trials. Unlike deletion strategies, this genetic modification was not cancer, but tissue specific. The first virus CG 7060 contained an E3 deletion and E1A expression under the control of prostate specific antigen (PSA) promoter-enhancer elements. The second CG 7870 contained no gene deletions and expressed E1A under the control of the rat probasin promoter and E1B under control of the PSA promoter-enhancer elements. Clinical trials evaluating IT administration of these viruses validated the cancer targeting strategy and led to the production of many

more adenovirus vectors with varying cancer targeting strategies, however, no complete responses were observed (DeWeese, van der Poel et al. 2001; Small, Carducci et al. 2006).

Telomelysin is a serotype 5 adenovirus with E1A and E1B promoter regions replaced by the human telomerase reverse transcriptase gene (hTERT) promoter (Takakura, Kyo et al. 1999). As telomerase is inactive in differentiated tissues but active in tumours, this causes tumour specific replication of this virus. In a phase I clinical trial, following a single IT administration of telomelysin to patients with a variety of solid tumours, 1/16 patients had a partial response and 7/16 patients were reported as having stable disease (Nemunaitis, Tong et al. 2009). It was also reported, however, that in 3/16 patients tumour biopsies displayed necrosis that may, or may not have been treatment induced.

OVs with Transgenes to Enhance Anticancer Activity

As well as genetic modification to enhance cancer selectivity, modifications have also been made to enhance anticancer potency.

JX-594 is an engineered vaccinia virus containing an inserted granulocyte macrophage colony stimulating factor (GM-CSF) encoding gene. The rationale behind this virus design was not only to restrict virus replication to tumour cells but to induce anti-tumour immune responses by stimulating immune cells with GM-CSF. JX-594 also bears a deletion of the thymidine kinase (TK) gene to increase its cancer selectivity. A Phase I clinical trial showed safety and a complete response in 1/7 patients with cutaneous melanoma following IT virus injections (Mastrangelo, Maguire et al. 1999). In an on-

going phase II trial of JX-594 in combination with the protein kinase inhibitor sorafenib for the treatment of advanced hepatocellular carcinoma, preliminary results show 11/13 patients responded to therapy in weeks 6-12 (Heo 2012).

OncoVEX$^{GM\text{-}CSF}$ is a HSV-1 virus with deletions in the γ34.5 gene and replacement of the α47 gene with a gene encoding GM-CSF. A phase II clinical trial of this virus was conducted involving 50 stage IIIc (10) or stage IV (40) melanoma patients receiving OncoVEX$^{GM\text{-}CSF}$ alone as therapy. GM-CSF expression was detected by RTPCR and ELISA and found to be present in tumours and serum, at input-dose related levels. A 26% response rate was observed with a 52% 2-year survival rate and 8/50 patients with complete responses (Senzer, Kaufman et al. 2009). This promising outcome has led to initiation of a phase III trial. Intriguingly, although delivery in these studies was by IT injection, regression of non-injected deposits was also observed, perhaps indicating a GM-CSF mediated systemic anti-cancer effect.

Overall Clinical Observations

A range of viruses from different families have proven the sound principles of oncolytic virotherapy and the toxicity profiles observed are favourable compared to conventional chemotherapy and radiotherapy (Prestwich, Errington et al. 2008). The numerous reports of tumour re-sensitisation to chemotherapy after virotherapy also show that by utilising treatments with differing mechanisms of cell kill, cancer can be treated more effectively. It is feasible that provided side effects are non-overlapping and mechanisms of action are distinct, that multiple viruses could potentially be used in combination, as well as with chemotherapeutic agents (Pandha, Melcher et al. 2009).

1.1.5 Limitations to Successful Virotherapy

Several pre-clinical and clinical studies of oncolytic agents have shown that virotherapy can be successful in treating cancer. The outcomes of virotherapy treatments both in animal and human studies have shown significant variability between subjects. A 100% curative rate has not been observed for any oncolytic virus in clinical trials, however, several complete responses in individual patients have been documented. Where virotherapy is unsuccessful it is likely that either the initial dose reaching tumours was insufficient to establish an infection, or that having established tumour infection, spread of virus through the whole tumour was prevented. This could be a consequence of physical barriers, such as extracellular matrix components or the contents of lysed cells, anti-viral responses from innate immune cells or conferred resistance through IFN signalling, or lastly, a pre-existing inability of the oncolytic agent to infect or kill all tumour cells.

It could be argued that oncolytic activity alone is insufficient to completely eradicate tumours in immune competent hosts and that the clinical success of virotherapy is borne of activation of host anti-tumour immune responses. This claim is refuted though, by numerous studies showing anti-tumour efficacy of oncolytic agents in immune deficient mice (Stanford, Bell et al. 2010). It may be that the presence of an immune system and the formation of adaptive immune responses against OVs prevents their complete spread through, and eradication of tumours. Where complete tumour regression in immune competent hosts is observed it may be that oncolysis is not directly responsible, but that OV replication in tumour sites leads to the induction of anti-tumour immune responses which then eradicate tumours. The role the immune system plays in limiting oncolysis but enhancing tumour cell kill is likely to depend on the rate of oncolysis and the

immune modulation genes expressed by each particular virus. Understanding these events better will assist the design of more effective viruses.

1.1.5.1 Delivery

A major issue for favourable therapeutic outcome is delivering sufficient OV to tumours to establish infections. This is a significant barrier in the treatment of disseminated metastases or tumours in sites inaccessible for surgical resection. Such metastatic disease is of huge clinical importance due to its high prevalence and high associated mortality, and in order to treat such tumours, systemic delivery is essential. The immune system, however, has evolved over millions of years to be efficient in deactivating and clearing blood-borne viruses. Due to the size of virus particles, their movement *in vivo* is dictated by convective forces. A virus particle, therefore, may circulate the body many times before encountering its cellular receptor. As a result, the majority of intravenously administered OV dose is inactivated by a range of mechanisms before entry to target tumour cells, including those shown in Figure 1.1. It is therefore necessary to enhance the stability of OVs that are efficiently neutralised upon systemic delivery, or to utilise viruses with inherent resistance to these mechanisms.

A number of strategies are under investigation to increase the efficiency of OV delivery including; the use of polymer coating of virus particles to increase resistance to neutralisation and clearance of adenovirus (Green, Hale et al. 2012), using virus infected blood borne cells as *in vivo* virus factories (Power and Bell 2008), delivery of liposome encapsulated RNA (Fu and Zhang 2001) or DNA (Kwon, Kang et al. 2011) virus

genomes or direct administration of polymer coated (Kim, Kim et al. 2012) or "naked" nucleic acid virus genomes (Hadac, Kelly et al. 2011).

Viruses that encounter blood during their natural life cycles have evolved in the presence of blood neutralisation and clearance mechanisms. Based on their success despite exposure to blood on host-host transfer, it is probable they have acquired resistance to these mechanisms over the course of their evolution. The use of such viruses as systemically delivered agents has not been extensively studied. Some members of one such virus family, *Alphavirus*, however, have been studied as anticancer therapeutics as discussed in Chapter 1.2.

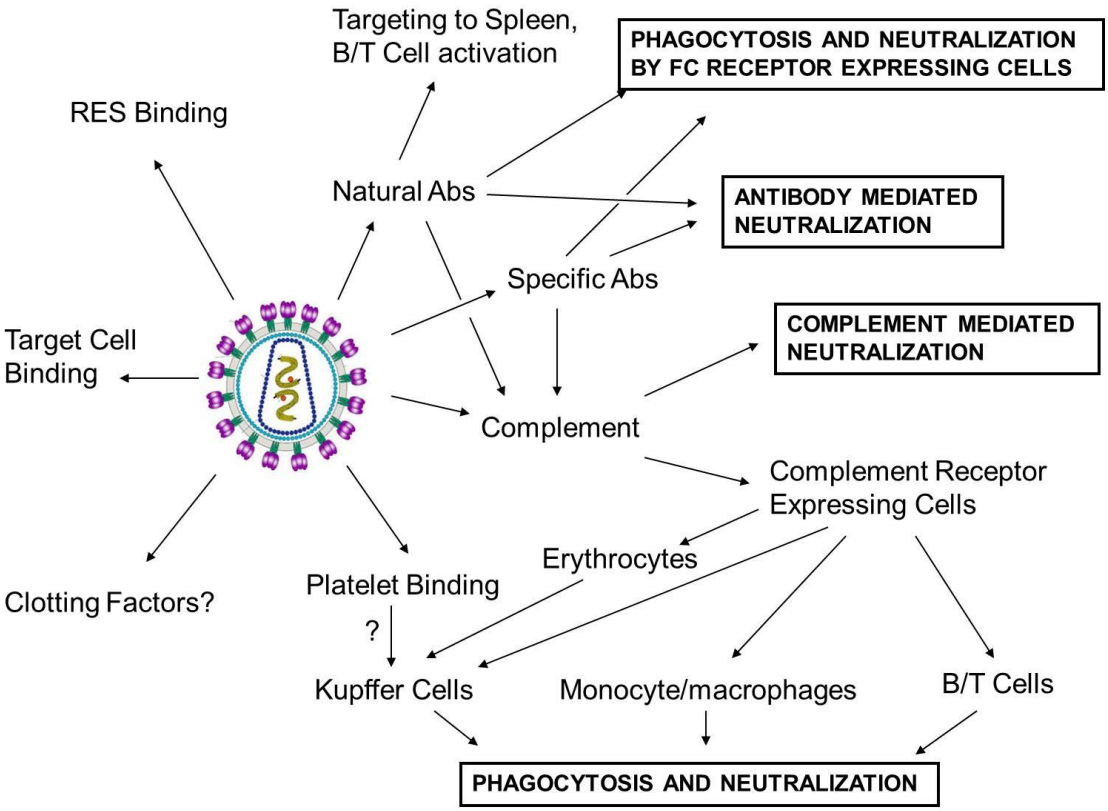

Figure 1.1: Clearance of Intravenously Delivered Virus – Boxes; points of neutralisation, RES; reticuloendothelial system, Abs antibodies (Kueberuwa, Cawood et al. 2010)

A second concern for oncolytic virus delivery, besides neutralisation by immune components, is successful accumulation of input virus in target metastases. The size of virus particles leads to their preferential accumulation at tumour sites compared to normal tissues due to the "enhanced permeability and retention" (EPR) effect. This effect is a consequence of increased gaps between endothelial cells in tumour associated vasculature (380-780nm) versus normal vasculature (6-7nm) (Wisse, Jacobs et al. 2008). Although this effect, and therefore virus particle size is advantageous to virotherapy, it is also thought to lead to phagocytosis by Kupffer cells - liver resident macrophages, and splenic macrophages.

1.1.5.2 Spread

The factors that prevent complete spread of virus and oncolysis of tumours are not clearly understood, but evidence suggests that the spread of viruses which exit cells through lytic processes are inhibited by cellular debris from dead cells. Also, the dense and disorganised connective tissue (extra cellular matrix (ECM)) in tumours may inhibit viral spread. High interstitial fluid pressure within the tumour removes convective forces from the vasculature to the centre of the tumour making the movement and spread of virus reliant on diffusion alone, an inefficient process considering the size of virus particles. It is possible that hypoxic regions of tumours present a barrier to the

spread of at least some types of OVs based on changes in replication efficiency in the presence of hypoxia induced factors (HIFs), however, measured changes are small and may not be of clinical relevance. Functional IFN signalling may prevent OV infection of all tumour cells. This may be due to pre-existing populations of tumour cells with intact IFN signalling or increased IFN accumulation upon OV infection of tumours leading to priming uninfected cells. Even if IFN responses are partially defective, this could confer some degree of resistance to viral infection. It is also apparent that a great deal of heterogeneity exists with tumours (Marusyk, Almendro et al. 2012), hence engineering OVs to be selective for the presence of particular mutations might render them unable to infect and kill all cell subpopulations within a tumour.

Strategies to increase the efficiency of OV spread through tumours include; the use of viruses with intrinsic spread mechanisms such as the cell associated form of vaccinia which utilises actin polymerisation to aid spread to neighbouring cells (Condit 2010), genetic engineering to express enzymes to degrade components of the ECM and connective tissue (Dmitrieva, Yu et al. 2011; Schaefer, Weibel et al. 2012), and utilising OVs with natural or engineered membrane fusogenic peptides, which allow cell-cell viral spread without contact with extracellular moieties (Chen, Cawood et al. 2010; Durupt, Koppers-Lalic et al. 2011). TGFβ signalling has been targeted to reduce the collagen content of tumours and enhance macromolecule spread which can potentially be applied to OVs (Lammerts, Roswall et al. 2002). This concept is of interest as it may also help relieve immune suppression in the tumour environment (Jarnicki, Lysaght et al. 2006). Also, IFN signalling has been targeted by utilising viruses expressing IFN antagonists to prevent signalling (Fu, Rivera et al. 2012) as well as combining OV

treatment with immune suppressive agents (Alvarez-Breckenridge, Yu et al. 2012; Peng, Myers et al. 2012).

It is possible that there is a window in time, before the stimulation of adaptive immune responses, in which OVs can replicate relatively freely to de-bulk tumours. After this window, spread will be significantly inhibited by antiviral antibodies and potent cytotoxic T lymphocyte (CTL) responses against virus infected cells. It is, therefore, attractive to utilise an oncolytic agent with a short replication cycle, so that maximum amount of spread through tumours can be achieved before adaptive antiviral immune responses are generated. With this in mind, the *Alphavirus* family again present themselves as prime candidates for use as oncolytic agents. As discussed in Chapter 1.2, *Alphavirus* infected cells start budding infectious daughter virions just 4 hours after infection.

1.1.5.3 Stimulation of Anti-Tumour Immunity

Clinical success of virotherapy has largely been in cases where the oncolytic virus expresses an immune stimulatory gene. It could be that oncolysis alone is insufficient to eradicate tumours, however, the nature of viruses mean they have the potential to prime the host against antigens of the tumour cells they infect.

Priming of anti-tumour immune responses by the expression of tumour associated antigens has been shown for several cancer vaccines, although with limited success of clinical outcome. It has been shown that with *Alphavirus* based cancer vaccines the induction of apoptosis leads to the production of potent anti-tumour immune responses

due to increased uptake of tumour associated antigens (TAA) by dendritic cells (DCs) (Albert, Sauter et al. 1998; Ying, Zaks et al. 1999). As replication competent oncolytic alphaviruses also kill by apoptosis, it is feasible that these viruses could provide a natural combination of virotherapy and stimulation of anti-tumour immunity.

1.2 Anticancer Applications of Alphaviruses

1.2.1 Alphaviruses as Anti-cancer Vaccines

In 1975 the interest in utilising alphaviruses as anticancer agents was sparked by the report that mice could be protected from cancer by an immune mediated mechanism following immunisation with cell membranes of Semliki Forest virus (SFV) infected cancer cells. WEHI-11 fibrosarcoma cells were infected with SFV *in vitro*, sonicated, heat treated, then administered to BALB/c mice by intraperitoneal (IP) injection. 6/10 mice were protected from subsequent SC challenge with 10^4 WEHI-11 cells (Griffith, Crook et al. 1975). Although this experiment proves a principle of the ability to induce an anti-tumour response with alphaviruses, the protection rate is relatively low considering challenge was with only 10^4 cancer cells. It is also of note that immunisation with irradiated whole influenza infected cancer cells gives an increased rate of protection (17/20) (Boone 1974) compared to membranes of SFV infected cells.

Alphavirus replicons are not capable of productive infection as the structural genes, which are required for the formation of daughter virus particles, are deleted. The main context in which alphaviruses have been used as anti-cancer vaccines is by genetically engineering viruses to express TAAs as replicons. This concept was validated by protecting mice from β-galactosidase (β-gal) expressing tumours by immunising with plasmids encoding Sindbis Virus (SV) or Semliki Forest Virus (SFV) replicons where structural genes were replaced with LacZ (which encodes β-gal) under the viral subgenomic promoter. Immunising with these replicons protected mice against subsequent IV challenge with β-gal expressing CT-26 colon carcinoma cells (CT-26 β-

gal) whilst CMV-β-gal plasmids (pCMV- β-gal) could not. Also the survival of mice with pre-established IV administered CT-26 β-gal lung metastases was significantly increased by replicon encoding plasmids compared to PBS whilst immunisation with pCMV-β-gal had no therapeutic effect. The increased efficacy in utilising SV and SFV replicons to express β-gal compared to pCMV-β-gal was not thought to be due to increased levels of expression, as similar amounts of protein was produced, but due to induction of apoptosis by replicons. This is induced by intracellular dsRNA receptors and leads to increased uptake by DCs and in the context of "danger" signals known to be key in promoting strong antigen responses (Ying, Zaks et al. 1999; Leitner, Ying et al. 2000).

Numerous subsequent studies have been conducted analysing the ability of SV, SFV and Venezuelan equine encephalitis virus (VEE) replicons expressing TAAs to induce anti-tumour immune responses. *Alphavirus* replicon RNA, packaged by providing virus structural genes in trans are known as virus like particles (VLPs), as although they have identical structure to their parental virus particles, they lack genes required for productive infections. VLPs and DNA plasmids encoding replicons have both been successful in protection from challenge and increasing survival in mice bearing established tumours, as well as breaking tolerance self-antigens. Mouse tumour models in which immunisation with antigen expressing *Alphavirus* replicons elicited significant therapeutic effects include; breast (Human epidermal growth factor receptor 2 (HER2), cervical (human papilloma virus (HPV) E6 and E7), colorectal (carcinoembryonic antigen (CEA)), mastocytoma (P815), melanoma, (tyrosinase, tyrosine related protein 1 (TRP-1), gp100, melanoma associated antigen (MAGE) and melanoma cell adhesion molecule (MCAM)) and prostate (six transmembrane epithelial antigen (STEAP) and

prostate stem cell antigen (PSCA)) (Lachman, Rao et al. 2001; Leitner, Hwang et al. 2003; Cassetti, McElhiney et al. 2004; Goldberg, Bartido et al. 2005; Wang, Wang et al. 2005; Yamanaka and Xanthopoulos 2005; Leslie, Zhao et al. 2006; Garcia-Hernandez, Gray et al. 2007; Näslund, Uyttenhove et al. 2007; Garcia-Hernandez, Gray et al. 2008). Anticancer activity in gp100 melanoma and HPV E7 and E8 cervical models was enhanced by concomitant administration of replicons expressing interleukin 18 (IL-18), an inducer of type 1 helper T cell (Th1) responses and interleukin 12 (IL-12), a natural killer (NK) cell activator, respectively.

A phase I/II clinical trial has been conducted to evaluate the safety and induction of anticancer immune responses against colon cancer using a VEE VLP expressing CEA. Results showed that with multiple VLP injections, immune tolerance to CEA was broken and T cell and antibody responses to CEA developed. This occurred despite rapidly increasing levels of anti-VLP antibodies on repeated administrations, which had been a stumbling block for prime-boost strategies with adenovirus and vaccinia vectors (Kundig, Kalberer et al. 1993; Sumida, Truitt et al. 2005). In this study there were not enough patients to statistically evaluate the therapeutic effect of vaccination, however, 1/24 patients had a complete response to a liver metastasis and 2/24 were reported as having stable disease (Morse, Hobeika et al. 2010). A phase III trial is required to evaluate the efficacy of this agent but, importantly it has shown that *Alphavirus* VLPs can be safely be used in humans and suggests when using *Alphavirus* vectors, development of neutralising antibody responses may not present an insurmountable hurdle.

1.2.2 Alphaviruses as Immune Modulating agents

Immune regulatory cytokines have proven efficacy in animal models and clinical trials. *Alphavirus* vectors expressing GM-CSF, IL-12, IL-15 or IL-18 have shown anticancer efficacy in colon adenocarcinoma, fibrosarcoma, glioma, ovarian and melanoma mouse models (Klimp, van der Vaart et al. 2001; Chikkanna-Gowda, Sheahan et al. 2005; Rodriguez-Madoz, Prieto et al. 2005; Yamanaka and Xanthopoulos 2005). Efficacy in athymic mice suggests that suppression of angiogenesis rather than immune stimulation is key, however, CTL depletion in immune competent mice ablated efficacy. In addition, many models in which these cancer vaccines were tested utilised tumour transplantation, where anti-tumour immune responses may be easier to induce. However, it is of note that efficacy has been reported for a SFV replicon expressing IL-12 in a woodchuck model of hepatitis B virus (HBV) induced hepatocellular carcinoma (HCC) (Rodriguez-Madoz, Prieto et al. 2005). A phase I/II clinical trial protocol was reported in 2003 for the evaluation of the safety and efficacy of a SFV replicon expressing IL-12 coated in cationic liposomes to be delivered by intratumoural infusion to patients with glioblastoma multiforme (Ren, Boulikas et al. 2003). The results of this trial have not yet been published.

1.2.3 Oncolytic Efficacy of Alphaviruses

During the use of alphaviruses as cancer vaccines, it was observed that anti-tumour immune responses induced by VLPs were stronger than those induced by plasmid encoded replicons (Ni, Lin et al. 2004). Fully replication competent alphaviruses can, therefore, potentially induce anti-tumour immune responses in addition to directly

killing cancer cells. Two replication competent alphaviruses, SFV and SV, have been evaluated for their anticancer efficacy in mice.

1.2.8.1 SFV

The SFV strain A7 is attenuated by repeated tissue culture (TC) passage and is not virulent in adult mice (unlike the virulent L10 and SF4 strains). In 2006, it was shown to replicate in, and cause regression of, A2058 melanoma xenografts implanted by subcutaneous (SC) injection in severe combined immunodeficient (SCID) mice by IT, IP or IV delivery (Bradish, Allner et al. 1971; Vähä-Koskela, Kallio et al. 2006). Subsequent testing in partially immune competent mice, however, revealed limitations of systemic delivery of SFV A7.

The natural tropism of SFV for neuronal cells was utilised to treat partially immune competent Balb/c mice inoculated intracranially (IC) or SC with U87 human glioblastoma cells. After a single IV delivery of SFV A7, 5/5 orthotopic IC tumours completely regressed without recurrence. In the same study, the complete response rate for SC implanted U87 tumours was reduced to 3/6, despite receiving three IV doses of virus (Heikkilä, Vaha-Koskela et al. 2010). The disparity in success of treatment of IC versus SC U87 tumours is probably due to differences in richness of blood supply and the influence of surrounding tissues on implanted tumour cells which affect SFV uptake, replication or spread. It may also be a consequence of the immune privileged status of the brain, suggesting the immune system plays a role in inhibiting oncolytic activity of SFV. As these mice were also not fully immune competent these results highlight insufficiency of SFV A7 as a systemically delivered oncolytic agent.

Combination of SFV with vaccinia virus, with both expressing ovalbumin (OVA), gave good therapeutic efficacy in the syngeneic murine ovarian surface epithelial carcinoma (MOSEC) model. This study not only combines two viruses with different oncolytic mechanisms but also combines oncolysis and anti-tumour immune activation, and shows that immune activation enhances anti-cancer activity compared to non-OVA expressing viruses used in combination (Zhang, Tsai et al. 2010). Significantly, the burden of producing a single curative oncolytic agent is relieved in the knowledge that multiple viruses may be used in combination. Clinically evaluating treatment with multiple viruses in one trial, however, may provide a significant challenge. It is of note that SFV A7 has been significantly attenuated and other less attenuated strains of the virus may prove more potent as oncolytic agents, although safety concerns must be addressed.

1.2.8.2 SV

Sindbis virus is described in more detail in Chapter 1.3. As an oncolytic agent, SV has shown promise in animal models. In SCID mice, SV administration has achieved complete regression in 4/5 mice with SC BHK tumours following IP delivery. In the same model, SV treatment significantly inhibited the growth of LS174T (human colon adenocarcinoma), HT-29 (human colon adenocarcinoma) and CFPAC (human pancreatic adenocarcinoma) tumours compared to PBS (Tseng, Levin et al. 2002).

In models designed to investigate whether systemic administration of SV could be used to treat tumours at different tissue sites in SCID mice, it was seen that SV administered IP was able to infect BHK and ES-2 tumour metastases implanted by IP injection. Also, IV administered SV was able to infect lung tumours established by injection of BHK

cells IV. As well as being capable of infection of IP implanted ES-2 tumours, IP administered SV expressing LacZ or IL-12 was also capable of significantly inhibiting tumour growth compared to PBS treated mice (Tseng, Levin et al. 2004).

The above studies utilise SCID mice and human tumours, leaving doubt as to whether tumour selectivity is based on preference of SV for human cells in general and whether systemic SV delivery and replication in tumours can take place in the presence of an intact immune system. To remove such doubt, anticancer activity of SV was evaluated in immune competent mice utilising syngeneic or spontaneously forming cancer models.

The MOSEC cell line is derived from a C57BL/6 mouse (Chalikonda, Kivlen et al. 2008), hence can establish tumours in this immune competent mouse strain. In mice bearing MOSEC tumours a single IP delivered dose of SV was sufficient to enhance survival, suggesting that SV infection of tumours and subsequent anti-cancer activity is not a consequence of tumour and host species differences (Tseng, Hurtado et al. 2004).

The Pan02 cell line (murine pancreatic adenocarcinoma) is also derived from the C57BL/6 mouse strain. Growth of subcutaneously implanted Pan02 tumours in this model was significantly inhibited by daily SV treatment over a period of 14 days (Tseng, Levin et al. 2004). This suggests that the development of an adaptive immune response does not negate the anticancer efficacy of SV.

Another immune competent model, in which transgenic MSV-RGR/p15$^{+/-}$ mice spontaneously develop fibrosarcomas, it was shown that systemically delivered SV selectively infected tumour cells. This is significant as spontaneously arising tumours are immune edited and hence more closely mimic the physiological development of cancer (Tseng, Levin et al. 2004).

1.3 Sindbis Virus

Sindbis virus is a positive stranded RNA virus discovered in 1952, Cairo, Egypt, isolated from a pool of mosquitoes of the species *C. pipiens* and *C.univittatus.* Sindbis Virus belongs to the *Togavirus* family of the *Alphavirus* genus. Alphaviruses are categorised in group IV in the Baltimore virus classification system, of which all possess single stranded positive sense RNA (+ssRNA) genomes. Hosts of Alphaviruses include vertebrates such as humans, horses, rodents, fish and birds, as well as several invertebrate species.

1.3.1 Transmission

Transmission of SV and indeed all alphaviruses occurs through infection of haematophagous arthropod vectors, typically mosquitoes, where infection causes no pathological symptoms, hence its classification as an arbovirus (arthropod borne virus).

There is evidence of SV infections throughout the old world in Europe, Asia, Africa and Australia (Tesh 1982). SV is maintained in the wild by alternating infection of arthropod and vertebrate hosts. Upon arthropod infection SV replicates in the gut and spreads to other tissues leading to the accumulation of virus particles in salivary glands, after which, mammals on which they feed are susceptible to infection during subsequent blood meals. Once in vertebrate hosts SV replicates rapidly causing a period of viraemia, during which, feeding arthropods can be infected during blood meals. Apart from in humans, adult vertebrate hosts show no pathological symptoms during infection (Heise, Simpson et al. 2000; Kurkela, Manni et al. 2004).

The most complete epidemiological data regarding SV infection has been collected in Finland where it is the causative agent of seven yearly outbreaks of Pogosta disease (Kurkela, Manni et al. 2004). In this setting the arthropods responsible for transmission of the virus are the *Aedes, Culiseta* and *Culex* mosquito species. It is thought that in particular, *Culex torrentium* transmits SV through the fieldfare (*Turdus pilaris*) redwing (*Turdus iliacus*) and song thrush (*Turdus philomelos)* bird populations and that the mosquito species *Aedes cinereus* is largely responsible for spread to humans as it feeds regularly on birds and occasionally on humans (Turell, Lundstrom et al. 1990).

Upon human infection with SV, after an incubation time of 2-10 days (Luukkainen, Laine et al. 2000), symptoms of arthralgia, rash, fatigue and itching are experienced by the majority of patients. Less common are reports of fever, muscle pain, headaches nausea, papules in the mucosal membrane of the mouth, enlarged lymph nodes and dizziness (Kurkela, Manni et al. 2005). The fact that humans can be infected during mosquito bites means that, at least in some humans, SV has sufficient resistance to neutralisation by the multiple blood based defence mechanisms to establish infection (Figure 1.1) (Kueberuwa, Cawood et al. 2010). In addition, the long lasting symptoms observed in some patients could be due to persistent virus survival and replication in hosts. Evidence for this includes the detection of IgM antibodies long after acute infection suggesting continued expression of viral antigens. Nevertheless, samples taken from patients with chronic symptoms have not confirmed the presence of SV RNA in blood or synovial tissue samples (Levine, Hardwick et al. 1994).

1.3.2 SV Structure and Cell Entry

SV virions are enveloped in a phospholipid membrane derived from the cytoplasmic membrane of their producer cell and measure ~70 nm in diameter (Ferreira, Hernandez et al. 2003). At the nucleus of the virion is the 11.7Kb +ssRNA genome, coated in 80 capsid proteins. On the surface are 80 spikes formed from trimers of 240 copies of E1-E2 protein heterodimers, these directly interact with the 240 capsid proteins through the phospholipid membrane, this feature makes the envelope of SV rigid and means the capsid:glycoprotein ratio is 1:6 (Figure 1.2).

The primary receptor for SV in mammalian cells has been shown to be the 67kDa high affinity laminin receptor (67LR) (Wang, Kuhn et al. 1992). The 67LR binds laminin-1, a component of the ECM and the major glycoprotein in the basement membrane in all tissues, with high affinity and plays an important role in adhesion of cells to the laminin network (Cavalieri, Rotoli et al. 2005).

Spikes protruding from the surface of SV formed from trimers of E1-E2 dimers are responsible for virus particle binding and entry to cells. Residues 170-220 on the E2 glycoprotein are of particular importance in attachment of virus particles to cells although SV particles lacking E2 are still capable of entry (Strauss and Strauss 1994).

Entry of SV into cells is achieved through fusion of the viral lipid envelope with the cytoplasmic membrane of the host cell (Li, Jose et al. 2010). A 17 amino acid stretch on the E1 glycoprotein has been shown to be responsible for membrane fusion; SV particles lacking E1 are not capable of infection (Kondorkoch, Burke et al. 1983; Mukhopadhyay, Zhang et al. 2006). Although membrane fusion has been observed on the cell surface, a change to low pH environment is required for the fusion peptide to be

exposed, strongly suggesting that SV particles are endocytosed and membrane fusion occurs upon endosome acidification (Helenius, Kielian et al. 1985).

After fusion with the cell, the virus nucleocapsid breaks down by a mechanism that has yet to be fully defined, as during an infectious cycle capsids both disassemble on entry and assemble prior to release within the cytoplasm. One explanation for this discrepancy is that interactions with the large ribosomal subunit are responsible for disassembly and that during the course of an infection, ribosomal subunits are saturated with newly produced capsid proteins, triggering a switch to assembly later in an infectious cycle. There has been data to refute this, however, with ribosomal saturation measured at only 20% during late stage infection (Ulmanen, Soderlund et al. 1979). Other explanations suggest that mature capsids differ from those newly produced, that acidified endosomes cause a structural change in capsid protein and that in normal cellular Na^+ and K^+ concentrations capsids disassemble, whereas later in infection, when these concentrations change, capsids are driven to associate.

Once the SV nucleocapsid is disassembled, genomic RNA is released and is translated by host cell machinery in the cytoplasm.

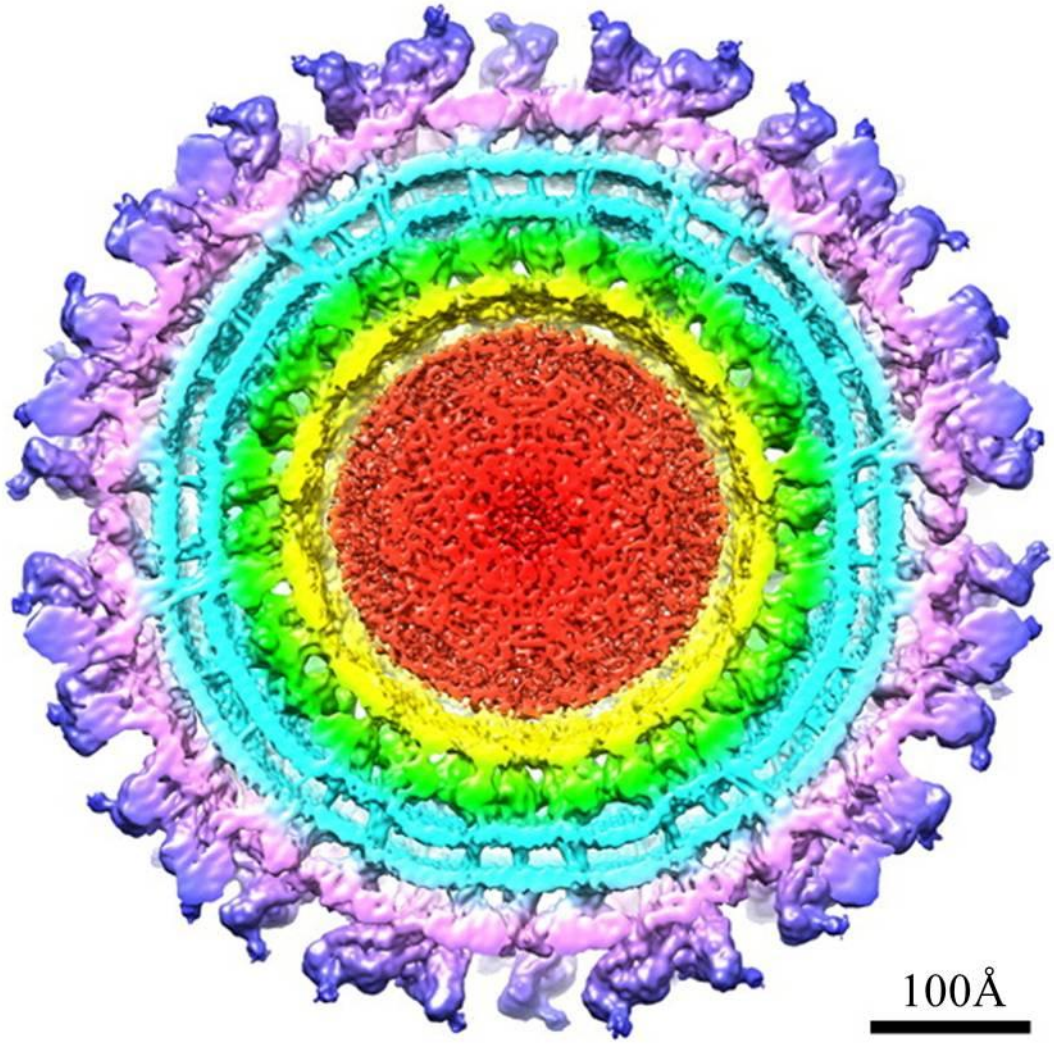

Figure 1.2: SV Virion Structure – This structure was computed from an average of cryoEM images by Tang *et al*. Spikes of E1-E2 trimers (blue) and the underlying skirt (magenta). Outer and inner leaflets of the viral membrane appear as two concentric, roughly spherical shells of density (cyan), crossed by distinct E1 and E2 TM helices (also in cyan). Protease domains of the capsid protein (green) lie beneath the membrane and surround a layer of density (yellow) that is attributed primarily to the N-terminal segments of the capsid protein. The remaining disorganized density (red) at the core of the virion is attributed primarily to the RNA genome. Adapted from (Tang, Jose et al. 2011).

1.3.3 SV Replication

Like mature messenger RNA (mRNA) the SV genomic RNA is capped and polyadenylated. This results in stability in the cytoplasm by conferring resistance to 5' and 3' exonucleases and enhances the efficiency of translation initiation. The genome encodes two polyproteins, one a precursor for the non-structural proteins nsp1-4 and the other a precursor for structural proteins capsid, E1, E2, E3 and 6K (Figure 1.3).

Cap dependent translation of SV genomic RNA produces P123, the polyprotein precursor of nsp1-3, after the nsp3 coding region there is an opal stop codon (Sanz, Castello et al. 2009). At this point in mammalian cells, read-through translation occurs with an efficiency of < 5%, where an arginine, tryptophan or cysteine residue is inserted in the position of the UGA codon; this produces P1234, a precursor polyprotein of nsp1-4 (Shirako and Strauss 1994) (Figure 1.3). It has been shown that a cytosine base immediately downstream of the opal stop codon is the cause of read-through translation, as when this is replaced by any other nucleotide read-through translation ceases (Li and Rice 1993).

The C-terminal residues 460-807 of nsp2 form a papain-like protease responsible for processing the non-structural polyproteins. P1234 is able to self-cleave, thus forming P123 and nsp4 which form a complex that binds the 3'UTR of positive sense genomic RNA and functions as the minus strand synthase (Strauss and Strauss 1994). Nsp4 has a GDD motif characteristic of viral RNA polymerases and is thought to be the SV RNA dependent RNA polymerase (Kamer and Argos 1984).

The nsp2 protease is also responsible for the processing of P123 to nsp1, nsp2 and nsp3, this occurs through a bimolecular reaction which requires the cellular concentration of

P123 to reach a threshold (Hardy and Strauss 1989). A complex formed by nsp1, nsp2, nsp3 and nsp4 functions as the SV plus strand RNA synthase. Thus SV temporally regulates RNA synthesis so that synthesis of minus strand RNA occurs early in infection, followed by a switch, after 3-4 h, to plus stranded RNA synthesis. The role of nsp3 is unclear, yet it is required for RNA replication and is heavily phosphorylated by one or more host cell kinases (Li, Lastarza et al. 1990).

From negative sense genomic RNA, positive sense genomic and subgenomic RNA are produced by the plus strand replicase, initiating at the 49S genomic and 26S subgenomic promoter respectively (Figure 1.3). Nsp1 is required for 5' capping of genomic and subgenomic RNA during transcription and is responsible for their methylation (Cross and Gomatos 1981).

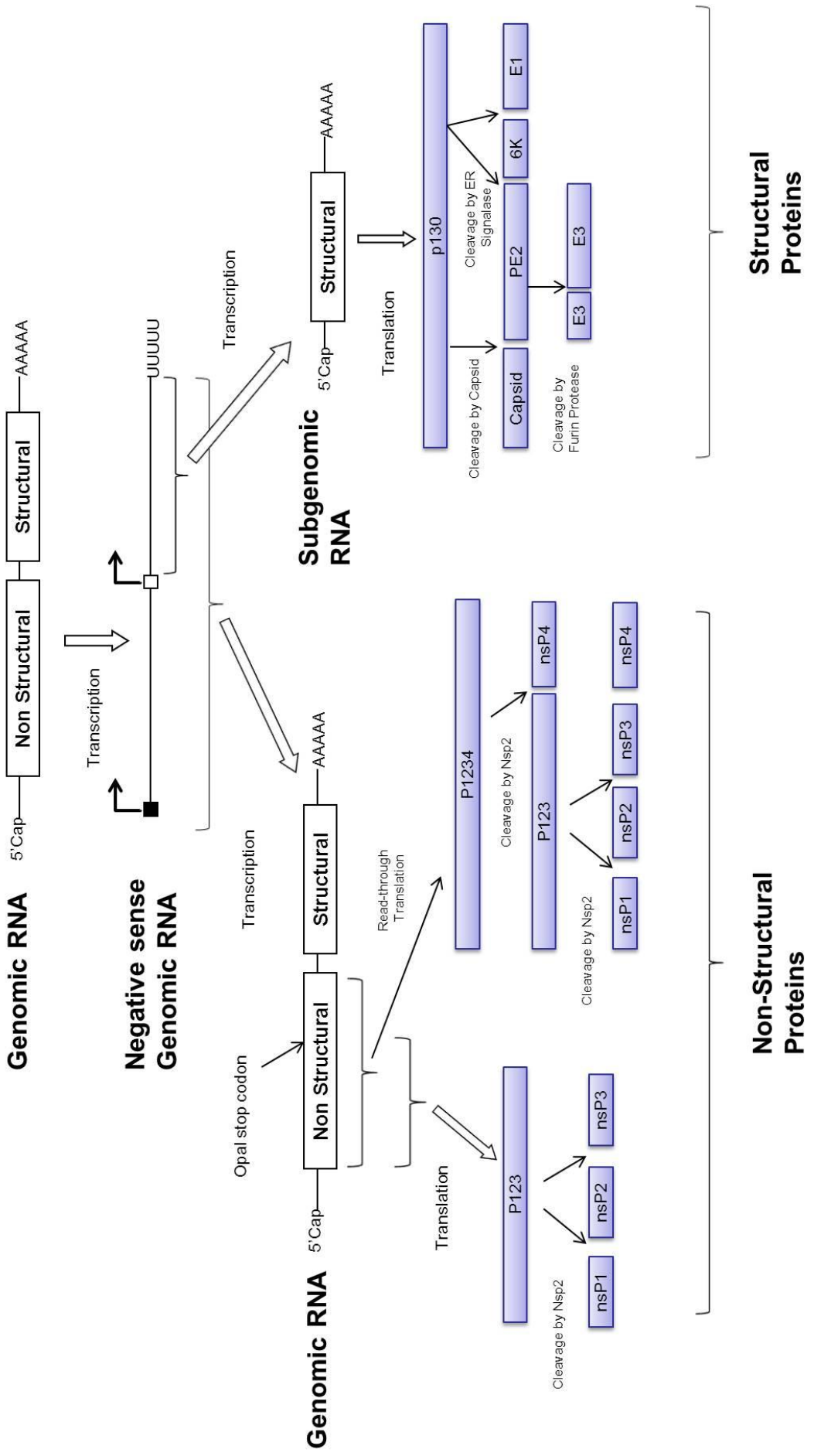
Genomic RNA
5'Cap
Non Structural
Structural
AAAAA
Transcription
Negative sense Genomic RNA
UUUUU
Transcription
Subgenomic RNA
5'Cap
Structural
AAAAA
Translation
p130
Cleavage by ER Signalase
E1
6K
PE2
E3
E3
Cleavage by Capsid
Capsid
Cleavage by Furin Protease
Structural Proteins
Transcription
Opal stop codon
Non Structural
Structural
AAAAA
Read-through Translation
P1234
Cleavage by Nsp2
nsP4
P123
nsP4
nsP3
nsP2
nsP1
Cleavage by Nsp2
Genomic RNA
5'Cap
Translation
P123
nsP3
nsP2
nsP1
Cleavage by Nsp2
Non-Structural Proteins

Figure 1.3: Overview of SV RNA Replication, Translation and Protein Processing – nsp = non-structural protein, ■ = 49S genomic promoter, □ = 26S subgenomic promoter.

The subgenomic RNA encodes the structural proteins; these are produced as a polyprotein which is inserted into the ER. Capsid protein possesses protease activity and cleaves itself from the polyprotein co-translationally and remains in the cytoplasm. The ER signalase cleaves the remainder of the polyprotein yielding glycoprotein E1, 6K and PE2, which are all membrane anchored (Figure 1.3). E1 and PE2 are glycosylated at every accessible site during transit through the golgi apparatus, with sites that become inaccessible through folding receiving less complex glycosylations. E1, 6K and PE2 are all palmitoylated; these palmitic acid modifications are not necessary for correct transport to the cell surface but are essential for virus budding (Gaedigknitschko, Ding et al. 1990; Gaedigknitschko and Schlesinger 1991). PE2 is further cleaved by cellular furin protease to yield glycoproteins E2 and E3. E2 remains anchored protruding into the ER lumen and E3 is freed but associates with E1-E2 dimers that are subsequently formed. After transport through the golgi complex, glycoproteins are transported to the cell surface through the *trans* golgi network. Here they associate with nucleocapsids during the budding process.

Unlike many other viruses, SV does not form virions with empty capsids. This is because initiation of nucleocapsid formation relies on a direct interaction of capsid protein with a specific RNA sequence between 746 and 1226 (Weiss, Nitschko et al. 1989). After one capsid protein binds a genomic RNA molecule a cascade of binding is initiated which leads to 240 monomers completely encapsulating the SV genome. Assembly and budding of newly synthesized SV virions requires a high intracellular

concentration of Na^+ ions. As mentioned above, this may be required for nucleocapsid formation. Direct sequence recognition of genomic RNA by capsid protein also prevents the formation of non-infectious particles that may otherwise result from the packaging of subgenomic RNA (Weiss, Nitschko et al. 1989). Once formed, nucleocapsids accumulate at the cell membrane where they are bound by the intracellular cytoplasmic domain of E2 glycoproteins. The energy change in this binding is thought to be sufficient to cause complete circularisation of cytoplasmic membrane around the nucleocapsid and hence release enveloped SV particles from the cell surface (Strauss and Strauss 1994).

Newly budded SV virions have been detected as soon as 4 hours post infection (PI) and infected cells continually shed virus until death by apoptosis (Strauss and Strauss 1994). SV triggered apoptosis takes approximately 72 hours from initiation to completion. This is likely a host mechanism which has evolved in order to limit viral spread; it seems that this has imposed a large selective pressure on SV to replicate rapidly for the release of the maximum number of virions possible before apoptotic death occurs. It is also of note that non-viral induction of apoptosis is reported to take < 24 hours, suggesting SV slows apoptosis, which may confirm that it imposes a significant selective pressure (Saraste and Pulkki 2000).

Intracellular antiviral sensors that recognise dsRNA are activated during SV infection (Ryman, Meier et al. 2005). This leads to shut down of cellular translation by PKR-phosphorylation of eIF2α and the induction IFN signalling. The PKR response induces a global knockdown of translation, thus virus protein synthesis is repressed at the cost of also shutting down host protein synthesis. SV, however, can initiate translation in the absence of active eIF2α through a hairpin structure that forms in viral RNA that

interacts with ribosomes. Hence, whilst cellular translation is unable to continue, virus protein synthesis is uninhibited (Ventoso 2012). This rather elegant mechanism of SV takes advantage of a host cell response which is normally anti-viral, to direct maximum cellular resources into the production of new virus particles.

Despite resistance to host cell translational shutoff, SV replication is extremely sensitive to IFN. Intracellular viral RNA sensors such as toll like receptors (TLRs) 3, 7 and 8, retinoic acid inducible gene I (RIG-I) like receptors (RLRs) and nucleotide-binding oligomerisation domain (NOD) like receptors (NLRs) are activated during SV infection, and lead to the production of IFN and the secretion of pro-inflammatory cytokines. The time taken for this to occur is around 12 hours and has probably provided a major selective pressure for the rapid replication of SV (Atkins and Lancashire 1976).

1.3.4 Underlying Causes of SV Tumour Selectivity

The natural tumour selectivity of SV has been attributed to increased infection of tumour cells and more efficient replication once within them.

The receptor 67LR used during SV infection is up-regulated in neoplastic tissues and increased expression has been shown to correlate with increased invasion and metastasis. Although the 67LR is ubiquitously expressed, overexpression in neoplastic tissues is thought to result in more unoccupied receptors on the surface of cancer cells than normal cells (Tseng, Levin et al. 2004). It has been suggested that this increased number of unoccupied receptors is responsible for more efficient attachment and uptake

of SV particles in tumours than in normal tissues. Studies showing the ability of SV to utilise more than one receptor in mammals, one of which has been identified as heparin sulphate proteoglycan (HS), cast doubt on this hypothesis. It is well accepted that upon TC passage on BHK cells, SV changes receptor tropism to utilise HS (Byrnes and Griffin 2000). Studies showing SV utilisation of HS as a receptor could, therefore, be a consequence of the investigation of different strains of SV at different stages of TC adaptation. Given the presence of HS binding motifs in both TC adapted and *in vivo* passaged SV, it is reasonable to postulate that HS contributes to cell attachment, bringing SV particles into close proximity of the 67LR but not allowing entry in itself. It is of note that *in vivo* tissues analysed for 67LR levels showed that tumours permissive to SV had higher expression than other tissues in which SV replication was not detected (Tseng, Levin et al. 2004) and that down-regulation of the 67LR using siRNA causes decreased SV infectivity (Tseng, Hurtado et al. 2004).

An alternative theory is that the cancer selectivity of SV is governed by intracellular determinants rather than surface receptor levels. Considerable evidence for this proposal was recently presented by Huang *et al* who showed that in a range of cancer cell lines *in vitro*, the degree of SV infectivity did not correlate with the amount of 67LR present, but with the functionality of IFN signalling status of cells (Huang, Guo et al. 2011).

Comparison of an eGFP encoding SV and two lentivirus vectors encoding eGFP, the first pseudotyped with SV glycoproteins and the second pseudotyped with VSV glycoprotein G (VSV-G) showed that cells resistant to SV infection were still susceptible to lentivirus infection and expression of eGFP. Furthermore, psuedotyping with SV or VSV-G glycoproteins did not give significantly different profiles of eGFP expression by lentivirus, strongly suggesting that intracellular mechanisms, rather than

surface expression of SV receptors, are responsible for determining the efficiency of SV transgene expression and replication in different cells. The same group went on to characterise the functionality of the IFN signalling pathways in a range of cell lines and showed a correlation of compromised signalling with increased permissivity to SV infection (Huang, Guo et al. 2011).

The weight of evidence, therefore, indicates that dysfunctional IFN signalling in cancer cells is the major determinant of SV tumour selectivity. This would provide an explanation of the ability of SV to infect such a wide variety of tumour types, and conforms to existing theories for the tumour selectivity of the oncolytic viruses NDV and VSV. IFN sensory and effector pathways, however, may exist at varying levels of functionality between tumours and indeed between subpopulations of cancer cells within individual tumours. This could mean heterogeneity in permissivity to productive infection by SV; if so, as complete tumour regression requires elimination of all tumour cells, this could limit the anti-cancer efficacy of SV.

1.3.5 Mechanism of SV Oncolytic Activity

It is well documented that SV induces apoptosis in vertebrate cell lines *in vitro*. This has been shown to be triggered through multiple mechanisms, the most significant being through activation of acid sphingomyelin phosphodiesterase (aSMase). This occurs concomitantly with virus-cell membrane fusion and later through neutral sphingomyelin phosphodiesterase (nSMase). Sphingolipids are a cofactor for SV virion-cell membrane

fusion; during this process aSMase hydrolyses sphingomyelin, releasing phosphocholine and ceramide, in this context ceramide triggers caspase dependent apoptosis (although ceramide accumulation can also lead to caspase independent apoptosis) (Taha, Mullen et al. 2006). The SV protein nsp2 is also toxic to cells due to shutoff of host cell transcription to a point where the cell cannot survive, although this leads to toxicity in itself, it may contribute to the increased time required for completion of apoptosis (Garmashova, Gorchakov et al. 2006).

Early models of SV anti-tumour efficacy designate the mechanism of tumour regression as complete spread of SV through tumours and hence induction of apoptosis throughout. Recent studies, however, have provided evidence that SV stimulates anti-tumour immune responses. This suggests that although widespread apoptosis in tumours contributes to oncolytic efficacy, it is likely that the immune system contributes to tumour clearance (Huang, Guo et al. 2011). This is unsurprising, given observations of efficacy in *Alphavirus* replicon induction of anti-tumour immune responses. The mechanism by which *Alphavirus* vaccines are thought to prime immune responses is shared by oncolytic alphaviruses. Like other viruses, SV causes the induction of inflammatory cytokine signalling and the release of tumour antigens, however, because of its strong induction of apoptosis, it causes increased production apoptotic bodies which are taken up by DCs. Cancer cell antigens are, therefore, taken up in the context of *Alphavirus* induced inflammatory signals, leading to the induction of stronger immune responses than free antigens (Ying, Zaks et al. 1999; Leitner, Ying et al. 2000).

1.4 MicroRNA

1.4.1 Discovery

MicroRNAs (miRs) are nucleotides 21-25 bp in length that post-transcriptionally regulate host gene expression (He and Hannon 2004). The first characterised miRNA was lin-4 in *C.elegans* whose larval development takes place in 4 stages, designated L1-4. It was shown that mutations in lin-4 caused a block in larval development where cells were "stuck" in the L1 phase, whereas mutations in the lin-14 gene caused premature initiation of the L2 phase (Chalfie, Horvitz et al. 1981; Ambros and Horvitz 1984; Ambros 1989). It was later found that lin-4 did not encode a protein but a non-coding RNA, 22 bases in length with partial complementarity to the protein coding lin-14 gene (Lee, Feinbaum et al. 1993). Lin-14 encodes a nuclear protein down-regulated during the transition between L1 and L2 and down-regulation is dependent on 3'UTR sequences with partial complementarity to Lin-4. In addition, Lin-28 was also down-regulated by Lin-4 in an analogous, 3'UTR dependent fashion.

These experiments demonstrated that protein expression could be regulated at the mRNA level by antisense miRNA. Since their discovery, 367 more mature miRNAs have been identified in C.elegans and thousands more across the chromalveolatan, metazoan, plantae, unikont and virus kingdoms, including 1921 in humans (miRBase 2012).

1.4.2 MiRNA Production

Cellular miRs are produced as shown in Figure 1.4; miR precursors, called primary miRNAs (pri-miRs) are produced in the nucleus by transcription carried out by RNA polymerase II (RNA pol II). DNA template for pri-miRs is either non-translated RNA or introns of translated RNAs which are subject to splicing. The length of pri-miRs ranges from hundreds to thousands of nucleotides in length. Within pri-miRs are 21-25 nucleotide miR sequences that form part of an imperfect stem loop structure about 80 nucleotides in length (Cullen 2004). Pri-miRs can contain the sequence of one, or of several miRs. In vertebrate cells, a dimer of Drosha, the cellular RNase III enzyme, and DGCR8, recognise and cleave stem loop structures within pri-miRs yielding stem loops about 60 nucleotides in length with 2 nucleotide overhangs at the 3' ends called pre-miRNAs (pre-miRs) (Lee, Ahn et al. 2003). A minority of intron encoded pri-miRs (mirtrons) are processed by the spliceosome independently of Drosha (Ruby, Jan et al. 2007). 2-nucleotide overhangs at the 3' end of pre-miRs facilitate binding to dimers of exportin 5 (Exp5) and Ras related nuclear protein (Ran) (Zeng and Cullen 2004). Exp5-Ran dimers transport bound pre-miRs through the nuclear pore complex to the cytoplasm, a process which requires GTP hydrolysis (Yi, Qin et al. 2003). Once in the cytoplasm, pre-miRs are bound by a dimer of HIV-1 transactivating response (TAR) RNA-binding protein (TRBP) and another cellular RNase III enzyme, Dicer; again dependent on 3', 2 nucleotide overhangs (Chendrimada, Gregory et al. 2005). Dicer cleaves the terminal loops of pre-miRs creating an RNA duplex. This duplex is transferred from Dicer to Argonaute 2 (Ago2) which becomes part of the RNA induced silencing complex (RISC) and the complementary RNA strand, termed the passenger

strand, is degraded, leaving the mature miRNA sequence bound to RISC (Maniataki and Mourelatos 2005).

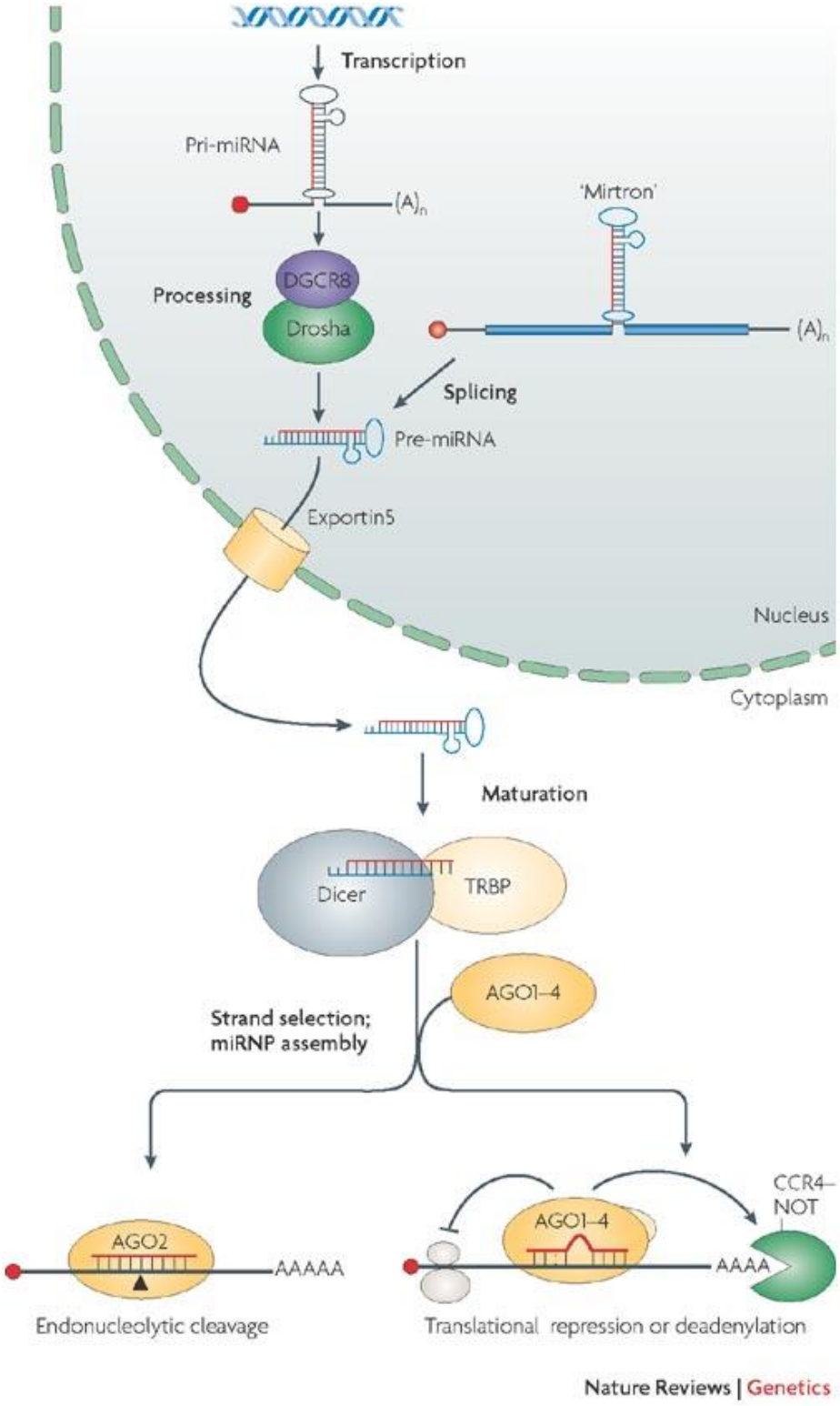

Figure 1.4: MiRNA Processing – Ago = Argonaute, TRBP = HIV-1 transactivating response (TAR) RNA-binding protein, DGCR8 = Pasha, CCR4-NOT = de-adenylation complex. Used, with permission, from (Filipowicz, Bhattacharyya et al. 2008)

1.4.3 MiRNA Regulation of Gene Expression

Assembled RISC complexes contain miRNA molecules which recruit RISC to messenger RNA (mRNA) molecules through perfect or partial complementary base pairing (Figure 1.4). Recruitment of RISC causes down-regulation of mRNA translation; as a general rule, increased complementarity between miRNA and mRNA causes increased translational inhibition. All eukaryotic mRNA transcripts contain methylated 5' guanine cap (5'm7Gppp N), one role of which is to promote translation through interactions with eukaryotic initiation factor 4E (eIF4E). eIF4E, in concert with other eIFs, recruits the 40S ribosomal subunit which leads to initiation of translation (Sonenberg and Hinnebusch 2009). The RISC has been shown to inhibit mRNA translation by repressing 5'cap-eIF4E mediated ribosomal recruitment (Mathonnet, Fabian et al. 2007). RISC also inhibits translation by causing ribosomes that successfully initiate translation to prematurely dissociate from their template mRNAs (Petersen, Bordeleau et al. 2006). As well as directly inhibiting the translation of target mRNAs, the RISC causes removal of their 5'cap and polyA tails which normally protect them from exonuclease degradation (Rehwinkel, Behm-Ansmant et al. 2005; Giraldez, Mishima et al. 2006). The mechanisms by which RISC mediates these processes, their timing and links to one another, are not fully understood, but many proteins have been identified which clearly play crucial roles (Fabian and Sonenberg 2012).

Perfect complementarity between the RISC loaded miRNA and target mRNA leads to direct target cleavage mediated by Ago2 although this does not seem to be a major mechanism of cellular post-transcriptional gene regulation (Hutvágner and Zamore 2002; Liu, Carmell et al. 2004).

1.4.4 Tissue Specific MiRNA Expression

It is estimated about 30% of genes in the human genome are subject to post transcriptional regulation by miRNAs. Tissues are able to carry out their specialised functions as a consequence of cellular expression of distinct sets of genes; however, each somatic cell contains an identical genomic template. Gene expression is regulated at multiple levels; accessibility of genomic regions are regulated by chromatin modifications, transcription is regulated by a plethora of promoters, and once expressed, proteins are regulated by a number of modifications affecting their activity or localisation. It is not surprising, following the discovery of translational regulation by miRNAs that, as with proteins, the expression of some miRNAs are restricted to specific tissues (Figure 1.5).

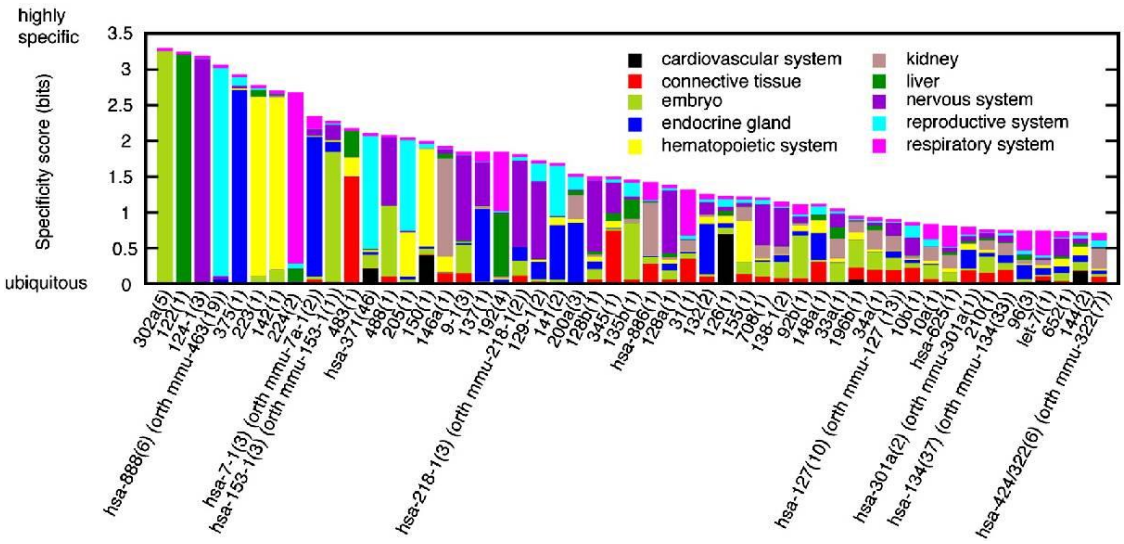

Figure 1.5: Tissue Specific miRNAs in Humans – The 51 most specific miRNA precursor clusters for human and mouse are depicted. The total height of each bar represents the tissue specificity. Each bar is split into coloured stacks depicting the miRNA expression in given tissue types (Landgraf, Rusu et al. 2007).

1.4.5 Interactions Between Viruses and MiRNAs

Given the importance of miRNA in regulating gene expression it is unsurprising that viruses interact with this component of cellular machinery. Several viruses, in fact, express miRNAs as a means of regulating the expression of cellular genes, many of which, as one would expect, are involved in antiviral and immune stimulatory signalling pathways.

The initial processing step of miRNA is cleavage of pri-miRs by Drosha, which resides in the nucleus. This restricts the advantageous use of miRNAs to viruses which have a replication step in the nucleus with a DNA stage; RNA viruses typically replicate in the cytoplasm so do not have access to Drosha, and if they did this cleavage step would result in destruction of genomic material. Also, if genes are down-regulated at the mRNA level, there is a lag time, dependent on the half-life of existing target protein. As most RNA viruses have rapid replication cycles, it is unlikely that changes which take such a time to come in to effect may be advantageous. In line with these observations, no RNA viruses have been identified to express miRNAs except for retroviruses which undergo genomic integration (miRBase 2012). It has, however, been shown that genetically engineered pri-miR sequences in both SV and influenza resulted in a detectable level of miRNA production, although achieved through different machinery than identified for normal processing. The produced miRs, as expected, caused RISC mediated cleavage of target genomic material (Shapiro, Varble et al. 2010).

Every herpesvirus analysed has been found to encode miRNAs, as do several polyomaviruses, perhaps highlighting the importance of miRNAs in conferring

resistance to apoptotic signalling and suppression of immune responses during latent infections.

Roles beyond latency are highlighted by SV40 and adenovirus encoded miRs; these two viruses are both lytic. MiR-S1, an SV40 encoded miR, is expressed in the late stage of virus replication. It is perfectly complementary to viral RNAs that are expressed in the early stage of infection and are no longer needed. Degradation of early viral RNAs results in decreased expression of viral T antigen, reducing susceptibility of virally infected cells to lysis by CTLs (Sullivan, Grundhoff et al. 2005).

Adenovirus non-coding virus associated (VA) RNAs I and II are produced in high numbers during early infection. Replication levels of adenovirus serotype 2 (Ad2) lacking regions encoding VAs I and II were 60 fold lower than wild type. The increased replication efficiency mediated by VA I and II is thought to be due to saturation of RISC which prevents normal cellular mRNA regulation of genes through miRs, as well as targeting mRNA of genes involved in cell proliferation and DNA repair for RISC induced cleavage. However, the major contributing factor seems to be binding of PKR which prevent its activation and subsequent phosphorylation of cellular targets that mediate antiviral signalling and inhibition of cellular translation (Carnero, Sutherland et al. 2011). Thus it is clear that virus encoded miRs can be advantageous in settings other than latency, it is expected that in the coming years, many more virally encoded miRs with novel functions will be discovered.

It is of note that all viruses tested so far are sensitive to inhibition through RNAi, this suggests that there is a strong evolutionary pressure for viruses to avoid

complementarity to existing cellular miRs. It has been postulated that this plays a key role in determining the tissue tropism of viruses (Kelly and Russell 2009).

Invertebrate cells, which lack 2'-5' oligoadenylate synthase, PKR and IFN, depend on RNA interference (RNAi) to suppress intracellular virus replication. Long dsRNA, associated with virus replication is cleaved by a protein called dicer-2 (Dcr2) into fragments 21-25 base pairs in length. These are unwound and loaded onto RISC, which as a result, cleaves RNA species from which RNA fragments are produced. It has been shown that SV replication in mosquito cells is repressed by this mechanism (Campbell, Keene et al. 2008). Whether this mechanism is relevant in vertebrate cells is a matter of controversy, although processing of dsRNA structures and loading onto the RISC can occur, whether this contributes to an antiviral mechanism is unclear (Shapiro, Varble et al. 2010; Jeang 2012).

In contrast to all our knowledge of miR function, the hepatitis C virus (HCV) genomic RNA possesses 2 complementary sequences to miR122 near its 5' end, and binding of miR122 actually promotes translation initiation and physically stabilises the HCV genome (Shimakami, Yamane et al. 2012). The mechanism of translation enhancement is not well understood, but increased genomic stability is thought to occur by RISC stearically inhibiting 5' exonuclease digestion. It is conceivable that HCV RNA-miR122 interactions prevent cleavage by the RISC and render it permanently attached to HCV RNA preventing its degradation. It seems that dependence on miR122 expression is a major factor restricting HCV to the liver. This is the only known scenario in which miR targeting leads to enhancement rather than inhibition of RNA translation and stability. Whether this is a unique phenomenon or something which occurs more widely remains to be seen.

1.4.5 MicroRNA Control of Viral Vectors

Exploiting our knowledge of tissue miR expression profiles and miR mediated mRNA translational repression and degradation, it is possible to repress virus replication and transgene expression in a manner specific to tissue types. This was first shown to be efficacious in allowing increased gene transfer of a lentiviral vector in mice. Lentiviral transgene expression in antigen presenting cells (APCs) normally leads to induction of an anti-transgene immune response. MiR142-3p is a miR specifically expressed haematopoietic cells. Addition of miR response elements (MREs), sequences perfectly complementary to a miR of choice, specific for miR-142-3p into the 3'UTR of a lentivirus expressing GFP, led to decreased transgene expression in haematopoietic cells, including APCs, without decreasing expression in non-haematopoietic cells (Brown, Venneri et al. 2006).

An adenovirus vector expressing HSV thymidine kinase (HSV-TK) causes non-toxic ganciclovir to be phosphorylated to a highly toxic substance only in vector transduced cells expressing HSV-TK. In murine models the tumour selectivity of this vector allows killing of tumour and surrounding tissues by toxic phosphorylated ganciclovir, but transduction of hepatic cells causes off target toxicity. Engineering MREs to liver specific miR122 into this adenovirus vector led to a huge reduction in liver toxicity without affecting tumour HSV-TK expression, effectively increasing the limiting dose and therefore therapeutic efficacy of this vector (Suzuki, Sakurai et al. 2008).

1.4.6 MicroRNA Control of Replicating Viruses

MiRNA regulation through the introduction of MREs has proved successful for vaccination strategies where virus replication is attenuated without affecting immunogenicity. Poliovirus (PV) which causes poliomyelitis upon infection of neurons was genetically modified by the introduction of MREs to either the neuronal specific miR124a, or the ubiquitously expressed miR-Let7a, in the 5'UTR and between capsid and P2 encoding regions. Infection of mice with both viruses with an otherwise lethal dose was safe and induced potent immune responses (Barnes, Kunitomi et al. 2008). It is of note that the PV targeted by Let7a (PVL7) which is attenuated in all cells, led to a less potent immune response than PV124 which is only attenuated in neuronal cells, this has been attributed to an increase in danger signals associated with increased replication in other tissues, even though replication in these tissues gives no adverse symptoms. A similar strategy has also been applied to influenza A where MREs complementary to miR-93, which is expressed in human and mouse lungs, but not chickens, allowed growth of the virus to high titre in chicken eggs but led to attenuation in mice when administered as a vaccine (Perez, Pham et al. 2009).

1.4.7 MicroRNA Controlled Oncolytic Viruses

The evidence presented thus far indicates MREs could be used to attenuate the replication of oncolytic viruses in tissue sites that contribute to pathological symptoms without affecting anti-tumour potency. Since the undertaking of this project this has indeed been achieved for oncolytic VSV, adenovirus, coxsackievirus and HSV.

Neurotoxicity of VSV was substantially reduced through addition of 4 MREs to miR125, which is highly up-regulated in glial, astrocyte and neuronal cells of the brain, into the 3'UTR. Furthermore anti-tumour efficacy in BALB/c mice following SC inoculation with CT26 colon carcinoma cells was not reduced compared to WT VSV (Kelly, Nace et al. 2010).

Ad5 with 4 miR122 MREs in the E1A mRNA reduced liver toxicity in mice without loss of anticancer efficacy compared to wild type (WT) Ad5 in nude mice bearing SC HepG2 tumours (Cawood, Wong et al. 2011). Also, experiments with an Ad5 with E1A under the control of the promoter of chromogranin-A (CgA), a neuroendocrine tumour marker, and 6 miR122 sites showed that a combination of transcriptional and post transcriptional targeting could completely ablate replication in Huh-7 cells *in vitro* (Leja, Nilsson et al. 2010).

A strain of coxsackievirus, CVA 21, which normally causes lethal myositis in mice, was attenuated in muscle cells by the addition of 2 mir133 and 2 miR206 MREs to the 3'UTR. Notably, in this study it was shown *in vitro* that this combination of 2 miR133 + 2 miR206 was better than 4 of either in achieving attenuation in TE671 human rhabdosarcoma and L6 murine myoblast cell lines. Treatment of SCID mice bearing SC SQmel624 melanomas with wild type CVA 21 led to tumour shrinkage but concomitant hind limb paralysis and subsequent death. In contrast, mice treated with miRNA targeted (miR-T) CVA21 survived with complete tumour regression (Kelly, Hadac et al. 2008). In this study it is of note that mutations in MREs occurred in some cases leading to pathological symptoms.

Based on the observation that miR143 and miR145 are ubiquitously highly expressed except in prostate tissue, 5 MREs to these miRNAs were engineered into the 3'UTR of the HSV-1 ICP4 gene mRNA, in order to confer prostate selectivity for the treatment of prostate cancer. Both miR143-T and miR145-T HSV-1 showed decreased virulence in normal tissues compared to non-miR-T HSV-1 and demonstrated anti-tumour efficacy in nude mice bearing SC LNCaP, human prostate adenocarcinoma cell tumours (Lee, Rennie et al. 2009).

1.5 Thesis Objectives

1.5.1 Hypothesis

Insufficient dose of OV reaching tumours when delivered systemically has been identified as a significant barrier to the successful treatment of cancer by virotherapy.

We hypothesise that:

- The stability of Sindbis Virus in human blood may be superior to existing OVs.

Although wild type SV has many characteristics that make it a potentially effective oncolytic agent, it also causes pathological symptoms in humans. Although symptoms are mild in most patients, they can be moderate, and can last for years (Laine, Luukainen et al. 2000). Attenuation of SV infection in non-target tissues could alleviate potential side effects thereby improving its clinical safety profile.

We therefore hypothesise that:

- The introduction of MREs into the SV genome that are complementary to miRs located specifically in non-target tissues in which SV replication causes adverse clinical symptoms, may provide a means of increasing virus safety, without affecting its oncolytic potency in target cancer cells.

The central aim of this project is, therefore, to produce a blood stable SV, suitable for the treatment of tumours in an immune competent *in vivo* model and to attenuate SV in specific tissues which may contribute to pathological symptoms in humans, without diminishing oncolytic potency.

2 Materials and Methods

2.1 Production of Heat Shock Competent E.Coli Cells

Heat Shock DNA competent E. coli cells were produced from Xl-10 Gold Ultracompetent or JM110 stocks (Agilent technologies, UK) by inoculating 5 mL 2xYT broth media (16 g/L Bacto Tryptone, 10g/L Yeast Extract, 5g/L NaCl, pH 7.0 (pH adjusted with 5M NaOH)) with a single colony of E. coli cells and shaking at 37°C for 4 hours. This 5 mL 2xYT broth media was then transferred to a further 200 mL fresh pre-warmed 2xYT broth media and placed at 37°C in a shaking incubator until the optical density at 550 nm (OD550) reached 0.480. Cells were then pelleted at 3000 rpm in a swing out centrifuge at 4°C for 10 minutes. Cells were re-suspended in a total of 80 mL cold TFB1 (30 mM KC2H3O2, 100 mM RbCl, 10 mM CaCl2·2H2O, 50 mM MnCl2·4H2O, 15% v/v glycerol, adjusted to pH 5.8 using 0.2 M CH3COOH, filter sterile). Cells were spun as above and re-suspended in 8mL of TFB2 (10 mM MOPS, 10 mM RbCl, 75 mM CaCl2·2H2O, 15% v/v glycerol, adjusted to pH 6.6 using 5 M KOH, filter sterile). 100 µl aliquots of cells were pipetted into pre-chilled 1.5 mL microfuge tubes and frozen on dry ice. Tubes were then transferred to -80 C for long term storage.

2.2 Bacterial Transformation

Plasmids were amplified by utilising the Xl-10 Gold Ultracompetent strain of *E.Coli* (Agilent Technologies, UK), which were prepared for efficient delivery of large DNA plasmids by heat shock. Where unmethylated DNA was required for downstream restriction digests the Dam and Dcm DNA methylase deficient *E.Coli* strain JM110 (Agilent Technologies, UK) was used; *E.Coli* cells were stored in single use aliquots at -80°C.

DNA transformations were performed by thawing aliquots on ice and incubating on ice for 20 minutes with 5-100 ng of DNA followed by a three minute heat shock at 37°C. 900 µL of lysogeny broth (LB) medium (Sigma, UK) was then added followed by a further 15 minute incubation at 37°C before adding to LB agar (35 g/L, Sigma, UK) plates impregnated with the appropriate selection antibiotic (Ampicillin or Kanamycin, 50 µg/mL, Sigma, UK). Plates were incubated overnight at 37°C and successfully transformed clones were picked by colony isolation. Transformed clones were amplified by incubating overnight at 37°C in LB medium (20 g/L, 5 mL miniprep, 250 mL maxiprep) containing 50 µg/mL of the appropriate selection antibiotic in a shaking incubator (SANYO Electric Biomedical Co. Ltd, USA) set to 220 rpm (revolutions per minute).

Plasmid DNA was purified from bacterial cultures using the QIAprep Spin Miniprep kit (QIAgen, UK) or the Pure Yield Plasmid Maxiprep System (Promega, UK). Plasmid clones were selected by restriction digest screening and DNA sequencing (Source Bioscience, UK).

2.3 DNA Restriction Digests

Restriction endonuclease enzymes were used to create DNA fragments with sticky ends for subsequent ligation to produce desired genetic constructs or for screening for the success of ligations performed. All restriction digests were performed under conditions recommended by the manufacturer (New England Biolabs, UK). In order to determine the size of DNA fragments produced by digestion, agarose gel electrophoresis was performed alongside a DNA ladder (Hyperladder I, Bioline, UK).

2.4 DNA Ligation

Donor (insert) and recipient (vector) DNA were digested with restriction enzyme(s) resulting in the production of DNA overhangs (sticky ends) compatible for complementary base pairing. Digested insert DNA was purified using the QIAquick PCR Purification Kit (Qiagen, UK), or where necessary, DNA electrophoresis was performed and DNA bands were visualised using a Dark Reader Transilluminator (Clare Chemical Research, USA). Bands of desired size were excised and DNA was purified using the QIAquick Gel Extraction Kit (Qiagen, UK). Digested vector DNA was dephosphorylated with 2 µl calf intestinal alkaline phosphatase (CIAP, Invitrogen, UK) for 1 hour at 37°C to prevent vector re-ligation then purified using the QIAquick PCR Purification Kit (Qiagen, UK). All purified DNA was eluted in nuclease-free water (Applied Biosystems, UK). Ligation reactions were prepared using T4 DNA Ligase (New England Biolabs, UK) according to the manufacturer's protocol.

2.5 Agarose Gel Electrophoresis

Separation of DNA fragments based on size was performed using 1% (w/v) agarose (Sigma, UK) gels containing 0.5 µg/mL ethidium bromide in TAE running buffer (20mM Tris, 10mM acetic acid, 0.5mM EDTA, pH 8.4). RNA gels did not contain ethidium bromide but 1 µg was added directly to RNA samples before loading into wells. Gels were run in horizontal DNA electrophoresis gel boxes (BioRad Laboratories,

UK) at 10 Volts/cm for 40 minutes and DNA bands were visualised by UV transillumination (Alpha Imager, Alpha Innotech, USA).

2.6 Quantitation of purified DNA and RNA

DNA was quantified using a Nanodrop spectrophotometer (Thermo Scientific, UK). Prior to analysis, equipment was blanked using the medium in which the DNA or RNA had been eluted, (nuclease free water except for RNA produced from *in vitro* transcriptions which used Megaclear elution buffer, (Applied Biosystems, UK)). Samples were tested in triplicate and data was interpreted using the ND-1000v 3.1.0 software according to the manufacturer's instructions. The final quantity of DNA was expressed as nanograms/microliter (ng/μl).

2.7 Polymerase Chain Reaction

Primers for polymerase chain reactions (PCR) were designed according to the requirements of the genetic manipulation, sequencing or screening procedures. Primers less than 51 base pairs (bp) in length were purchased from Sigma, UK and those over 51 bp were purchased from Invitrogen, UK). Primers were re-suspended in nuclease free water to generate 100 μM stocks, aliquoted and stored at -20°C,

For production of DNA fragments for sub-cloning, Phusion High-Fidelity PCR Kit (New England Biolabs) was used and where PCR products were used for screening

purposes Platinum Taq DNA Polymerase (Invitrogen, UK) was used. Reactions were carried out according to manufacturer's recommendations and where necessary primer concentration and primer annealing temperature gradients were used to identify optimal reaction conditions. PCR reactions were performed using a Tetrad PTC-225 Thermo Cycler (MJ Research, USA).

2.8 *In Vitro* Transcription

DNA templates were linearised by restriction digestion with Xho I (New England Biolabs, UK) and cleaned up using the QIAquick PCR Purification Kit (Qiagen, UK). Concentrations of purified linearised DNA were determined using a Nanodrop. 1 µg of linearised DNA was used as template for *in vitro* transcription using the mMessage mMachine SP6 Kit (Applied Biosystems, UK). All transcription reactions were carried out according to the manufacturer's recommendations; briefly, reactions were set up as standard with the addition of 3 µl GTP (20mM, (supplied)) per reaction and a total incubation time of 2 hours (h) in view of the substantial length of SV genomic RNAs produced (>10Kb). Following transcription, reactions were treated with Turbo DNase (provided) for 15 minutes at 37°C to degrade DNA template, RNA was then purified using MEGAclear (Applied Biosystems, UK). The concentration of purified *in vitro* transcribed RNA was determined using a Nanodrop and all RNA samples were stored at -80°C.

2.9 Transfection of Sindbis Virus Genomic RNA

BHK cells to be transfected with SV genomic RNA were plated in 6 well plates 24 hours before transfection at a density of 250 000 cells/well so that wells were ~80% confluent at the time of transfection. DOTAP transfection complexes were prepared according to the manufacturers recommendations; briefly, 5 μg of SV genomic RNA was diluted to 0.1 μg/μl in a total volume of 50 μl HEPES ((4-(2-hydroxyethyl)-1-piperazineethanesulfonic acid) buffered saline (HBS, Sigma, UK) and mixed with DOTAP liposomal transfection reagent (3:10 v/v, Roche Applied Science, Germany) in 100 μl HBS. RNA-DOTAP complexes were allowed to form by incubating at 25 °C for 15 minutes before adding formed complexes directly to the supernatant of BHK cells. After 4 hours BHK cells were washed 3 times with warm PBS and media was replaced with fresh DMEM. 24 hours after transfection, supernatant was collected to harvest virus.

2.10 Transfection of Pre-miR MicroRNA Precursors

In order to express desired micro-RNAs (miRNAs) in non-endogenous cell lines, Pre-miR, miRNA precursor molecules, were used (Applied Biosystems, UK). Upon transfection these precursors are processed to yield mature miRNAs bound to the RISC. Transfection of pre-miRNAs was carried out using Lipofectamine RNAiMAX (Invitrogen, UK) according to the manufacturer's reverse transfection protocol. 96 well plates were seeded at a density of 10^4 cells per well 24 hours before infection with miRNA controlled SVs.

2.11 Virus Luciferase *In Vitro* Assay

Cells were plated 24 hours before infection in 96 well plates at a density of 10^4 cells/well and SVLuc infections were carried out by adding virus diluted in serum free DMEM to cell monolayers and incubating at 37°C for 30 minutes. Cell monolayers were then washed 3 times with pre-warmed PBS and fresh, pre-warmed cell culture medium was added. Cells were incubated for 16 hours at 37°C before cell culture medium was removed and 1 x lysis buffer was added (Promega, UK). Cells were freeze/thawed to achieve complete lysis then luciferase activity was assayed with the Luciferase Assay System (25µl cell lysate: 25µl luciferin, 10 second measurement, Promega, UK) using a Lumat LB 9507 tube luminometer (Berthold Technologies UK Ltd). Protein levels were also assayed in order to determine the activity of luciferase/µg protein in each well.

2.12 Protein Assay

The protein content of cell lysates was determined by BCA (bicinchoninic acid) assay using the Quantipro BCA Assay Kit (Sigma, UK). This assay relies on the formation of protein-Cu^{2+} complexes followed by reduction of Cu^{2+} to Cu^{+}; the amount of reduction is proportional to the amount of protein present. Reduction of Cu^{2+} to Cu^{+} by protein occurs through peptide bonds as well as cysteine (including cysteine dimers), tryptophan and tyrosine side chains. BCA forms a blue-purple complex with Cu^{+} under alkaline conditions providing a means to measure the extent of Cu^{2+} reduction by proteins.

Protein assays were carried out by adding 50 µl reaction mixture (produced according to the manufacturer's protocol) to 50 µl of cell lysate as well as 50µl samples of a BSA standard curve ranging in concentration from 0.5-30 mg/well. Colour was developed for 2 hours at 37 °C or 16 hours at 25 °C. Absorbance at 595 nm was measured using a Wallac 1420 Victor^2 multi-label counter (PerkinElmer Life and Analytical Sciences, UK) and standard curve absorbance was correlated with that of cell lysate in order to determine protein content.

2.13 Flow Cytometry

Cells were washed 3 times with pre-warmed PBS before treating with trypsin-EDTA solution (Sigma, UK). Trypsin was neutralised by addition of DMEM containing 10% FCS, cells were pelleted by centrifugation at 500 X g for 5 minutes and re-suspended in 300 µl in PBS containing 4% paraformaldehyde. Flow cytometry was carried out using a FACSCalibur flow cytometer (BD Biosciences, USA) and analysed using CellQuest Pro software (BD Biosciences, USA).

2.14 MTS Assay

Cell viability was measured using the CellTiter 96 Aqueous One Solution Cell Proliferation Assay (Promega, UK). This assay contains a tetrazolium compound [3-(4,5-dimethylthiazol-2-yl)-5-(3-carboxymethoxyphenyl)-2-(4-sulfophenyl)-2H-tetrazolium, inner salt; MTS] and an electron coupling reagent (phenazine ethosulfate; PES). In metabolically active cells the MTS tetrazolium compound is reduced,

presumably by NADH, yielding a coloured formazan product which is soluble in tissue culture medium. The quantity of this product correlates with metabolic activity of cells and can be measured by absorbance at 490 nm.

Cells were seeded in 96 well plates and treated as per experimental design. To measure cell viability, cell culture media was removed and replaced with 120 μl/well of DMEM containing MTS reagent (5:1). Cells were incubated for 30 minutes at 37 °C then absorbance at 490 nm was measured using a Wallac 1420 Victor^2 multi-label counter (PerkinElmer Life and Analytical Sciences, UK).

2.15 Reverse-Transcription Polymerase Chain Reaction

SV preparations were sequenced by first extracting RNA from cell culture supernatant using the QIAamp Viral RNA Mini Kit (Qiagen, UK) then creating cDNA by reverse transcription with the SuperScript III First Strand Synthesis System for RTPCR (Invitrogen, UK) primed with random hexamers. PCR was then performed using the Platinum Taq DNA Polymerase kit (Invitrogen, UK) and custom made primers (Sigma, UK) for regions of interest on a Tetrad PTC-225 Thermo Cycler (MJ Research, USA). PCR products were cleaned up using the QIAquick PCR Purification Kit (Qiagen, UK), analysed by agarose gel electrophoresis and sequenced (Source Bioscience, UK).

2.16 Reverse Transcription Quantitative Polymerase Chain Reaction

Where quantitative real time reverse transcription polymerase chain reaction (RTQPCR) was carried out to quantify the amount of virus RNA in cell culture supernatant, blood or tissue homogenates, total RNA was isolated using the QIAamp Viral RNA Mini Kit (Qiagen, UK, supernatant and blood samples) or the RNAqueous Kit (Applied Biosystems, UK, tissue homogenates). Standard curves were prepared by making serial dilutions of known amounts of viral RNA produced by *in vitro* transcription measured using a Nanodrop.

A standard curve was produced for each experiment, for detection of RNA in cell culture supernatant, standard curve RNA was produced by serial dilution of known amounts of RNA in nuclease free water. Example standard curves for the detection of nsp1 and luciferase are shown in Figure 2.1 which relates to Figure 3.11, as well as standard curves for the detection of nsp1 and eGFP (Figure 2.2) which relates to Figure 3.16.

Where RNA was extracted from organ samples, homogenates of each tissue were spiked with known amounts of SV genomic RNA and extracted using the same method as samples to be analysed in order to take into account the efficiency of RNA extraction in each tissue. The limit of detection in these experiments was determined as the point after which the relationship between threshold cycle number (C_T) value and the amount of spiked RNA was no longer linear. Standard curve points outside the linear range were excluded in analysis and any samples below the lowest standard curve point in the linear range were recorded as undetected.

RTQPCR reactions were carried out using the TaqMan RNA-to-CT 1-Step Kit according to the manufacturer's protocol (Applied Biosystems, UK). Custom primers and probes for RTQPCR were synthesised by Sigma, UK. Primer pairs and corresponding probes for detection of SV nsp1, eGFP and luciferase are shown in Table 2.2.

For the analysis of micro-RNA levels of cell lines or tissue homogenates by RTQPCR, TaqMan microRNA Assays (Applied Biosystems, UK) were used. RNA was extracted using the mirVana miRNA Isolation Kit (Applied Biosystems, UK). RNA extracts were reverse transcribed using the TaqMan MicroRNA Reverse Transcription Kit, (Applied Biosystems, UK) specific primers for miRNAs of interest (supplied) and a Tetrad PTC-225 Thermo Cycler (MJ Research, USA). Synthesised cDNA was used in subsequent quantative real time PCR reactions. Relative amounts of miRNAs were determined by comparative C_T experiments according to the manufacturer's recommendation's using either 293 or BHK cellular RNA as a reference sample and ubiquitously expressed Let-7a miRNA as an endogenous control.

All RTQPCR reactions were carried out on an Applied Biosystems StepOne Real-Time PCR system and results were analysed using StepOne Software v2.1 (Applied Biosystems, UK).

Target Gene	Oligonucleotide	Sequence	Amplicon Length (bp)
Nsp1	Forward Primer	5'-TCGTTCCCTGTGTGCACGTA-3'	67
	Reverse Primer	5'-CCGTGGCCATTATACCAGTCA-3'	
	Probe	[JOE]5'-ATC CCG GCC ACC ATA TGC GAT CA-3'[BHQ1]	
eGFP	Forward Primer	5'-TCCGCCCTGAGCAAAGAC-3'	61
	Reverse Primer	5'-GAACTCCAGCAGGACCATGTG-3'	
	Probe	[FAM]5'-CCAACGAGAAGCGCGA-3'[TAMRA]	
Luciferase	Forward Primer	5'-TGCACATATCGAGGTGGACATC-3'	57
	Reverse Primer	5'-TGCCAACCGAACGGACAT-3'	
	Probe	[FAM]5'-CTTACGCTGAGTACTTCGA-3'[TAMRA]	

Table 2.2: RTQPCR Primer and Probe Sequences – Fluorophores and quenchers of probes at 5' and 3' ends are shown, as well as the amplicon lengths produced by each primer pair.

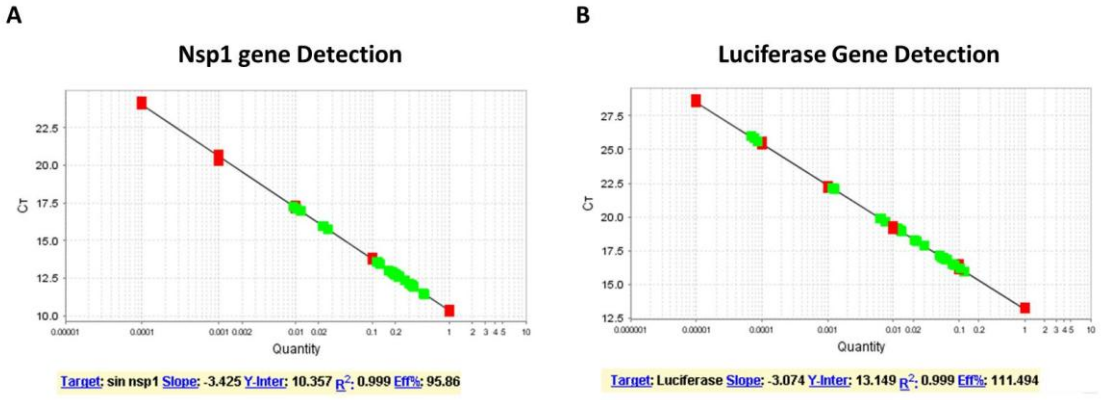

Figure 2.1: RTQPCR Standard Curves for Detection of SV *In Vitro* – A) Nsp1 and **B)** Luciferase were detected in virus containing cell culture supernatant. RNA was extracted and 2 µl samples of RNA extracts were analysed by RTQPCR alongside serial dilutions of *in vitro* transcribed RNA in order to quantify the amount of RNA present. Red = standard curve RNA CT, green = sample RNA CT.

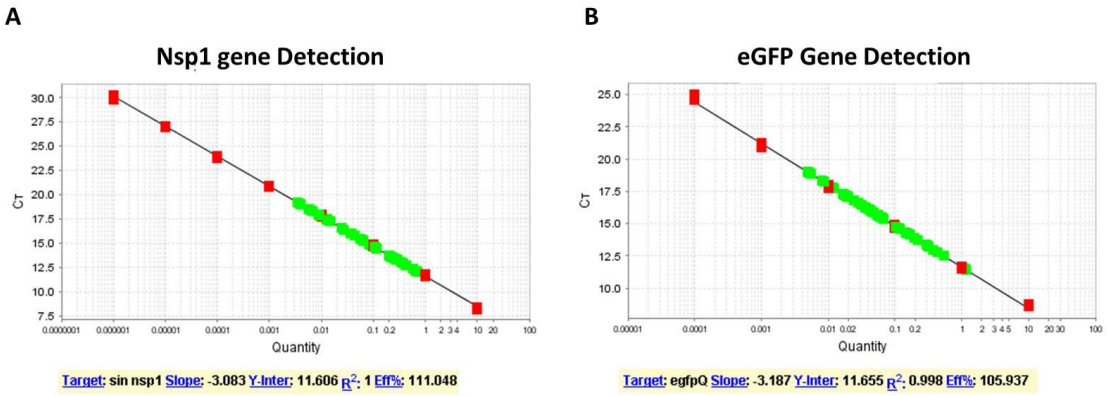

Figure 2.2: RTQPCR Standard Curves for nsp1 and eGFP - Virus containing cell culture supernatant was RNA extracted and 2 µl samples of RNA extracts were analysed by RTQPCR alongside serial dilutions of *in vitro* transcribed RNA in order to quantify the amount of RNA present. Red = standard curve RNA CT, green = sample RNA CT.

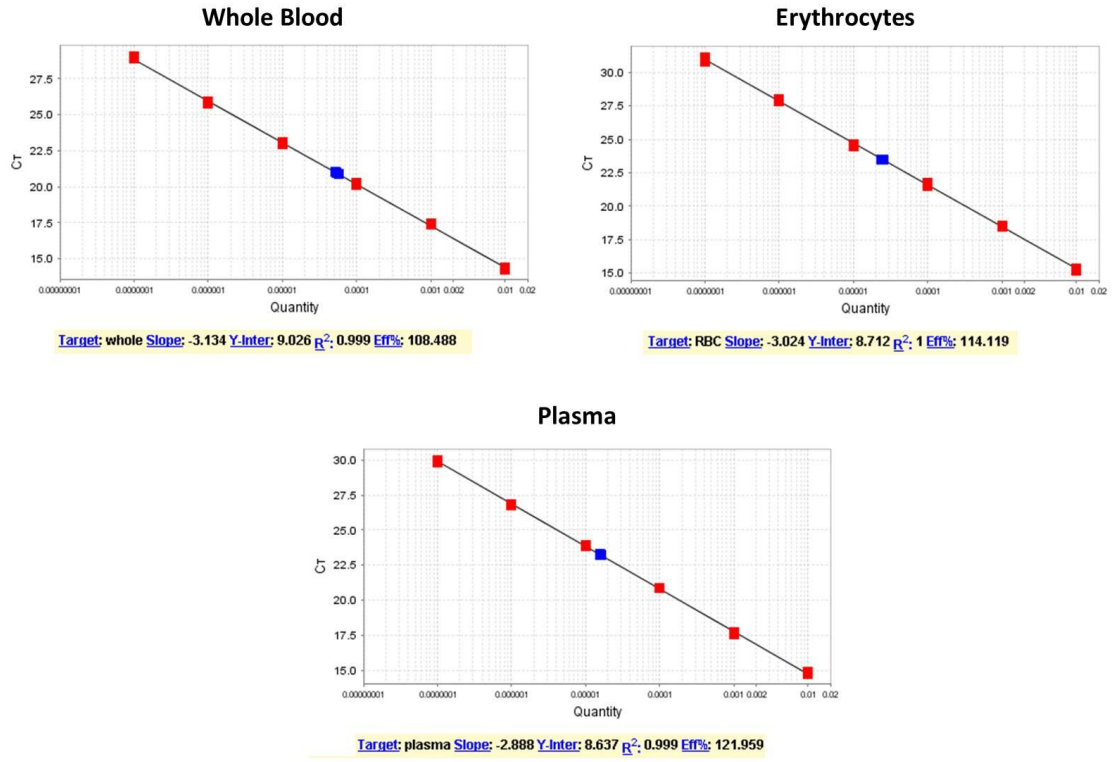

Figure 2.3: RTQPCR Standard Curves for Nsp1 Detection in Human Blood Fractions – Whole blood was incubated with SVLuc DSG then 15 µl volumes of whole blood, erythrocytes or plasma were RNA extracted and analysed by RTQPCR. Standard Curves were constructed from serial dilutions of whole blood plasma or serum spiked with 10ng/µl *in vitro* transcribed SVLuc DSG RNA. . Red = standard curve RNA, blue = sample triplicates with high SD.

Liver

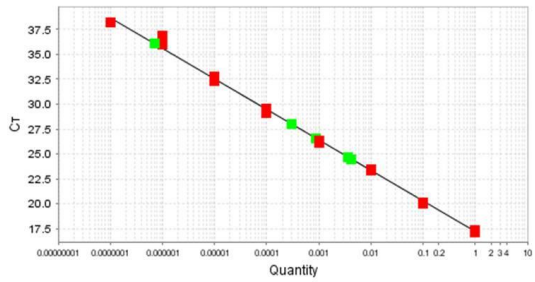

Target: Liver Slope: -2.764 Y-Inter: 15.247 R^2: 0.998 Eff%: 130.042

Brain

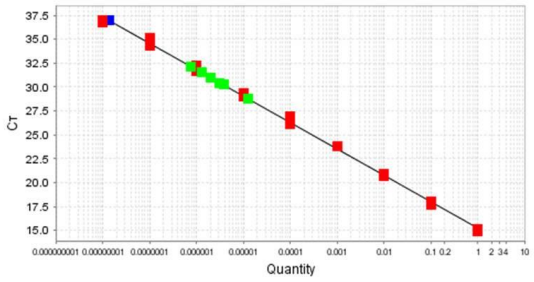

Target: Brain Slope: -3.069 Y-Inter: 17.19 R^2: 0.993 Eff%: 111.747

Tumour

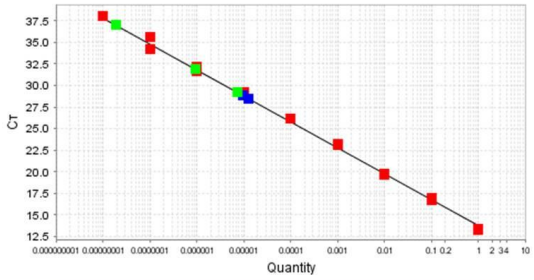

Target: tumour Slope: -3 Y-Inter: 11.054 R^2: 0.998 Eff%: 115.449

Kidney

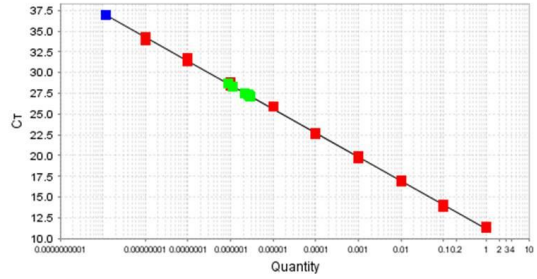

Target: Kidney Slope: -2.912 Y-Inter: 9.293 R^2: 1 Eff%: 120.487

Spleen

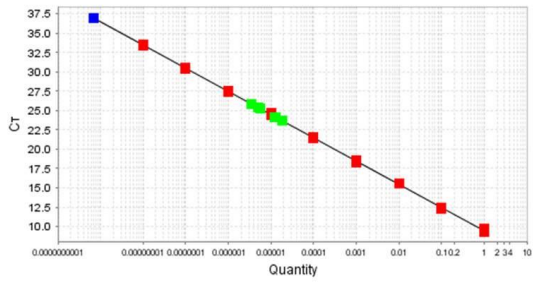

Target: sin nsp1 Slope: -3 Y-Inter: 9.456 R^2: 1 Eff%: 115.438

Lung

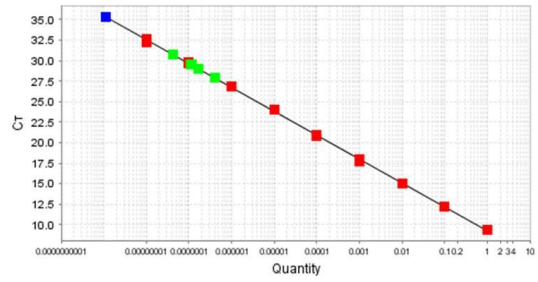

Target: Lung Slope: -2.889 Y-Inter: 11.196 R^2: 0.999 Eff%: 121.861

Muscle

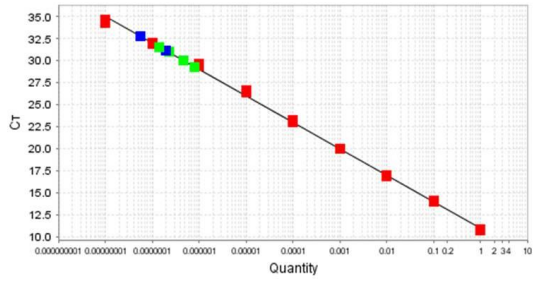

Target: sin nsp1 Slope: -3.003 Y-Inter: 13.814 R^2: 0.997 Eff%: 115.262

Figure 2.4 Standard Curve for Detection of VD SV and ID SV *In Vivo* – Organs harvested 60 mins PI IV delivery of SVLuc DSG were homogenised in 10 µl lysis buffer /mg tissue and 300 µl homogenate was RNA extracted. Standard curve was created by spiking homogenates of control mouse organs with known amounts of genomic SV RNA and performing RNA extraction. Red = standard curve RNA, green = sample RNA, blue = sample triplicates with high SD. Standard curve points in the non-linear range were excluded and any samples appearing below the linear standard curve range was recorded as undetected.

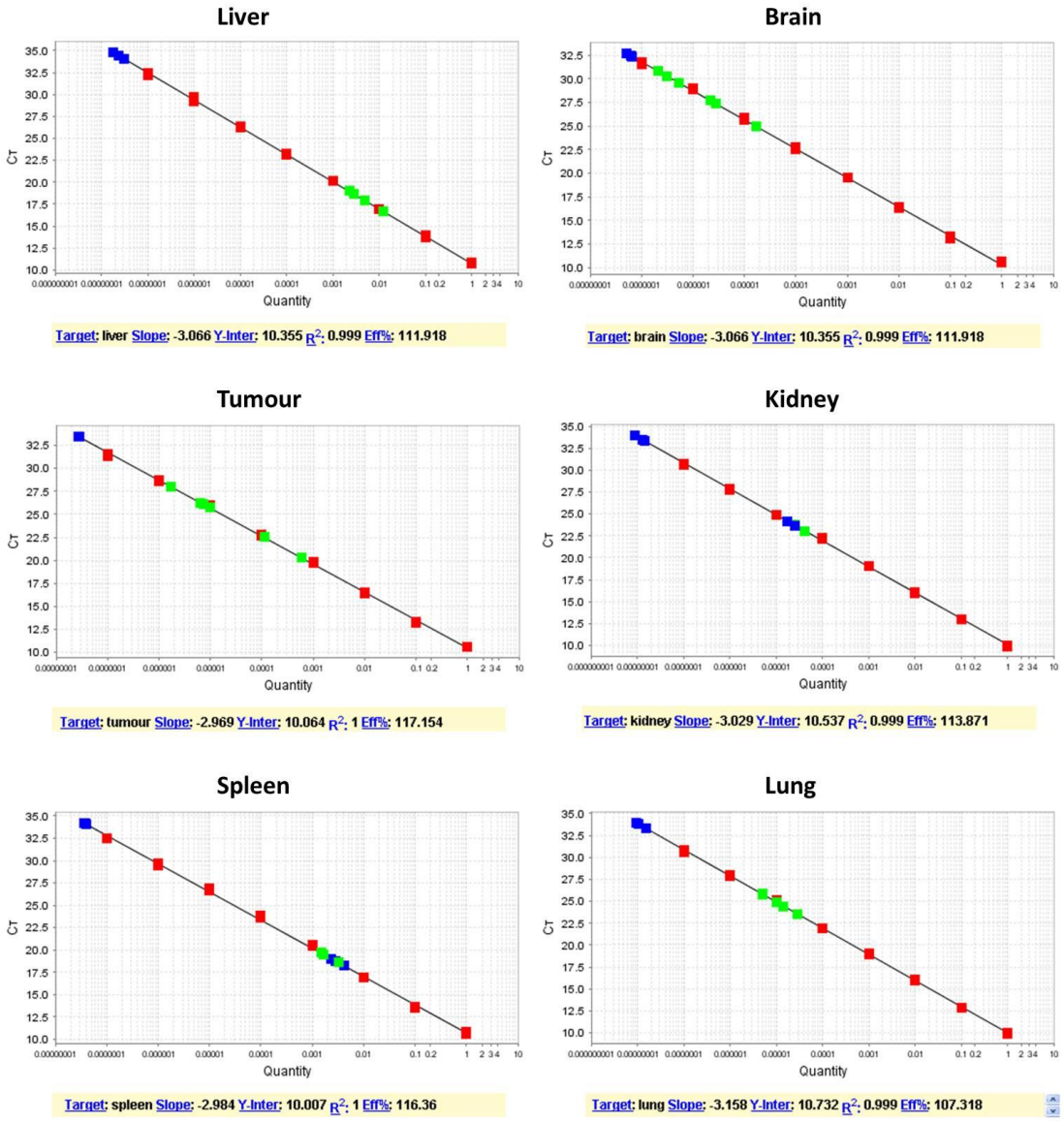

Figure 2.5 Standard Curves for Detection of SV *In Vivo* after Clodronate Liposome Treatment – Organs harvested 60 mins PI IV delivery of SVLuc DSG were homogenised in 10 µl lysis buffer /mg tissue and 300 µl homogenate was RNA extracted. Standard curve was created by spiking homogenates of control mouse organs with known amounts of genomic SV RNA and performing RNA extraction. Red = standard curve RNA, green = sample RNA, blue = sample triplicates with high SD. Standard curve points in the non-linear range were excluded and any samples appearing below the linear standard curve range was recorded as undetected.

2.17 Cell Culture

All cells were cultured with 10% foetal calf serum (FCS; PAA Laboratories, UK), and 1% penicillin (104 units/mL)-streptomycin (10 mg/mL) (pen/strep) solution (Sigma, UK) in a humidified, 5% CO_2 environment at 37 ºC except the C6/36 cell line which was kept at 27 °C. Cells were split by washing with PBS and incubating with Trypsin/EDTA at 37 °C for 5 minutes. After cells were detached, culture medium containing 10% FCS was added to neutralise trypsin, and cells were seeded in new flasks with fresh tissue culture medium. C6/36 cells were split by physically detaching cells with a cell scraper. Details of cell lines and specific growth media used are shown in Table 2.1.

Cell Line	Description	Origin	Culture Medium
A549	Human Caucasian lung carcinoma	ECACC	DMEM
BHK-21	Baby Hamster Kidney Fibroblasts	ATCC	DMEM
B16-F10	Mouse melanoma	ATCC	DMEM
C2C12	Mouse myoblasts	*	DMEM
C6/36	Aedes albopictus larvae	**	EMEM
HCT116	Human colon carcinoma	***	McCoys 5A
HEK 293A	Adherent human embryonic kidney	ECACC	DMEM
Huh7	Human Asiatic hepatocellular carcinoma	ECACC	DMEM
IGROV-1	Human Caucasian ovarian adenocarcinoma	ECACC	DMEM
MCF-7	Human Caucasian breast adenocarcinoma	ECACC	DMEM
OVCAR-3	Human Caucasian ovarian carcinoma	ATCC	RPMI
PC3	Human Caucasian prostate adenocarcinoma	ATCC	DMEM
SHSY-5Y	Human neuroblastoma	****	F12: DMEM (1:1)
SK-OV-3	Human Caucasian ovarian adenocarcinoma	ATCC	DMEM
U-87-MG	Human Caucasian glioblastoma astrocytoma	ECACC	EMEM
U-937	Human Caucasian histiocytic lymphoma	ECACC	RPMI
ZR-75-1	Human Caucasian breast carcinoma	ECACC	RPMI

Table 2.2: Details of Cell Lines and Culture Media – ECCAC = European Collection of Cell Cultures, ATCC = American Type Culture Collection, DMEM = Dulbecco's Modified Eagle Medium, RPMI = Roswell Park Memorial Institute, EMEM = Eagle's Minimum Essential Medium, McCoy's medium 5A and Ham's F12: DMEM (1:1) were supplemented with 2mM Glutamine, * Kindly provided by Professor Matthew Wood, University of Oxford, ** Kindly provided by Professor Nicole Zitzmann, University of Oxford, *** Kindly provided by Professor Patrick Johnston, Queens University, Belfast, **** Kindly provided by Dr Richard Wade-Martins.

2.18 Differentiation of Myoblasts

The C2C12 mouse myoblast cell line was established from muscle tissue from a normal adult C3H mouse following a crush injury. Upon differentiation these cells form myotubes *in vitro*. Differentiation was performed by seeding cells at 40-60% confluence and culturing for 5 days in DMEM containing either 2% horse serum (HoS) or 2% FCS. The extent of differentiation was analysed by observing myotube formation by bright field microscopy.

2.19 Microscopy of Live Cells

Phase-contrast and fluorescent images of live cells were captured using a Nikon Eclipse 80i microscope with a Nikon DS-5M camera. Green and red fluorescence were visualised by illuminating samples with UV radiation from a mercury short arc bulb (OSRAM, Germany) and using B-2A and G-2A excitation filters (Nikon, UK) respectively. Images were captured using NIS Elements Imaging Software AR 3.0.

Time lapse bright field microscopy was performed using a custom made sealed chamber slide (Dr David Barlow and Gray Institute for Radiation Oncology and Biology Workshop, University of Oxford) containing pre-gassed culture medium in an outer moat enabling buffering of media over the course of time lapse experiments. Phase contrast and differential interference contrast (DIC) time lapse microscopy was captured using a modified Olympus U-TB190 microscope (Olympus, UK) mounted with an Olympus DP71 camera (Olympus, UK) and Cell^P Imaging Software (Olympus, UK).

Images were captured at a rate of 1/minute throughout time lapse experiments and converted to videos with a playback rate of 25 frames/second.

Phase contrast fluorescent time lapse microscopy was carried out using a custom made sealed chamber and an automated time lapse microscope (A Nikon TE2000 microscope maintained at 37 °C, fitted with a motorised stage, mounted with an ORCA-ER camera (Hamamatsu Photonics, UK), controlled with MetaMorph Software (Molecular Devices, USA). Utilisation of a moving stage allowed the sequential acquisition of bright field and fluorescent images of pre-defined field coordinates every 10 minutes during time lapse experiments. Images were converted into videos using ImageJ software (NIH, USA) with a playback rate of 7 frames /second.

2.20 Microscopy Primary Tissue Samples

Primary tissue samples were sectioned and analysed by fluorescent microscopy in order to detect the presence of SV expressed eGFP transgene. Samples were collected and immediately added to optimum cutting temperature compound (OCT, VWR International), snap frozen with liquid nitrogen and stored at -80 °C. Samples were sectioned using a Bright OTF 5000 Cryostat (A-M Systems, USA) and mounted onto glass slides which were stored at -80°C until they were analysed by microscopy. Cells were mounted and nuclei were stained using VECTASHIELD Mounting Medium with DAPI (4'-6-diamidino-2-phenylindole, Vector Biolabs, USA). Bright field and fluorescent images were acquired using a Nikon ECLIPSE 80i microscope (Nikon, UK)

mounted with an ORCA-ER camera (Hamamatsu Photonics, UK) and NIS Elements Imaging Software AR 3.0.

2.21 Determination of Viral Titres by $TCID_{50}$

The $TCID_{50}$ (tissue culture infectious dose causing pathological change in 50% of cultures) method utilises the observation of cytopathic effect (CPE) induction to determine viral titres. Cells were seeded in 96 well plates at a density of 10^4 cells/well prior to infection. On the day of infection virus containing culture medium was subject to 10 fold serial dilutions in fresh cell culture medium and 100 µl aliquots of each dilution step were added to 10 well rows in a 96 well plate. Media in each well was "topped up" with an additional 100 µl cell culture media and plates were incubated for 5 days in a 37 °C humidified 5% CO_2 incubator. $TCID_{50}$ /100 µl inoculum were determined using the Karber method, outlined by the equation:

$$T=10^{1+D(S-0.5)}$$

Where D = Log_{10} serial dilution factor (1 for a 10 fold dilution) and S = Sum of the ratios of CPE in each row (if CPE was observed anywhere in a well it was counted as positive).

Wells with no cytopathic effect had zero plaque forming units present upon infection but those which display CPE had 1 or more present. By applying Poisson distribution where P(o) is the proportion of wells free from cytopathic effect and "m" is the mean number of PFU/100 µl inoculum:

$P(o) = e(-m)$.

For any titer expressed as $TCID_{50}$

$P(o) = 0.5$,

So $e(-m) = 0.5$

and $m = -\ln 0.5$

Thus $m = 0.7$

Therefore multiplication of $TCID_{50}$ values/100 µl by 0.7 gives PFU/100 µl.

This mathematically derived conversion has been confirmed to be accurate by experimental observations (Qbiogene, USA). All $TCID_{50}$ assays were carried out in triplicate after 1 freeze thaw cycle to be consistent with virus aliquots stored at -80°C and thawed immediately prior to infections.

2.22 Isolation of SV Clones by Serial Dilution

The $TCID_{50}$ method was followed and after 5 days wells showing CPE were identified. Supernatant was collected from wells showing CPE at the highest dilution factor and 5 µl samples of this supernatant was added to BHK cells seeded 24 hours earlier at a density of 10^4 cells/well. 16 hours post infection transgene expression was analysed either by *in vitro* luciferase assay or by observation by fluorescence microscopy. Due to the possibility of the isolation of 2 or more clones, the highest expressing virus

containing supernatants were subject to 2 more rounds of selection, followed by amplification by adding to BHK cells pre-seeded in 6 well plates at a density of 2.5 x 10^5 cells/well overnight. Supernatant was filtered using 0.45 μm pore filters (Whatman International) aliquoted and stored at -80 °C.

2.23 Collection and Preparation of Human Blood

Human blood was collected from healthy adult donors typically with lithium heparin coated Vacutainers (Becton Dickinson, UK) between the hours of 9 am and 12 noon and immediately placed on ice. To collect plasma and erythrocyte fractions whole blood was separated by centrifugation at 1000 x g for 5 minutes at 4 °C. For the collection of serum, blood was collected in glass vacutainers (Becton Dickinson, UK) and incubated for 1 hour at room temperature to allow complete clotting; centrifugation at 1000 X g for 5 minutes at 4 °C cleared serum for collection.

All whole blood and plasma samples were used on the day they were collected whilst some serum samples were stored at -80 °C for further use. During the hour required for whole blood to clot, plasma or erythrocyte fractions were stored on ice until serum was collected.

2.24 Measurement of Complement Activation

Activation of both the classical and alternative complement pathway lead to the conversion of C3 to C3a and C3b. C3a anaphylatoxin is rapidly cleaved to C3a-desArg,

a stimulator triacylgycerol synthesis, by carboxypeptidases B and N. This was detected by ELISA as a measure of the amount of C3a, hence extent of complement activation.

C3a-desArg was detected using the BD OptiEIA Human C3a ELISA Kit (Becton Dickinson, UK). A monoclonal antibody specific for human C3a-desArg immobilised on a 96 well plate is used to bind the C3a-desArg in the samples. Wells are washed and a mixture of biotinylated polyclonal anti-human C3a antibody and streptavidin-horseradish peroxidase is added, producing an antibody-antigen-antibody "sandwich". Horseradish peroxidase converts TMB (3,3',5,5'-Tetramethylbenzidine) to its terminal diimine oxidation product (3,3',5,5'- tetramethylbenzidine diimine) which has a peak absorbance at 450 nm on addition of acidic stop solution; hence measuring the of samples absorbance at 450 nm in conjunction with a standard curve can be used to determine the C3a content of samples.

Plasma and serum samples to be tested were incubated with SV for 30 minutes, complement activation was terminated by the addition of 10 mM EDTA. Samples were then diluted 1/500 in provided diluent (animal serum with 0.09 % sodium azide preservative). Standard curves were created by serial (1:2) dilutions of a standard human serum sample containing 5 ng/µl C3a-desArg. Standards and samples were incubated in wells for 2 hours at room temperature, washed 5 times with 300 µl wash buffer. 100 µl working detector, containing a mixture of biotinylated polyclonal anti-human C3a antibody and streptavidin-horse radish peroxidase, was added per well and plates were incubated for 1 hour at room temperature, wells were washed 7 times, each time incubating for 1 minute with 300 µl wash buffer. 100 µl of TMB One-Step Substrate Reagent (containing 3,3',5,5'-Tetramethylbenzidine) was then added to each well and plates were incubated for 30 minutes at room temperature in the dark. 50 µl stop

solution was added per well and absorbance at 450 and 570 nm was measured. The absorbance at 570nm was subtracted from that at 450nm to correct for non-specific absorption. Stands were plotted and the standard curve used to determine the quantity of C3a in samples.

2.25 Tyrosinase Assay

B16 melanoma cells express tyrosinase and other enzymes required for the synthesis of melanin which are lacking in most cell tissues. Measurement of tyrosinase levels was therefore used to determine the number of B16-F10 cells present in the lung as metastases following IV injection. Tyrosinase catalyses the conversion of L-DOPA to the orange coloured dopachrome, which is subsequently converted to eumelanine. The accumulation of eumelanin can be quantified by measuring absorbance at 450 nm. In conjunction with a standard curve it is possible to determine the amount of tyrosinase or the number of B16-F0 cells in a given sample.

A standard curve was constructed by pelleting known numbers of B16-F10 cells by centrifugation at 500 x g for 5 minutes at 25 °C. Cells were lysed by re-suspending in 300 µl lysis buffer, ((20mM phosphate buffer (pH 6.8, Sigma, UK), 1mM PMSF (phenylmethanesulphfonylfluoride, Sigma, UK) and 1% Triton X-100 (Sigma, UK)), freeze thawing and vortexing for 30 seconds. Lung samples were lysed by homogenisation in 10µl lysis buffer/mg lung tissue using a motorised homogeniser (Ultra Turrax IKA T18 Basic, Fisher Scientific, UK), freeze thawing and vortexing for 30 seconds. 50 µl of cell lysates were mixed in triplicate with 50 µl reaction mixture

(50mM phosphate buffer (pH 6.8), 25mM L-DOPA) or 50 µl PBS as background in a 96 well plate. Plates were incubated for 3 hours at 37 °C then absorbance at 450 nm was measured. The amount of B16-F10 cells in each sample of lung homogenate was determined by correlating absorbance with the standard curve.

2.26 Animal Experimentation

All animal experimentation was performed in accordance with the terms of the UK Home Office guidelines and the UKCCCR Guidelines for the Welfare of Animals in Experimental Neoplasia. These experiments were conducted under the home office personal licence (PIL) number 30/8554 and the home office project license (PPL) numbers 30/2333 and 30/2819. All experiments were conducted with approval of the Medical Sciences Animal Ethics Committee, University of Oxford.

2.27 Statistical Analysis

Statistical analyses were performed using 2-tailed T-tests for experiments containing two sets of data. Where variance between data sets was significantly different, 2-tailed T-tests with Welch's correction were performed. For comparison of more than 2 sets of data one-way analysis of variance (ANOVA) was performed and where the effects of two variables were compared two-way ANOVA was performed. Prism was used for all analyses. Standard deviation is shown where n = 3 or 4 and ± standard error of the mean (SEM) where n = 5 or above. * = $P < 0.5$, ** = $P < 0.01$, *** = $P < 0.001$. Data

presented are representative of experiments carried out a minimum of 3 times unless otherwise stated

3 Physical and Genetic Stability of SV

3.1 Introduction

SV is an arbovirus that replicates in mosquitoes. It's confirmed mosquito host families include *Anopheles, Culex, Aedes,* and *Culiseta*, which allows spread to a large range of host birds and mammals on which these mosquitoes feed. The constant exchange between vertebrate and invertebrate hosts required for virus transmission means that mutations causing increased fitness in either host are not maintained if they significantly hamper fitness in the other. This evolutionary pressure is thought to be responsible for the ability of alphaviruses to infect such a broad host range by selecting for infection via a single receptor conserved across phylogenetic boundaries, or through the use of multiple receptors, each with distinct phylogenetic profiles of expression (Wang, Kuhn et al. 1992).

As the discovery of SV pre-dates that of the reverse transcriptase enzyme, after the isolation of SV from mosquitoes in 1952, it was maintained in the laboratory by *in vitro* serial passage for many years. In contrast to selective pressures in the wild, *in vitro* the major selective pressure is for mutations that give more efficient replication in cell lines used. Over time, such mutations accumulate, diverging *in vitro* passaged virus from wild type strains. It was not until 1970 when reverse transcriptase was discovered, that RNA viruses such as Sindbis could be "frozen" in DNA form and it became possible to work with a true master stock virus.

In selecting a virus for molecular engineering we were keen to obtain a cDNA version of an SV strain that had not been attenuated by repeated *in vitro* serial passage and that would be compatible with insertion of a reporter transgene and microRNA target sites. We received as a gift from Stephen Higgs the genome of Sindbis AR339 strain after it

had been serially passaged on mouse brains *in vivo* in order to ablate mutations picked up from extensive tissue culture and return the virus to a more wild type "neuro-adapted" phenotype. The neuro-adapted SV genome was "frozen" by reverse transcription and cloned into a plasmid backbone, allowing insertion of a duplicated subgenomic promoter.

In wild type SV, the plus strand synthase complex binds the genomic and subgenomic promoter and subsequently produces positive sense genomic or subgenomic RNA respectively (see Chapter 1.3.3). Where the subgenomic promoter has been duplicated in our construct, two subgenomic RNAs are produced; one encoding the structural polyprotein and any transgene inserted downstream, the other encoding just the inserted transgene (Figure 3.1). For ease of monitoring virus replication both *in vitro* and *in vivo,* we inserted firefly luciferase, eGFP and TurboRFP encoding regions into our SV plasmid under the control of the second subgenomic promoter.

There are several published methods of purifying SV; of these, 2 were compared in order to evaluate which was best for the neuro-adapted variant of SV, as it is possible it differs in physical properties to previous lab strains used.

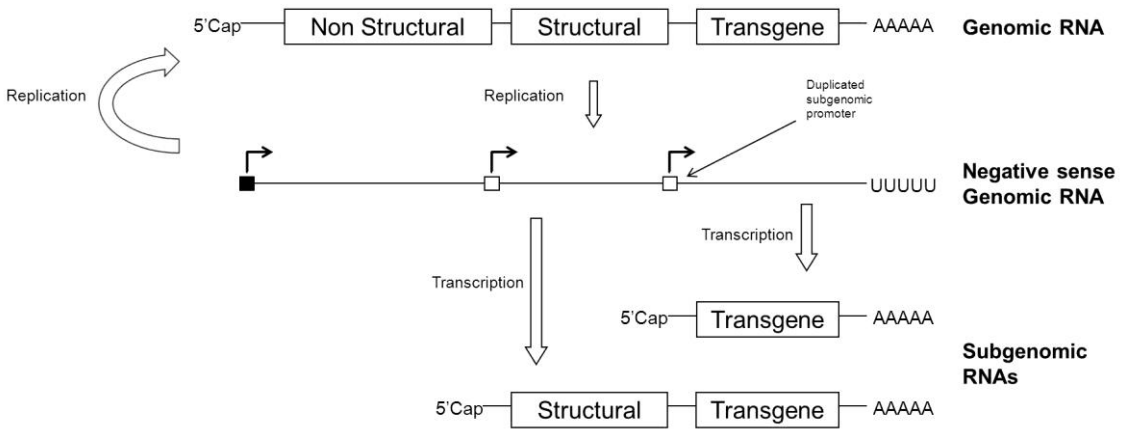

Figure 3.1: RNA species produced by SV DSG – During early infection, genomic SV RNA is transcribed into negative sense genomic RNA by the minus strand synthase. Later in infection when levels of the minus strand synthase have reached a threshold, its constituents P1-3 and nsp4, are proteolytically cleaved to form mature forms of nsp1, nsp2, nsp3 which associate with each other and nsp4 to form the plus strand synthase. Positive sense genomic and subgenomic RNAs are produced by the plus strand synthase transcription after binding the genomic or subgenomic viral promoters. ■ = genomic promoter, □ = subgenomic promoter.

3.1.2 Aims

- To engineer Sindbis Viruses expressing with Luciferase and GFP and RFP under the control of the duplicated virus subgenomic promoter in order to gain a reporter virus system for SV infectivity and replication
- To compare virus purification strategies and select one for routine use
- To assess the physical and genetic stability of rescued viruses
- To establish *in vitro* conditions in which to test biological activities of SV

3.2 Results

3.2.1. Insertion of Luciferase, eGFP and TurboRFP Genes into Sindbis Virus cDNA Sequence

In order to produce reporter viruses we initially cloned firefly luciferase, enhanced GFP (eGFP) and TurboRFP into our Sindbis Virus construct containing the duplicated subgenomic promoter (pSV DSG).

Luciferase and eGFP encoding genes were cut out of their respective plasmids pCMVLuc, pEGFP-C1 with NheI and XbaI, two restriction endonucleases that produce sticky ends compatible for ligation with one another. Both plasmids were cut with these enzymes and the transgene fragments were gel extracted and cleaned up. The TurboRFP gene was PCR rescued from the pTurboRFP plasmid with primers adding and NheI site upstream and XbaI site downstream of the TurboRFP coding region. The PCR rescued TurboRFP coding fragment was gel extracted, digested with NheI and XbaI, and cleaned up. Each transgene fragment was ligated with XbaI cut, dephosphorylated pSV DSG. This produced three separate plasmids; pSVLuc DSG, pSVGFP DSG and pSVRFP DSG, encoding SV with luciferase, eGFP or TurboRFP reporter transgenes downstream of the duplicated SV subgenomic promoter respectively (Figure 3.2 A, B and C).

The above described method of cloning results in ligation products with transgenes inserted in either forward or reverse orientation, relative to the virus genome encoded in the plasmid construct. When XbaI and NheI sticky ends anneal, the product is a hybrid of the recognition sequences of both restriction enzymes. This hybrid sequence is no longer a six base palindrome and can be cut by neither enzyme, therefore, it is possible

to screen for plasmids with luciferase, eGFP or TurboRFP transgene inserts in correct orientations (Figure 3.2 D).

All 3 transgenes used have an NheI site upstream, which means upon ligation into pSV DSG, the surviving XbaI site is downstream of the inserted gene in the context of the plasmid backbone, if it in the correct orientation. An enzyme with a recognition site in the pSV DSG backbone, XhoI was used to cut in combination with XbaI. Plasmids with transgenes in the correct orientations gave a ~0.5 Kb fragment, representing the distance between XbaI and the downstream XhoI site, whereas plasmids with the luciferase transgene in the reverse orientation gave a larger fragment of ~2.5kb and plasmids with eGFP or TurboRFP in the reverse orientation gave fragments of ~1.6 Kb (Figure 3.2 E and F).

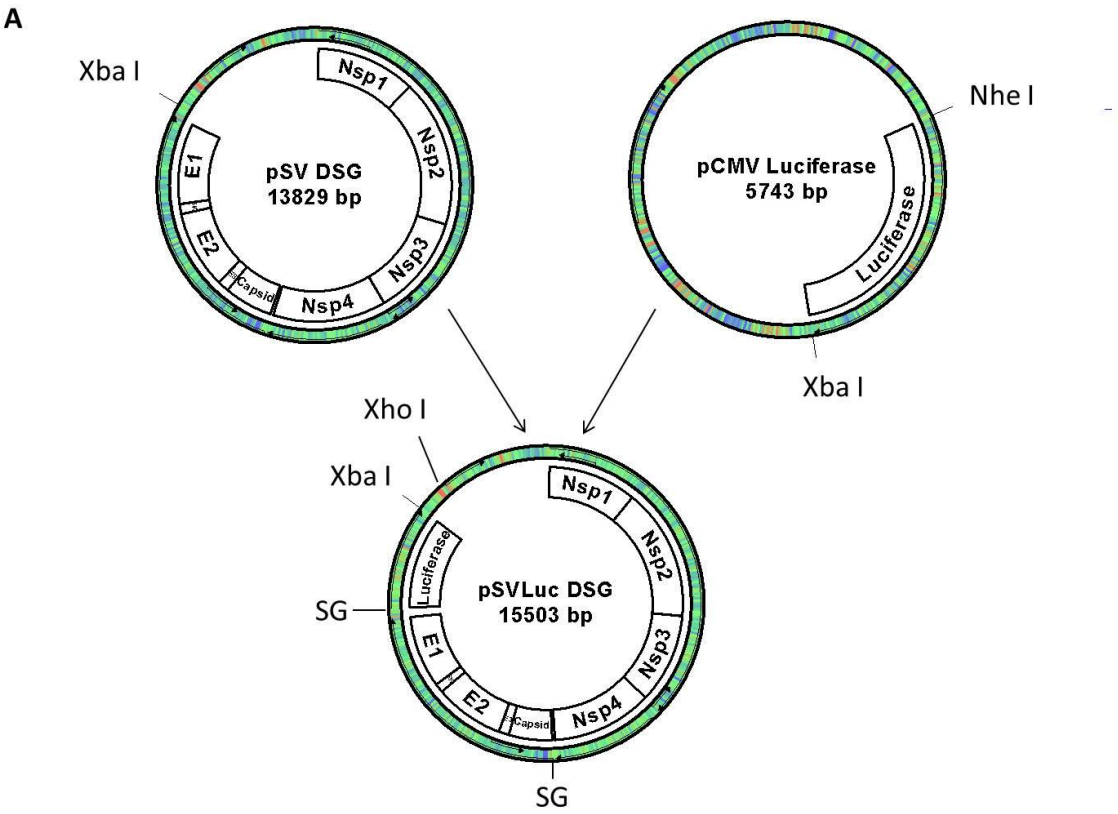
A
Xba I
Nsp1
Nsp2
Nsp3
Nsp4
Capsid
E2
E1
pSV DSG
13829 bp
Nhe I
pCMV Luciferase
5743 bp
Luciferase
Xba I
Xho I
Xba I
SG
Luciferase
Nsp1
Nsp2
Nsp3
Nsp4
Capsid
E2
E1
pSVLuc DSG
15503 bp
SG

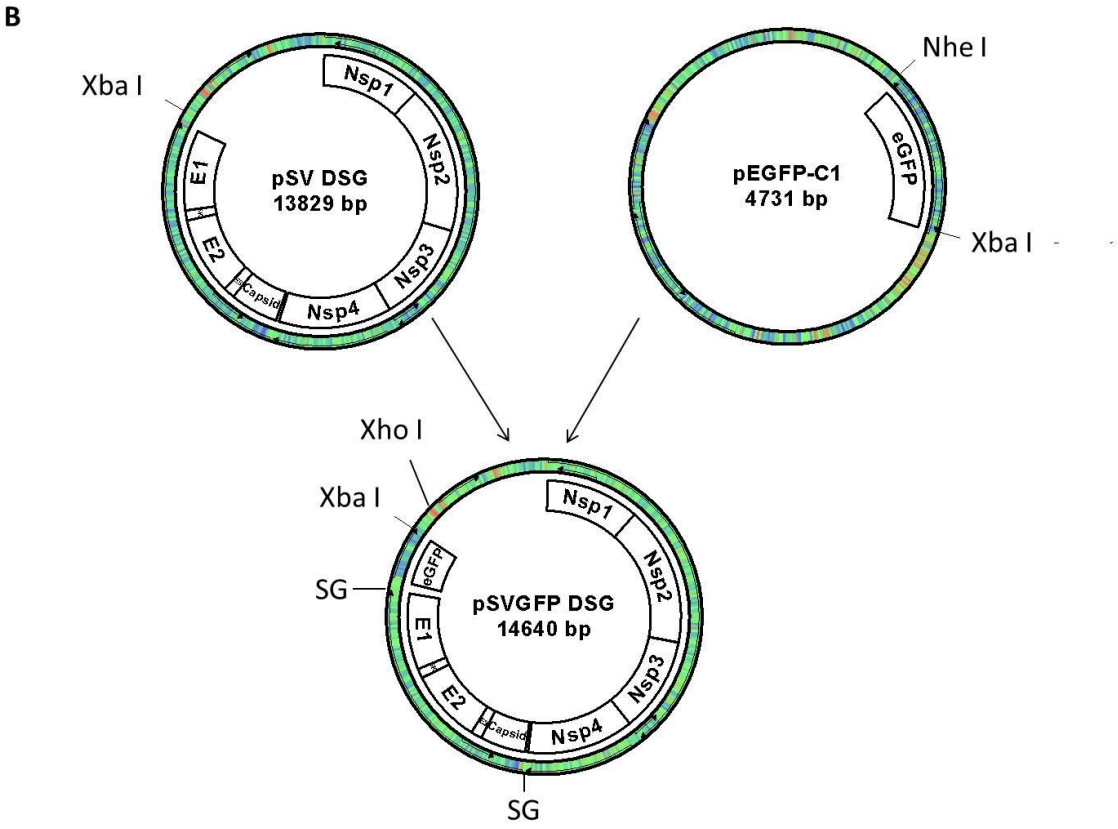
B
Xba I
Nsp1
Nsp2
Nsp3
Nsp4
Capsid
E2
E1
pSV DSG
13829 bp
Nhe I
pEGFP-C1
4731 bp
eGFP
Xba I
Xho I
Xba I
SG
eGFP
Nsp1
Nsp2
Nsp3
Nsp4
Capsid
E2
E1
pSVGFP DSG
14640 bp
SG

C

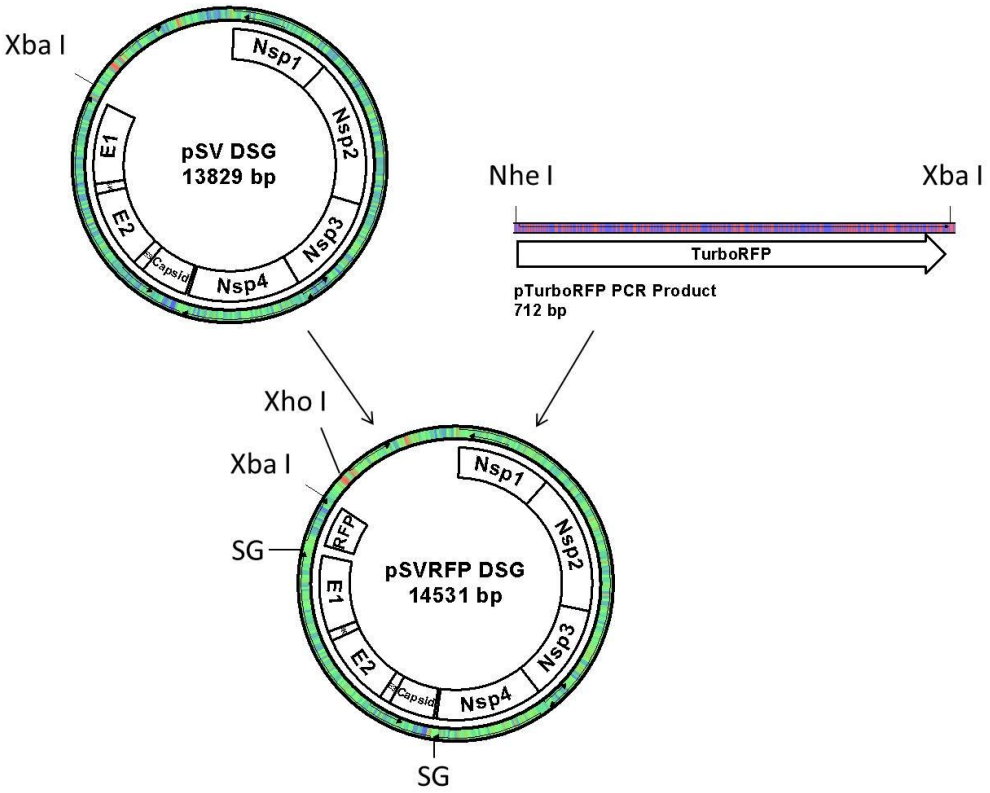
Xba I
Nsp1
Nsp2
Nsp3
Nsp4
Capsid
E2
E1
pSV DSG
13829 bp
Nhe I
Xba I
TurboRFP
pTurboRFP PCR Product
712 bp
Xho I
Xba I
SG
RFP
pSVRFP DSG
14531 bp
SG

D

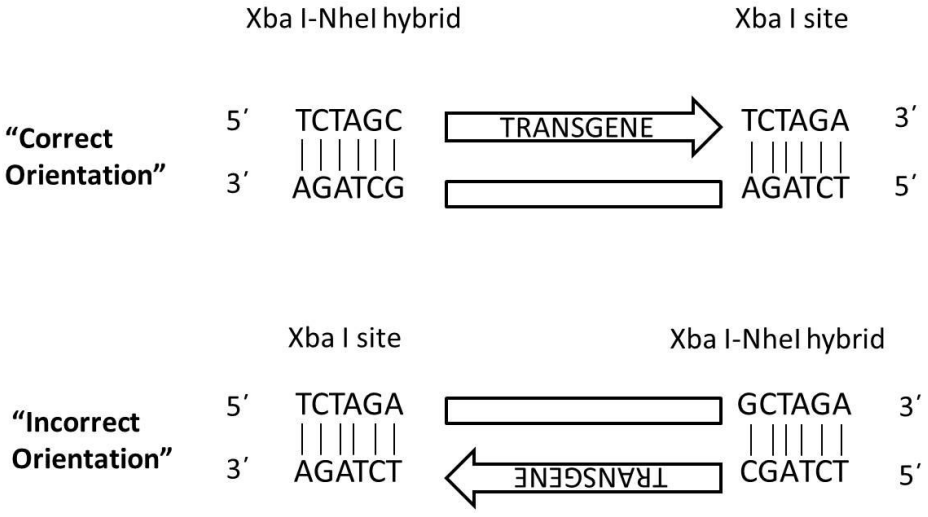
Xba I-NheI hybrid
Xba I site
"Correct Orientation"
5′ TCTAGC
3′ AGATCG
TRANSGENE
TCTAGA 3′
AGATCT 5′
Xba I site
Xba I-NheI hybrid
"Incorrect Orientation"
5′ TCTAGA
3′ AGATCT
TRANSGENE
GCTAGA 3′
CGATCT 5′

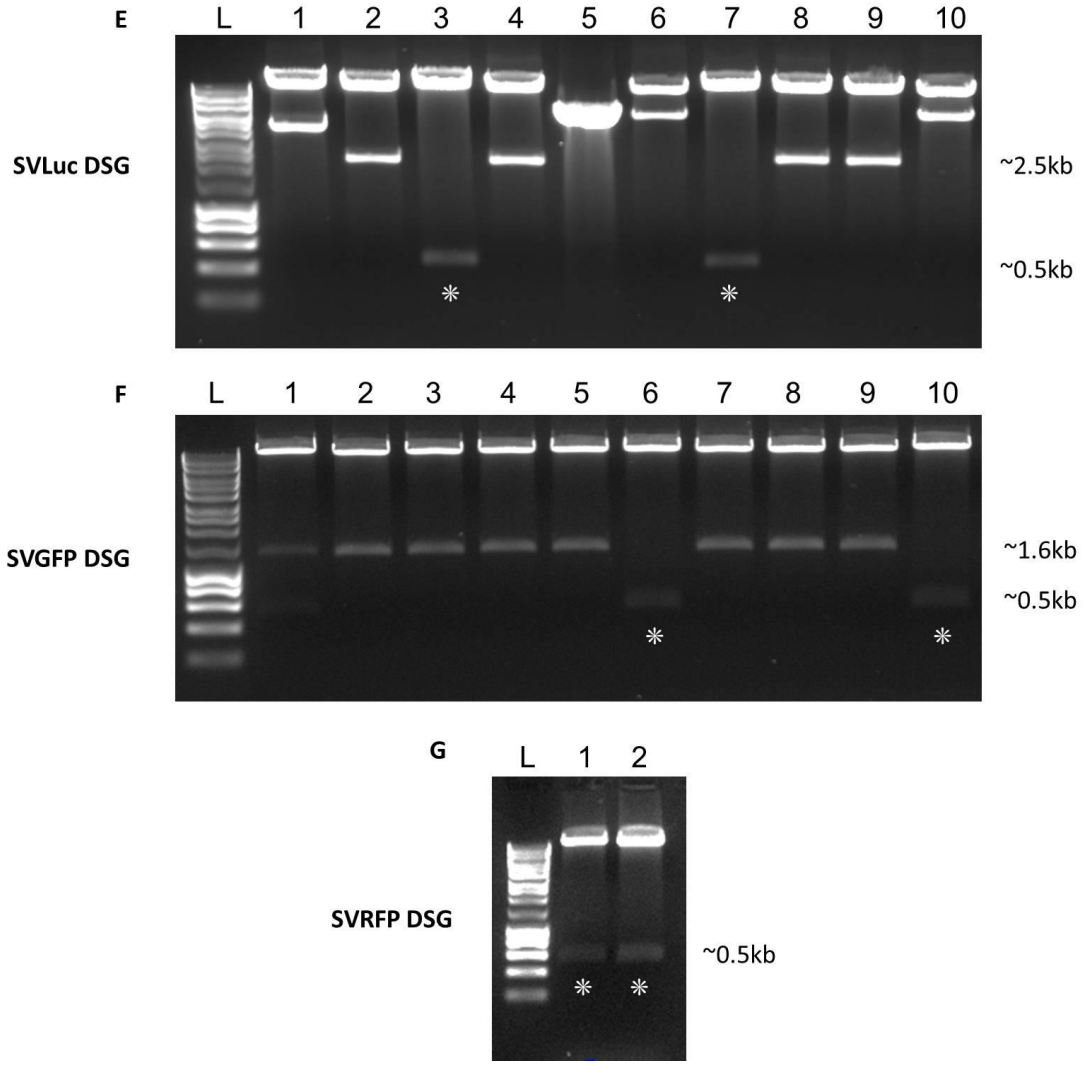

Figure 3.2: Insertion of reporter transgenes into pSV DSG - A), **B)** and **C)** Overview of cloning strategies for production of pSVLuc DSG, pSVGFP DSG and pSVRFP DSG respectively. For each, transgene encoding DNA was cut with NheI and XbaI and ligated into pSV DSG linearized with XbaI and dephosphorylated to prevent re-circularisation. The position of NheI and XbaI restriction enzyme sites utilized in cloning are indicated, as is the XhoI site subsequently utilized for screening for transgene insertions in the correct orientations. SG indicates the positions of the two identical viral subgenomic promoters **D)** Illustration of the resulting position of the XbaI restriction enzyme site resulting from both possible transgene orientations following ligations **E)**, **F)** and **G)** Screening the orientation of luciferase, eGFP and TurboRFP transgenes in SVLuc DSG, SVGFP DSG and SVRFP DSG respectively. L = Hyperladder I, 1-10 = clones, * = clones with transgenes in the correct orientation.

3.2.2. Rescue of Reporter Sindbis Viruses

The pSV DSG construct does not contain a mammalian promoter for transcription, therefore, transfection of DNA into mammalian cells would not rescue virus without the insertion of a mammalian promoter upstream of the virus encoding region. The presence of an SP6 RNA polymerase promoter sequence upstream of the virus coding region, however, allows *in vitro* transcription of virus RNA, which can then be transfected into mammalian cells capable of supporting replication for rescue of virus particles (VPs); It is well documented that BHK cells (baby hamster kidney fibroblasts) can be used to produce high titres of SV utilising this method.

Due to the highly processive nature of SP6 RNA polymerase it is necessary to linearise plasmid DNA template. This avoids producing multiple transcribed copies of the DNA template in a single mRNA molecule, resulting from the polymerase circumnavigating the plasmid many times before dissociating. Plasmids were therefore linearized via an XhoI site 9bp downstream of the viral polyA signal and *in vitro* transcribed. *In vitro* transcribed RNA was cleaned up and transfected into BHK cells using lipofectamine LTX and virus containing supernatant was collected 24 h post transfection.

3.2.3 Characterisation of Rescued Viruses

In order to confirm successful virus rescue, supernatant collected from transfected cells was added to fresh BHK cells and luciferase eGFP and TurboRFP expression analysed 24 h PI by luminometry or UV microscopy respectively (Figure 3.3)

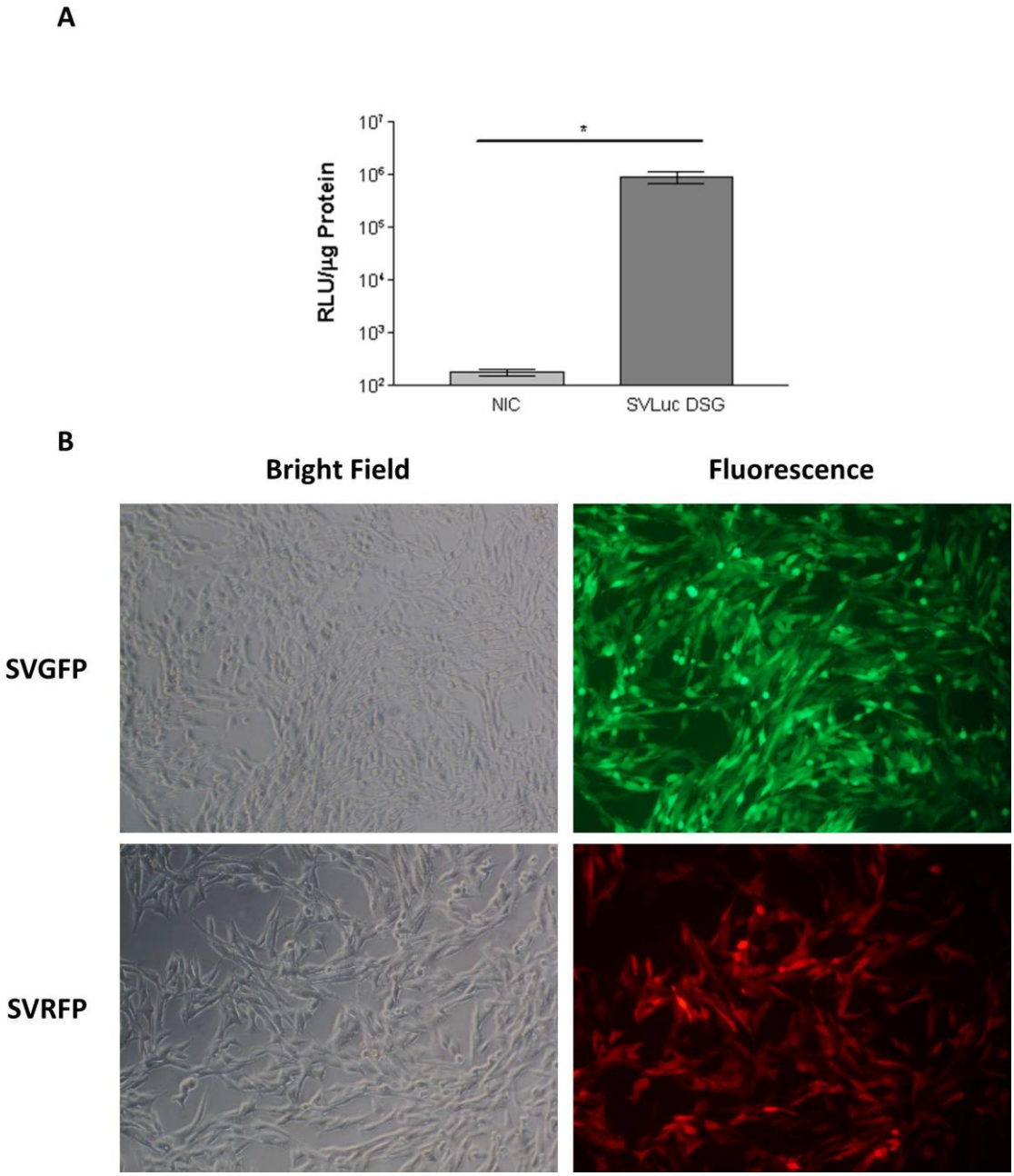

Figure 3.3: Confirmation of SV Rescue by Reporter Gene Expression – A) Luciferase Expression of SVLuc DSG was measured by luminometry as described in Chapter 2.11. Statistical analysis was performed using a two tailed T test with Welch's correction. Error bars show ± SEM, n = 5, (* = P < 0.05). **B)** Visualisation of SVGFP DSG, eGFP expression and SVRFP DSG, TurboRFP expression respectively, by fluorescence microscopy. All infections were carried out on BHK cells at an MOI of 1 PFU/cell and analysed 24 h PI.

3.2.4 Purification

As SV is a budding virus, collection from the supernatant is necessary in order to recover enveloped virions. Due to the significant volume of media required to cover monolayers of cells *in vitro*, the concentration of virus that can be harvested from cells is low compared to non-budding viruses, which produce infectious particles intracellularly and can be harvested from cell pellets. In an attempt to gain the highest possible titres, two published methods of concentrating SV were compared to purification by passing virus-containing supernatant through a 0.45μM pore syringe filter:

1) Centrifugation of 9 mL virus-containing supernatant through a 1mL 20% sucrose cushion for 2 hours at 25,000 RPM in a Beckman tube followed by re-suspension of sedimented virus in 1 mL serum free DMEM (Byrnes and Griffin 2000; Lee, Knight et al. 2002; Lundstrom 2012).
2) Passing virus-containing supernatant through a 0.45μM pore syringe filter then centrifugation at 30,000 RPM for 90 mins followed by re-suspension of sedimented virus in 1 mL serum free DMEM (Marie H 2006).

A pair of primers and a probe were designed for RTQPCR of a region of the nsp1 gene, so that SV genomic, but not subgenomic RNA could be detected. The number of SV genomes per mL was measured by RTQPCR of RNA extracted from input and purified samples. Methods (2) and (3) both successfully increased virus particle concentration (Figure 3.4 A). However, when equal 5 µl volumes of the product of each purification method were used to infect monolayers of BHK cells, the transgene expression of virus concentrated by methods (1) and (2) was significantly lower than virus prepared by filtration alone. This was in spite of at least having ~50 fold higher numbers of virus particles per µl (Figure 3.4 B). This suggests that high speed centrifugation may compromise SV particles, impairing their ability to infect cells. In light of these results, purifying virus by filtering through a 0.45 µM pore syringe filter to remove any cell debris was adopted as standard.

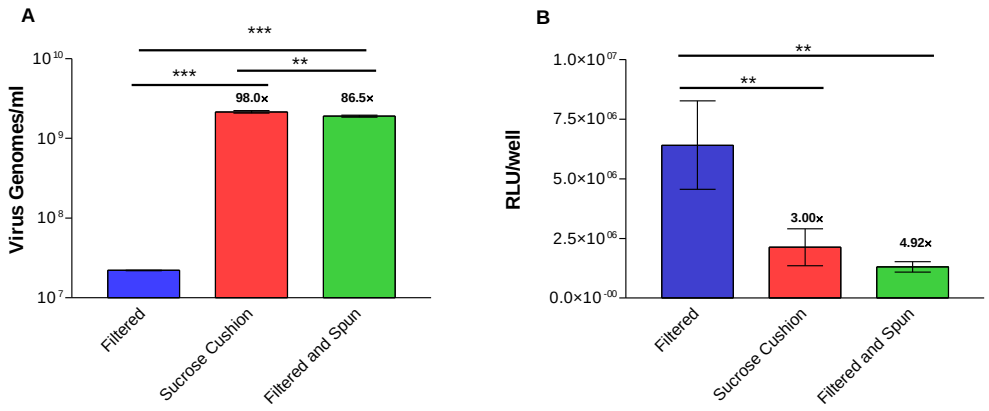

Figure 3.4: Assessment of Virus Quality - A) VP titres produced by different purification methods. Filtered: Virus containing supernatant was filtered through a 0.45µM pore syringe filter. Sucrose cushion: 9 mL Virus containing supernatant was centrifuged on a 1mL sucrose cushion for 2 hours at 25,000 RPM in a Beckman tube followed by re-suspension in 1 mL serum free DMEM. Filtered and spun: Virus containing supernatant was filtered through a 0.45µM pore syringe filter then centrifuged at 30,000 RPM for 90 mins followed by re-suspension in 1 mL serum free DMEM. RNA extraction and RTQPCR detection of virus genomes was carried out as describe in Chapter 2.16. Statistical analysis was performed using one-way ANOVAs and Tukey's multiple comparison post-tests. (** = P <0.01, *** = P <0.001). Fold increases in SV titre compared to non-concentrated virus are indicated on graph. **B)** BHK cells were infected with 5 µl aliquots of SVLuc DSG stocks produced by the indicated methods and luciferase expression was analysed 24 h PI infection as described in Chapter 2.11. Statistical analysis was performed using one-way ANOVAs and Tukey's multiple comparison post-tests. (** = P <0.01). Fold decreases in luciferase expression compared to non-concentrated virus are indicated on graph.

Measuring the number of virus genomes in a preparation gives an indication of the number virus particles present, however, it does not give any information about the viability of the virus particles present. In order to determine the amount of viable virus in a given preparation, it is necessary to measure the number of plaque forming units

(PFU) present; virus particles capable of productive infection, compared to the total number of particles. This is known as the VP/PFU ratio.

There are several reasons that any given VP may not productively infect a cell; some VPs have inherent disabling features that mean they are not capable, such as improper assembly or a disabling mutation in a gene encoding a protein necessary for a critical step in virus infection, replication or release. Of the VP that are able, some may not go on to form plaques due to degradation of virus particle structure over time, either during storage, or upon addition to new cells before they encounter their receptor. Alternatively, some VP may not encounter their receptor due to geometric factors or sequestration by binding of virus particles to non-target surfaces such as transfer pipette tips, molecules in tissue culture media, surface proteins or extracellular matrix components that do not lead to internalization. Also, VP may bind proteins or cell surface molecules that lead to internalisation, but into a cellular compartment in which an infection cannot be established.

It is of note that during virus infection, replication and release, each step operates with a given efficiency. The culmination of the efficiency of each required step in the replication cycle of a given virus (such as fusion of virus and cellular membranes, or breakdown of nucleocapsids once in the cytoplasm) sets an inherent upper limit for the VP/PFU ratio for that virus. In a perfect system where all steps in a replication cycle operate with 100% efficiency, and during infection of cells, all virus particles encounter their cellular receptors, the VP/PFU ratio would be one. In practice this value cannot be reached, however, VP/PFU ratios can be used as a guide to as to the quality of virus preparations.

Several viruses used in the laboratory, such as adenovirus, often require purification to remove virus particles produced with empty capsids lacking genomic material which are not capable of infection in order to decrease VP/PFU ratios. Alphaviruses, however, do not produce empty capsids because the virus genome is involved in a nucleation event where a single capsid protein binds an encapsidation signal in the virus genomic RNA. This is required for the rest of the virus capsid proteins to be "built" around the genome (Weiss, Nitschko et al. 1989). In addition, SV budding is a process driven by the free energy change between virus glycoproteins in the host cell membrane associating with capsid molecules through their C-terminal cytoplasmic domains, hence virions lacking nucleocapsids also cannot form (Strauss and Strauss 1994).

The VP/PFU ratio of Sindbis Virus preparations can be determined by using RTQPCR to determine the number of VPs per ml and plaque or $TCID_{50}$ assays to determine the number of PFU per ml. Ratios for virus preparations were typically about 10, but ranged from 3.5 to 67 VP/PFU.

3.2.5 Storage Conditions

It has been reported that SV binds to polystyrene surfaces (Hernandez, Sinodis et al. 2010) and hence any vessels used for the transfer or storage of virus particles should be made from another material. In order to investigate this, the level of depletion of SVLuc DSG transgene expression after storage in a range of commercially available containers, routinely used in the laboratory, was measured (Figure 3.5 A). SVLuc DSG aliquots were incubated at 37 °C in serum free DMEM for 30 minutes at a concentration of 10^5 PFU/ml in polystyrene, polypropylene or glass tubes with or without rotation on a Stuart

SB3/2 blood tube rotator (Bibby Scientific, UK). Upon subsequent infection of BHK cells, no significant effect on transgene expression was observed by any of the materials used compared to virus immediately collected and frozen in a standard polypropylene microcentrifuge tube (Eppendorf).

In order to determine suitable storage conditions for SV, SVLuc DSG transgene expression was analysed after storage at a range of temperatures for varying lengths of time (Figure 3.5 B). Results showed retention of SVLuc DSG infectivity when stored at 4 °C for up to 1 week, however, storage at 20 °C or 37 °C for 1 day or longer caused a significant reduction,

Many viruses are known to be compromised by repeated freeze/thaw cycles. However, the use of cryoprotectants, at least in some cases, can minimize the degree of damage, allowing multiple freeze/thaw cycles before significant activity is lost. To establish if this principle could be applied to SV, its infectivity was measured after being subjected to multiple freeze/thaw cycles with a range of potential cryoprotectants (Figure 3.5 C). Results show that 3 freeze/thaw cycles in PBS reduced SV infectivity, measured by luciferase transgene expression, to background levels. It appears that 10% DMSO and 5% sucrose may have some ability to protect SV from freeze/thaw damage. Observed differences, however, were not statistically significant. 10% FCS did significantly protect SV from freeze/thaw damage with only 11.2 fold lower infectivity after 5 freeze/thaw cycles. However, as planned subsequent experiments involved virus interactions with human and mouse serum components, and the presence of calf serum proteins could have a confounding influence on experimental results, FCS was not used as a cryoprotectant. Instead, SV was stored at -80 °C in single use aliquots.

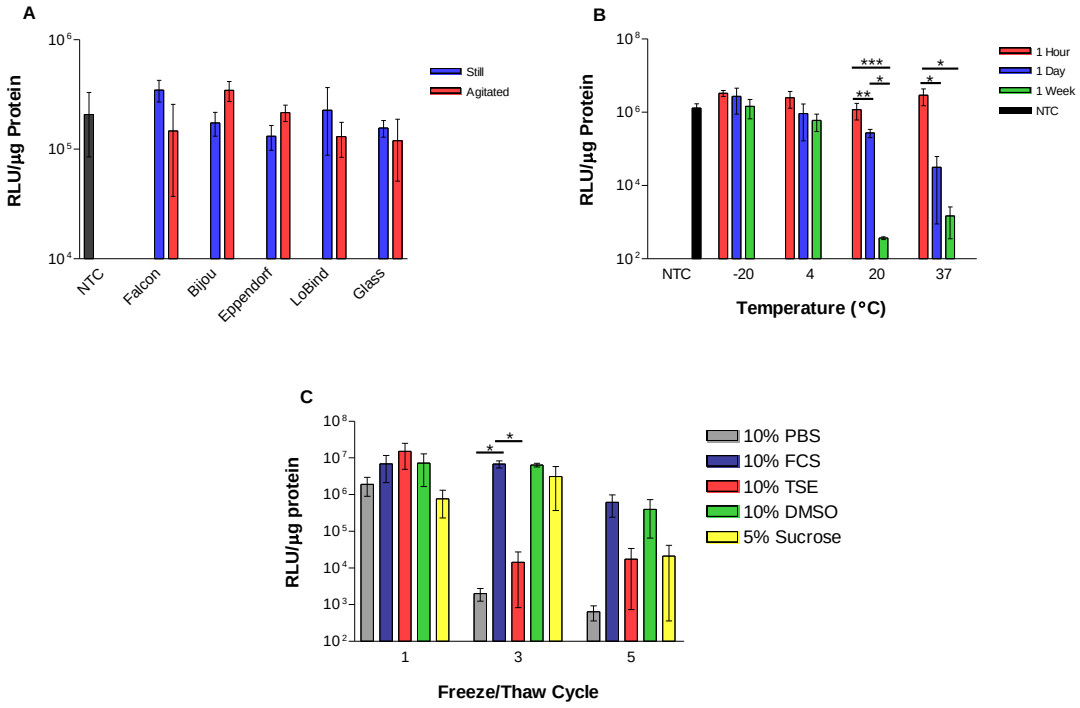

Figure 3.5 Physical Stability of SV - A) Storage of SVLuc DSG in serum free DMEM in a range of containers of differing materials: Polypropylene (Corning 15 ml (Corning BV, Netherlands), standard safelock microcentrifuge Protein LoBind microcentrifuge tubes (Eppendorf, UK)), polystyrene (7ml Bijou (Sterilin, UK)) and glass (Becton Dickinson, UK). Error bars show the SEM. Statistical analysis was using one way ANOVA was conducted on still and agitated treatment groups separately, no statistical significance compared to NTC was observed. **B)** Storage of SVLuc DSG in standard polypropylene microcentrifuge tubes (Eppendorf, UK) at varying temperatures for varying lengths of time. Error bars show the SEM. Statistical analysis was conducted groups of differing temperature treatment separately using one way ANOVA. Observations of statistically significant differences are indicated. (* = $P < 0.05$, * = $P < 0.01$, *** = $P < 0.001$) **C)** Exposure of SVLuc DSG to freeze/thaw cycles with a range of cryoprotectants. Freezing was at -80˚C and thawing at RT. Non-treated control was fresh virus stock stored at -80 °C in polypropylene Eppendorf tubes was used to infect cells immediately after thawing. Error bars show the SEM. Statistical analysis was conducted using one way ANOVA on groups of differing treatments at 1,3 or 5 freeze/thaw cycles. Observations of statistically significant differences are indicated. (* = $P < 0.05$). In all experiments SVLuc DSG was added at an MOI of 1 and luciferase expression in BHK cells was measured after cells were lysed 18 h PI. NTC:

3.2.6 Virus Replication and Transgene Expression

Reporter viruses SVLuc DSG and SVGFP DSG were made so that transgene expression could be easily measured as a surrogate for virus replication and virus protein expression. To facilitate studies of virus particle uptake, transgene expression and release of new particles, it was necessary to establish a set of standard experimental conditions for *in vitro* infection with SV.

To identify the optimum incubation time for SV infection of BHK cells, experiments were performed in which SV was incubated with BHK cells for various lengths of time. Cells were infected with SVLuc DSG at an MOI of 1 PFU/cell before washing and incubating with fresh media for 16-18h before analysis of luciferase expression (Figure 3.6 A). It is clear that uptake of SV is rapid and after about 10 minutes most virus has entered the cells. A plateau is reached after around 30 minutes where little more virus enters cells with increase incubation time. This implies that by this time, most infectious virus particles have entered cells, or that cells have become saturated with SV. Based on this data, the standard protocol for SV infections was incubation with cells for 30 minutes before washing.

The time taken for SV to express measurable amounts of transgene was analysed by infecting BHK cells with SVLuc DSG at an MOI of 1 PFU/cell for 30 minutes and measuring luciferase expression at 4, 8 or 24 hours PI (Figure 3.6 B). Measurement of luciferase transgene expression showed that virus proteins are produced as early as 4 hours PI and increase in levels over a 24 h period.

In order to assess changes in protein expression or virus replication, it is important to measure these parameters whilst their rate of increase is linear with respect to time,

before rate limiting factors convolute interpretation of the magnitude of differences. To determine the kinetics of SV replication and more accurately define the kinetics of transgene expression, a time-course experiment was conducted in which BHK cells were infected with SVLuc DSG at an MOI of 1 PFU/cell. At each time point, supernatant was analysed by RTQPCR for released virus genomes (Figure 3.6C) and cells were analysed for transgene expression by luminometry (Figure 3.6D).

Observed results show that the number of virus genomes, and therefore virus particles, in the supernatant increases about 10^3 fold in 12 hours and plateau at about 24h with around 10^{10} virus genomes/ml in the supernatant. Based on measured loss of infectivity, it seems SV particles are degraded at 37 °C in cell supernatant (Figure 3.5B), this plateau, therefore, probably represents a steady state where the rate of production of daughter virions equals the rate of virion degradation. A reduction from the initial rate of daughter virion release from 0-24 h is possibly due to decreased cellular resources such as lipid membrane utilised in virus budding, amino acids used in production of virus proteins or nucleic acids used in the replication of the SV genome. It may also be due to a general depletion of cellular energy stores. Data also shows that intracellular luciferase accumulated in a linear fashion over the first 18 hours PI, after which it too plateaued. Luciferase is known to have a half-life of 2 hours in mammalian cells (Ignowski and Schaffer 2004), suggesting the continued production of luciferase and therefore probably SV proteins during this plateau.

Based on the summation of the above observations, when analysing changes in transgene expression or replication, a standard protocol of infecting cells for 30 minutes, washing with PBS and analysis 16 h PI was adopted. Under these conditions, it is seen that transgene expression and replication correlate with one another from ~0–18 hours

PI, hence reporter transgene expression can be used a surrogate for virus replication during this period of time at an MOI of 1 PFU/cell.

As SV infectivity is reduced with increased time at 37 °C (Figure 3.5B), it is paramount when growing virus stocks, to collect the produced virus as early as possible to gain the highest quality virus preparation, however, it is also important to obtain the highest titres possible. These data show that virus titre does not significantly increase after 24 hours PI and hence indicate this as an optimal time for harvesting SV stocks, assuming the initial MOI is 1.

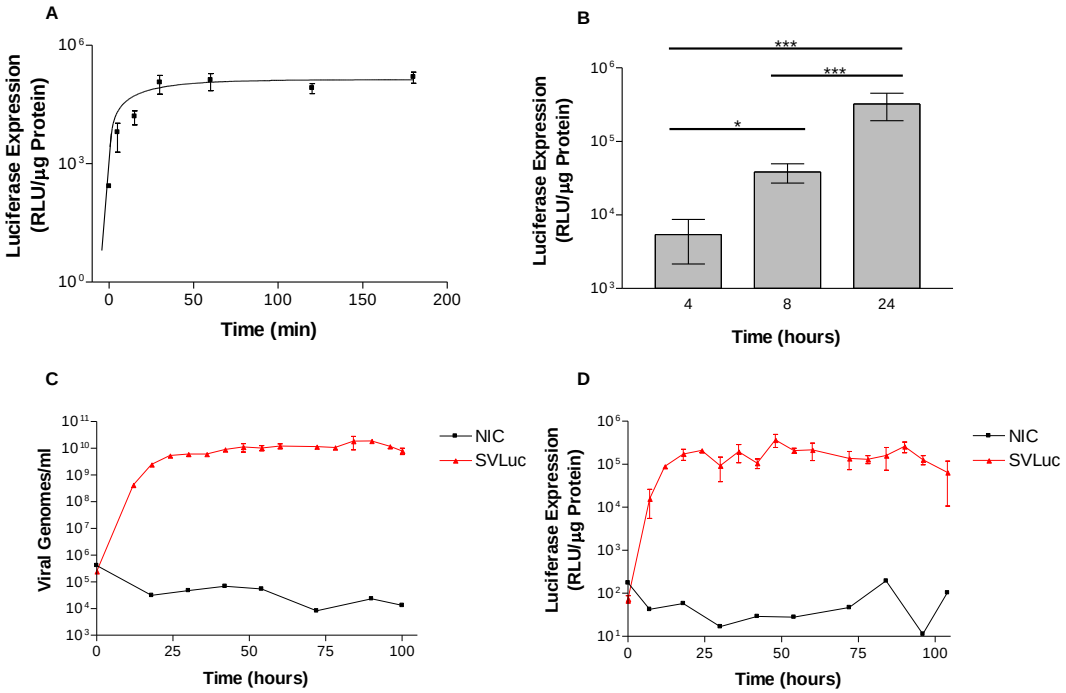

Figure 3.6: Analysis of SV Uptake, Transgene Expression and Release - A) Luciferase expression after varying lengths of infection. SVLuc DSG was incubated with BHK cells for varying lengths of time before washing and allowing infection to proceed for 16-18 hours after which luciferase expression was then analysed as described in Chapter 2.11. **B)** Time taken for SVLuc DSG to express luciferase. SVLuc DSG was incubated with BHK cells for 30 minutes after which they were washed with PBS and incubated at 37 °C for varying amounts of time before luciferase expression was analysed as described in Chapter 2.11. Statistical analysis was performed using one way ANOVA with Tukey's multiple comparison post-test. Error bars show ± SEM, n = 6. (* = $P < 0.05$, *** = $P < 0.001$) **C)** and **D)** Time-course of SVLuc DSG replication. BHK cells were infected with SVLuc DSG at an MOI of 1 for 30 minutes and luciferase expression measured at indicated times PI by RTQPCR and luminometry as described in Chapters 2.16 and 2.11 respectively. A), C) and D) Error bars show ± SD, n = 3.

3.2.7 Analysis of Sindbis Virus Cell Tropism

SV is able to infect and kill BHK cells efficiently. The IC_{50} of SV on BHK cells was determined by incubating serial dilutions of virus preparations with cells over a 5 day period, and was found to be an MOI of 6.5×10^{-4} PFU/cell (Figure 3.7 A).

This strain of SV has been passaged on mouse brains *in vivo* and hence may have differences in surface glycoproteins from the parental AR339 strain. Sequence analysis revealed an amino acid change in the E2 (Q55H) compared to the parental AR339 strain (data not shown) (Davis, Fuller et al. 1986). Heparin sulphate dependence is thought to be a consequence of extensive *in vitro* culture and causative of reduced virulence *in vivo*; however, the 2 putative heparin sulphate binding domains are still present in our

strain although it is possible structural changes caused by the amino acid change in E2 could make these regions less active.

The change noted in surface glycoprotein sequence could have consequences on cell tropism; it is possible that repeated passage on neuronal cells *in vivo* could have conferred a restriction or preference for neuronal cell types. To assess the ability of SV to infect and kill different cell types, a range of cancer cell lines were infected with SVLuc DSG and the levels of transgene expression and cell kill were measured (Figure 3.7 B). Where cell lines were susceptible to infection by SV, the level of transgene expression was inversely proportional to the viability of cells 48 h PI, suggesting that where SV is able to infect cells *in vitro*, it causes cell death. Toxicity to cells has been attributed to ceramide release upon cell entry (Taha, Mullen et al. 2006) and accumulation of nsp2 (Garmashova, Gorchakov et al. 2006) whilst high levels of SV transcription, protein expression and virus production may also contribute by causing cellular stress that leads to apoptosis.

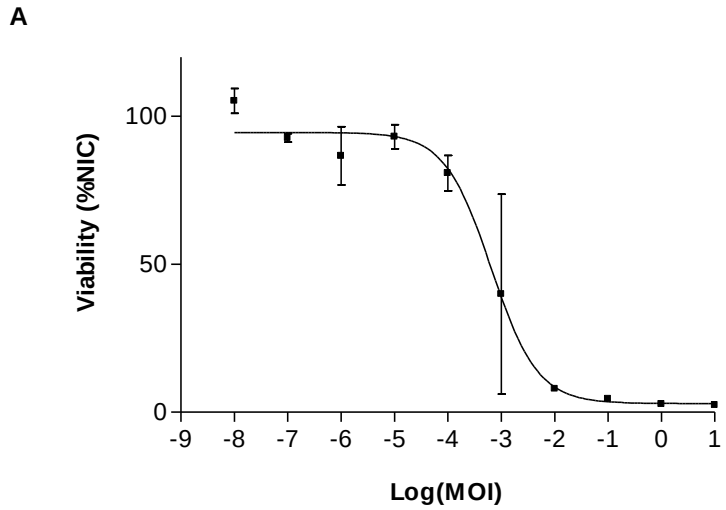
A
Viability (%NIC)
100
50
0
-9
-8
-7
-6
-5
-4
-3
-2
-1
0
1
Log(MOI)

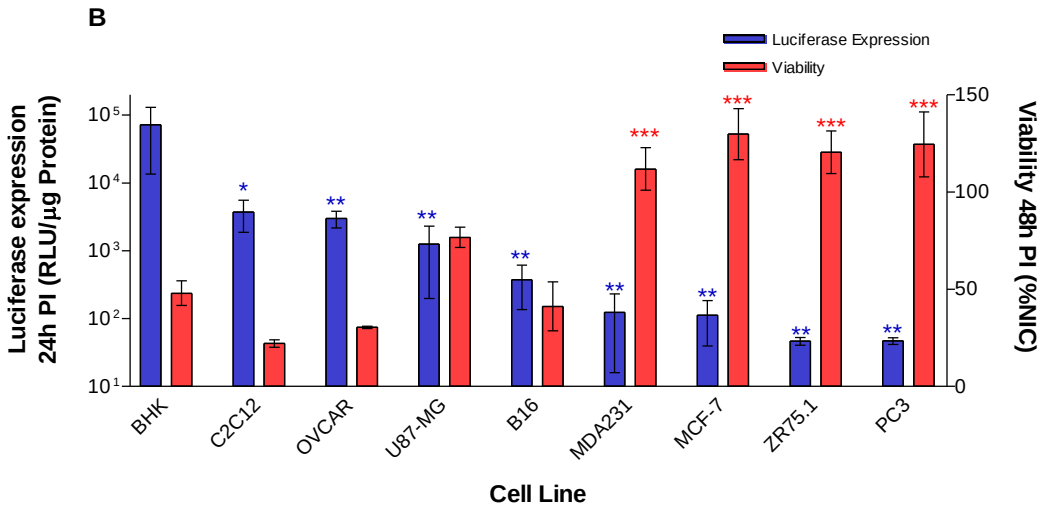
B
Luciferase Expression
Viability
Luciferase expression
24h PI (RLU/µg Protein)
Viability 48h PI (%NIC)
BHK
C2C12
OVCAR
U87-MG
B16
MDA231
MCF-7
ZR75.1
PC3
Cell Line

igure 3.7: Relation of transgene expression to cell killing – **A)** BHK cells were infected with SVLuc DSG at range of MOIs and cell viability was measured 5 days PI by MTS assay. Error bars show ± SD (n = 3). IC_{50} was calculated by non-linear regression curve fit. SVLuc DSG IC_{50} = an MOI of 0.00065 (CI = 0.0002448 to 0.00173). **B)** A range of cell lines were infected with SVLuc DSG at an MOI of 1. Luciferase expression and total protein content was measured 24 h PI by *in vitro* luciferase assay and BCA assay respectively. Cell viability was analysed 48 h PI by MTS assay. Statistical analysis of luciferase expression and cell viability was analysed separately by one way ANOVA with Tukey's multiple comparison post-test. Error bars show ± SD, n = 3. Significant difference in luciferase expression and cell viability following infection of BHK cells is denoted by asterisks above each data bar. (* = $P < 0.05$, ** = $P < 0.01$, *** = $P < 0.001$).

3.2.8 Possible Mechanisms of Loss of Transgene Expression

SVLuc DSG showed high variation in transgene expression between replicates, particularly when infection was at a low MOI. This was consistent in several experiments with separate batches of virus under experimental conditions defined above. This exposed the possibility that transgene expression could be lost by SVLuc DSG and this was subsequently studied in detail. There are several possible mechanisms by which loss of transgene expression by SVLuc DSG could occur:

3.2.8.1 Accumulation of point mutations, rendering the luciferase transgene inactive

The SV RNA-dependent RNA polymerase (RdRp), utilized for genome replication, lacks proofreading activity. The SV genome, therefore, is prone to accumulating mutations in any region which is not vital for infection, replication or release, such as an inserted reporter transgene.

The error rate of the SV RdRp is ~$10^{-6.8}$ (Durbin and Stollar 1986) , hence, on average it introduces one substitution mutation every $10^{6.8}$ (6.31 x 10^{6}) base pairs of copied RNA. Since the SV genome is 11860 base pairs long there are on average about 0.0019 substitutions mutations per genome copy. The SVLuc DSG genome is slightly longer at 13588 base pairs so this rate is increased slightly to 0.0022 substitutions per genome copy, hence about 1 in 464 SVLuc DSG virus particles produced by the RdRp has a substitution mutation.

Upon increased rounds of replication more point mutations will accumulate in the SVLuc DSG genome, however, during growth of virus stocks, virus replication proceeds for just 16 h meaning the numbers of rounds of genome replication is limited. In addition, SV displays superinfection exclusion, a phenomenon arising because host cell components required for genome replication are present in limiting amounts and are sequestered by virus genomes from initial or early infection. SV genomes produced within a cell therefore derived from a limited number of templates, so in order for genomes with introduced point mutations to pass these on to subsequent virus generations they must be released in virus particles and infect new cells. Typically, the efficiency of BHK transfection with genomic SV RNA is ~ 80 % efficient, this means that the vast majority of virus particles produced over 16 h are derived from the original RNA produced from *in vitro* transcription. Furthermore, point mutations that lead to the

production of non-functional luciferase enzyme do not confer a selective advantage to virus replication hence are unlikely to be selected for.

3.2.8.2 Transfection of BHK cells with incomplete SVLuc DSG RNA

Incomplete *in vitro* transcription could offer an alternative explanation as to loss of the inserted luciferase transgene. As described above, SVLuc DSG is produced by *in vitro* transcribing a linearized virus-encoding plasmid and transfecting the resultant RNA into BHK cells (3.2.2). As the processivity of the SP6 RNA polymerase is very high, any incomplete transcription occurring is likely to be the result of inadequate amounts of ATP provided in reaction buffers. A small proportion of incomplete transcription products, however, is likely to be present derived from incomplete RNA molecules at the time termination of *in vitro* transcription reactions. To check for shorter length transcripts, as well as any degradation of RNA transcripts produced, genomic RNA was analysed by agarose gel electrophoresis (AGE) (Figure 3.8). These gels showed no evidence of shorter length genomes resulting from premature transcription termination, however the amount of ssRNA required to be visible on a gel is > ~50 ng for bands less than 10 kb in length so species could be present in small amounts. In the case of incomplete transcripts transfected into cells during SVLuc DSG production, components of the 3'UTR would be lost. Sequence elements within the 3'UTR are required for initiation of the production of negative sense SV genomic RNA through interactions with the negative strand synthase (Strauss and Strauss 1994), hence replication of these virus genomes could not occur. It is possible, however, that co-infection/transfection alongside full length replication competent genomes could lead to packaging of incomplete genomes through capsid association with the nucleation signal in the nsp1

coding region (Chapter 1.3.3). These would still not be replication competent upon infection of any subsequent cells hence would not amplify, or be packaged, unless again co-infection with full length genome SV occurred. This would mean that with increasing rounds of virus replication, non-transgene containing variants would be selected against.

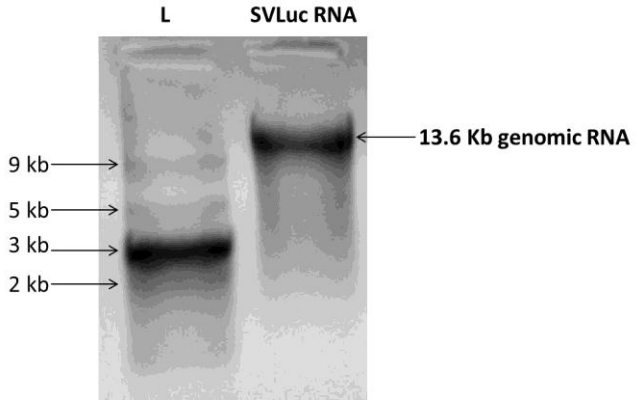

Figure 3.8: RNA agarose gel electrophoresis of SV RNA – Genomic SVLuc DSG RNA was analysed by agarose gel electrophoresis as described in Chapter 2.5. All equipment was cleaned with RNAse Zap before use to inactivate RNase degradation of sample RNA and buffers were made up using di-ethyl pyrocarbonate (DEPC) treated water. RNA was produced by *in vitro* transcription as described in Chapter 2.8. 500 ng SVLuc genomic RNA and 1 µg ssRNA ladder were added to 2x loading buffer and 1 µg ethidium bromide before gel loading. L: ssRNA Ladder.

3.2.8.3 RNA-RNA recombination

A third possible explanation is that transgene deletion from SV occurs through intracellular RNA-RNA recombination where the RdRp skips from one part of a template genomic RNA molecule to another. In this case, any resulting luciferase deleted clone would have a competitive advantage; hence outgrow luciferase expressing counterparts over increasing cycles of replication.

It may be that sequences brought into close proximity through the formation of RNA loop structures allow this manner of template "skipping". It may also be possible that the SV RdRp skips from one genomic RNA molecule to another analogous to previously described "template switching" (Raju, Subramaniam et al. 1995). In order for this to occur, separate genome molecules would need to be brought into close proximity. It could be that during SV infections at low MOI, genomic RNA is rapidly sequestered by host proteins and hence there is little free RNA. This could mean that upon transfection SV RNA to cells, or at high MOIs, there are higher numbers of free RNA SV RNA molecules in a cell, and hence a higher likelihood of RNA-RNA molecule interactions which may facilitate recombination.

It is of note that SV may not have evolved any mechanisms to prevent RNA-RNA recombination as with such a short genome, the vast majority of coding and non-coding RNA sequences are required for successful productive virus infection. The loss of any essential region would therefore be strongly selected against. In contrast, in the case of SV reporter viruses encoding a non-essential reporter transgene, any recombination product lacking the transgene encoding region would be at a selective advantage. This is by virtue of a shorter time required for genome replication and a lower metabolic burden on infected cells due to the production of 1 less protein.

3.2.9 Analysis of the Mechanism of Loss of Transgene Expression

To check whether observed losses of luciferase expression are the consequence elimination of the whole luciferase transgene or production of non-functional protein, clones from SVLuc DSG stocks were analysed. Clones were isolated by serially diluting stock virus and collecting supernatant from wells showing CPE after 5 days. The luciferase expression capacity of each clone was analysed after 16 hour infections of fresh BHK monolayers, those with differential luciferase expression were selected for analysis. In cells infected with clones 8.2 and 8.1, levels of luciferase expression was zero, whilst levels of luciferase expression on infection with clones 4.5 and 4.4 were ~ 3 x 10^5 RLU/μg protein (Figure 3.9 A). The total number of virus particles in each clonal preparation was similar, as the numbers of copies of nsp1, detected by RTQPCR, were not significantly different (Figure 3.9 B). To test whether the luciferase gene had been deleted or was present upon measured loss of expression/function, RNA was extracted from non/expressing clones and reverse transcription with random hexamers was used to create cDNA libraries of each clone. These were analysed by PCR with primers overlapping the SV genome and 5' and 3' ends of the luciferase gene. Results showed that in non-expressing clones, the luciferase gene was lost (Figure 3.9 C). This interpretation discounts the unlikely scenario that multiple point mutations had occurred in both 5' and 3' regions of the gene in which primers were designed to anneal.

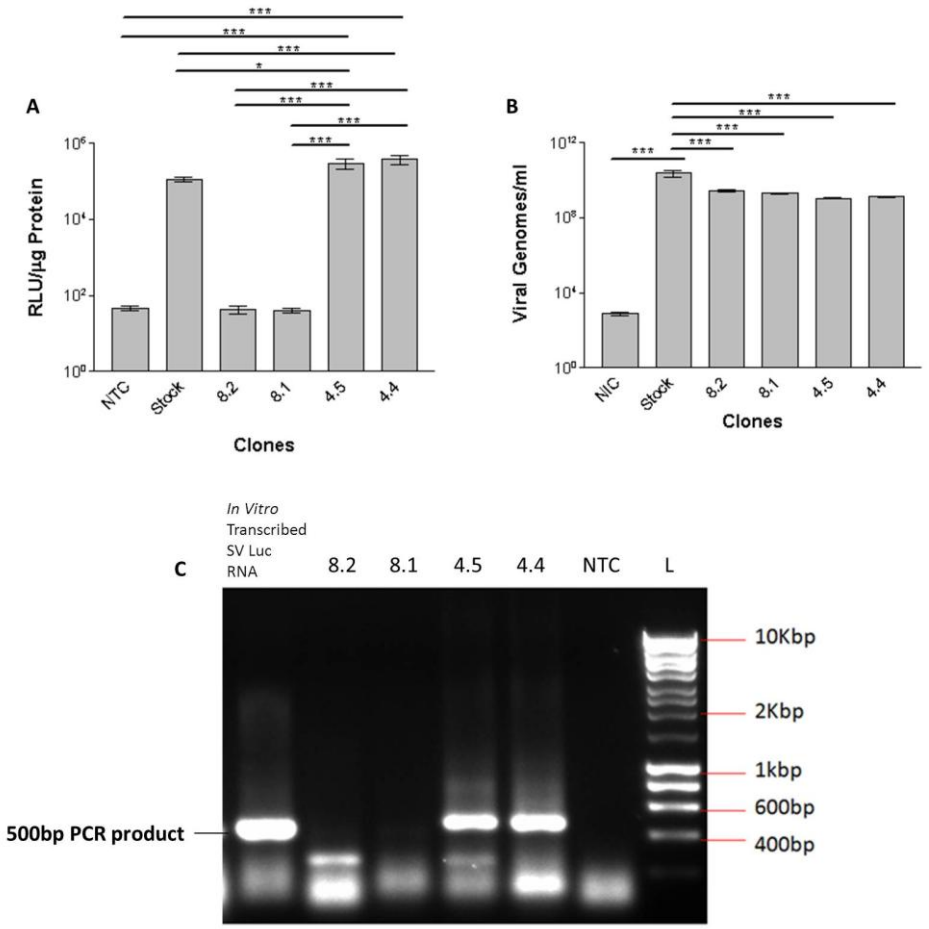

Figure 3.9: Luciferase Expression of SVLuc DSG Clones – A) Luciferase expression of SVLuc DSG clones 8.2, 8.1, 4.5 and 4.4 by luminometry following infection of BHK cells with equal volumes of virus containing supernatant 24h PI. B) Virus titers of each clone as detected by RTQPCR using primers and probes for the nsp1 polymerase encoding region of the Sindbis genome. C) Detection luciferase encoding RNA in SVLuc DSG clones. Primers used were designed to overlap the luciferase and E3 encoding region and the Sindbis genome. NTC: non-template control, L: Hyperladder II. **A)** and **B)** Statistical analysis by one way ANOVA with Tukey's multiple comparison post-test. Error bars show $\pm$ SD, n = 3. Statistical significance is indicated on each graph. (* = $P < 0.05$, *** = $P < 0.001$)

SVLuc DSG, produced by transfection of *in vitro* transcribed RNA into BHK cells, was serially passaged ten times for in order to further examine loss of luciferase expression. As initial stocks express luciferase, it was predicted that conversion to a non-expressing phenotype, and the kinetics of such a conversion, may offer insights into whether luciferase loss observed in previous experiments was due to accumulation of point mutations or deletion of the luciferase transgene. Passage 1 consisted of infection of BHK cells in a 6 well plate at an MOI of 1 PFU/cell and collection of 140 µl supernatant 16 h PI for RNA extraction, and 50 µl for subsequent passage; this was repeated until passage 10. Analysis of the presence of luciferase in SV of differing passages was achieved by extracting RNA form virus-containing supernatant. First, the number of copies of the essential nsp1 gene was quantified by RTQPCR as a surrogate for viral titre, which is at a distant site in the genome from luciferase (Figure 3.10 A). Also, the presence of the luciferase gene was analysed qualitatively by 2-step RTPCR detection using the same extracted RNA as in Figure 3.10. Reverse transcription was performed using random hexamers and PCR was performed using primers for a 500 bp region spanning the 5' portion of the luciferase gene and overlapping the SV genome (Figure 3.10 B). Results show a rise in SV titre between passages 1 and 3 after which it remains reasonably constant. This suggests by passage 3, the maximum number of virions able to be produced under these conditions is reached. With increasing passage number the number of virus particles containing the luciferase transgene is reduced whilst titre remains unaffected. It is of note that due to the exponential nature of PCR detection, DNA bands seen from passages 1-8 that appear similar in intensity, may represent considerable variations in the number of luciferase gene copies initially present in virus-containing supernatant due to “topping out” of either PCR reagents or saturation of

exposure during picture acquisition. This observation is in line with the predicted for transgene loss by RNA-RNA recombination (Chapter 3.2.8.3).

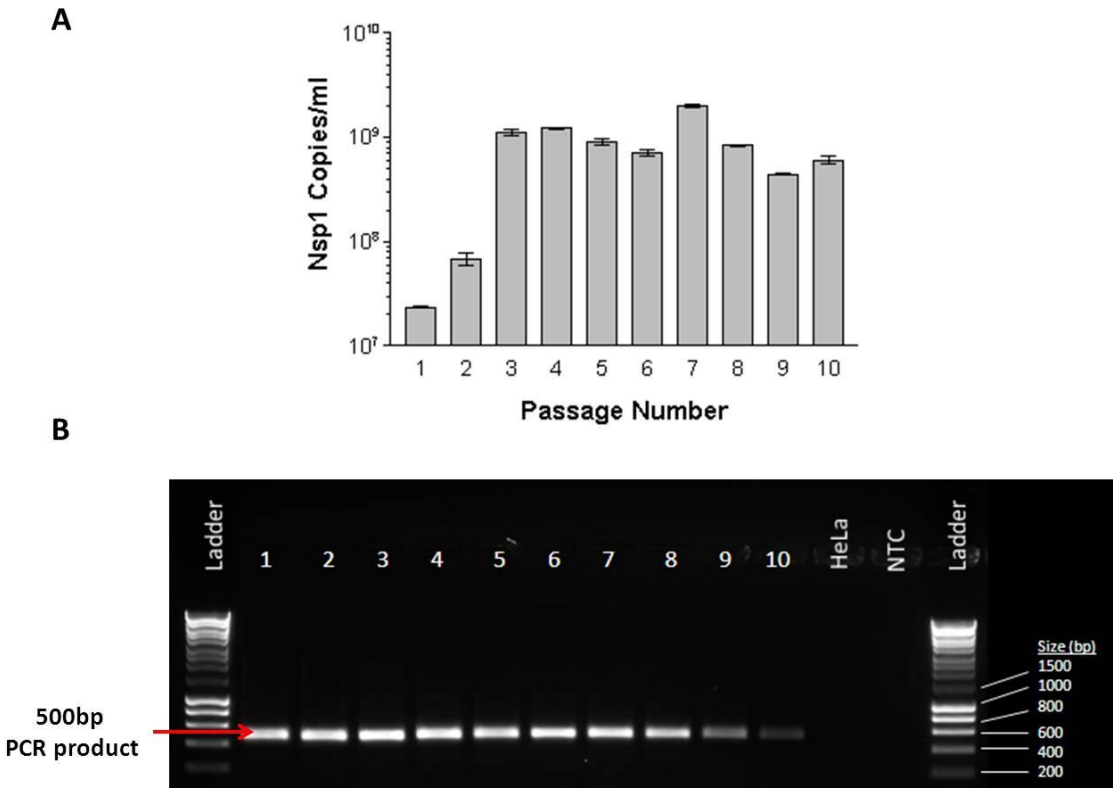

Figure 3.10: SVLuc DSG Loss of Luciferase Gene upon Passage – 6 well plates seeded with 2.5 x 10^5 BHK cells and infected at an MOI of 1 PFU/cell. 16h PI 140 µl supernatant was collected for RNA extraction and 50 µl for subsequent passage; this was repeated until passage 10 **A)** Nsp1 copies were detected by RTQPCR with primers and probe for the nsp1 encoding region of the genome as described I Chapter 2.16. **B)** Luciferase gene copies were detected by RTPCR with primers spanning a region overlapping E3 and the 5' luciferase encoding region as described in Chapter 2.15. RTPCR products were gel extracted using the QIAquick Gel Extraction Kit (Qiagen, UK) and analysed by agarose gel electrophoresis as described in Chapter 2.7 and 2.5 respectively. Equal volumes of extracted RNA were loaded into RTQPCR, RTPCR reactions and agarose gels. 1 – 10 = Passage numbers, L = Hyperladder I, HeLa = DNA extracted from HeLa cells, NTC = Non template control.

As data from Figure 3.10 B is not quantative, a set of primers and a probe were designed targeting the luciferase gene to accurately quantify the amount of virus genomes containing the luciferase gene. RTQPCR detection of luciferase and nsp1 gene copies was carried out simultaneously (Figure 3.11). Results revealed a sigmoidal decay curve of luciferase gene loss and that the amount of virus particles encoding the luciferase gene in our initial stock was only about 40% and this fell to about 0% by passage 8. The shift of the virus population to a non-luciferase expressing phenotype could be due to the presence of contaminating, non-luciferase expressing clones in initial virus stocks or deletion of luciferase from initially expressing clones. The observed pattern of sigmoidal decay suggests non-expressing SVLuc DSG variants outgrow their expressing counterparts, and appears to be in an exponential fashion. If the starting proportion of contaminating luciferase encoding SVLuc DSG particles is decreased, the half-life of luciferase gene expression, with respect to passage number, could therefore be increased. To apply this, a method to isolate luciferase expressing clones was developed.

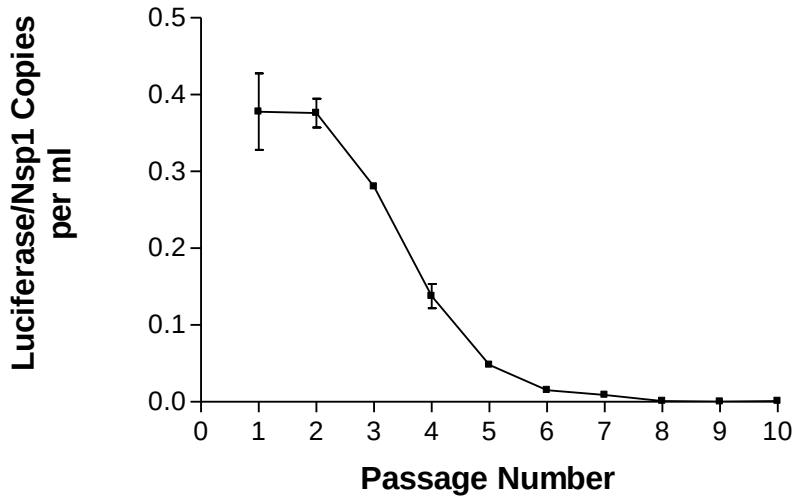

Figure 3.11: Proportion of Luciferase Transgene Encoding SVLuc DSG Particles – RNA extracts from serially passaged SVLuc DSG from Figure 3.10 were analysed for the ratio of nsp1 and luciferase gene copy numbers by detection of the total number of each utilising nsp1 and luciferase specific primers and probes as described in Chapter 2.16.

3.2.9 Prevention of Transgene Loss

To select clones of SVLuc DSG, limiting dilution method was utilized. Serial dilutions of virus containing supernatant were added to BHK cell monolayers and 5 days PI supernatants were collected from wells showing CPE at the highest dilution factor. These were analysed for luciferase expression by a 24 h infection of fresh BHK monolayers and the variant showing the highest luciferase expression was taken to the next round of selection. This was repeated three times and resultant viruses were grown (Figure 3.12 A). The purified SVLuc DSG clone containing an intact luciferase gene was serially passaged ten times. RTQPCR was used to detect the number of nsp1 and luciferase genes to determine if serial clonal isolation decreased the rate of luciferase gene loss from SVLuc DSG preparations (Figure 3.12 B). Growth of SVLuc DSG from an isolated luciferase expressing clone increased the initial proportion of luciferase encoding SVLuc DSG particles compared to stocks collected 16 h after *in vitro* transfection of genomic RNA. The rate of luciferase gene loss, however, was similar. This suggests conversion of virus particles from a luciferase expressing to non-expressing phenotype through transgene deletion. This observation could prove massively detrimental in any clinical setting in which the SV encodes a therapeutic transgene. If delivered in low amounts and virus replication at the site of action is

required for therapeutic effect as transgene expression will rapidly be lost. With this in mind, we looked to utilize a genetic construct that could offer more genetic stability.

A

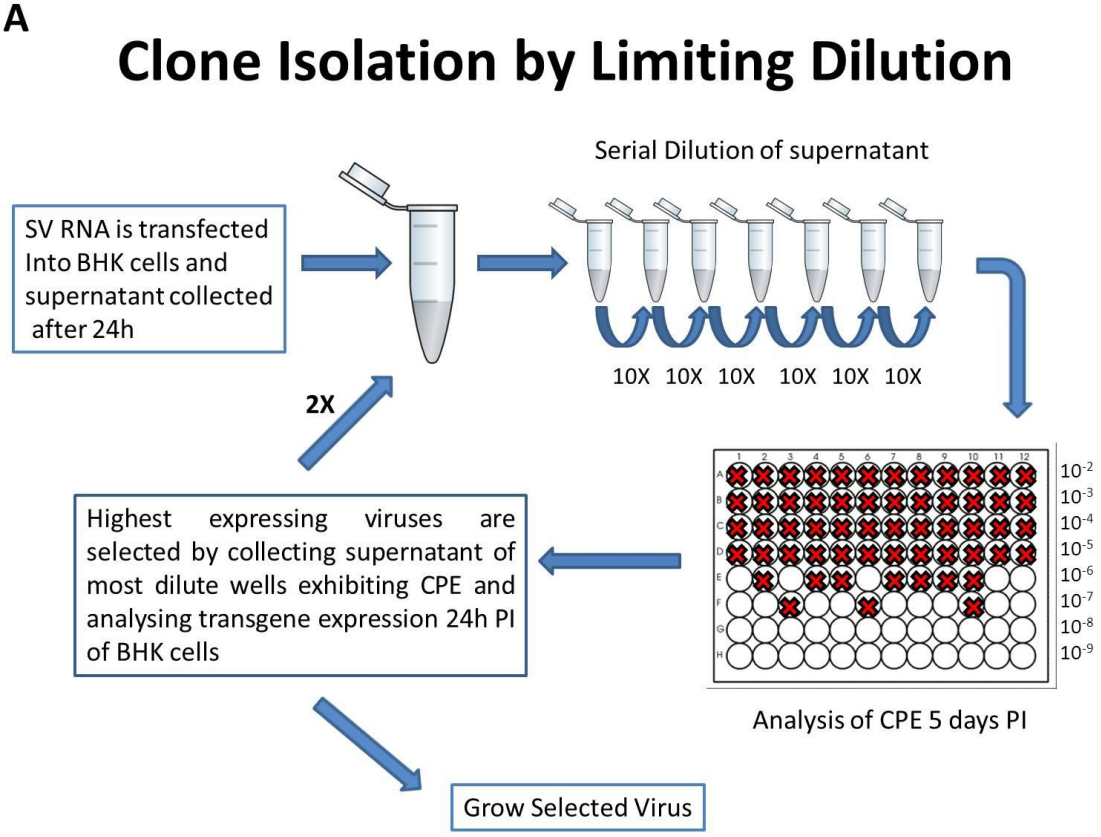
Clone Isolation by Limiting Dilution
Serial Dilution of supernatant
SV RNA is transfected Into BHK cells and supernatant collected after 24h
10X 10X 10X 10X 10X 10X
2X
Highest expressing viruses are selected by collecting supernatant of most dilute wells exhibiting CPE and analysing transgene expression 24h PI of BHK cells
10-2 10-3 10-4 10-5 10-6 10-7 10-8 10-9
Analysis of CPE 5 days PI
Grow Selected Virus

B

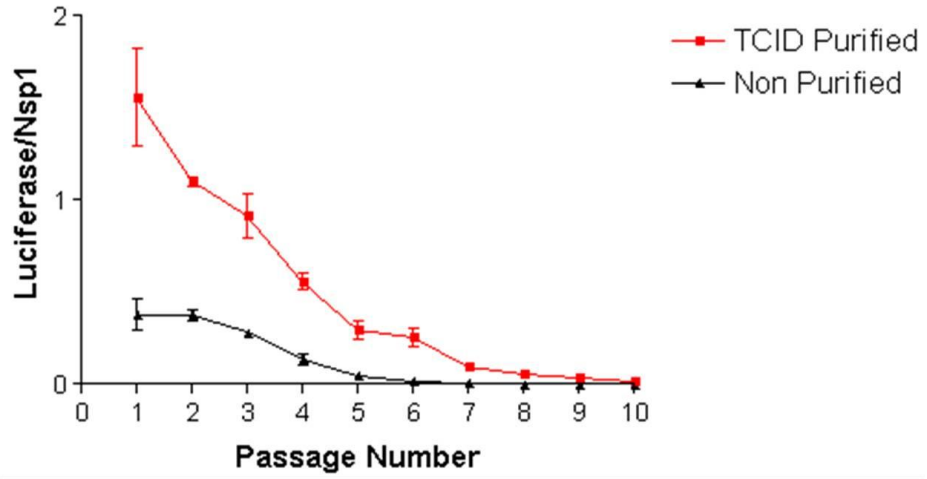
TCID Purified
Non Purified
Luciferase/Nsp1
Passage Number
0
1
2
0 1 2 3 4 5 6 7 8 9 10

Figure 3.12: Analysis of Clonal SVLuc DSG Upon Serial Passage - A) Overview of purification of luciferase expressing SVLuc DSG clones. Virus preparation from transfection of BHK cells with *in vitro* transcribed RNA was serially diluted and incubated with BHK cells in 96 well plates for 5 days. Supernatant was collected from wells at the highest dilution factor displaying SV induced CPE, 5 µl samples of this virus-containing supernatant was analysed for luciferase expressing capacity through infection of fresh BHK cells. The remainder of supernatant with the highest level of luciferase expressing activity was serially diluted and the process repeated twice. **B)** Clonally derived SVLuc DSG was serially passaged as in Figure 3.10 and proportion of nsp1 and luciferase genes present analysed as in Figure 3.11.

3.2.10 FMDV2A Self Cleavable Transgene System

The insertion of transgene in the 3'UTR in the SVLuc DSG and SVGFP DSG may allow high rates of reversion to wild type phenotype as any RNA-RNA recombination events in this region are unlikely to involve RNA that encodes virus proteins essential for productive SV infection. To investigate this, a Sindbis Virus was constructed with the desired transgene, either luciferase or eGFP, encoded as part of the structural polyprotein but produced as a free protein because of the non-peptide bond formation function of the Foot and Mouth Disease Virus 2A peptide (FMDV2A).

The structural proteins of SV are produced as a polyprotein (Figure 1.2) from which the capsid protein is self-cleaved and proteins PE2, 6K and E1 are cleaved by endoplasmic reticulum Signalase. PE2 is further cleaved into E2 and E3 by furin protease in the golgi apparatus (Figure 3.13). Luciferase and eGFP transgenes were inserted between capsid and PE2 in the structural polyprotein so that any RNA-RNA recombination events leading to loss of the inserted transgene would also likely lead to interruption of adjacent RNA that encodes the SV structural polyprotein. Mutations causing frame

shifts in this region would cause loss of replication competence, as would any mutations affecting protein encoding regions of essential function. This system, therefore, may provide a degree of selective pressure for SV to retain the inserted transgene, potentially, decreasing the rate of wild type reversion of SV reporter viruses.

Insertion of the FMDV2A peptide downstream of the inserted transgene is to provide a means of separation of the transgene from the viral polyprotein by non-peptide bond formation without terminating RNA translation. The mechanism by which this occurs is outlined below (Brown, Ryan et al. 2010):

- Firstly, interactions between the FMDV2A nascent peptide in the ribosomal exit tunnel cause stearic strain on the C terminal peptide in the peptidyl transferase center of the ribosome. This inhibits nucleophilic attack of $tRNA^{gly}$ by prolyltRNA in the A site stalling of the ribosome with prolyl-tRNA in the "A" site (Donnelly, Luke et al. 2001).
- Prolyl-tRNA exits the "A" site
- eRF1/3 (eukaryotic translation release factors 1 and 3) enter the "A" site and hydrolyse the bond between the terminal glycine of the nascent peptide and its tRNA causing release of the peptide relieving inhibition of protein synthesis (Doronina, de Felipe et al. 2008).
- Either translation terminates or reinitiates to translate the rest of the mRNA molecule sequence bound to the ribosome with proline on the N-terminus of the downstream peptide.

During SV replication, subgenomic RNA is translated to form a polyprotein which is subsequently cleaved to yield the viral structural proteins (Figure 1.2). Capsid protein contains a fold analogous to that of chymotrypsin by which it cleaves itself off the polyprotein. Whilst the structural polyprotein is being translated the capsid protein folding process places the cleavage recognition sequence in the protease active site. In this way, capsid cleaves the polyprotein to which it is attached, releasing itself. After cleavage, the protease active site remains occupied, preventing capsid protein from cleaving any subsequent peptides. PE2 (which is subsequently cleaved to give E2 and E3 by host furin protease), 6K and E1 are released by cleavage at two sites by the signalase of the ER lumen (Figure 3.13). Utilising the FMDV2A peptide a transgene can be expressed as part of the SV structural polyprotein whereby it is released by stop/start translation.

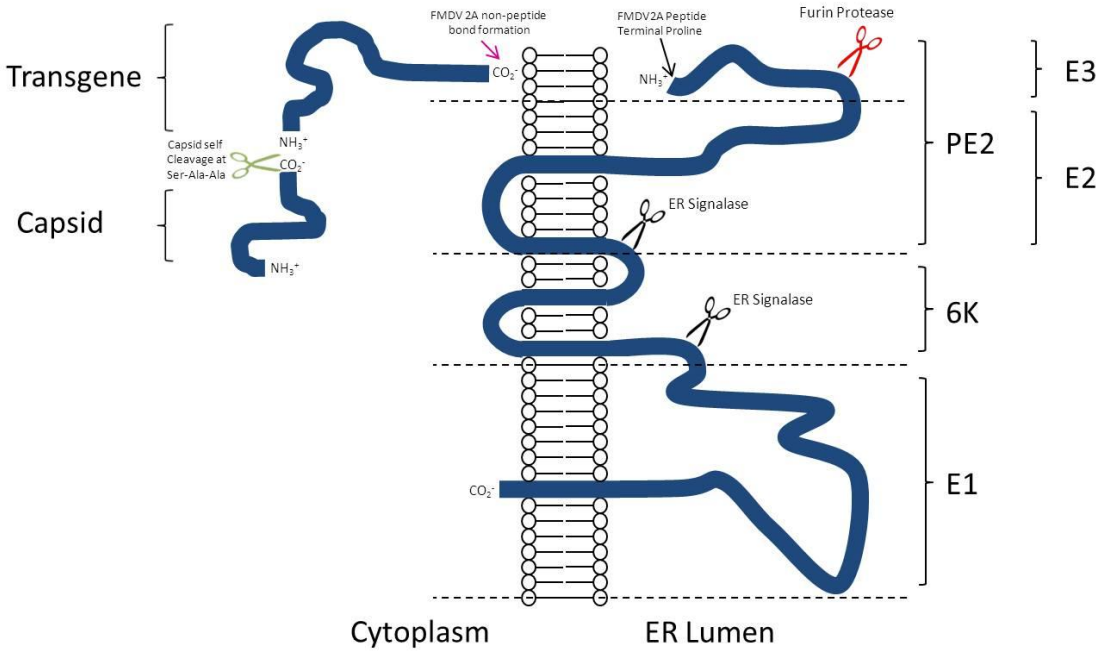

Figure 3.13: Processing of the Structural Polyprotein – As the SV structural polyprotein is translated, the capsid protein folding causes Ser-Ala-Ala, the cleavage sequence of capsid protease activity is positioned in its active site. This sequence is cleaved but remains in the active site, leaving capsid protein in the cytoplasm without additional protease activity. In the SV2A system, the FMDV peptide following the inserted transgene causes non-peptide bond formation between transgene and PE2, which has an ER localization signal. This causes retention of the transgene in the cytoplasm whilst PE2 contains a signal for ribosomal association with the rough ER and insertion of the remainder of the structural polyprotein into the ER membrane before subsequent cleavage by the ER signalase and furin protease.

3.2.11 Production of SVGFP 2A

In order to insert eGFP and FMDV2A sequence between capsid and PE2. a plasmid was synthesized along with the SV genome up to the next unique restriction sites in both directions (Aat II and Bcl I). The eGFP gene was synthesized with the start and stop codons removed and flanked by unique restriction sites (Nhe I and Xba I) for subsequent insertion of any other transgenes of interest followed by a region encoding the FMDV2A peptide. On inserting the transgene the first 9 base pairs of the PE2 encoding region were retained at the 3' end of the capsid as they encode the Ser-Ala-Ala sequence recognition site for the capsid protease to facilitate its release from the polyprotein.

A plasmid encoding pSVGFP 2A was produced by utilizing Aat II and Bcl I restriction sites that naturally occur in the virus genome to insert the edited region encoding eGFP and FMDV2A peptide (Figure 3.14 A). To produce a luciferase reporter construct site directed mutagenesis was used to remove start and stop codons from the luciferase gene. Nhe I and Xba I were used to insert the mutated gene into the synthesized plasmid upstream of the FMDV2A encoding sequence. Aat II and Not I were then used to insert the edited region into full the pSVGFP 2A plasmid with the GFP encoding region removed by digestion with the same restriction enzymes and AGE and gel extraction (Figure 3.14 B).

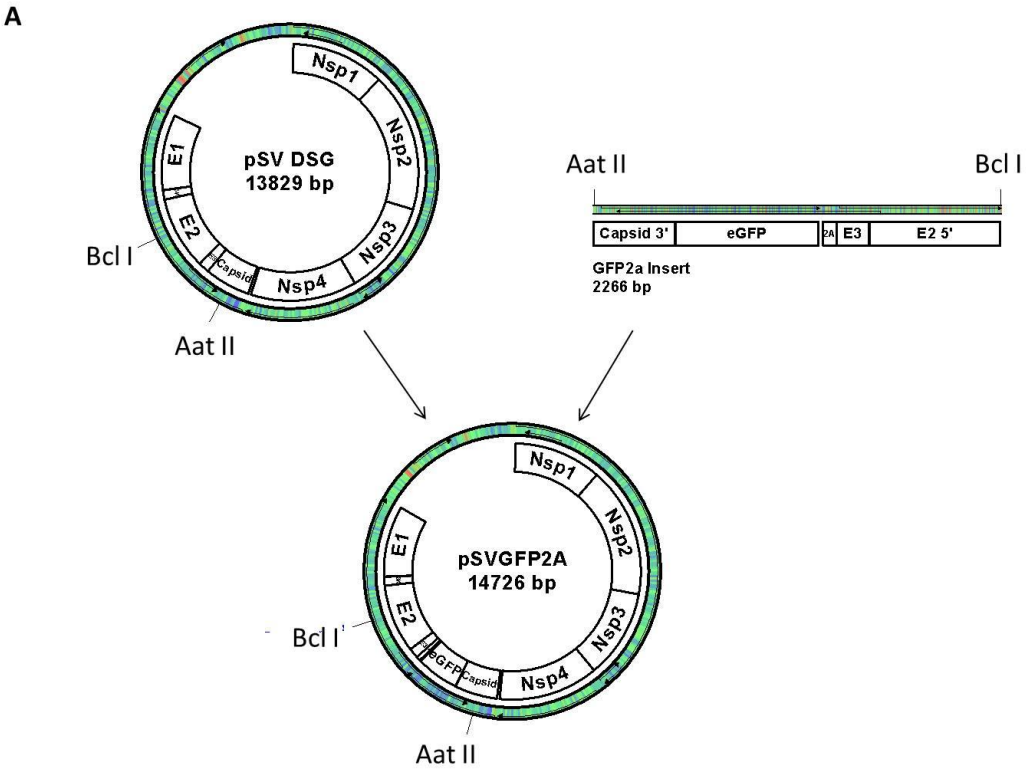
A
pSV DSG
13829 bp
Nsp1
Nsp2
Nsp3
Nsp4
E1
E2
Capsid
Bcl I
Aat II
Aat II
Bcl I
Capsid 3'
eGFP
2A
E3
E2 5'
GFP2a Insert
2266 bp
pSVGFP2A
14726 bp
Bcl I
Aat II
B
pSVGFP2A
14726 bp
Not I
Aat II
Aat II
Not I
Capsid 3'
Luciferase
E3
E2'
Luciferase 2A
3105 bp
pSVLuc2a
15559 bp
Not I
Aat II

Figure 3.14: Production of SV with eGFP or Luciferase Expressed as Part of the Structural Polyprotein- Overview of cloning strategies for production of pSVGFP 2A and pSVLuc 2A respectively. **A)** SVGFP 2A was produced by ligating DNA produced by cutting synthesised DNA and pSV DSG with Aat II and Bcl I as described in Chapters 2.3 and 2.4 **B)** The same strategy was applied to produce pSVLuc2A using pSVGFP 2A produced in A) and the restriction enzymes Aat II and Not I.

3.2.12 Rescue of SVLuc 2A and SVGFP 2A

Plasmids pSVGFP 2A and pSVLuc 2A were linearized with PVU I, *in vitro* transcribed and transfected into BHK cell as in the production of SV DSG (Chapter 3.2.2). SVGFP 2A could be reliably rescued (Figure 3.15) whereas several attempts to rescue SVLuc 2A were unsuccessful. As with all major cloning steps, the sequence of pSVLuc 2A was confirmed by sequence analysis, suggesting firefly luciferase may not be compatible with the FMDV2A system, however, this has been successful in the context of lentivirus transgene expression (Lin, Cheung et al.).

SVGFP 2A consistently grew to titres about 10 fold lower than SVGFP DSG, possibly due to premature termination events during translation (Chapter 3.2.10).

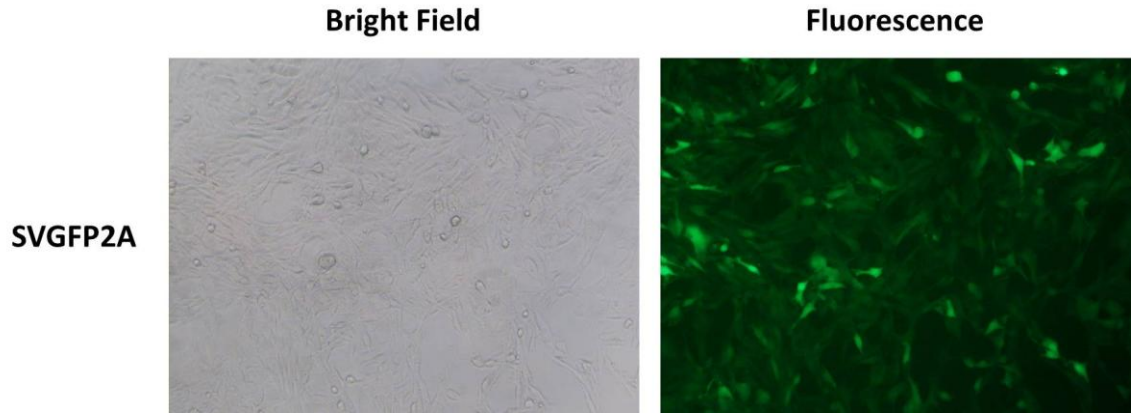

Figure 3.15: Confirmation of SV Rescue by Reporter Gene Expression – Visualisation of SVGFP 2A eGFP expression by fluorescence microscopy. Infection was carried out on BHK cells at an MOI of 1 PFU/cell and analysed 24 hours PI.

3.2.13 Comparison of SVGFP DSG and SVFGP2A

As rescue of SVLuc 2A failed, the effects of transgene insertion position was analysed utilising SVGFP DSG and SVGFP 2A.

To analyse whether loss of transgene expression upon serial passage was reduced by insertion of eGFP into the polyprotein coding region rather than under a duplicated subgenomic promoter, SVGFP DSG and SVFGP2A were compared. Each was serially passaged ten times on BHK cells and relative quantities of nsp1 and eGFP coding RNA were measured by RTQPCR (Figure 3.15). This experiment revealed first that the SV encoding eGFP appeared to be stable for more serial passages than SV encoding luciferase (3 compared to 6) (Figure 3.16 vs Figure 3.12). Second it showed that expressing the eGFP transgene as part of the viral structural polyprotein had little effect

on the number of passages before significant loss of transgene encoding regions compared to SVGFP DSG.

Deletion of eGFP is advantageous to SV as it shortens replication time, a major selective pressure *in vitro*. Concurrent loss of eGFP transgene and an increase in SVGFP 2A titre is probably due to the increased number of daughter SV virions which can be released before the terminal stages of apoptosis.

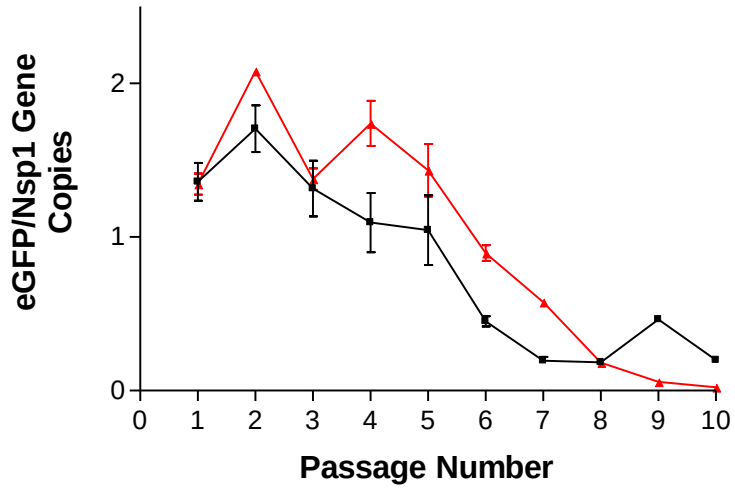

Figure 3.16: Comparison of the Rate eGFP Loss from SVGFP DSG and SVGFP 2A – SVGFP DSG and SVGFP 2A were serially passaged on BHK as in Figure 3.10 and the ratio of nsp1 and eGFP gene copies was determined after measuring the total numbers of each by RTQPCR as in Figure 3.11 with primers and probes for nsp1 and eGFP genes as described in Chapter 2.16.

3.2.14 Mechanism of Transgene Loss

Based on observations of loss of the luciferase gene by SVLuc DSG, it was originally hypothesized that the mechanism by which transgene RNA was eliminated from the SV genome was through RNA-RNA recombination events. It was postulated that these recombination events would interfere with adjacent RNA sequences, but as the transgene is encoded in the 3'UTR of this virus, that such recombination events could occur without interrupting essential protein encoding genomic regions (Figure 3.1 and Chapter 3.2.10). Data from Chapter 3.2.13 however, shows that the eGFP transgene, is eliminated from SVGFP DSG and SVGFP 2A at a similar rate, suggesting a shared underlying mechanism that does not interrupt other genomic regions, or at least does so at a low enough rate that replication competent recombination products arise rapidly.

Sequence analysis of serially passaged SVGFP 2A was carried out following RNA extraction and RTPCR of serial passages 1-10 using primers spanning the transgene encoding region. Results reveal that the SVGFP 2A eGFP transgene was deleted upon serial passage (Figure 3.17), as was the case with SVLuc DSG and its luciferase transgene (Chapter 3.2.8). Furthermore, it was seen that upon increasing passage, the genomic sequence of the SVGFP 2A population shifted to a dominant proportion containing a complete deletion of the eGFP transgene and FMDV2A peptide, except 13 terminal bases. This included a nucleotide mutation in the terminal nucleic acid of capsid protein (A801C), in a vital Ser-Ala-Ala encoding region susceptible to capsid protease activity and required for capsid release from the SV structural poyprotein. This mutation, however, results in a change of the terminal codon from GCA to GCC, which still encodes alanine as in wild type SV (Figure 3.17 - underlined). The terminal 13 residues of the FMDV2A peptide were retained this region encodes the “PGP” motif

required for non-peptide bond formation. The PGP motif, however, is unlikely to be functional as the full length FMDV2A peptide is absent, which plays an essential role in ribosome stalling (Chapter 3.2.10).

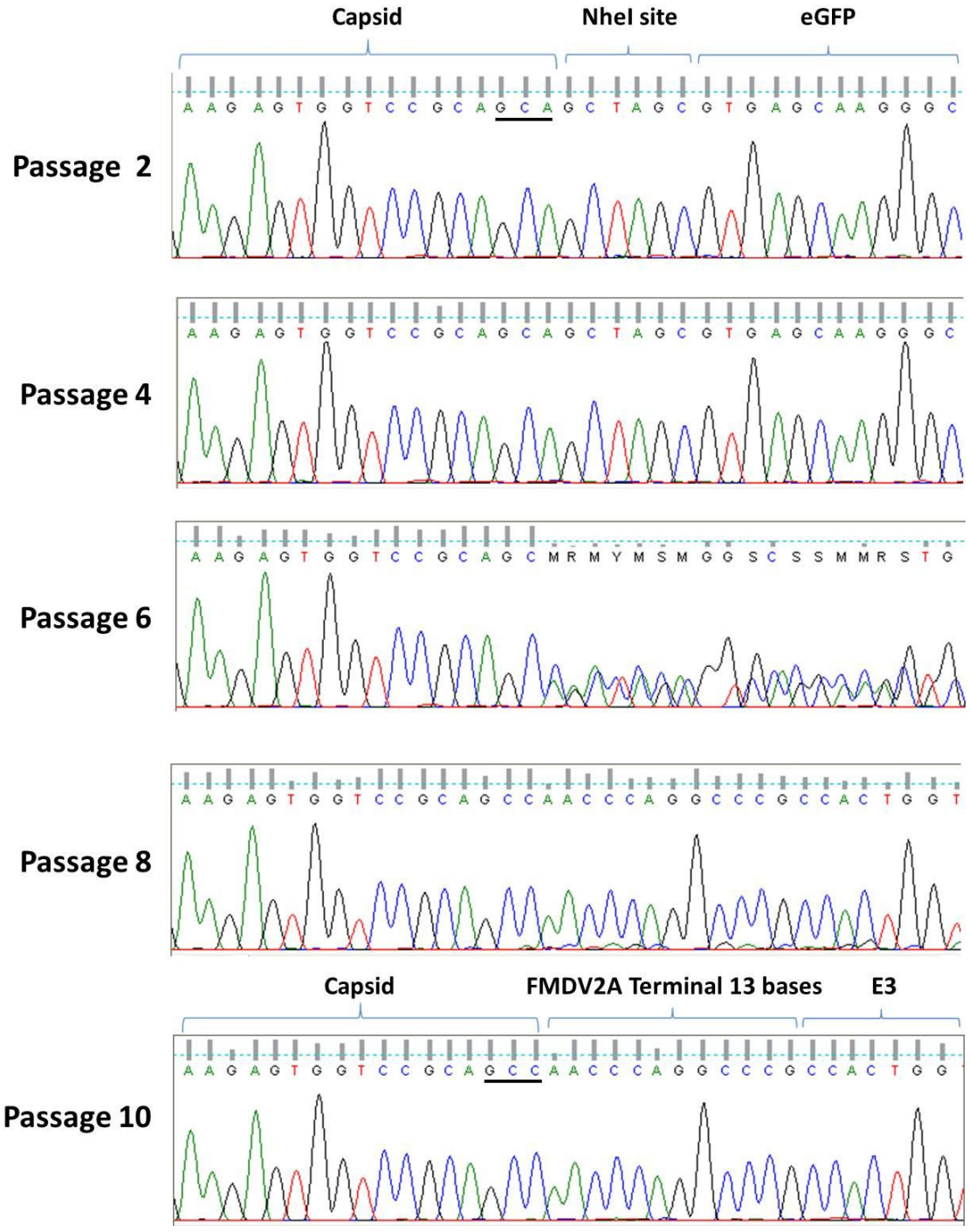
Capsid
NheI site
eGFP
Passage 2
Passage 4
Passage 6
Passage 8
Capsid
FMDV2A Terminal 13 bases
E3
Passage 10

Figure 3.17: Chromatogram of Early and Late SVGFP 2A Passages – RNA from serially passaged SVGFP 2A produced as in Figure 3.16 was converted to cDNA using specific primers binding in the SV genome (capsid and E3) spanning the eGFP encoding region. PCR was performed using the same primers, RTPCR products were purified using the QIAquick Gel Extraction Kit (Qiagen, UK). DNA sequencing was performed by Source Bioscience, UK and sequence analysis was carried out using FinchTV, PDraw32 and Microsoft Word.

Based on sequence analysis the way in which inserted transgenes are deleted from SV could be through a mechanism in which the virus RNA polymerase skips past transgene encoding regions. One way this might occur is through release of template RNA, by the viral plus strand or minus strand synthase, followed by re-association at another point on the same, or another, virus genome. This type of mechanism could be facilitated by the formation of hairpin secondary structures in viral genomic RNA, bringing genomically distant regions together spatially.

3.3 Concluding Discussion

Assessment of the yield and quality of stocks produced by multiple methods provides evidence that virus particles are damaged during high speed centrifugation. Thus, a standard protocol of purification of SV by filtering without centrifugation was established. It was also observed that SV can be stored in any standard labware vessel and at 4 °C for 1 week without losing infectivity. Freeze thawing severely decreases SV particle infectivity as surrounding water molecules participate in formation of ice crystals, generating shear forces on interrupting virus particles. DMSO, FCS and 5% sucrose all reduced loss of infectivity resulting from freeze/thawing, probably as clathrate structures formed around guest solute molecules in water interrupt ice crystal growth. Upon freezing, water bound to virus surface proteins through hydrogen bonds participate in crystal lattice ice structures. This often involves an entropy driven change in orientation, creating push, pull and shear forces on bound virus surface proteins. The replacement of bound water molecules with cryoprotectants prior to freezing can aid retention of biological conformation as upon freezing, cryoprotectant molecules do not participate in ice crystal formations.

SV is efficiently taken up into cells at 37 °C and uptake plateaus at around 15 minutes at an MOI of 1. The level of transgene expression and release of new daughter virions also plateaus at around 24 hours. Based on these observations, the standard protocol for SV infections was set as incubation with cells for 30 minutes, washing cells with warm PBS, and measuring transgene expression or virus replication 16 h PI.

It was shown that SV is capable of infecting a wide range of cell lines as is the case with the parental AR339 strain, showing that *in vivo* passage on mouse brains has not restricted virus tropism to neuronal cell types.

SV expressing non-essential reporter transgenes rapidly reverts to a wild type phenotype. This was demonstrated with purified SVLuc DSG and SVGFP DSG clones to be through a mechanism resulting in complete loss of the inserted gene. Reversion to wild type of SVLuc DSG was more rapid than SVGFP DSG with loss of ~50% transgene from the virus population at serial passage 4 and 6 respectively. This is presumably due to the increased length of the luciferase gene (1.7 Kb) compared to eGFP (0.8 Kb), meaning the selective advantage to SV having deleted the former gene is greater. Comparison of SVGFP DSG which encodes eGFP in the 3'UTR to SVGFP 2A, which encodes eGFP as part of the SV structural polyprotein, revealed that this phenomenon occurred at a similar rate irrelevant as to the position of the inserted transgene. These findings are in contrast to a previously published study that reported retention of GFP or bluetongue virus VP7 protein for 10 serial passages when using an analogous Sindbis virus FMDV2A peptide cleavage system for transgene expression (Thomas, Klimstra et al. 2003). RTQPCR, however, was not used to accurately quantify relative numbers of virus genomic and transgene encoding RNA.

SV deletion of inserted transgenes is a remarkable efficient process. In order to calculate the maximum possible number of rounds of SV genome replication it was assumed that upon serial passage of SVGFP 2A, each daughter virus genome is produced by doubling of a parental genome. Based on the numbers of SV genomes measured by RTQPCR of input and output virus at each passage, the total number of genome doublings was 49.6 over 10 serial passages. Based on the measured fidelity of the SV RdRp, one would

expect to observe 1 mutation per 497 copying events of the SVGFP 2A. This mutation rate would therefore yield an insignificant number of mutated genomes at this point.

Furthermore, it is known that superinfection exclusion occurs in SV infections (Chapter 3.2.8.1) so a limited number SV genomes are the templates of all the new virus particles released from that cell. This means that in order for mutations introduced to daughter genomes to be passed on to further generations of virus progeny, daughter genomes bearing mutations must successfully infect a new cell. Upon 10 serial passages of SVGFP 2A, therefore, there are only around 10 successive genome copying events, hence the observation that transgene is completely lost from SVGFP 2A by passage 8 cannot be reconciled by RdRp infidelity.

The complete lack of any transgene encoding sequence by passage 8, suggests that revertant virus has a dramatic ability to outgrow the original virus pool, whatever its mechanism of creation. Superinfection exclusion probably has a large role to play in this outgrowth as it means that the first viruses to enter an uninfected cell can pass on their genomes to virus progeny. Those that arrive after cellular machinery required for replication is already saturated with other SV genomes cannot, hence are rapidly outcompeted from the population.

This strongly suggests that any oncolytic or gene therapy approach utilising SV, cannot expect continued expression of any inserted gene, such as a pro-drug activator or immune modulating cytokine, unless it confers a selective advantage to the virus. Unless this problem can be addressed, potential applications of transgene expressing SV will be limited to those that require a short duration of expression, such as production of high levels of an antigen to prime immune responses.

4 MicroRNA Controlled Sindbis Virus

4.1 Introduction

A significant drawback to the development of SV as an oncolytic agent is that virus pathogenesis in *in vivo* mouse models does not correlate with that in humans. In infant mice SV infection is neurotropic and causes severe encephalitis, paralysis and death, whilst in adult mice there are no apparent symptoms of pathology. In humans, SV is the causative agent of Pogosta disease, causing symptoms such as fever, rash and polyarthritis, with joint symptoms lasting for a number of years in some patients (Kurkela, Manni et al. 2005). Although such side effects might be acceptable if accompanied by high anticancer potency of the virus, it would be ideal if these side effects could be eradicated. One way to achieve cell-selective attenuation of SV without reducing its oncolytic activity could be through the use of MREs.

As discussed in Chapter 1.4.4, the expression of many miRNA molecules is tissue-specific (Landgraf, Rusu et al. 2007). This affords the possibility of producing tissue de-targeted replicating viruses by inserting MREs into the viral genome, which are complementary to miRs expressed specifically in tissues. This can be used to prevent replication in the tissues in which the wild type virus causes pathological symptoms (Edge, Falls et al. 2008; Cawood, Chen et al. 2009; Kelly and Russell 2009). In the context of virotherapy, this is ideal, allowing production of viruses that show wild type replication in tumours whilst being attenuated at sites of potential pathology.

When RISC loaded miRs bind mRNA, and sequences are not perfectly complementary, protein synthesis is inhibited through repression of translation; mRNAs are targeted to P-bodies and subjected to accelerated 5' de-capping (Valencia-Sanchez, Liu et al. 2006). As well as inhibiting protein expression through inhibition of translation, target mRNA

sequences can be directly cleaved by the RISC. Endonucleolytic cleavage by the RISC is generally favoured by perfect base-pairing between the miR and target mRNA, although some mismatches can be tolerated and still allow cleavage to occur (Mallory, Reinhart et al. 2004; Yekta, Shih et al. 2004; Guo, Xie et al. 2005) (Figure 4.1). MiR directed cleavage activity of RNA by the RISC has been utilized in the attenuation of a number of viruses through the introduction of MREs, as discussed in Chapter 1.4.5-7. This concept has been shown to be possible through the incorporation of MREs into viral genomes of RNA viruses or transcripts of genes of DNA viruses essential for replication (Cawood, Chen et al. 2009; Kelly and Russell 2009).

4.1.1 Aims

- To produce SVmiR-T viruses by introducing MREs to miRs specifically expressed in liver, neuronal, muscle and haematopoietic tissues
- To assess whether SVmiR-T viruses can be attenuated by the presence of complementary miRs by transfecting pre-miRs into a non-expressing cell type prior to infection
- To identify cell lines that express high levels of miRs of interest and assess the level of attenuation of SVmiR-T variants in these cells
- To test miR mediated attenuation of SVmiR-T in human tissue

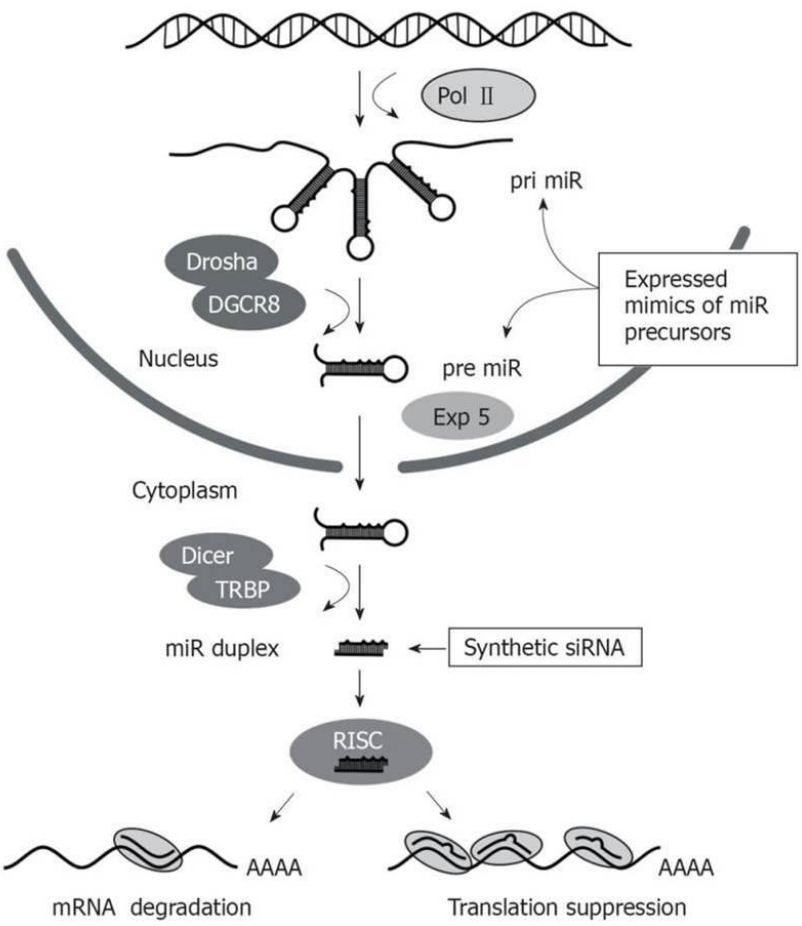

Figure 4.1: Micro RNA processing – Pri-miRs are transcribed in the nucleus, processed to pre-miRs by DGCR8 and Drosha, and exported to the cytoplasm by exportin 5. Once in the cytoplasm, pre-miRs are loaded onto the RISC complex and guide it's mRNA degradation and translational repression (Arbuthnot and Thompson 2008).

We hypothesize the potential sites of pathological SV replication in humans to be:

- Neurons: In mouse models immature mice succumb to Sindbis Virus induced encephalitis. Also, the closely related *Alphavirus* (SFV) displays preferential replication in neuronal cells (Graham, Walker et al. 2006)
- Muscle: Myalgia is a symptom of Pogosta disease whose causative agent is Sindbis virus (Ryman, Klimstra et al. 2000). This might reflect tissue damage due to virus replication.
- Macrophages and joints: Patients with Pogosta disease show symptoms of joint aches for periods of up to 2 years. This could be due to chronic infection and inflammatory response of macrophages resident in connective tissue, or direct infection of connective tissue itself.
- Liver: The liver receives about 30% of the resting cardiac output. It is a common site of accumulation for any IV delivered viruses, probably due to their particulate nature and surface properties. Virus particles are likely to be phagocytosed by Kupffer cells and may also infect hepatocytes, hence SV may infect a variety of cell types in the liver.

On analysis of a mammalian miRNA expression profile (Landgraf, Rusu et al. 2007), we identified miRNAs expressed with high specificity in each of the tissues mentioned above (Figure 4.2). Previous research has shown that the greater the number of copies of MREs present in a virus genome, the more efficient the attenuation in tissues expressing complementary miR (Cawood, Chen et al. 2009). With a greater number of MRE copies, however, comes a greater the risk of the formation of secondary RNA structures,

which may interfere with virus replication. With this in mind we incorporated 4 MREs into the 3'UTR of SV. Each MRE bears perfect complementarity to the corresponding tissue specific miR selected. This design means that both positive-sense genomic and subgenomic RNAs of Sindbis Virus should be able to bind cognate miR, if present, and hence be cleaved by RISC (Figure 4.1 and Figure 4.3 B).

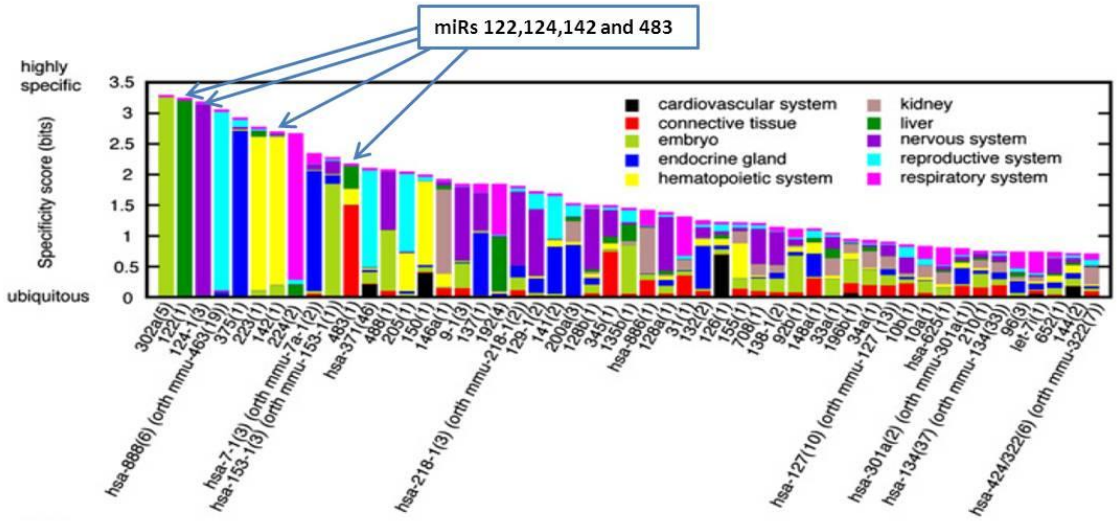

Figure 4.2: - Human Tissue miRNA Profile - Highlighted miRs have highly specific expression in tissues that may contribute to pathological symptoms during SV infection of humans. Reproduced from (Landgraf, Rusu et al. 2007), with permission.

4.2 Results

4.2.1 Selection of Regulatory MiRs

Sequences with perfect complementarity to tissue specific miRs were inserted into the 3'UTR of SV, so that upon infection of corresponding tissues, endogenous miRs will guide RISC mediated degradation of SV RNA.

MiRs with high specificity to tissues in which SV replication potentially causes pathological symptoms in humans, were identified. Those conserved between mice and humans were selected for engineering into SV on the premise that they could be tested in human and mouse models both *in vitro* and *in vivo* (Table 4.1). On this basis, liver specific miR122, neuron specific miR124-1, muscle specific miR133a and 206 and haematopoietic specific miR 142-3p were selected for development. Joint specific miR483 was not taken forward as it does not have paralleled tissue specific expression in joints in mice as it does in humans hence, would not be suitable for evaluation in mouse models.

4 identical MREs, perfectly complementary in sequence to selected tissue specific miRs, were engineered into the 3'UTR of SV to create separate tissue de-targeted variants. Muscle tissue de-targeted SV, in contrast, had a combination of 2 miR133a MREs and 2 miR206 MREs. This difference in design was based on previous research by Kelly et al (Kelly, Hadac et al. 2008), who showed that the introduction of 4 MREs to either miR133a or miR206 was less efficient at attenuating coxsackievirus in muscle cells than a combination of 2 + 2 of each.

MiRNA	Tissue of Expression	Sequence of miRNA	Comparison to Murine miRNA Sequence
Hsa-miR-122	Liver	15 -uggagugugacaaugguguuug - 36	Single forms with identical binding sites mice and humans
Hsa-miR-124-1	Neuronal	53 - uaaggcacgcggugaaugcc - 72	In mice and humans consists of forms 124-1, 2+3, but all binding sites are of the same sequence
Hsa-miR-133a	Muscle	53 –uuuggucccuucaaccagcug - 74	In humans and mice consists of forms 133a-1, a-2 and b.b forms differ with a single change of the terminal g to a
Hsa-miR-142-3p	Macrophages	16 – uguaguguuuccuacuuuaugga - 36	miR142 and miR142-5p are produced from the same precursor, sequence is conserved in humans and mice
Hsa-miR-206	Muscle	53 -uggaauguaaggaagugugugg- 74	Single forms with identical binding sites mice and humans

Table 4.1: Sequences of Tissue Specific MiRNAs – Perfect reverse complement sequences of these miRs were encoded in SV in order to attenuate virus replication and protein expression in these tissues.

4.2.2 Cloning of SV DSG MiR-T variants

Site directed mutagenesis was utilized to insert a unique Not I restriction enzyme site directly downstream of an existing Xba I site in the 3' UTR of the SV genome in the pSV DSG plasmid.

Single stranded DNA oligomers were chemically synthesised containing the required MRE sequences. Reverse complement sequences were also synthesised and complementary oligos were annealed together to make dsDNA with sticky end overhangs of Xba I and Not I restriction enzyme sites at the 5' and 3' ends respectively.

First, Not I restriction enzyme sites were introduced into pSVGFP DSG before insertion of miR-T sequences. Restriction digestion of pSV DSG with Xba I and Not I, dephosphorylation, purification and ligation with annealed oligos, allowed the production of 4 SV variants; each with MREs to miRs expressed in specific tissue types. Once plasmids of SV variants had been cloned, plasmids were sequenced to confirm insertion of MREs. Genomic maps of the 3′ regions of the resulting viruses are shown (Figure 4.3 A).

4.2.3 Rescue of MiR-T SV Variants

Viruses were rescued by linearization of encoding plasmids, *in vitro* transcription, transfection of resulting viral RNA into BHK cells, and collection of virus-containing supernatant 18 h post transfection. Virus clones were selected as described in Chapter 3.2.9 and selected clones were grown up, filtered, aliquoted and stored at -80° C in single use aliquots (Chapter 2.22). Viral titres were determined and transgene expression analysed as described in (Chapter 2.21 and Chapter 3.2.4). Titres of SV variants containing MREs were similar to those without, with the exception of those containing the combination of miR133a and miR206 MREs, which consistently grew to lower titres. Titres could not be significantly raised in comparison to SVGFP DSG by growth in either 293 or Huh7 cells. This suggests that the observed reduction in titres was not a consequence of the presence of miRs specific for introduced MREs, but an intrinsic debilitation of the virus.

MRE containing, eGFP expressing SV variants (SVGFPmiR-Ts) were designated names according to their MREs (e.g. SVGFP122-T DSG) and muscle de-targeted SV was

named according to both MREs it encodes in its open reading frame (SVGFP133,206-T DSG). MRE sites in the 3' UTR of the SV genome means that during a replication cycle all viral positive sense genomic and subgenomic RNA species will be targeted for RISC mediated cleavage as described in Chapter 1.4.3 (Figure 4.3 B).

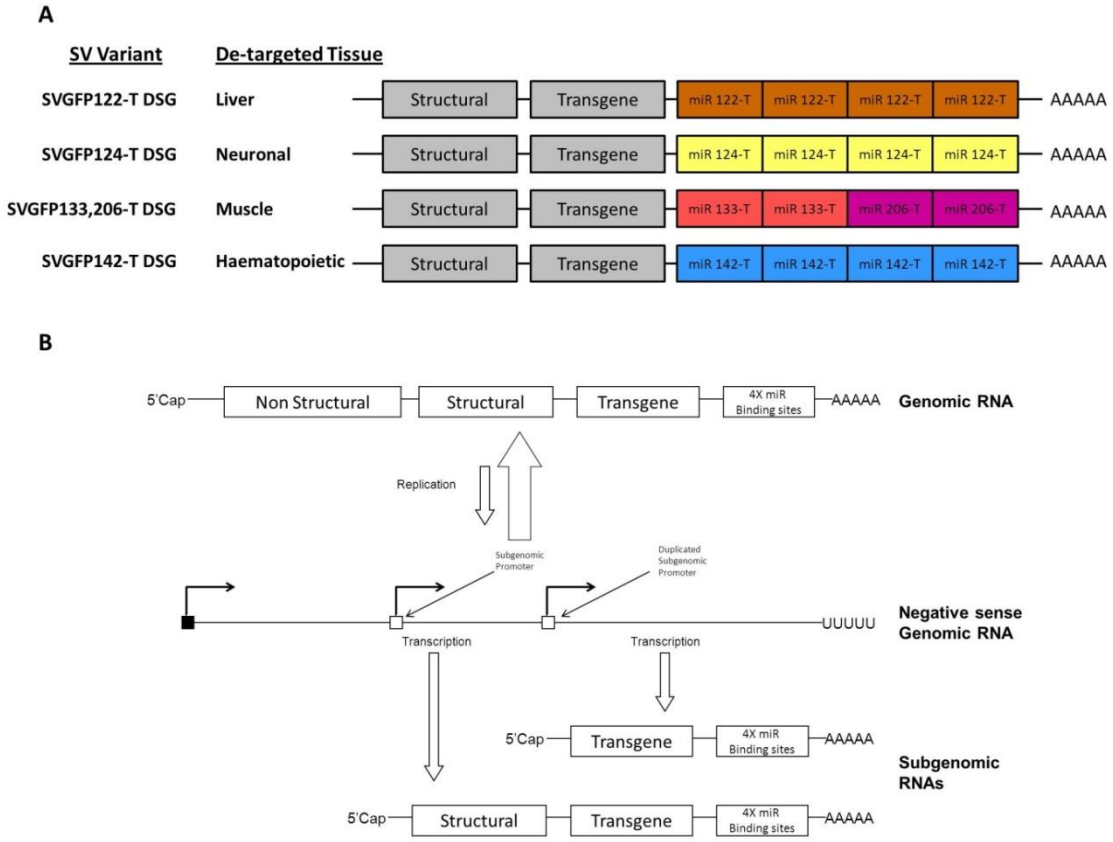

Figure 4.3: Schematic diagram of miR-T sites – A) Maps of selective tissue de-targeted SV variants. 4 identical copies of miR-T sites with perfect complementarity to their cognate miRs were inserted into the 3'UTR SV with the exception of muscle de-targeted SV where previous research has shown that a combination of 2 miR133-T and 2 miR206-T is better for reducing coxsackievirus replication in muscle cells than 4 identical sites of either one. Structural: structural polyprotein, transgene: either luciferase or eGFP. **B)** RNA replication cycle of SV with miR binding sites shown on RNA species. nsp = non-structural protein, ■ = genomic promoter, □ = subgenomic promoter.

4.2.4 Inhibition of SV DSG MiR-T by Ectopically Expressed MiRs

As a model to evaluate miR control of MRE containing SV, it is possible to introduce or up-regulate miR expression in a given cell by transfection of the miR precursors, pre-miRs. Transfection leads to pre-miRs joining the normal processing pathway as endogenous pre-miRs that have been exported from the nucleus. They are hence processed and loaded onto the RISC in the same fashion as endogenously expressed miRs (Figure 4.1).

Utilising this technology it is possible to test whether the introduction of cognate miRs attenuates miR-T SV. Although miR expression varies between cell lines, there are also other factors that vary. Using the same cell line to test miR attenuation of SVmiR-T strains means that host cell-virus interactions are unchanged and, therefore, changes in virus transgene expression levels are likely to be the direct result of changes in miR levels achieved by transfection. In order to test all the SV miR-T variants in one cell line it is necessary to find a cell line which is permissive to SV infection but does not express significant levels of any miRs of interest.

Several cell lines were screened by RNA extraction and RTQPCR with specific primers and probes for miRs. BHK cells, used to grow SV stocks, were found to express significant amounts of both miR133a and miR206 hence were unsuitable, whereas 293 cells were identified to meet the above mentioned criteria. As 293 cells are routinely used in the production of viruses to good manufacturing practice (GMP) grade their lineage and gene expression profile is well characterized, providing a good model in which to work.

293 cells were transfected with cognate miRs before infection with SVGFP DSG miR-Ts or control SVGFP DSG. As a transfection control, a negative control pre-miR was used, consisting of random sequence, shown to have no identifiable effects on cellular miR function (Applied Biosystems, UK).

Expression of eGFP was analysed after eGFP encoding SVmiR-T virus infection of 293 cells. These were either non-transfected, transfected with negative control pre-miR, or transfected with pre-miR precursors of miRs complementary to miR-T sequences introduced into the 3'UTR of SV (Figure 4.4). The eGFP reporter gene was used as a marker of infected cells and the percentage of virus infected cells was determined by flow cytometry. Fluorescence intensity of eGFP positive cells was used as an indicator of the expression levels of eGFP. As fluorescence intensity was recorded on a logarithmic scale, the geometric mean, taken together with the number of eGFP positive cells, was used to calculate the total fluorescence of infected cell samples, an overall measure of virus protein expression.

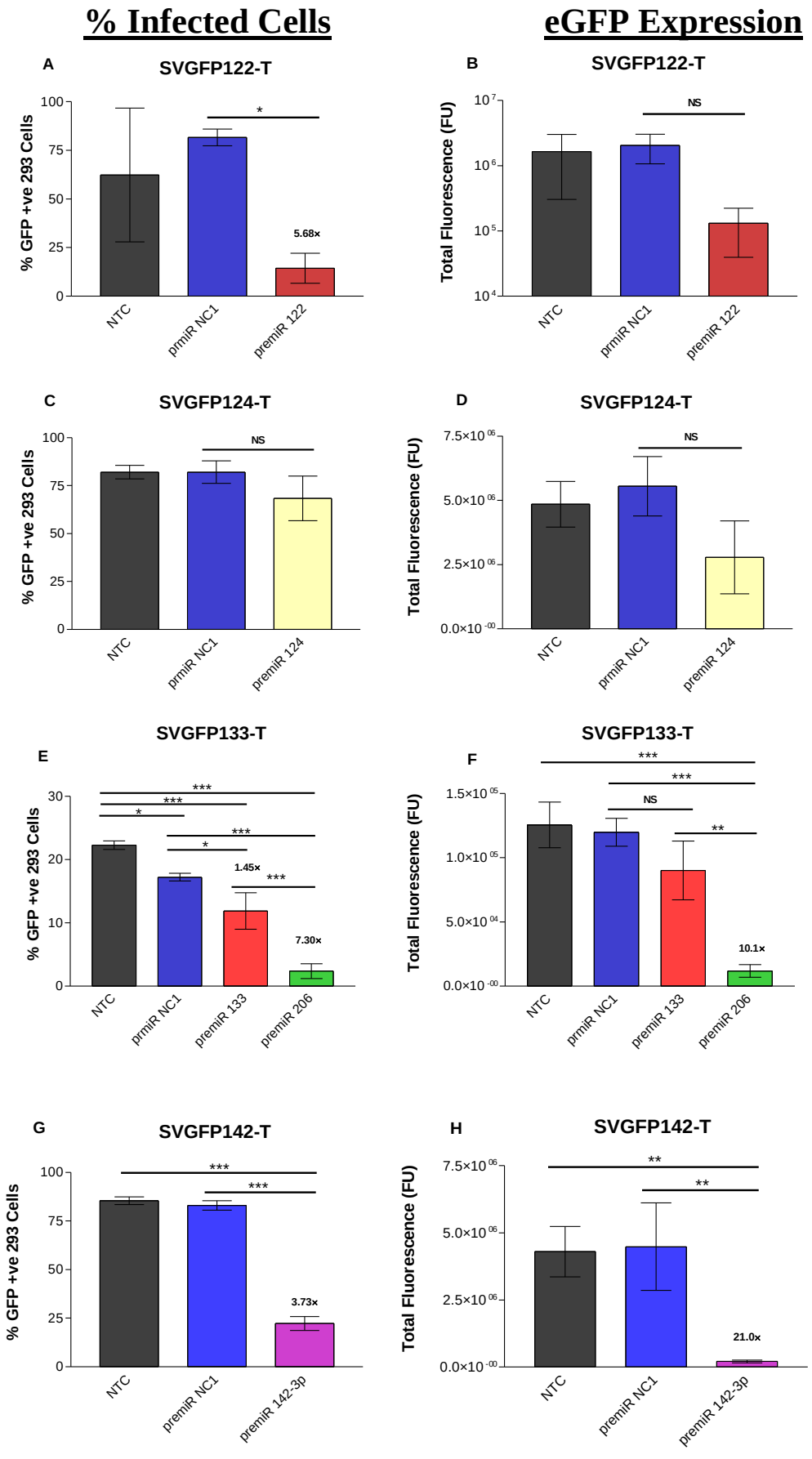
% Infected Cells
eGFP Expression
A
SVGFP122-T
% GFP +ve 293 Cells
100
75
50
25
0
*
5.68×
NTC
prmiR NC1
premiR 122
B
SVGFP122-T
Total Fluorescence (FU)
10 7
10 6
10 5
10 4
NS
NTC
prmiR NC1
premiR 122
C
SVGFP124-T
% GFP +ve 293 Cells
NS
NTC
prmiR NC1
premiR 124
D
SVGFP124-T
Total Fluorescence (FU)
7.5×10 06
5.0×10 06
2.5×10 06
0.0×10 -00
NS
NTC
prmiR NC1
premiR 124
SVGFP133-T
E
% GFP +ve 293 Cells
30
20
10
0
***
***
*
***
*
1.45×
***
7.30×
NTC
prmiR NC1
premiR 133
premiR 206
SVGFP133-T
F
Total Fluorescence (FU)
1.5×10 05
1.0×10 05
5.0×10 04
0.0×10 -00
***
***
NS
**
10.1×
NTC
prmiR NC1
premiR 133
premiR 206
G
SVGFP142-T
% GFP +ve 293 Cells
***
***
3.73×
NTC
premiR NC1
premiR 142-3p
H
SVGFP142-T
Total Fluorescence (FU)
**
**
21.0×
NTC
premiR NC1
premiR 142-3p

Figure 4.4 Attenuation of SVmiR-T Viruses by Transfected MiRs – 293 cells were reverse transfected with the indicated pre-miRs using lipofectamine RNAiMAX 24 hours prior to infection by adding cells in suspension to wells of 48 well plates containing transfection complexes. Infections were carried out at an MOI of 1 in serum free DMEM, for a duration of 30 minutes, after which cells were washed in warm PBS and left for 48 hours. **A), C), E)** and **G)** The percentage of virus infected cells. **B), D), F)** and **H)** Total eGFP expression levels calculated from the percentage of infected cells and the geometric mean of the fluorescence intensity of infected cells. These parameters were measured by flow cytometry as described in Chapter 2.13. NTC: non-transfected control, FU: fluorescence units, NS: not significant. Error bars show $\pm$ SD (n = 3). Statistical analysis was performed using one way ANOVA and Tukey's multiple comparison post-test. (* = $P < 0.05$, ** = $P < 0.01$, *** = $P < 0.001$). Where there is statistically significant difference between control pre-miR and cognate pre-miR transfected cells, fold differences are indicated on each graph.

Results show that upon infection of 293 cells with miR-T viruses, both the number of 293 eGFP positive cells and the total fluorescence resulting from infection are reduced when complementary miRs to SV genomic and subgenomic RNA were ectopically expressed compared to 293 cells transfected with a control pre-miR.

The frequency of 293 cell infection by SVGFP122-T DSG, SVGFP133,206-T DSG and SVGFP142-T DSG viruses was significantly reduced following transfection with precursors to cognate miRs, compared to transfection with a control pre-miR. This provides evidence that miR targeted cleavage by the RISC can successfully attenuate SVmiR-T viruses (Figure 4.4 A, E and G). In the case of SVGFP124-T DSG, however, no reduction in the proportion of virus infected cells was observed (Figure 4.4 C); this was the case in several separate experiments.

The total fluorescence of 293 cells (calculated as the average fluorescence intensity multiplied by the total number of fluorescent cells) transfected with appropriate pre-miRs appeared to be reduced in all SVmiR-T variants; however, statistical significance was not consistently observed.

Attenuation of SV by ectopically expressed miRs establishes the principle of miR mediated SV attenuation, however, in some cases attenuation was not of great magnitude, perhaps questioning the biological significance of any such attenuation. Ectopically expressed miRs through pre-miR transfections may be at much lower levels in comparison to their endogenously expressed counterparts (Kelly, Nace et al. 2010). MiR mediated attenuation of SV observed through this method, therefore, may not be representative of the magnitude of SVmiR-T virus suppression that could be achieved in cells that naturally express miRs of interest.

4.2.5 Identification of Cell lines Expressing MiRs

In order to identify cells that endogenously express miRs of interest, RTQPCR using specific reverse transcription and PCR primers and probes were used to measure levels of these miRs in cell lines derived from liver, neuronal, muscle and haematopoietic tissues.

In each case the measured miR expression levels were compared to an internal control miR; Let7a, which has a role in controlling cell proliferation through negative regulation of the oncogene Ras (Esquela-Kerscher and Slack 2006) and is ubiquitously expressed to similar levels in most tissues (Davoren, McNeill et al. 2008).

It has been reported that the level of muscle specific miR133a and miR206 are increased upon differentiation of the mouse myoblast cell line C212. Two methods of differentiation were compared, replacing growth media, DMEM containing 10% FCS, with DMEM containing either 2% horse serum or 2% FCS for a period of 5 days. Differentiation results in cellular fusion and the production of myotubes and the extent of differentiation in both conditions were similar (Figure 4.5 A). As FCS is used routinely in the culture of other cell lines (Table 2.1) 5 day incubation with DMEM containing 2% FCS was adopted as the routine method of C2C12 differentiation. Comparison by RTQPCR of the miR133a and miR206 levels relative to Let7a in undifferentiated and C2C12 cells differentiated using this protocol showed a significant increase in levels of both miRs in differentiated cells by factors of 836 and 266 fold respectively (Figure 4.5 B). These relative increases appeared to be due to an increase in the absolute number of miR133a and miR206 molecules present as the CT at which miRlet7a was detected remained reasonably constant.

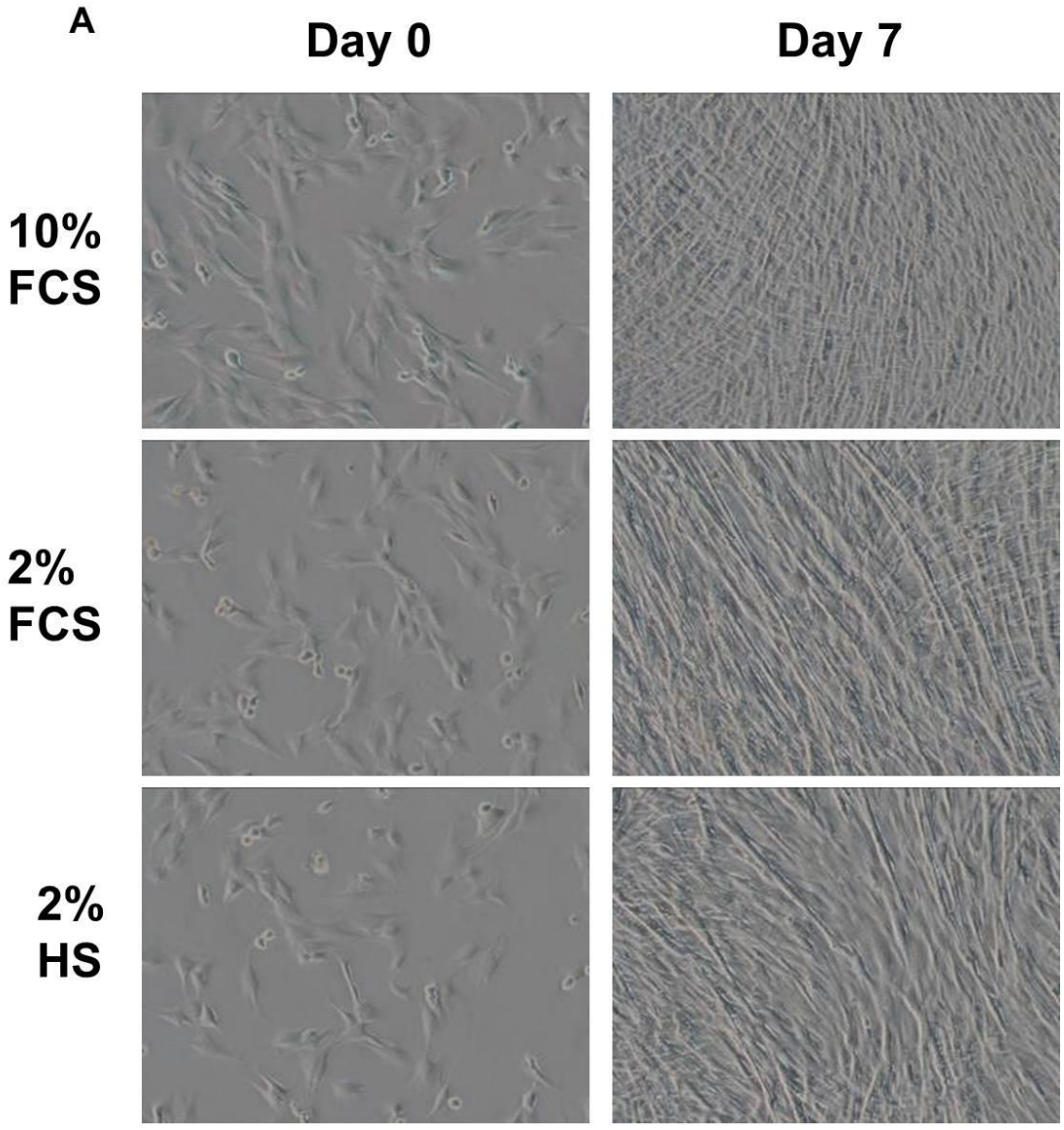
A
Day 0
Day 7
10% FCS
2% FCS
2% HS

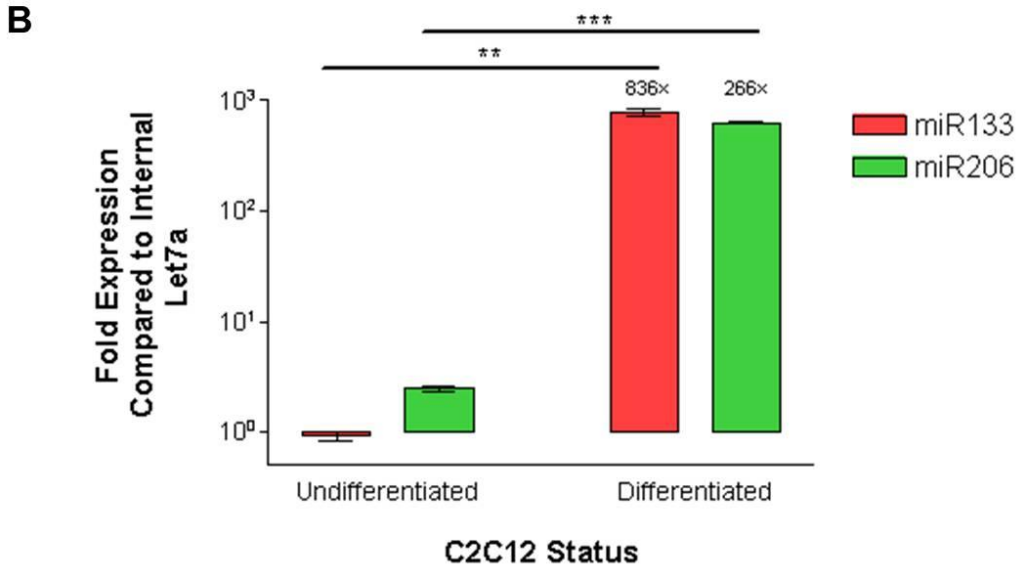
B
***
**
836×
266×
miR133
miR206
Fold Expression Compared to Internal Let7a
10³
10²
10¹
10⁰
Undifferentiated
Differentiated
C2C12 Status

Figure 4.5 Increase of Muscle Specific MiR levels Upon C2C12 Cell Differentiation – A) C2C12 cells were differentiated by replacing growth medium with DMEM containing either 2% horse serum or 2% FCS and incubating for 5 days at 37 °C in a humidified 5% CO_2 environment. Pictures were acquired as described in Chapter 2.19. **B)** MiR133a and miR206 levels in differentiated or undifferentiated C2C12 levels were measured by RTQPCR as described in Chapter 2.16. Statistical; analysis was carried out using 2 separate unpaired Students T tests with Welch's correction as in both cases variances were not equal. (Fold increases are indicate by x, ** = $P < 0.01$, *** = $P < 0.001$).

RTQPCR using specific primers and probes for miRs of interest were used to detect miR levels in a range of cell lines as for miR133and miR 206 in Figure 4.5. Cell lines that showed high levels of tissue specific miRs relative to Let7a were compared to the relative expression of each miR to Let7a in 293 cells as a control. For liver specific miR 122, neuronal specific miR124-1, muscle specific miR133a and miR 206 and haematopoietic miR142-3p a cell line was selected that showed high levels of tissue specific miR expression relative to 293 cells and also susceptibility to SV infection (Figure 4.6 A-E). Liver derived Huh7 cells had 5.68×10^4 fold higher expression of liver specific miR122 relative to Let7a than 293 cells, whilst SHSY5Y neuron derived cells had 10.9 fold higher expression of miR124-1, muscle derived C2C12 cells had 612 and 5.95×10^5 fold higher expression of muscle specific mi133a and miR 206 respectively and dendritic DC2.4 cells had 4.37 fold higher expression of haematopoietic specific miR 142-3p. The absolute levels of miRLet7a in each cell line were also shown to be similar, validating its use as a reference miR (Figure 4.6 F).

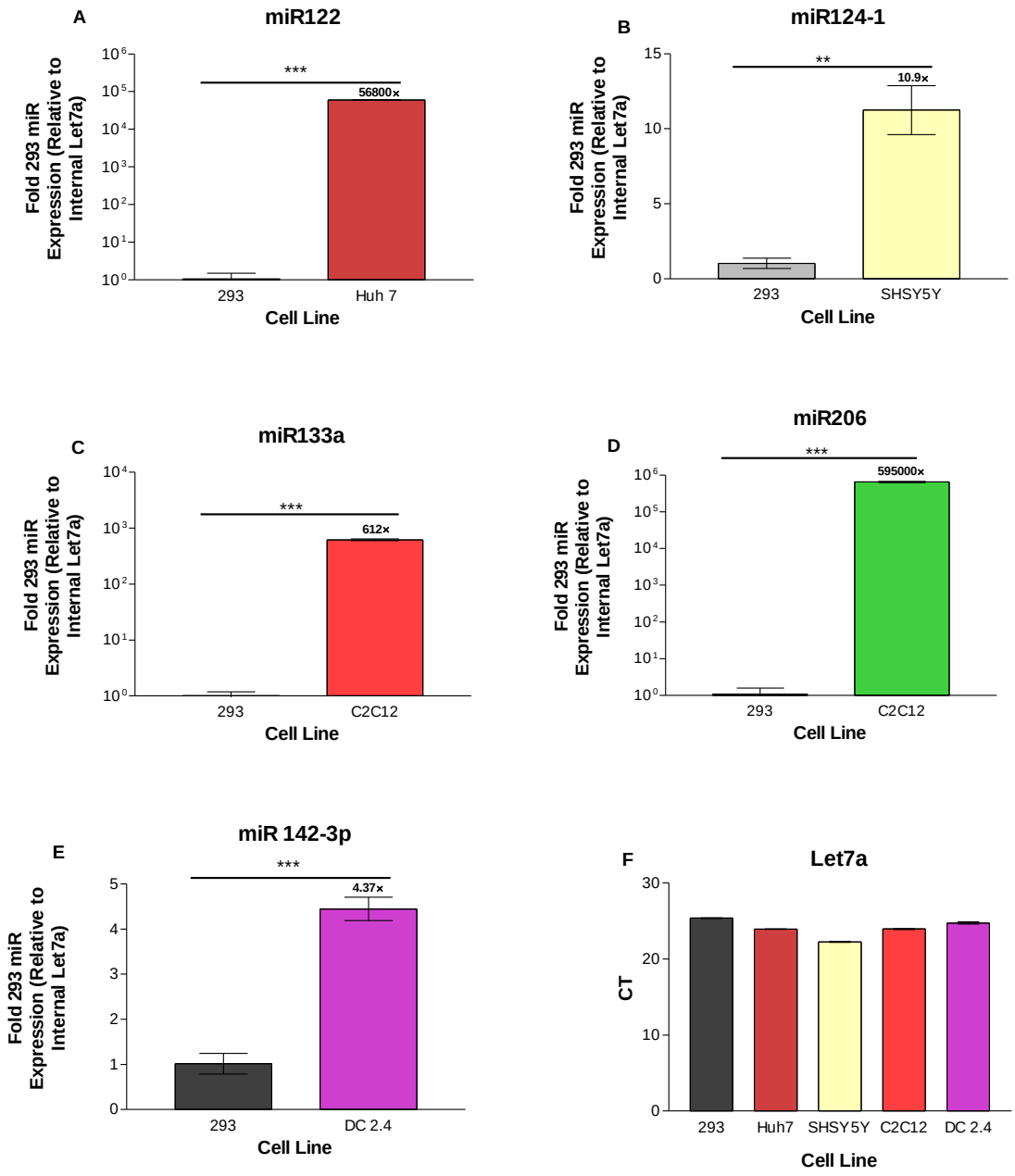

Figure 4.6: Expression of Tissue Specific MiRs in Selected Cell lines - RNA was extracted from cell lines and miR levels relative to internal Let7a analysed. **A)-E)** miR expression displayed as fold expression of 293 cells. **F)** C_Ts of Let7a detection in each cell line. RNA extraction and RTQPCR was performed as described in Chapter 2.16, Error bars show ± SD (n = 3). Statistical analysis was performed using one way ANOVA and Tukey's multiple comparison post-test (* = $P < 0.05$, ** = $P < 0.01$, *** = $P < 0.001$). Fold differences in miR expression are indicated on each graph

4.2.6 Inhibition of SV DSG MiR-Ts by Endogenously Expressed miRs

Having identified cell lines that express high levels of tissue specific miRs, the ability of these miRs to attenuate SV variants bearing complementary MREs was assessed by flow cytometry. The level of virus infection and protein expression of SVGFP DSG miR-T variants was compared to SVGFP DSG, which lacks MREs, in miR expressing cell lines and in miR negative 293 cells. Infection and protein expression in each cell line was standardized as a percentage of that in 293 cells in order to control for the difference in susceptibility of different cell lines to SV infection. Comparison to SVGFP DSG allowed inference that any difference in the percentage expression in 293 cells was due to the presence of MREs in SVmiR-T variants (Figure 4.7).

For each cell line and SVmiR-T variant, standards were optimized by varying the MOI of SV variants used so that by the time of measurement of infected cells and eGFP levels (48 h PI) cell monolayers had not been saturated and hence become a limiting factor in for productive SV replication.

Each SV variant was significantly attenuated in cell lines expressing miRs complementary to miR-T sites present in the 3'UTR except for in the case of SV124-T. The extent of reduction of virus infected cells was 13.2 fold for both SVGFP122-T DSG and SVGFP133,206-T DSG in Huh-7 cells and differentiated C2C12 cells respectively, and 378 fold for SVGFP142-T DSG in DC2.4 cells. The total eGFP expression was reduced 4.86 fold for SVGFP122-T DSG in Huh7 cells, 4.84 fold for SVGFP133,206-T DSG in differentiated C2C12 cells and 852 fold for SVGFP142-T DSG in DC2.4 cells. No significant reduction of the number of eGFP positive cells, nor the total expression of eGFP was observed for SVGFP124-T DSG in SHSY5Y cells.

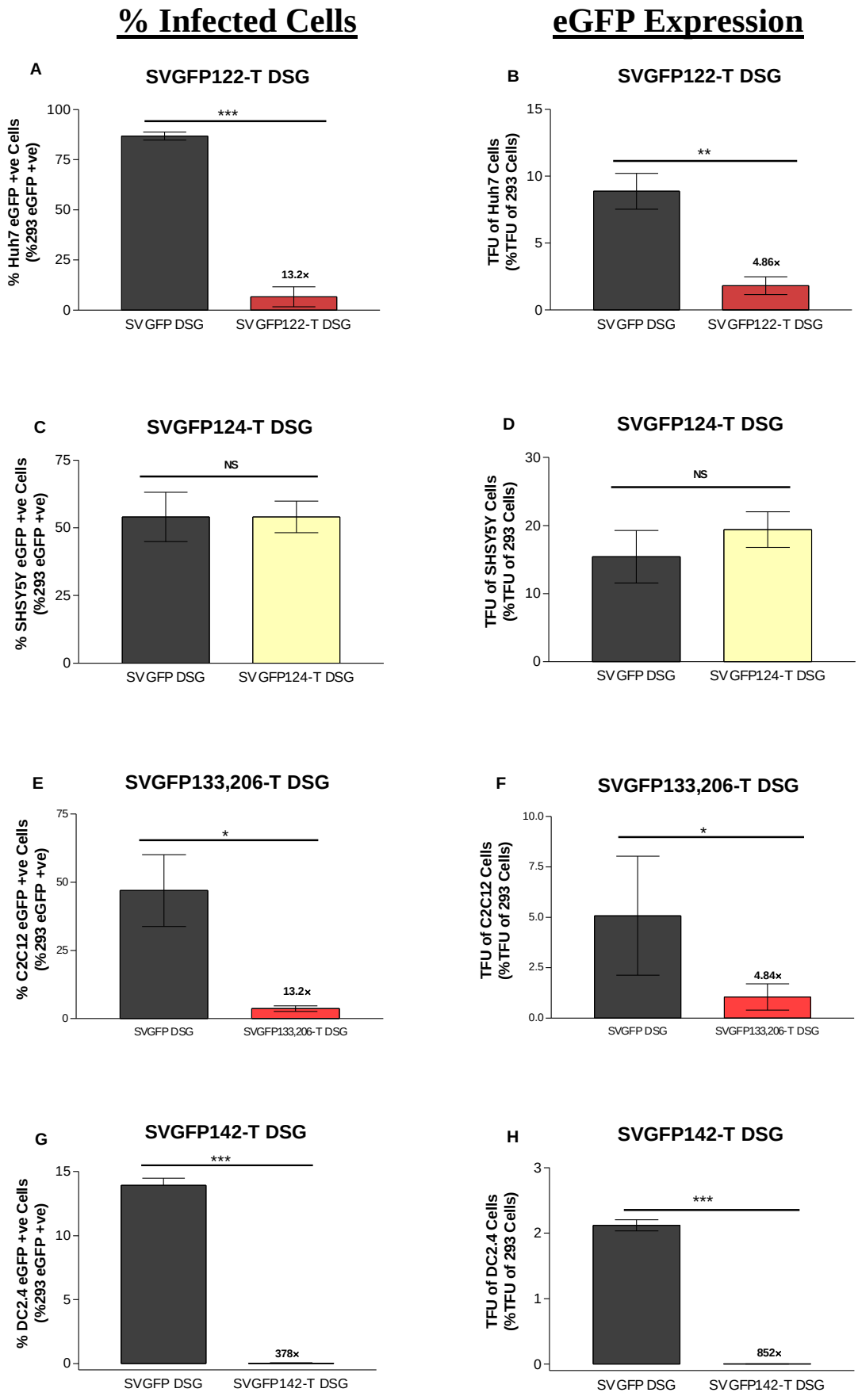
% Infected Cells
eGFP Expression
A
SVGFP122-T DSG
% Huh7 eGFP +ve Cells (%293 eGFP +ve)
***
13.2×
SVGFP DSG
SVGFP122-T DSG
B
SVGFP122-T DSG
TFU of Huh7 Cells (%TFU of 293 Cells)
**
4.86×
SVGFP DSG
SVGFP122-T DSG
C
SVGFP124-T DSG
% SHSY5Y eGFP +ve Cells (%293 eGFP +ve)
NS
SVGFP DSG
SVGFP124-T DSG
D
SVGFP124-T DSG
TFU of SHSY5Y Cells (%TFU of 293 Cells)
NS
SVGFP DSG
SVGFP124-T DSG
E
SVGFP133,206-T DSG
% C2C12 eGFP +ve Cells (%293 eGFP +ve)
*
13.2×
SVGFP DSG
SVGFP133,206-T DSG
F
SVGFP133,206-T DSG
TFU of C2C12 Cells (%TFU of 293 Cells)
*
4.84×
SVGFP DSG
SVGFP133,206-T DSG
G
SVGFP142-T DSG
% DC2.4 eGFP +ve Cells (%293 eGFP +ve)
***
378×
SVGFP DSG
SVGFP142-T DSG
H
SVGFP142-T DSG
TFU of DC2.4 Cells (%TFU of 293 Cells)
***
852×
SVGFP DSG
SVGFP142-T DSG

Figure 4.7: Attenuation of SVmiR-T DSGs by Endogenously Expressed MiRs – Cell lines derived from differing tissues expressing high amounts of tissue specific miR (liver - Huh7 - miR122, neuronal - SHSY-5Y- miR124-1, muscle – differentiated C2C12- miR133a and miR206 and haematopoietic - DC2.4- miR142-3p) as well as 293 cells were infected with SVGFP DSG and their respective SVGFPmiR-T DSG bearing cognate miR binding sites in the 3'UTR. The MOI of infection of 293 cells (1), Huh7 cells (1), SHSY5Y cells (0.1), C2C12 cells (1) and DC2.4 cells (10) was adjusted so that monolayers were not saturated at the time of comparison by FACS or RTQPCR. Infections were carried out in serum free DMEM, for a duration of 30 minutes, after which cells were washed in warm PBS. 48h PI the percentage of virus infected cells and the geometric mean of the fluorescence intensity were measured by flow cytometry as described in Chapter 2.13. FU: fluorescence units, NS: not significant. Error bars show $\pm$ SD (n = 3). Statistical analysis was performed using unpaired T tests. Where variances were unequal T test were performed with Welch's correction (* = $P < 0.05$, ** = $P < 0.01$, *** = $P < 0.001$). Where there is statistically significant difference, fold differences are indicated on each graph.

4.2.7 Production of MiRNA Targeted SVGFP 2A

Though significant miR based attenuation of SV was observed, it is known that conserved sequence elements (CSE) and 3 copies of a 40 nucleotide repeated sequence located in RNA structure in the 3'UTR are involved in genome replication. These regions play an important in the production of negative sense genomic RNA (Frolov, Hardy et al. 2001); the CSE interacts with the RdRp whilst repeated sequence elements have a role through interactions with host cell proteins. It is possible that proteins binding the 3'UTR regions interfere with miR mediated RISC cleavage of SVmiR-T RNA through stearic hindrance. In order to investigate this, SVmiR-T variants were

constructed with miR-T sites in the polyprotein encoding region of the SV genome that is not thought to be involved RNA protein complexes (excluding during transcription and translation). To achieve this, the SVGFP 2A system was utilized, where miR-T sites were inserted between eGFP and the FMDV2A peptide (Figure 4.8 A). These miR-T binding sites are hence present in positive sense SV genomic and subgenomic RNA species, hypothetically conferring them both sensitive to complementary tissue specific miR mediated RISC cleavage (Figure 4.8 B).). As above, tissue de-targeted SVGFP 2A miR-T variants were designated names according to their miR-T sites (eg. SVGFP122-T 2A) and muscle de-targeted SV was named according to both miR-T sites in its open reading frame (SVGFP133,206-T 2A).

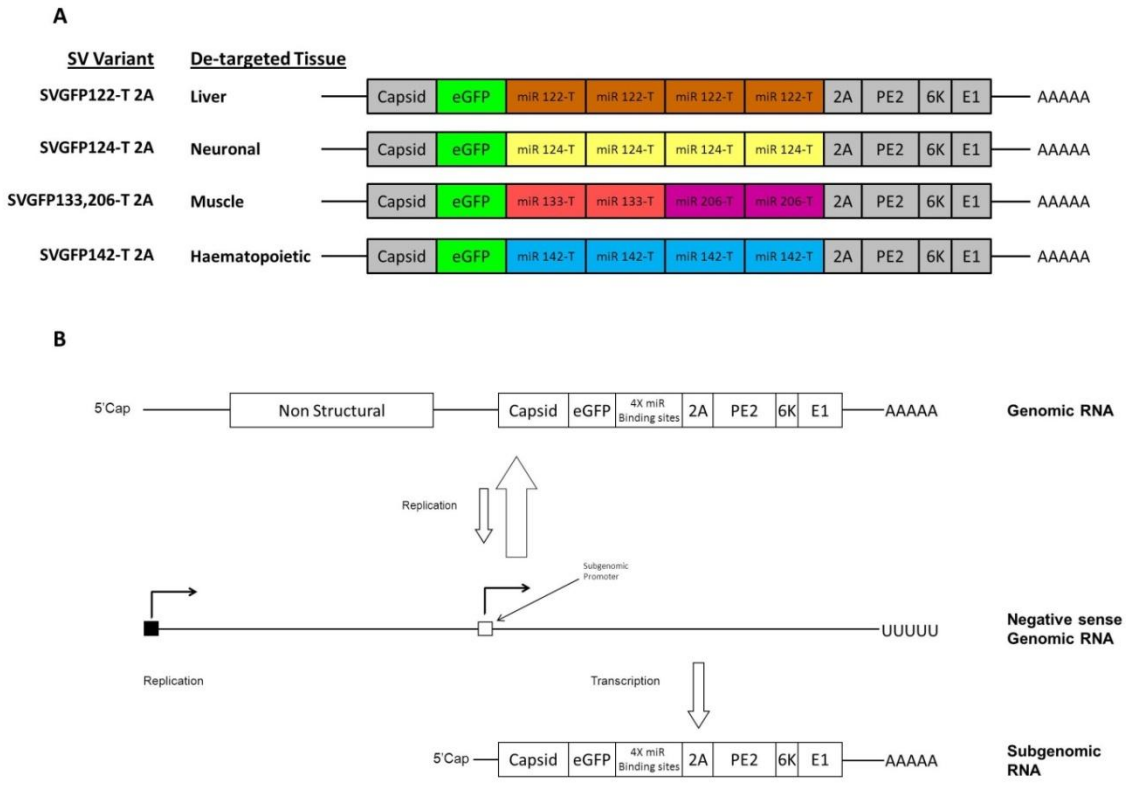

Figure 4.8: Schematic Diagram of MiR-T Sites in SVmiR-T 2A Variants – A) Maps of selective tissue de-targeted SVmiR-T 2A variants. 4 identical copies of miR-T sites with perfect complementarity to their cognate miRs were inserted into the 3'UTR SV with the exception of muscle de-targeted SV where previous research has shown that a combination of 2 miR133-T and 2 miR206-T is better for reducing virus replication in muscle cells than 4 identical sites of either one. Structural: structural polyprotein, transgene: either luciferase or eGFP. **B)** RNA replication cycle of SVmiR-T2A with miR binding sites shown on RNA species

4.2.8 Inhibition of SV 2A MiR-T by Ectopically Expressed MiRs

In order to test whether MREs located in RNA encoding the virus structural polyprotein caused more efficient miR mediated attenuation of SVmiR-Ts than those located in the 3'UTR, each virus was analysed as in Chapter 4.2.4. The frequency of infection and level of transgene expression of SVmiR-T 2A variants were analysed upon infection of 293 cells transfected with pre-miRs of cognate miRs by flow cytometry (Figure 4.9). As controls, 293 cells were uninfected, untreated and infected, or transfected with a control pre-miR then infected.

Results show significant attenuation of SVGFPmiR-T 2A variants by ectopic miR expression, again except for in the case of neuronal specific miR124-1. Statistical significance of inhibition of SVGFP133,206 2A was not consistently seen, probably due to the presence of half the number of active MREs in this setting compared to other variants. It is of note that miR206 seems to mediate more inhibition than miR133a.

Statistically significant attenuation of SVmiR-T 2A variants by exogenously expressed miRs was observed more consistently than with SV variants with MREs in the 3'UTR under the same experimental conditions. The magnitude of attenuation, however, was similar.

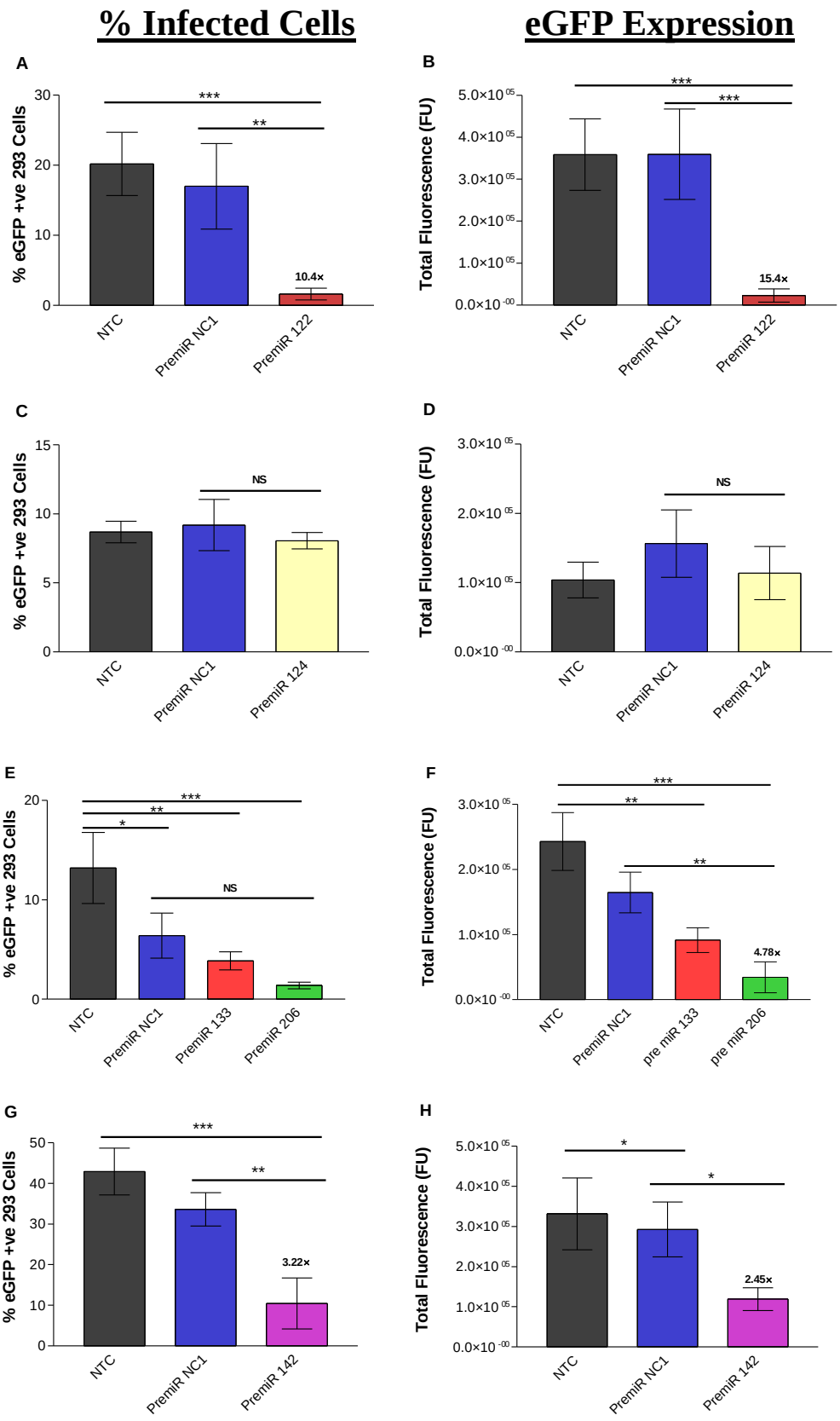
% Infected Cells
eGFP Expression
A
% eGFP +ve 293 Cells
***
**
10.4×
NTC
PremiR NC1
PremiR 122
B
Total Fluorescence (FU)
***
***
15.4×
NTC
PremiR NC1
PremiR 122
C
% eGFP +ve 293 Cells
NS
NTC
PremiR NC1
PremiR 124
D
Total Fluorescence (FU)
NS
NTC
PremiR NC1
PremiR 124
E
% eGFP +ve 293 Cells
***
**
*
NS
NTC
PremiR NC1
PremiR 133
PremiR 206
F
Total Fluorescence (FU)
***
**
**
4.78×
NTC
PremiR NC1
pre miR 133
pre miR 206
G
% eGFP +ve 293 Cells
***
**
3.22×
NTC
PremiR NC1
PremiR 142
H
Total Fluorescence (FU)
*
*
2.45×
NTC
PremiR NC1
PremiR 142

Figure 4.9 Inhibition of SVGFPmiR-T 2A Viruses by Transfected Pre-miRs – 293 cells were reverse transfected with the indicated pre-miRs using lipofectamine RNAiMAX 24 hours prior to infection. Infections with SVGFPmiR-T 2A viruses were carried out at an MOI of 1 in serum free DMEM, for a duration of 30 minutes, after which cells were washed in warm PBS and left for 48 hours. The percentage of virus infected cells and the geometric mean of the fluorescence intensity were measured by flow cytometry as described in Chapter 2.13. NTC: non-transfected control, FU: fluorescence units, NS: not significant. Error bars show ± SD (n = 3). Statistical analysis was performed using one way ANOVA and Tukey's multiple comparison post-test (* = $P < 0.05$, ** = $P < 0.01$, *** = $P < 0.001$). Where there is statistically significant difference between control pre-miR and cognate pre-miR transfected cell, fold differences are indicated on each graph.

4.2.9 Inhibition of SV 2A MiR-T by Endogenously Expressed miRs

The level of attenuation of SVmiR-T DSG variants was greater in endogenously expressing cell lines than 293 cells ectopically expressing cognate miRs. To determine if this was also the case for SVmiR-T 2A variants, and if attenuation in these variants was greater than their counterpart variant with 3'UTR MREs, each was tested in cell lines expressing elevated levels of the corresponding miR as described in Chapter 4.2.6 (Figure 4.10).

Again, each SV variant was significantly attenuated in cell lines expressing miRs complementary to miR-T sites present in the 3'UTR except for in the case of SV124-T. The extent of reduction of virus infected cells was 7.8 fold for SVGFP122-T 2A in Huh-7 cells, 17.1 fold for SVGFP133,206-T 2A in differentiated C2C12 cells and 905 fold for SVGFP142-T 2A in DC2.4 cells. The total eGFP expression was reduced 22.7 fold

for SVGFP122-T 2Ain Huh7 cells, 16.6 fold for SVGFP133,206-T 2A in differentiated C2C12 cells and 6100 fold for SVGFP142-T 2A in DC2.4 cells. No significant inhibition in either the number of eGFP positive cells, or the total expression of eGFP was observed for SVGFP124-T 2A in SHSY5Y cells.

Based on the magnitudes of attenuation of reporter transgene expression in all SVmiR-T variants, SV is more effectively attenuated by miR when MREs are inserted in the structural polyprotein encoding region of the genomic RNA than those inserted in the 3'UTR.

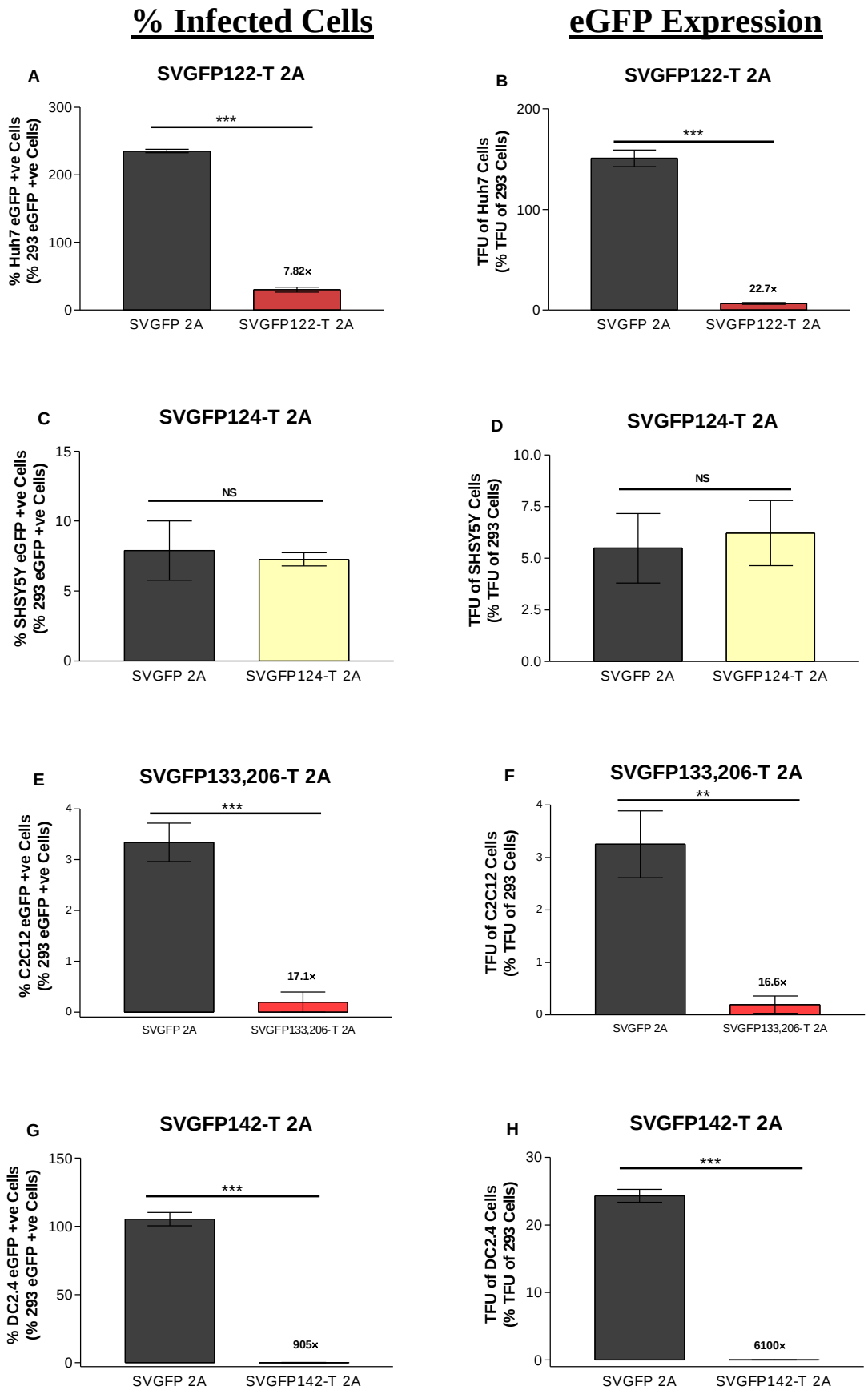
% Infected Cells
eGFP Expression
A
SVGFP122-T 2A
% Huh7 eGFP +ve Cells (% 293 eGFP +ve Cells)
***
7.82×
SVGFP 2A
SVGFP122-T 2A
B
SVGFP122-T 2A
TFU of Huh7 Cells (% TFU of 293 Cells)
***
22.7×
SVGFP 2A
SVGFP122-T 2A
C
SVGFP124-T 2A
% SHSY5Y eGFP +ve Cells (% 293 eGFP +ve Cells)
NS
SVGFP 2A
SVGFP124-T 2A
D
SVGFP124-T 2A
TFU of SHSY5Y Cells (% TFU of 293 Cells)
NS
SVGFP 2A
SVGFP124-T 2A
E
SVGFP133,206-T 2A
% C2C12 eGFP +ve Cells (% 293 eGFP +ve Cells)
***
17.1×
SVGFP 2A
SVGFP133,206-T 2A
F
SVGFP133,206-T 2A
TFU of C2C12 Cells (% TFU of 293 Cells)
**
16.6×
SVGFP 2A
SVGFP133,206-T 2A
G
SVGFP142-T 2A
% DC2.4 eGFP +ve Cells (% 293 eGFP +ve Cells)
***
905×
SVGFP 2A
SVGFP142-T 2A
H
SVGFP142-T 2A
TFU of DC2.4 Cells (% TFU of 293 Cells)
***
6100×
SVGFP 2A
SVGFP142-T 2A

Figure 4.10: Attenuation of SVmiR-T 2A by Endogenously Expressed MiRs – Cell lines derived from different tissues expressing high amounts of tissue specific miR (liver - Huh7 - miR122, neuronal - SHSY-5Y- miR124-1, muscle – differentiated C2C12- miR133a and miR206 and haematopoietic - DC2.4- miR142-3p) as well as 293 cells were infected with SVGFP 2A and their respective SVmiR-T 2A. The MOI of infection of 293 cells (1), Huh7 cells (1), SHSY5Y cells (0.1), C2C12 cells (0.2) and DC2.4 cells (5) was adjusted so that monolayers were not saturated at the time of comparison by FACS or RTQPCR. Infections were carried out at an in serum free DMEM, for a duration of 30 minutes, after which cells were washed in warm PBS. 48h PI the percentage of virus infected cells and the geometric mean of the fluorescence intensity were measured by flow cytometry as described in Chapter 2.13. FU: fluorescence units, NS: not significant. Error bars show $\pm$ SD (n = 3). Statistical analysis was performed using unpaired T tests. Where variances were unequal T test were performed with Welch's correction (* = $P < 0.05$, ** = $P < 0.01$, *** = $P < 0.001$). Where there is statistically significant difference, fold differences are indicated on each graph.

During the early stages of virus infection *in vivo*, it is likely that the amount of virus replication is critical as to whether, and to what extent inflammatory symptoms occur. The magnitude of miR based attenuation of virus replication *in vitro* may therefore be a better predicator than transgene expression for successful elimination of virus pathogenesis *in vivo*. To determine the level of inhibition of SVmiR-T 2As by their complementary miRs, RTQPCR was used to measure the number of virus genomes released into the supernatant following infection (Figure 4.11). As with the analysis of transgene expression in Figures 4.7 and 4.10, supernatant virus titres were normalized to those on the control, miR negative 293 cell line. Results showed that compared to SVGFP 2A which contained no MREs, the titre of SVGFP122-T 2A was reduced by 69

fold, SVGFP133.206-T 2A 14 fold and SVGFP142-T 2A 42300 fold whilst there was no significant difference in the titre of SVGFP124-T 2A.

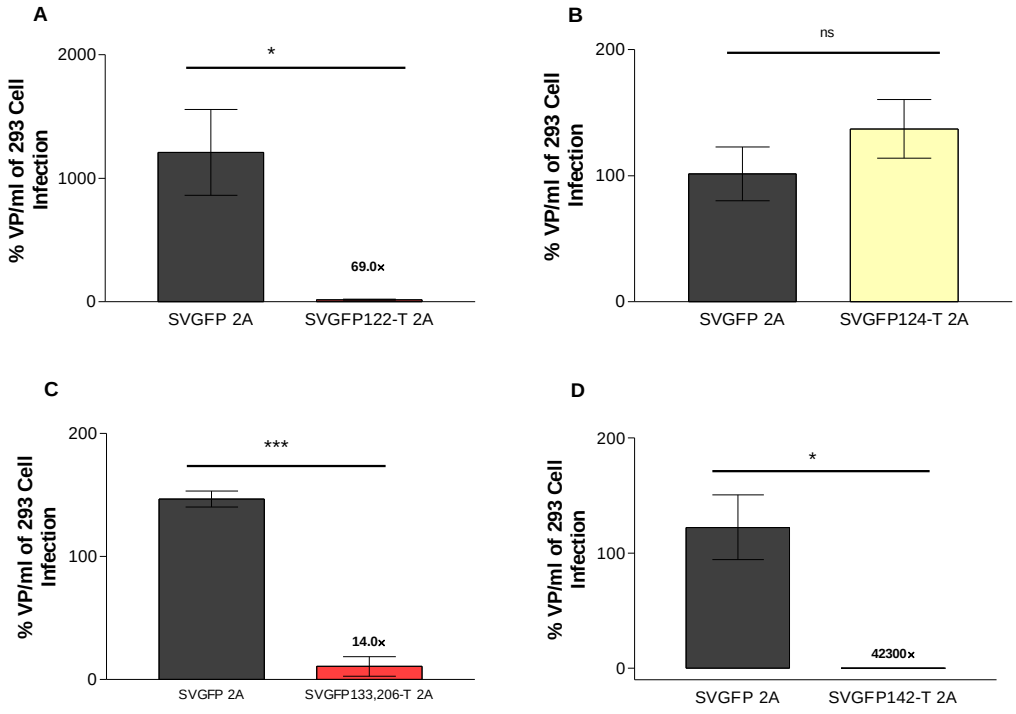

Figure 4.11: Attenuation of SVmiR-T 2A replication by Endogenously Expressed MiRs – Cell lines derived from differing tissues expressing high amounts of tissue specific miR (liver - Huh7 - miR122, neuronal - SHSY-5Y- miR124-1, muscle - CC12- miR133a and miR206 and haematopoietic - DC2.4- miR142-3p) as well as 293 cells treated as in Figure 4.10. 48 hours PI 140µl supernatant samples were collected, RNA extracted and analysed by RTQPCR as described in Chapter 2.16. NS: not significant. Error bars show ± SD (n = 3). Statistical analysis was performed using unpaired T tests. Where variances were unequal T test were performed with Welch's correction (* = $P < 0.05$, *** = $P < 0.001$). Where there is statistically significant difference, fold differences are indicated on each graph.

4.2.10 A Special Case for miR124?

In all experiments analysing miR knockdown of SVmiR-T variants there was no significant attenuation of either SVGFP124-T DSG or SVGFP124-T 2A. The levels of miR142-3p were 4.37 fold higher than in control 293 cells and this was capable of reducing SVGFP142-T 2A transgene expression and production of progeny virus by 6100 fold and 42300 fold respectively. In comparison, miR124-1 levels in SHSY5Y cells were 10.9 fold higher, suggesting that if inhibition could take place by the same mechanism, there would be sufficient levels of miR124 present for this to occur. It is possible that miR124 has a unique property in that it does not facilitate RISC mediated cleavage of SV RNA species making it unsuitable for its regulation. The successful use of miR124 specific MREs in attenuating VSV in neuronal tissues, however, make this explanation unlikely (Kelly, Nace et al. 2010).

Although the relative expression of miR124-1 in SHSY5Y cells was 10.9 fold, based on evidence suggesting that HEK 293 cells are actually of neuronal origin (Shaw, Morse et al. 2002), it is possible that the abundance of miR124-1 present in 293 cells is above a threshold required for SVGFP124-T DSG and SVGFP124-T 2A. In order to test this, cell lines with susceptibility to SV infection were screened for a reduced level of miR124-1 compared to 293 cells, with a view to their use as a negative control for miR124-1 mediated attenuation of SVmiR124-T 2A. It was found, using RTQPCR to detect miR124-1 relative to Let7a as an internal control miR, that there is a 1160 fold difference in miR124-1 levels in SHSY5Y compared to BHK cells (Figure 4.12 A). This is a much greater difference than the 10.9 fold difference observed between SHSY5Y cells and 293 cells (Figure 4.6 B).

As in Figure 4.10, the percentage of infected cells and the total level of eGFP expression following infection of SHSY5Y cells with SVGFP 2A and SVFP124-T 2A was analysed by flow cytometry. In this case, however, BHK cells were used as a negative control. Both the percentage infected cells and total fluorescence, calculated from the total number of infected cells and the geometric mean of fluorescent intensity of infected cells, were standardized as percentage of that observed in BHK cells (Figure 4.12 B and C). Results show that the percentage infected cells was reduced by 5.61 fold for SVGFP124-T 2A compared to SVGFP 2A and the total fluorescence was reduced 2.36 fold. This provides evidence that miR124-1 can indeed be used to inhibit SV bearing complementary MREs.

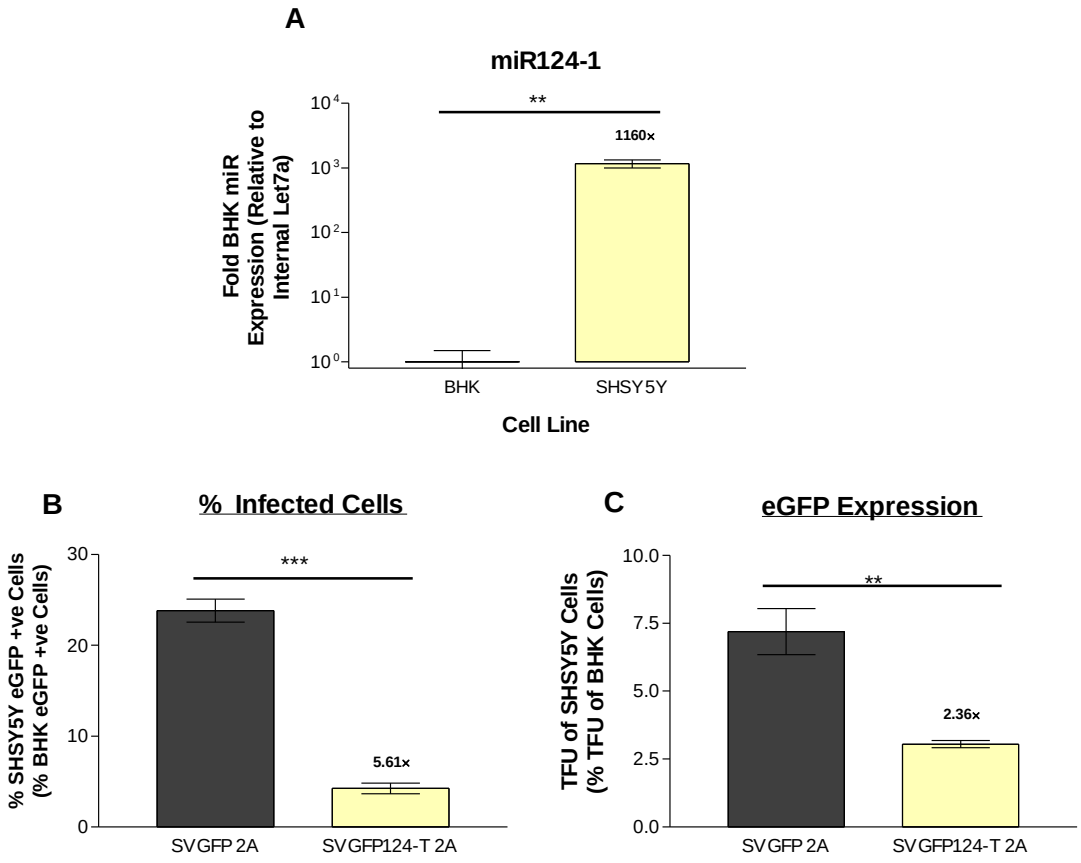

Figure 4.12: Re-Analysis of SVGFP124-T 2A - A) RNA was extracted from cell lines and miR levels relative to internal Let7a analysed. MiR expression is displayed as fold expression of BHK cells. RNA extraction and RTQPCR was performed as described in Chapter 2.16. **B)** and **C)** Neuronal SHSY5Y cells and BHK cells were infected with SVGFP 2A and SVGFP124-T 2A at an MOI of 0.1 such that monolayers were not saturated with virus at the time of comparison by FACS or RTQPCR (28 hours PI). Infections were carried out in serum free DMEM, for a duration of 30 minutes, after which cells were washed in warm PBS. 48h PI the percentage of virus infected cells and the geometric mean of the fluorescence intensity were measured by flow cytometry as described in Chapter 2.13. FU: fluorescence units. Error bars show $\pm$ SD (n = 3). Statistical analysis was performed using unpaired T tests. Where variances were unequal T test were performed with Welch's correction (** = $P < 0.01$, *** = $P < 0.001$). Where there is statistically significant difference, fold differences are indicated on each graph.

4.2.11 Ex Vivo Inhibition of SVmiR-T 2A

Whether the levels of miR mediated attenuation *in vitro* are sufficient to alleviate pathogenic side effects is unclear. In order to validate the SV was capable of replication *in vivo* SVLuc DSG was delivered IT to C57BL/6 mice and transgene expression was observed at 7h PI by IP administration of luciferin followed by *in vivo* luciferase imaging under isofluorane anaesthesia using an IVIS 1000 system (Xenogen, USA) and Living Image 2.50.1 software (Figure 4.13). Transgene expression was variable between the treated mice, probable due to leakage of administered virus dose out of the needle track in one mouse, however expression was present at 7 hours PI, but reduced to near background levels by 24 hours PI and did not re-appear thereafter.

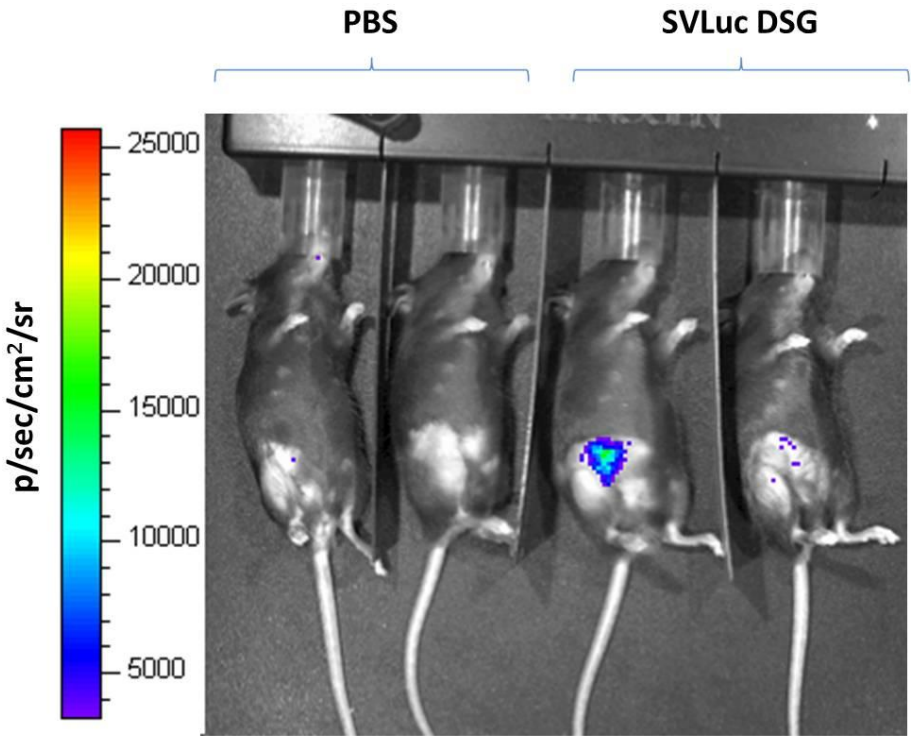

Figure 4.13: SVLuc DSG Gene Expression *In Vivo* – C57BL/6 mice bearing SC B16 tumours were inoculated IT with PBS or 7.5 x 10^6 PFU of SVLuc DSG in a volume of 50µl. 7 hours PI, mice were anaesthetised using isofluorane and injected IP with 100 µl luciferin and imaged for 5 minutes using an IVIS 1000 system and Living Image 2.50.1 software. p/sec/cm2/sr = photons/second/centimetre^2/steradian.

Given that SVLuc DSG was viable *in vivo*, it was investigated whether it indeed caused no pathogenesis in adult mice or if passage on mouse brains *in vivo* had conferred neuropathogenesis (Ryman, Klimstra et al. 2000). In separate experiments adult Balb/c and C57BL/6 mice were treated IP with SVLuc DSG and analysed for changes in gait, as a characteristic of encephalitis, weight loss and general outward signs of stress. No mouse treated with SVLuc DSG displayed any changes compared to control, PBS treated mice.

Due to lack of a suitable animal model with a pathological symptom with which to evaluate SVmiR-Ts, ex-vivo human samples were obtained in order to evaluate; first if SV can infect the tumours of patients with late stage cancers, second, if SV infects human liver tissue, and third, whether any such infection can be prevented through the use of MREs complementary to liver specific miR122.

Tissue from donors consisted of freshly resected liver metastasized colorectal cancer and surrounding normal liver tissue. Samples were placed in RPMI containing 10% heat treated FCS immediately after surgery and throughout experimentation. Tumour and liver were sliced immediately upon collection into approximate cylinders about 1 mm in depth and 3 mm in diameter and placed in 24 well plates with 1 ml media per well.

Tumour and liver samples were infected with 2 x 10^5 PFU of SVGFP 2A and SVGFP122-T 2A for 24 hours, washed with warm PBS and snap frozen in OCT. Samples were sectioned using a cryostat, mounted onto slides, stained with DAPI and then imaged by bright field and fluorescence microscopy as described in Chapter 2.20 (Figure 4.14). Liver sections did not show any infection by SV, perhaps suggesting that IV delivery of the virus will not lead to liver toxicity (Figure 4.14 A). Images of sectioned tumour showed foci of infection with both SVGFP 2A and SVGFP122-T 2A providing evidence that SV may be capable of human colorectal metastases *in vivo*. Images displayed, however, are of infected foci, the majority of tumour samples were uninfected, this could be due death of outer layers of cells upon e*x vivo* culture presenting barriers to SV spread, or could be indicative of a potential inadequacy of SV if delivered to humans i*n vivo* to treat such malignancies.

Upon analysis of further patient samples lack of liver infection was consistently seen, however, virus replication and transgene expression in tumours was also often absent. Patient history of the donor of tissue shown in Figure 4.14 reports an initial diagnosis with prostate cancer, before remission and later diagnosis with colorectal cancer which metastasized to the liver. This could mean that the tumour sample in Figure 4.14 is actually of prostatic tissue origin, and explain variation between this and other tumour samples that were well characterized as colorectal in origin.

Due to observations of little or no infection of liver tissue e*x vivo* miR mediated attenuation of SVGFP122-T 2A could not be evaluated in this setting.

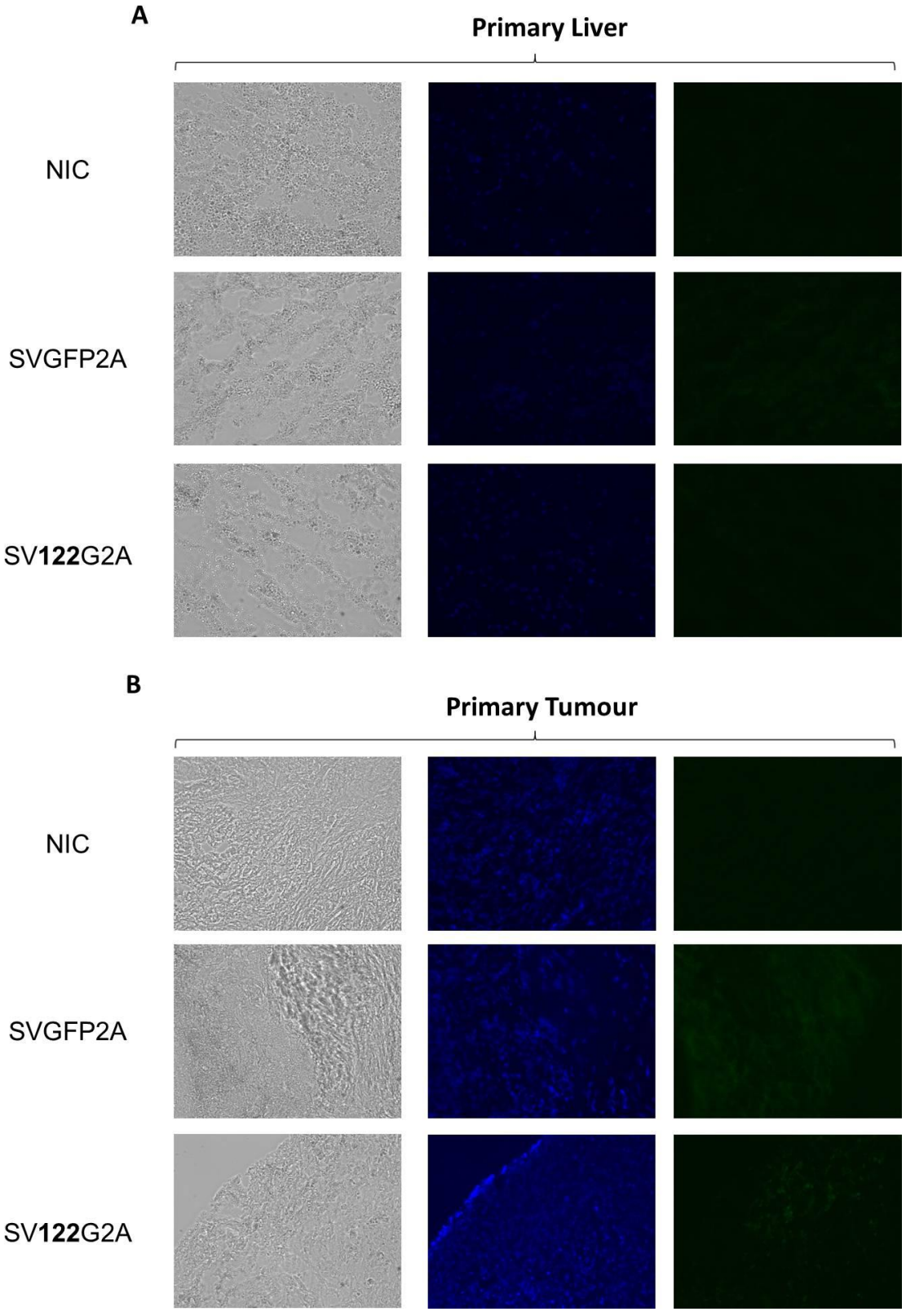
A
Primary Liver
NIC
SVGFP2A
SV122G2A
B
Primary Tumour
NIC
SVGFP2A
SV122G2A

Figure 4.14: Infection of Human Liver and Tumour – Freshly resected human **A)** liver and **B)** tumour samples were infected with 2 x 10^5 PFU of SVGFP 2A and SVGFP122-T 2A for 24 hours, washed with warm PBS and snap frozen in OCT. Samples were sectioned using a cryostat, mounted onto slides, stained with DAPI and then imaged by bright field and fluorescence microscopy as described in Chapter 2.20 (Figure 4.14)

4.3 Concluding Discussion

It was possible to inhibit both the transgene expression and replication of SVmiR-T variants *in vitro.* The magnitude of inhibition observed was greater in endogenously expressing cell lines than in 293 cells transfected with MRE specific miRs. The magnitude of miR mediated reduction in total transgene expression of SVmiR-T DSG variants with MREs located in their 3'UTRs was on average, about 5 fold lower than that of SVmiR-T 2A variants with MREs located in the structural polyprotein encoding region (Table 4.2). This may be, as hypothesized, due to interference of miR-MRE interactions through stearic hindrance of the RISC by other proteins that bind close by in the 3'UTR.

Specificity of MRE	Fold Reduction in eGFP Expression		Compared to Control Cell Line
	SVmiR-T DSG	SVmiR-T 2A	
miR122	4.86	22.7	293
miR124-1	N/A	2.36	BHK
miR133a	4.84	16.6	293
miR142-3p	852	6100	293

Table 4.2: Comparison of Levels of SVmiR-T DSG and SVmiR-T 2A Attenuation – Fold differences are shown to 3 significant figures. N/A = not available, MRE = miR response element.

The level of inhibition of replication of SVmiR-T 2A variants was in general greater than the level of transgene expression, perhaps because capsid assembly requires 80 monomers for each nucleocapsid, whilst each eGFP protein contributes to fluorescence measured. Also, nucleocapsid assembly is a process dependent on a threshold cytoplasmic concentration of capsid proteins, below which virus particles cannot be released.

SVmiR-Ts with MREs specific for different miR species were all significantly attenuated, however, the level of attenuation spanned a large range. In addition, the level of virus attenuation in endogenously expressing cell lines did not correlate with the amount of miR present as measured by RTQPCR. It is possible that miR species differ in their capability of directing RISC cleavage of RNA in general, or SV RNA. One way this could be explained is differing preferences of miRs for argonaute subunits recruited to the RISC, it is known that only when Ago2 is present, which has RNase H activity, can the RISC cleave mRNA, with any of the other 3 argonaute proteins only translational repression can occur. Assuming this is correct, translational repression through de-adenylation and de-capping before during or after targeting to P bodies is likely to take longer than direct cleavage of SV RNA. This might therefore mean that RISC complexes in the cell, loaded with MRE specific miRs become “engaged” and/or moved from the cytoplasm into P-bodies, allowing cytoplasmic SV RNA to complete replication, creating more RNA species and potentially overcoming the miR mediated suppression of productive replication.

Another explanation for the lack of correlation between the amount of each MRE specific miR present and the level of SVmiR-T attenuation observed is the probable variation in abundance mRNA targets present in each cell type. For example if miR122

and miR124-1 are expressed at equal levels but there are 10 target mRNA molecules with full or partial complementarity to miR122 in a liver cell and 1000 for miR124-1 in a neuronal cell, one can envisage the amount of free miRs remaining SV RNA will be different. It may well, therefore, be that the amount of free miR present is proportional to the level of SVmiR-T attenuation observed for each miR.

Identification of the limiting factors for SV attenuation by RISC mediated cleavage will allow increased efficacy of this system. If incomplete virus attenuation is due to insufficient miR interactions with MREs, it is likely that the introduction of an increased number of miR binding sites will increase the level of attenuation. If MRE specific miRs become overwhelmed by SV infection, it is likely that the introduction of MREs to more than one miR in a specific tissue will raise the level of SV attenuation. If the level of RISC, however, is a limiting factor, this technology may need to be combined with other strategies such as SV pseudotyping.

Though the only case of knockdown to background levels was observed was for SV142-T 2A infection of haematopoietic cells, it is impossible to know whether the level of SV attenuation of other variants is sufficient for a clinical improvement in pathological symptoms *in vivo* without direct testing.

Our assumptions of the cell types which contribute to SV pathogenesis are based on symptoms of patients with infection, however, more work is needed to validate or disprove such assumptions through immunohistochemical staining for virus proteins or isolation of replication competent virus from patient tissue samples.

Whether miR mediated attenuation of SV is sufficient to be of any therapeutic benefit requires *in vivo* animal models to validate this principle, ultimately, however, trials in

humans will be required to determine the level of clinical benefit, if any. In the absence of such a model, testing viruses in human *ex vivo* samples might provide a good indication as to whether this strategy can be useful *in vivo*.

Although SVmiR-T variants did not show mutation between rescue and production of virus stocks, given genetic instability shown in Chapter 3, it is more than likely that MREs are lost with increasing number of replication cycles. It is therefore feasible that if SV were used as a miR controlled oncolytic agent, upon replication in the tumour it may lose its tissue specific attenuation. Leakage from the tumour would then leave all tissue susceptible to infection with wild type SV; whether such leakage would occur and whether it would lead to pathological symptoms equal to or milder than wild type infections must be experimentally determined.

5 Blood Stability

5.1 Introduction

Stability in human blood is a prerequisite for any oncolytic agent that will be administered IV to treat metastatic disease. In addition, circulation kinetics and biodistribution following IV delivery must allow for sufficient virus doses to reach disseminated metastases to be therapeutic. Since SV is transmitted to humans through the bloodstream, we reasoned that it might display greater stability in human blood than other viruses currently being developed as oncolytic agents, such as HSV and adenovirus that are not transmitted via the bloodstream in their normal processes of infection. To test the stability of SV in blood, its infectivity was measured following exposure to neat whole blood, plasma or serum. As complement activation by SV *in vivo* may lead to direct neutralisation of virus particles as well as increased rates of clearance, the ability of SV to activate complement was analysed by ELISA. In order to further examine the compatibility of SV with IV delivery, its circulation kinetics and biodistribution in an *in vivo* mouse model were analysed.

As part of its life cycle, SV is capable of packaging in both vertebrate and invertebrate cells. Whilst most groups that have studied SV have made use of virus particles packaged in mammalian cells, the form that has been exposed to human blood during evolution is packaged in insect cells. Studies of SV produced from these different cells have shown differences in membrane cholesterol content and the extent of glycosylation of surface proteins (He, Piper et al. 2010). It is feasible that these differences have an impact on infectivity and blood stability of SV. Properties conferred by invertebrate cells might alter the susceptibility of SV to neutralisation by human blood, or may alter the efficiency of infection of specific vertebrate cell types. If so, SV produced in

invertebrate cells may be more efficient at establishing infection when passed to vertebrate hosts during transmission, compared to virions produced from host vertebrate cells. Should this hypothesis be correct, it could explain why SV, and indeed other alphaviruses, have remained as arboviruses; alternating infection between invertebrate and vertebrate hosts. More pertinently, it could mean that utilizing invertebrate producer cells for the production of SV could lead to increased blood stability and/or improved circulation kinetics following IV delivery, thereby increasing the dose of systemically delivered oncolytic SV that may reach tumours.

SV produced from BHK or C6/36 cells, was used to model SV particles produced from vertebrate or invertebrate cells respectively. Infectivity of a range of mammalian and insect cell lines, behaviour in human blood, particle kinetics and biodistribution in an immune competent mouse model were analysed to determine the influence of producer cell types.

5.1.1 Aims

- To assess the ability of SV to infect a range of human and mouse cancer cell lines
- To analyse the stability of SV in human and mouse blood
- To determine the circulation kinetics and biodistribution of SV in an immune competent *in vivo* murine model
- To determine whether SV can be efficacious as an oncolytic agent when delivered IV in an immune competent tumour bearing murine model
- To assess the influence of invertebrate, compared to vertebrate producer cells on the ability of produced virus to infect a range of cancer cell lines, its behaviour in blood and biodistribution in mice following IV administration

5.2 Results

5.2.1 Behaviour of SV in Human Blood

To what extent human blood components inhibit SV infection was investigated by incubation of the virus with whole human blood and blood fractions. An *in vivo* circulation half-life of 15 minutes might be sufficient for adequate access of input OV to tumour cells (Demers, Johnson et al. 2003), this duration represents about 15 circulations in an average human male. The effect of a 15 minute exposure of SV to neat human blood, plasma and serum at physiological temperature on its ability to infect BHK cells was therefore assayed. The concentration of SVLuc DSG in each incubation was based on the typical dose of 10^7 PFU/mouse in an *in vivo* experiment. After SVLuc DSG incubation with blood, preparations were diluted so that BHK cell monolayers were exposed to an input virus MOI of 10 PFU/cell.

Exposure of SVLuc DSG to whole human blood generally caused a modest fall in its ability to infect BHK cells (measured by luciferase reporter gene expression), although this was usually not statistically significant. A typical result is shown in Figure 5.1. Interestingly, incubation of SV in plasma seemed to actually enhance infectivity, although enhancement was not consistently statistically significant compared to incubation with DMEM. Incubation of SV with serum from the same donor led to significantly reduced infectivity compared to both DMEM and plasma.

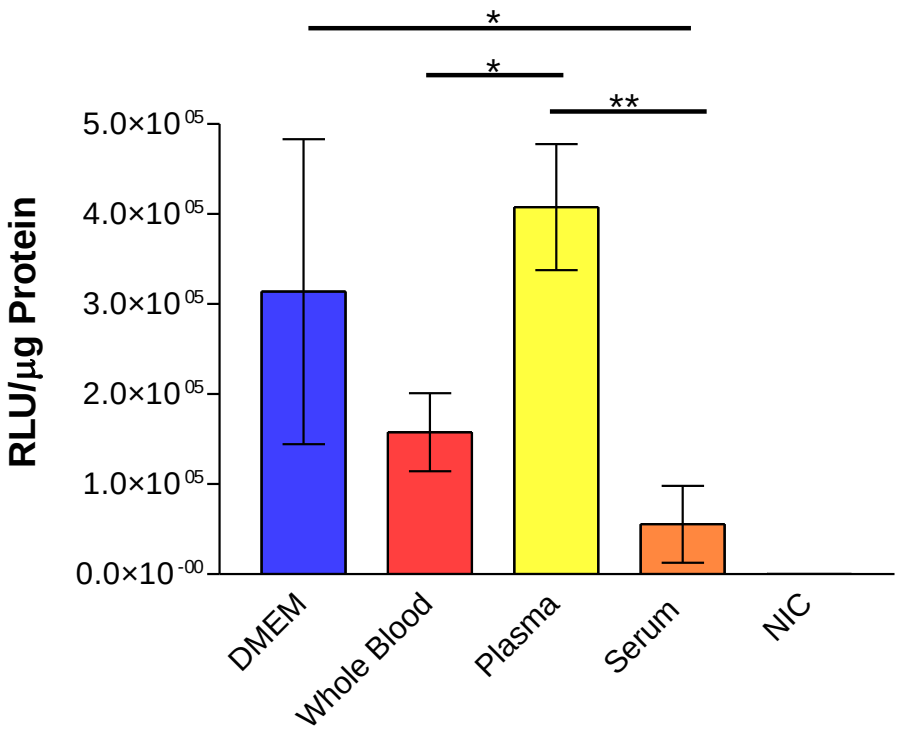

Figure 5.1: Effect of Blood Components on SV Infectivity – SVLuc DSG was incubated with serum free DMEM, whole blood, plasma or serum from donor L for 15 minutes at 37 °C at a virus-blood ratio similar to that predicted for *in vivo* experiments (where a mouse with a typical blood volume of 1.46 ml would receive a systemic injection containing ~ 10^7 PFU of SV). Incubations were then diluted in serum free DMEM and added to BHK monolayers in a 96 well plate such that cells were exposed to an MOI of 10 (PFU/cell) based on input virus amount, for 30 minutes at 37 °C. Monolayers were then washed 3 times with pre-warmed PBS and incubated at 37 °C for 16 hours. Luciferase transgene expression and protein content was determined by *in vitro* luciferase and BCA assay respectively. Blood was collected from donor L as described (Chapter 2.23) in lithium heparin coated (for plasma) or uncoated glass (for serum) vacutainers. NIC: non-infected control. Error bars show ± SD (n = 4). Statistical analysis was performed using one way ANOVA and Tukey's multiple comparison post-test (* = $P < 0.05$, ** = $P < 0.01$).

As these data, although reproducible with individual donors, were unexpected and rather counter-intuitive, blood was obtained from a larger panel of 13 healthy donors and analysis performed simultaneously. Figure 5.2 shows clear confirmation of the initial findings, that plasma enhances ($P < 0.001$), and serum inhibits ($P < 0.001$) SV infectivity compared to whole blood.

The key observation of these studies is that SV appears stable in whole blood for at least 15 minutes, suggesting it may be compatible for IV delivery in humans. However, the various effects of plasma and serum suggest there are factors exerting important effects that are not yet understood. Nevertheless, although we set out to identify these factors, the maximum level of inhibition observed is only about 5-fold in neat human serum; this is far lower than levels observed for other oncolytic viruses currently under development (unpublished data, Ying Di, University of Oxford).

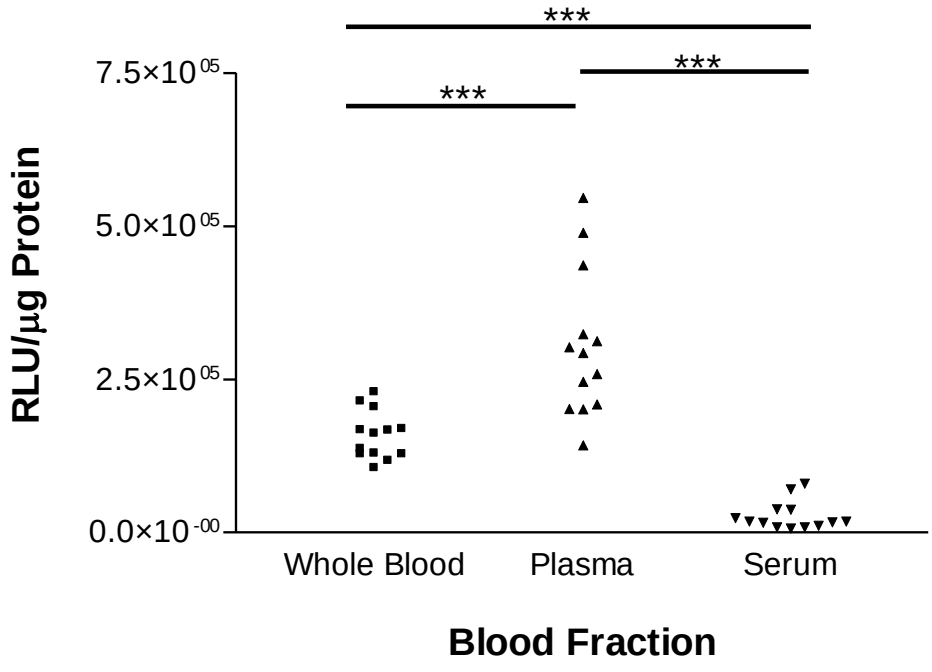

Figure 5.2: Effect of Blood Components on SV Infectivity from a Panel of Donors – Blood was collected from 13 donors in lithium heparin and glass vacutainers and whole blood, plasma or serum fractions were incubated with SVLuc DSG for 15 minutes at 37 °C before infection of BHK cells. Analysis of luciferase expression and protein content at 16 h PI was carried out as described in Figure 5.1 Each data point represents the mean value of quadruplicates of SVLuc DSG luciferase expression after incubation with whole blood plasma or serum from an individual donor. Statistical analysis was performed using one way ANOVA and Tukey's multiple comparison post-test (*** = $P < 0.001$)

5.2.2 SV May Bind Erythrocytes

Whole blood and plasma differ only by the presence of blood cells in the former; however, SV has enhanced activity upon exposure to plasma compared to whole blood. The ability of SV to bind erythrocytes, an interaction that may lower its infectivity by preventing association with target cell receptors (Carlisle, Di et al. 2009), was therefore analysed.

Several attempts were made to elucidate whether SV associates with erythrocytes. This was carried out by incubating virus with whole blood for 15 minutes, then collecting equal volumes of whole blood, plasma and erythrocyte fractions and analysing the number of SV genomes present by RNA extraction and RTQPCR. This procedure was technically difficult due to degradation of SV RNA by RNase present in human blood. Such difficulties were not experienced in RNA extraction from mouse blood or tissue and may be due to elevated levels of RNase present in human blood (Ambion 2012). It seemed that significant RNA degradation of samples occurred even in the presence of

RNase inhibitors in RNA extraction kits used. However, in a case where SV RNA degradation was incomplete, a significant fraction of SV genomes was associated with erythrocytes (Figure 5.3). It should be noted that erythrocytes were not washed, hence a considerable amount of virus would be expected to be trapped in the erythrocyte fraction in plasma occluded between cells. Nevertheless, if SV does not bind erythrocytes in whole human blood one would expect only a minority of SV RNA to be detected in the purified erythrocyte fraction compared to plasma. This suggests that SV in whole blood might indeed bind erythrocytes, either directly, or indirectly, through interactions with a component of blood. This may explain the decreased inhibition of infectivity of SV incubated in plasma compared to whole blood (Figure 5.2). It should be noted, however, that the recovery of SV RNA from whole blood was only 5.7% of the input dose, therefore differences observed may be an artifact arising from differential RNA degradation between samples.

The ability of SV to directly infect blood cells was tested by incubation of erythrocytes or buffy coats with SVGFP DSG and infection analysed by visualisation of eGFP expression utilising fluorescent microscopy. However, on no occasion was transgene expression observed (data not shown).

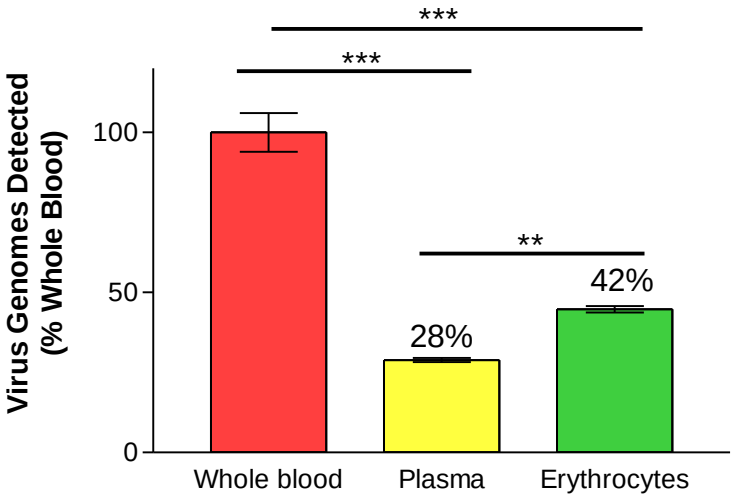

Figure 5.3: RTQPCR Detection of SVLuc DSG in Blood Compartments – Whole blood from donor "T" was incubated with SVLuc DSG (6.8 x10^6 PFU/ml) for 15 minutes at 37 °C. A 15 µl sample of whole blood was collected and stored on ice whilst the remainder of the whole blood separated into plasma and erythrocyte fractions by centrifugation for 5 minutes at 1000 x g, 4 °C. 15 µl samples of each were collected and RNA extracted and analysed by RTQPCR as described in Chapter 2.16

5.2.3 Effect of Anticoagulant on SV Neutralisation by Whole Human Blood and Plasma

Human serum inhibits SV infectivity compared to whole blood and plasma (Figure 5.2). One difference between blood and plasma, on one hand, and serum on the other, is the presence of lithium heparin, used as an anticoagulant, in the former. It is possible that lithium heparin might either directly stimulate SV infection, or interfere with the neutralisation mechanism mediated in serum. In order to assess the former possibility,

SV was incubated with DMEM in lithium heparin and glass tubes, and infectivity of BHK cells measured (Figure 5.4). A slight potentiating effect of SV infectivity in the presence of lithium heparin was observed, however, this was not statistically significant. This suggests previous effects observed in blood and plasma are likely to involve components of blood.

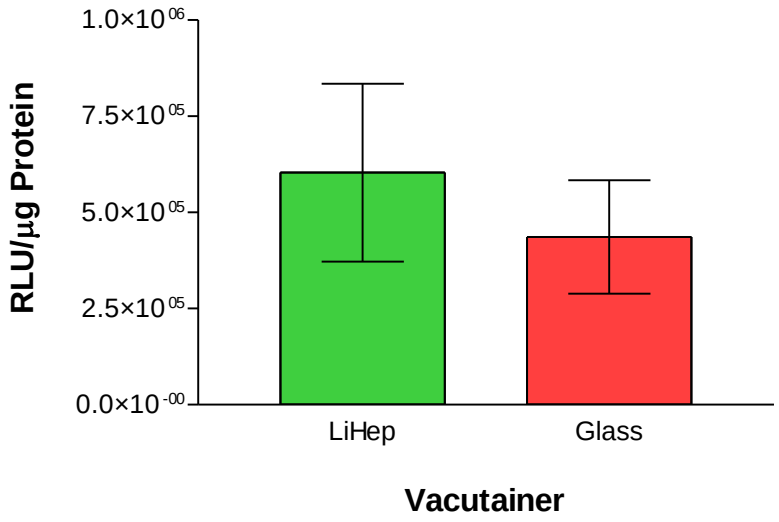

Figure 5.4: Lithium Heparin Does Not Directly Enhance SV Infectivity - SVLuc DSG was incubated with DMEM in either a glass or a lithium heparin coated vacutainer before infection. Infection of BHK cells, analysis of luciferase expression and protein content 16 h PI was carried out as described in Figure 5.1. Error bars show ± SD (n = 4). Statistical analysis was performed using an unpaired T test (two tailed), means were not significantly different (P = 0.2694).

In order to examine whether heparin contributes to the lack of SV neutralizing activity of whole blood or plasma *in vitro*, the neutralising activity of blood collected in lithium heparin coated tubes was compared with that of blood collected using another anticoagulant, acid citrate dextrose (ACD).

Heparin prevents clotting by activating anti-thrombin III, which inactivates factor IIa (thrombin) and to a lesser extent factor XIIa, XIa IXa, and Xa of the intrinsic coagulation pathway and Factor VIIa of the extrinsic coagulation pathway (Figure 5.5). In contrast, ACD prevents blood coagulation through citrate chelation of calcium, which is an essential cofactor for the formation of the prothrombinase complex, consisting of factor Xa and Va on negatively charged phospholipid membranes. Without association with the prothrombinase complex, the rate of conversion of prothrombin (factor II) to thrombin (factor IIa) by factor Xa is insignificant, hence coagulation does not occur (Figure 5.5).

.

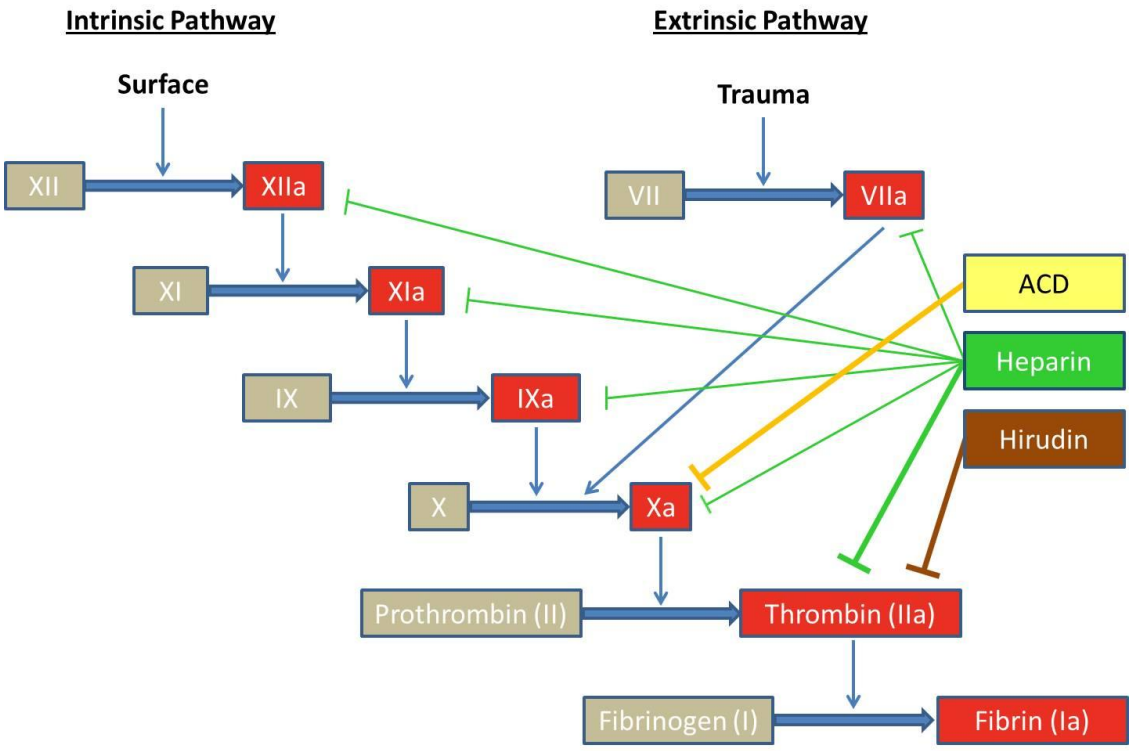

Figure 5.5: Anticoagulants and Activated Clotting Factors Present in Blood *in vitro* – The inhibition of clotting factors by anticoagulants used are highlighted on a simplified representation of the clotting cascade. Hirudin binds and irreversibly inhibits thrombin. ACD chelates calcium preventing the formation of the prothrombinase complex rendering factor Xa unable to convert prothrombin to thrombin. Heparin binds anti-thrombin III and causes a conformational change which exposes an active site and causes rapid binding and inactivation of activated clotting factors.

There was no difference in the SV-neutralising capacity of whole blood samples prepared using lithium heparin and ACD, or between corresponding plasma samples, or even between DMEM spiked with these anticoagulants (Figure 5.6). This suggests that SV resistance to neutralization by blood is not an artifact resulting from the anticoagulant used in blood collection procedures.

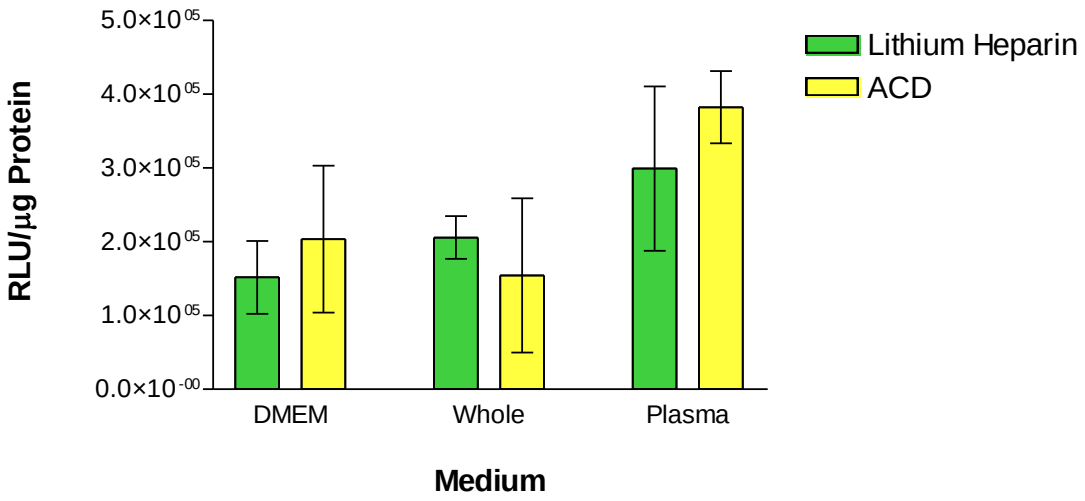

Figure 5.6: SV Stability in Whole Human Blood and Plasma Collected with Different Anticoagulants – Blood was collected from donor T in either lithium heparin or ACD containing vacutainers. 15 minute incubation with SVLuc DSG at 37 °C, infection of BHK cells, analysis of luciferase expression and protein content 16 hours PI was carried out as described in Figure 5.1. Error bars show ± SD (n = 4). Statistical analysis was performed using 3 separate unpaired T tests (two tailed), means were not significantly different (DMEM: P = 0.3868, whole blood: P = 0.3007, plasma: P = 0.7193).

5.2.4 Reversing the Neutralising Capacity of Human Serum

Serum mediated inhibition of SV infection could relate to the presence of products of the coagulation cascade. To test whether inhibition of SV infectivity by human serum could be relieved by the anticoagulants heparin or ACD, serum was collected by the

standard method described in Chapter 2.23, then transferred to vacutainers containing heparin or ACD.

It was observed that addition of lithium heparin relieved serum inhibition of SVLuc DSG infectivity (Figure 5.7). Addition of lithium-heparin in this way resulted in SV infectivity that was not significantly different from DMEM, whole blood or plasma collected in a lithium heparin coated tubes. Whilst the addition of ACD to serum appeared to relieve inhibition of SVLuc DSG infectivity to a lesser extent, this was not statistically significant.

It is possible that there is an agent in serum that inhibits SV infection which is sequestered or inhibited by lithium heparin. Lithium heparin is known to inhibit several proteases of the coagulation pathways by enhancing their inactivation by anti-thrombin III (Figure 5.5). In light of the ability of lithium heparin, but not ACD, to relieve inhibition of SV infectivity by human serum, SV might be neutralised by association with, or cleavage by one or several activated proteases of the coagulation cascade present in serum.

Another possibility is that SV is neutralized by complement which is known to be inhibited by ACD (Moini 2012) and heparin (Weiler, Yurt et al. 1978; Kadar, Parusel et al. 1992; Edens 1993; Lappegard, Fung et al. 2004). This could explain why serum inhibits SV infectivity and why addition of ACD or heparin to serum might have the ability to relieve this inhibition.

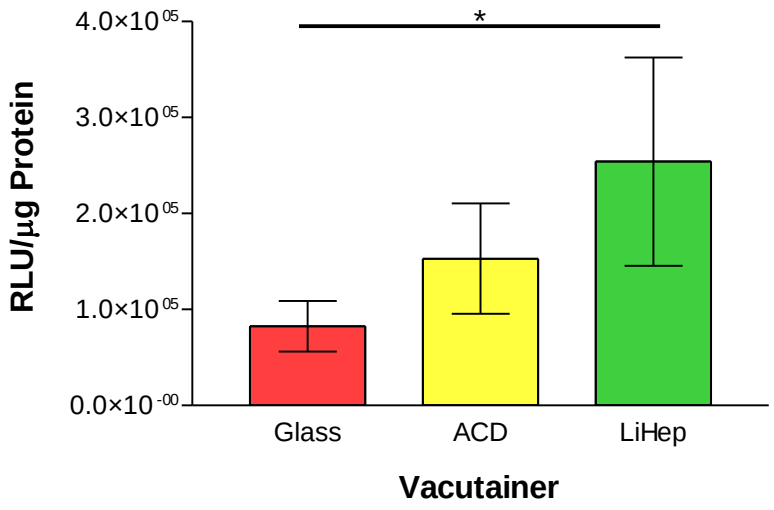

Figure 5.7 Anticoagulant Relief of Serum Inhibition of SVLuc DSG Infectivity – Serum was collected from donor "T" in a glass vacutainer and transferred to either ACD or heparin containing vacutainers before 15 minute incubation with SVLuc DSG and infection of BHK cells. Infection of BHK cells, analysis of luciferase expression and protein content 16 h PI was carried out as described in Figure 5.1. Error bars show ± SD (n = 4). Statistical analysis was performed using one way ANOVA. (* = $P < 0.05$).

5.2.5 Complement and SV Infectivity

It is known that heparin binds and interacts with several proteins in the complement cascade. It inhibits most steps in both the classical and alternative activation pathways and results in efficient dampening of complement activation (Edens 1993). This effect, has been shown to be concentration dependent, as at concentrations less than ~0.2 international units (IU)/ml of blood, heparin has been reported to enhance complement activation (Bexborn, Engberg et al. 2009). Inhibition of complement activation,

however, has been reported at 1 IU/ml (Bexborn, Engberg et al. 2009). The concentration of heparin present in blood coated collection tubes is 17 IU/ml (Becton Dickinson, UK), therefore it probably has an inhibitory effect on complement in these studies.

ACD inhibits the classical pathway of complement by chelating calcium ions required for C1 complex formation (Kadar, Parusel et al. 1992). Hirudin is a thrombin inhibitor produced and secreted by the leech *Hirudo medicinalis* that prevents blood clotting during feeding. Hirudin prevents coagulation by binding to, and irreversibly inactivating thrombin (Figure 5.5). Additionally it has been shown to have no effect on the rest of the coagulation cascade or complement activation (Bexborn, Engberg et al. 2009). To test whether complement inhibits infectivity of SV, blood was collected using hirudin as an anticoagulant (50 μg/ml) and incubated with SVLuc DSG before infection of BHK cells (Figure 5.8). It was seen that whole blood collected with hirudin, which contains active complement, did not significantly inhibit SV infectivity compared to DMEM. Complement, therefore, does not inhibit SV infectivity in these *in vitro* studies

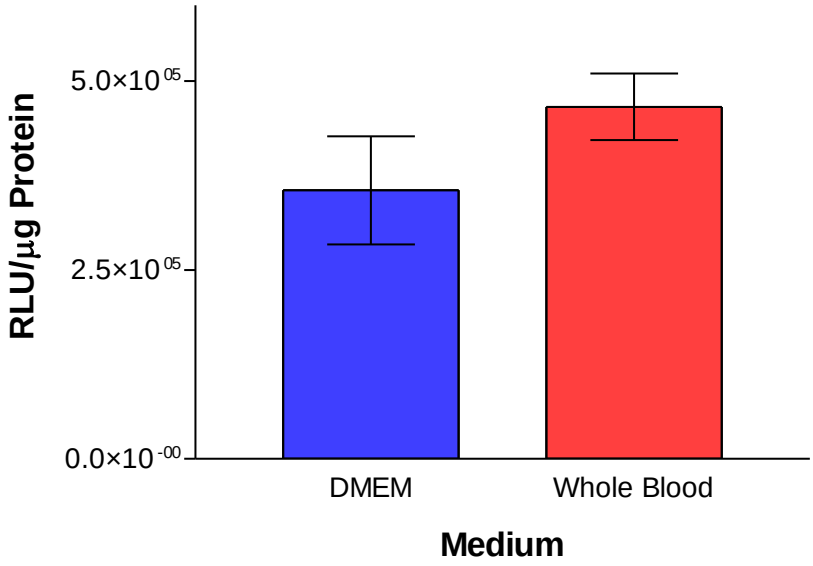

Figure 5.8: Complement Active Blood Collected with Hirudin Does Not Neutralize SV – Blood was collected from donor "T" in a glass vacutainer and 50 µg/ml hirudin added immediately. SVLuc DSG was incubated with whole blood or DMEM for 15 minutes at 37 °C before infection of BHK cells. Analysis of luciferase expression and protein content was performed 16 h PI as described in Figure 5.1 Error bars show ± SD (n = 3). Statistical analysis was performed using an unpaired T test (two tailed), means were not significantly different (P = 0.0848)

5.2.6 SV Behaviour in Human and Mouse Blood is Comparable

For testing the *in vivo* behaviour and oncolytic properties of SV, mouse models are widely used due to their well-defined characteristics and ease of use. In advance of investigating the PK and biodistribution properties of SV, stability in human and mouse blood was compared. SV infectivity following incubation with human or mouse blood (from donor "T" or the immune competent C57BL/6 strain) was not significantly different (Figure 5.9).

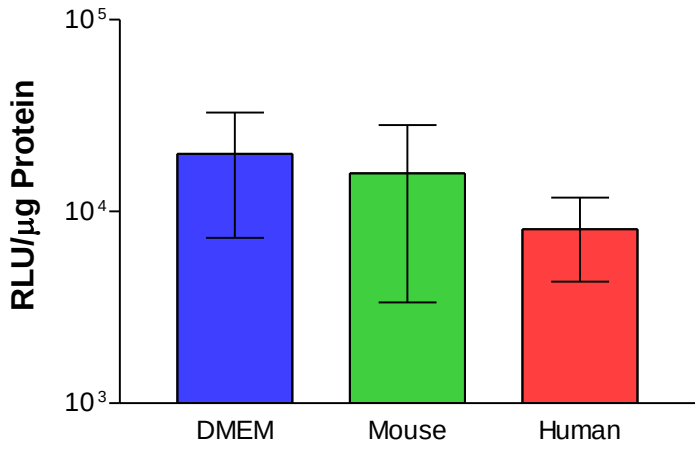

Figure 5.9: SV Neutralisation by Human and Mouse Blood – Human blood was collected from donor "T" and mouse blood was collected by exsanguination of 8 week old female C57BL/6 mice in lithium heparin coated vacutainers. SVLuc DSG was incubated with neat whole blood for 15 minutes at 37 °C before infection. Infection of BHK cells and analysis of luciferase expression and protein content 16 h PI was carried out as described in Figure 5.1. Error bars show ± SD (n = 5). Statistical analysis was performed using one way ANOVA. Means were not significantly different (P = 0.2300).

5.2.7 SV May Have a Direct Cell-Cell Spread Mechanism

As data indicate SV is stable in naïve human and mouse blood, it was investigated whether SV also possesses a mechanism of cell-cell spread that would render it resistant to neutralising antibodies. Initial bright field time lapse microscopy showed that SV kills by a mechanism that appears to be apoptotic and may involve direct cell-cell spread; the ability of SV to directly spread from one cell to another was therefore investigated. Time lapse videos were acquired as described in Chapter 2.19 with 1 image captured every minute over the course of SV infection. This high rate of image capture gives a high resolution of stages of active processes, as such, cell motility, blebbing and some vesicle trafficking can be seen.

A technical difficulty in capturing time lapse images of infected cells is caused by rounding up of cells when CPE is induced. Rounded cells refract light more than flat adherent cells hence have a bigger contrast with respect to background. This can cause autofocus functions to raise the plane of focus as a cell, or group of cells, round up. Once cells burst, the autofocus function, which only scans a depth of 6-12 μm, is often too far from the plane of focus of the remaining adherent cells to regain focus automatically, thus, significant numbers of time points can be missed. Phase contrast bright field microscopy is preferred to DIC for practical reasons. Although it yields less detailed images, light from a broader range of depths contributes to each image resulting in fewer cases of autofocus loss.

Uninfected BHK cells (Supplementary Figure 1.1, (DVD attached)) or BHK cells infected with SV at an MOI of 1 (Supplementary Figure 1.2 (DVD attached)) were analysed by phase contrast bright field microscopy with 1 image acquired every minute

over the course of 96 h. During SV infection, vesicles travelling from points of adhesion to the body of cells are more frequently observed. Whether these vesicles carry contents of the supernatant of one cell to the next is unclear, and interpretation is limited due to the quality of the images obtained.

In order to gain a more detailed view of such vesicular trafficking, SV infection of BHK was captured using DIC field microscopy with 1 image acquired every minute. Although, using this technique it took more attempts to collect data with images in focus throughout, it gave images with a much higher level of detail. Results clearly show characteristics of apoptotic death as well as possible cell to cell spread of SV through what appears to be trafficking of cytoplasmic components between cells (Figure 5.10 and Supplementary Figure 1.3 (DVD attached)). These trafficking events could be a result of SV manipulation of host cell machinery for spread to neighbouring cells in a way which would avoid neutralization by immune cells.

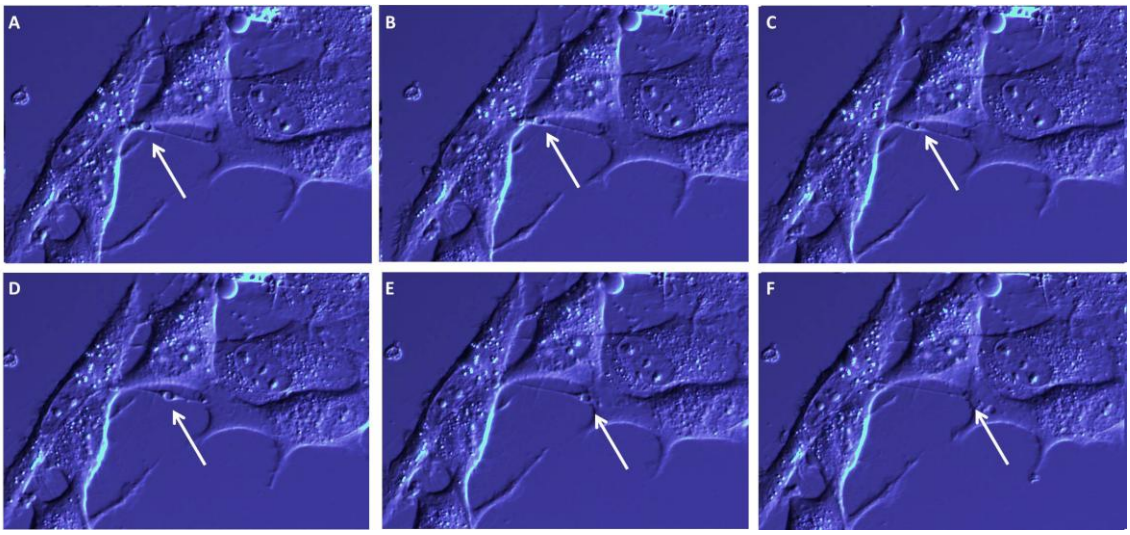

Figure 5.10: Possible Cell-Cell Spread of SV – BHK cells were infected at an MOI of 1, chambers were sealed 4 h PI and images acquired every minute. Videos have a playback rate of 25 frames/second (Supplementary Figures 1.1-1.3). Images A-F are each 10 minutes apart. A = 2190 minutes PI. Arrow denotes possible passage of vesicle between neighbouring cells.

5.2.8 Spread of SV in the Presence of Neutralising Antibodies

In order to analyse whether SV is capable of direct cell to cell spread, an assay was developed to test whether virus could spread in the presence of neutralizing antibodies. A serum sample from a patient with Pogosta disease (08PG365), characterized for IgG and IgM levels, a kind gift from Professor Vapalahti (University of Helsinki), was analysed for its ability to prevent SV infection of BHK cells *in vitro*. Results showed an IC_{95} of ~ 1/178 and an IC_{50} of ~ 1/668 dilutions (Figure 5.11).

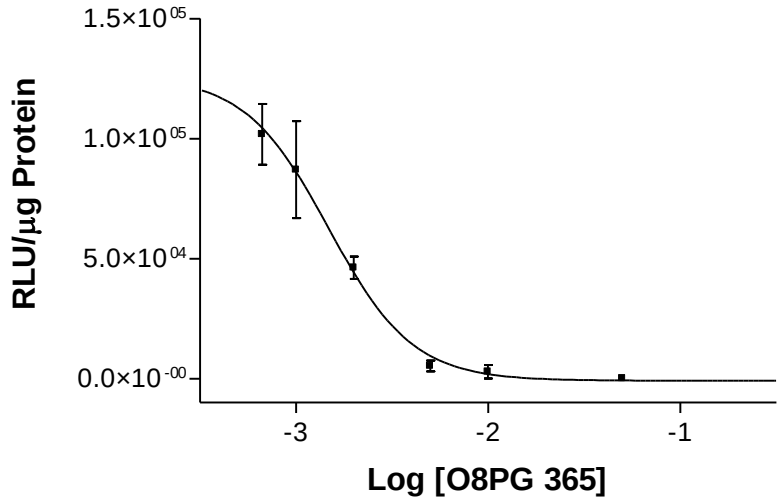

Figure 5.11: Inhibition of SVLuc DSG Infection by Immune Human Serum – Dilutions of 08PG365 over a range of concentration were made using SFDMEM. SVLuc DSG was incubated for 15 minutes at 37 °C with dilutions of 08PG365. Each dilution was constructed so that 100 µl contained 10^5 PFU of SVLuc DSG, equivalent to an MOI of 10 PFU/cell. Cells were lysed 16 h PI and analysed for luciferase expression and protein content as described in Chapter 2.11 and 2.12. Curve was fitted using PRISM 3 non-linear regression curve fit. Error bars show $\pm$ SD (n = 3).

Having validated the neutralizing capacity of 08PG365, in order to determine if SV could spread in the presence of neutralizing serum, an experiment was conducted in which two monolayers of BHK cells were seeded simultaneously. BHK cells seeded in a 24 well plate were infected with SVRFP DSG, SV expressing TurboRFP (As described in Chapter 3.1-3.3) at an MOI of 10 PFU/cell. 4 h PI the infected cell monolayers were washed and dissociated, re-suspended at a concentration of 2000 cells/ml in DMEM containing 08PG365 at final dilution factor of 1/20. This suspension was transferred to an uninfected monolayer of BHK cells pre-seeded in a chamber for time lapse microscopy (as described in Chapter 2.19) at a final ratio of 1 infected:100 uninfected cells. Bright field and fluorescent time lapse microscopy was used to monitor the cell monolayer during infection and TurboRFP transgene expression. Results show the rapid spread of SV in the absence of neutralizing antibodies with ~90% of cells showing TurboRFP expression after ~22 h (Supplementary Figure 1.4 (DVD attached)). In the presence of 08PG365 spread was not prevented, but delayed such TurboRFP expression in ~90% of cells occurs by ~70 h (Supplementary Figure 1.5 (DVD attached)).

In no field of view was vesicular trafficking observed to transfer red fluorescent supernatant directly from one cell to another, which would allow transfer of virus

genomes. This suggests that eventual spread in the presence of antibody may therefore be due to saturation of neutralizing antibodies, perhaps due to continued release of virus particles from initially infected cells through the course experiments. To test whether, neutralizing serum had become exhausted, inhibition of SVLuc DSG infection by "used" 08PG365 was tested. Supernatant from a time course experiment containing 08PG365 at a dilution factor of 1/20, where SVRFP DSG had successfully spread, was filtered and serially diluted alongside "fresh" 08PG365, and incubated with SVLuc DSG for 15 minutes prior to infection of BHK cells. Luciferase expression was analysed 16 h PI as a measure of SVLuc DSG infectivity (Figure 5.12 A).

"Used" 08PG365 showed decreased ability to neutralise SVLuc DSG compared to "fresh" 08PG365 at a dilution of 1/20, suggesting that it had lost SV neutralising capacity over the course of the above mentioned time lapse experiment (Figure 5.12 A). In fact, the neutralising activity of "used" 08PG365 is clearly compromised because it contains viable SVRFP DSG particles, as seen by fluorescent microscopy of BHK cells before analysis of luciferase expression (Figure 5.12 B). The observed infection of a proportion of BHK cells treated with "used" 08PG365 by SVRFP DSG is likely to have reduced the luciferase expression of monolayers due to competition with SVLuc DSG for BHK cell infection, especially when considering the effects of superinfection exclusion (described in Chapter 3.2.8).

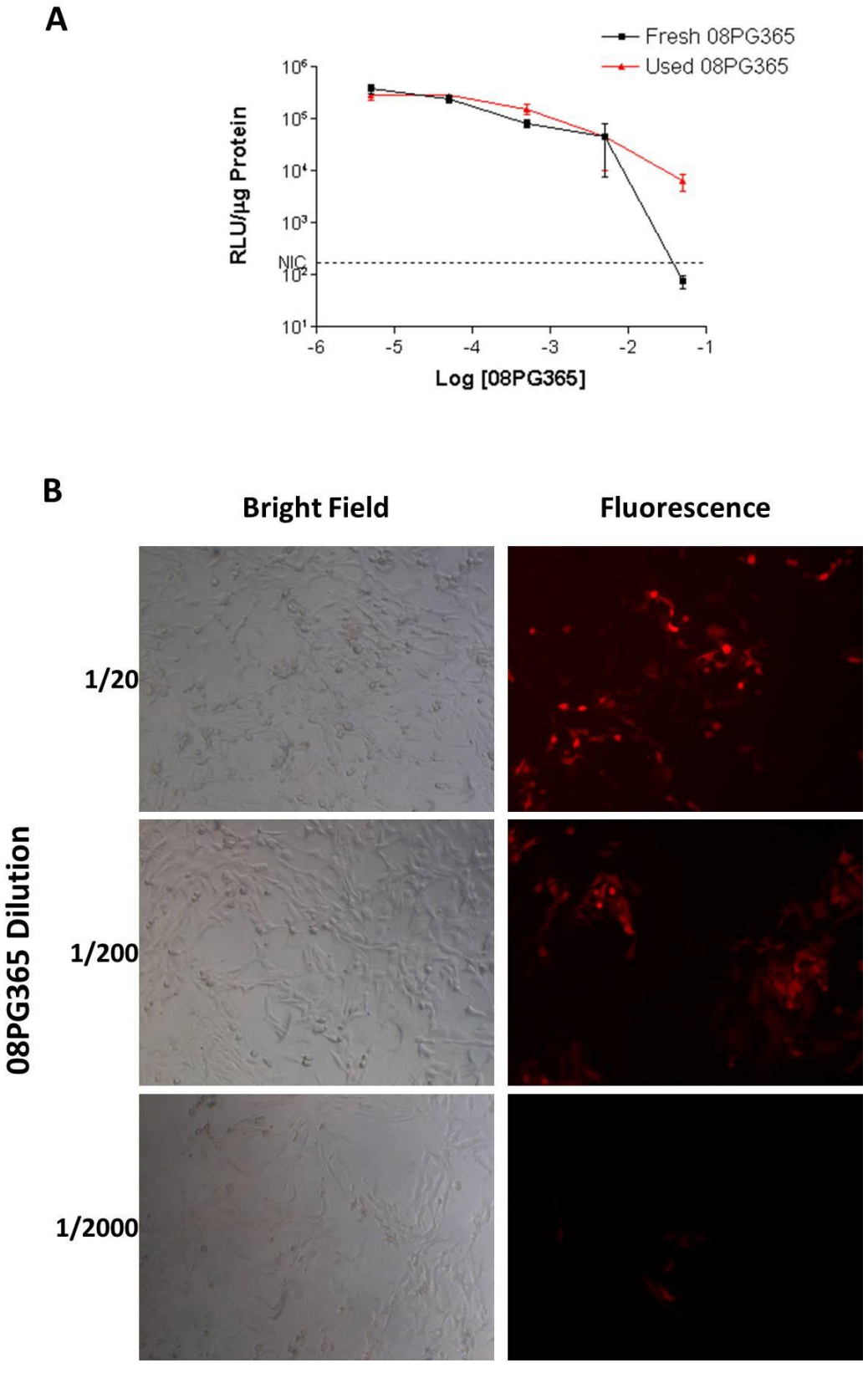
A
Fresh 08PG365
Used 08PG365
RLU/µg Protein
NIC
Log [08PG365]
B
Bright Field
Fluorescence
08PG365 Dilution
1/20
1/200
1/2000

Figure 5.12: Reduced Neutralising Capacity of "Used" 08PG365 – After the experiment shown in Supplementary Figure 1.5, "used" tissue culture media containing 08PG365 at a final dilution of 1/20 was serially diluted and incubated with SVLuc DSG as in Figure 5.11 alongside fresh 08PG365. Error bars show ± SD (n = 3). **A)** Luciferase levels and protein content of infected BHK cells were measured 16 h PI were measured as described in Chapters 2.11 and 2.12. **B)** Bright field and fluorescence microscopy of representative wells at different dilutions of used 08PG365 serum from A), immediately prior to lysis for luciferase expression analysis.

5.2.9 SV Infection of Invertebrate Cells

SV virions acquire their phospholipid membrane from the cytoplasmic membrane of the cells from which they bud and glycosylation of viral proteins is carried out by host cell machinery. Virus particles produced from vertebrate and invertebrate cells therefore differ in phospholipid content and surface protein glycosylation patterns. To assess whether these differing properties conferred differences in infectivity or stability in blood, SV produced from invertebrate (mosquito) and vertebrate (hamster) cells was compared.

To test whether SV could be successfully produced from invertebrate cells *in vitro* by simple infection, the *Aedes albopictus* (Asian tiger mosquito) cell line C6/36 was infected with SV produced from BHK cells as described in Chapter 3.2.2. SVGFP DSG transgene expression was visible 24 h PI by fluorescence microscopy; in addition, transgene expression was noted up to and beyond 10 days PI without visible CPE (Figure 5.13). This observation is in stark contrast to PI events in vertebrate cells, where after ~24 hours cells show CPE and after 72 hours die by apoptotic pathways (Figure 3.7).

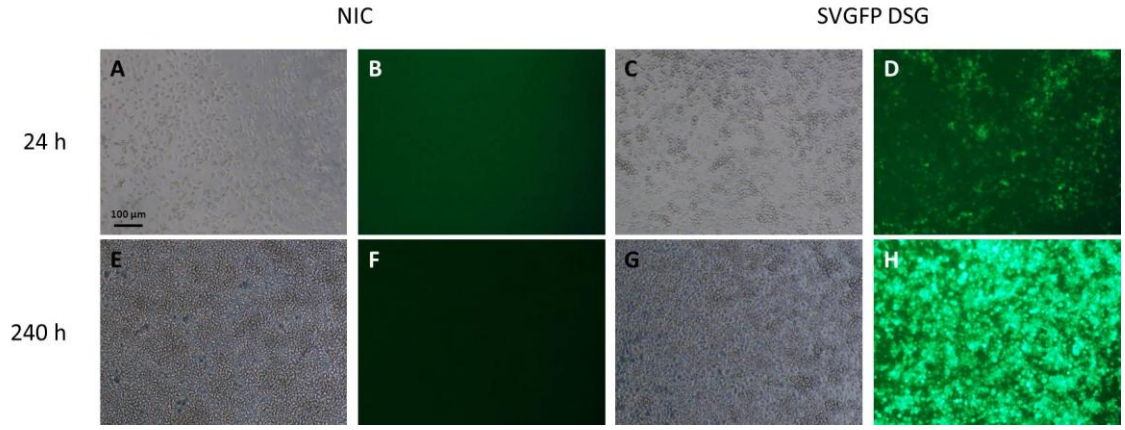

Figure 5.13: Transgene Expression in Mosquito Cells – C6/36 cells were either uninfected or infected with SVGFP DSG at an MOI of 1. A-D) 24 h PI, E-H) 240h PI, A,C,E and G) Bright field illumination, B,D,F and H) eGFP fluorescence (ultraviolet (UV) exposure, 6 sec).

Microscopy images suggested that C6/36 cells were resistant to killing by SV despite being susceptible to infection and permitting the expression of virally encoded eGFP. To test if cells were indeed resistant to killing by SV, cell viability was measured PI. Results show no significant difference in viability between C6/36 cells exposed to SV at an MOI 10 and non-infected cells 10 days PI (Figure 5.14)

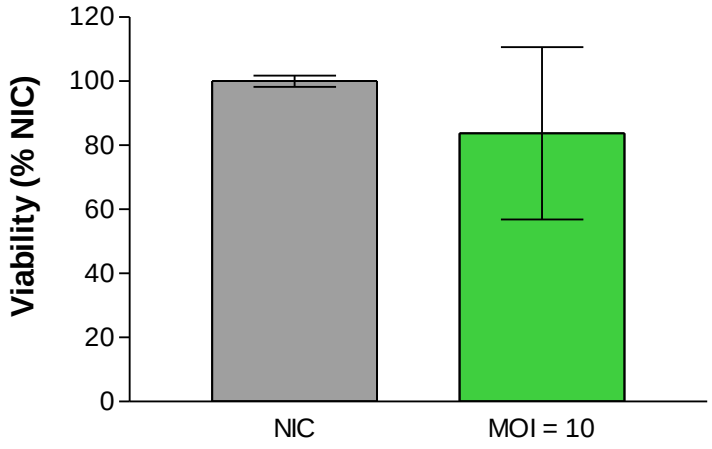

Figure 5.14: Mosquito Cells Resistant to Killing by SV – C6 /36 Cells were infected with SVGFP DSG and viability was measured 10 days PI by MTS assay as described (Chapter 2.14). Error bars show ± SD (n = 3). Variances were not equal as determined by an F test (P = 0.043) so statistical analysis was performed using an unpaired T test (two tailed) with Welch's correction. Means were not significantly different (P = 0.4054)

5.2.10 Production of SV from Invertebrate Cells

Evidence for the stable infection of invertebrate cells by other strains of SV has been widely reported along with data suggesting *in vivo* mosquito infection results in no pathological symptoms (Kosova 2003). It is possible that infected insect cells may interfere with a step in SV replication hence ablate infection related toxicity. To test whether persistently infected C6/36 cells stopped or reduced SV shedding, the supernatant of infected C6/36 cells was collected over the course of 10 days and analysed for SV genomes by RTQPCR (Figure 5.15 A). It was observed that persistently infected cells continue to produce and secrete virus particles with a steady state of virus production and decay reached at ~3 days PI.

Although C6/36 cells produced up to 10^9 VP/ml during infection as measured by RTQPCR, it is possible that virions released from insect cells may have an altered ability to infect and kill mammalian cells in tissue culture. To test this hypothesis, SV particles shed into the supernatant during infection of C6/36 cells were collected. The number of VP and PFU were determined by RTQPCR and $TCID_{50}$ (on BHK cells) respectively. Results showed VP/PFU ratios comparable to those observed for SV produced in BHK cells and these ratios did not significantly change for SV particles released from C6/36 cells over the course of 5 days (Figure 5.15 B). This suggests that persistent infection is a phenomenon derived from intracellular host-virus interactions and virus particles themselves are not impaired.

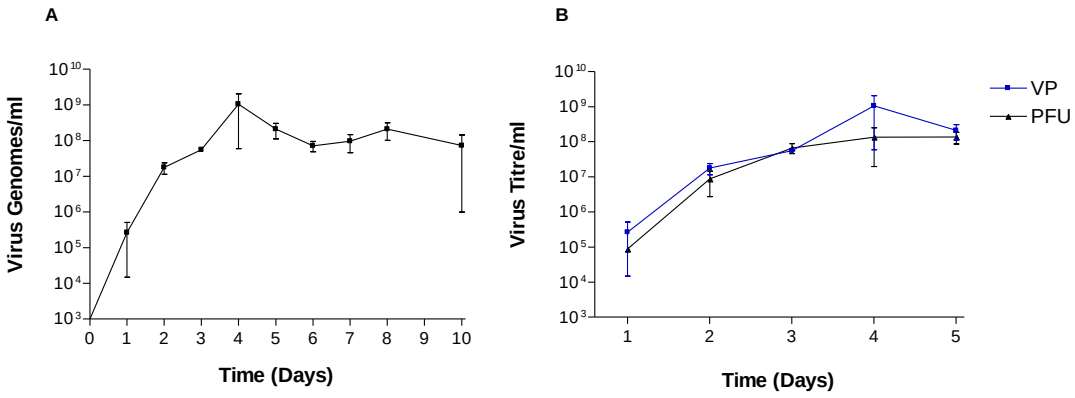

Figure 5.15 SV Shedding from Persistently Infected Invertebrate Cells – C6/36 cells were infected with SVGFP DSG at an MOI of 1 and supernatant samples were collected daily **A)** VP detection by RTQPCR analysis of supernatants over the course of 10 days, **B)** Comparison of supernatant VP and PFU by RTPCR and $TCID_{50}$ respectively. Error bars show ± SD (n = 3).

5.2.11 Tropism of Invertebrate and Vertebrate Cell Derived SV

It is known that virions produced from vertebrate and invertebrate cells differ in structure and physical properties (He, Piper et al. 2010). To analyse what, if any effects this has on the infectivity and toxicity to cell lines *in vitro*, vertebrate derived SVLuc DSG (VD SVLuc DSG) and invertebrate derived SVLuc DSG (ID SVLuc DSG) were compared for their luciferase expression 24 h PI and their cytotoxicity 48h PI. It was observed that infection was correlated with cell kill as seen by transgene expression and viability. SV produced in either cell type had a similar tropism but SV produced in vertebrate cells had a significantly higher infectivity in cell lines most susceptible to SV infection. This difference may be due to different VP/PFU ratios of the two preparations

as doses were normalised for VP equal to a VD SVLuc MOI of 1 PFU/cell as determined by $TCID_{50}$ on BHK cells. Only in MCF-7 and ZR75.1 cells did the luciferase expression observed with ID match that with VD. Cytotoxicity was equivalent for both viruses in all cell lines 72 h PI (Figure 5.16). It is probable that the significantly higher levels of transgene expression observed 24 h PI of BHK, C2C12 and B16 cells with VD compared to ID SVLuc DSG correlates with a decrease in viability at earlier time points than 72 h.

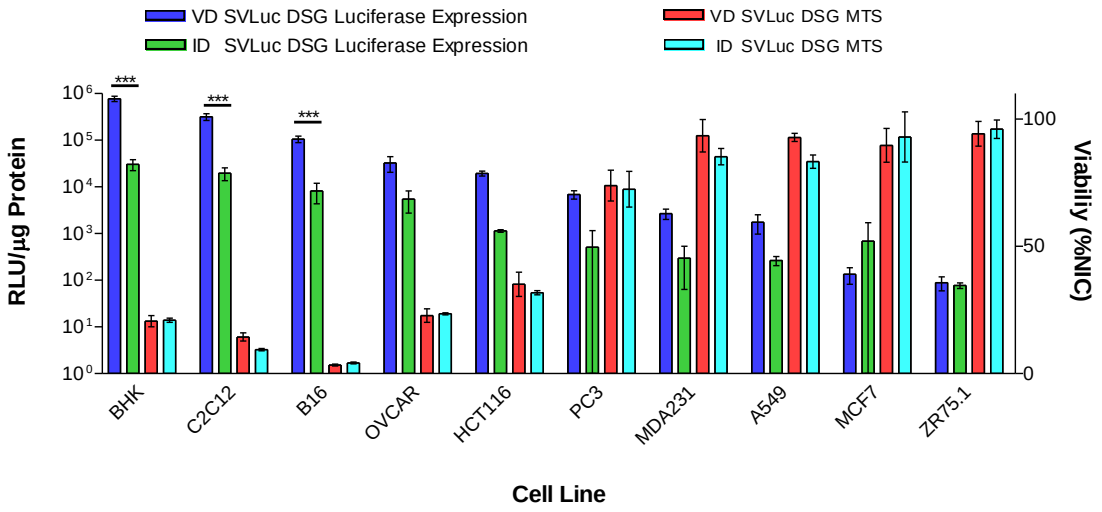

Figure 5.16: Tropism of Invertebrate and Vertebrate Derived SV – Cell lines were plated in triplicate in 2 separate 96 well plates for analysis of luciferase expression and cell viability. Both plates were infected concurrently with VD SVLuc DSG at an MOI of 1 as determined by $TCID_{50}$ on BHK cells or an equal particle number of ID SVLuc DSG as determined by RTQPCR. Luciferase expression and total protein content was analysed 24 h PI by *in vitro* luciferase assay and BCA assay whilst cell viability was measured by MTS assay 3 days PI (Chapter 2.11, 2.12 and 2.14 respectively). Error bars show ± SD (n = 3). Statistical analysis of luciferase expression and cell viability was performed using two separate two-way ANOVAs with Bonferroni post-tests. (*** = $P < 0.001$).

5.2.12 VD and ID SV Behaviour in Human Blood In Vitro is Similar

The infectivity of ID SV on a range of cell lines was unchanged compared to VD SV hence virus-target cell surface interactions are probably similar. It is possible, however, that differences in physical properties lead to changes in the interactions of VD and ID virus particles with blood components. In particular, differing membrane composition and glycosylation patterns derived from invertebrate cells may be the target of innate immune mechanisms.

To test whether there were any differences in the stability of VD and ID SV in human blood, each was incubated with whole blood, plasma or DMEM, then infectivity of BHK cells was analysed (Figure 5.17 B). Blood components had no significant effects on infectivity, however, as with previous experiments; ID SVLuc DSG had a significantly lower infectivity than VD SVLuc DSG.

SV stability in human blood could be due to lack of complement activation or resistance to complement effector mechanisms. C3a is produced upon activation of the complement cascade by either the classic or alternative pathway (Figure 5.17A). To test whether SV activates complement and whether there is any difference between VD and ID SV complement activation, C3a-desArg accumulation was directly measured using a sandwich ELISA.

There was no significant difference in C3a-desArg levels measured following incubation with either VD or ID SVLuc DSG compared to control plasma or serum (Figure 5.17 C). This data shows that SV does not activate complement when added to blood *in vitro* regardless of vertebrate or invertebrate origins of the cell line used for production.

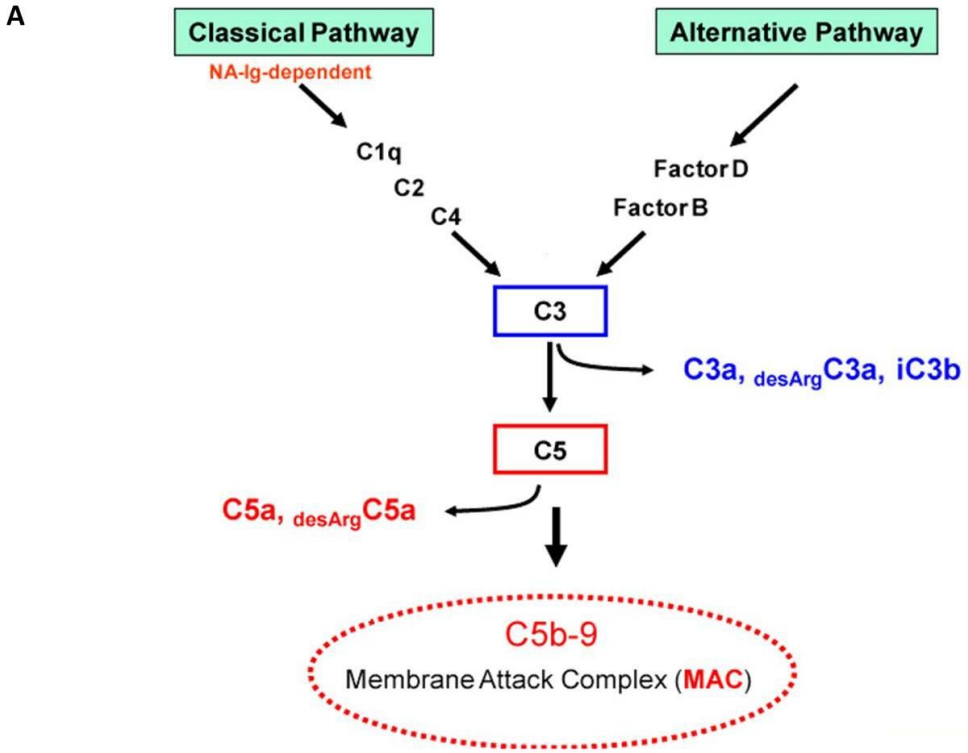
A
Classical Pathway
NA-Ig-dependent
Alternative Pathway
C1q
C2
C4
Factor D
Factor B
C3
C3a, desArgC3a, iC3b
C5
C5a, desArgC5a
C5b-9
Membrane Attack Complex (MAC)

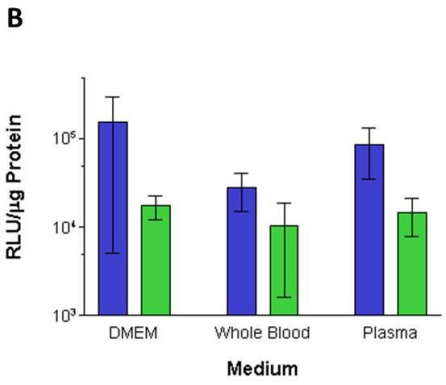
B
RLU/µg Protein
10⁵
10⁴
10³
DMEM
Whole Blood
Plasma
Medium

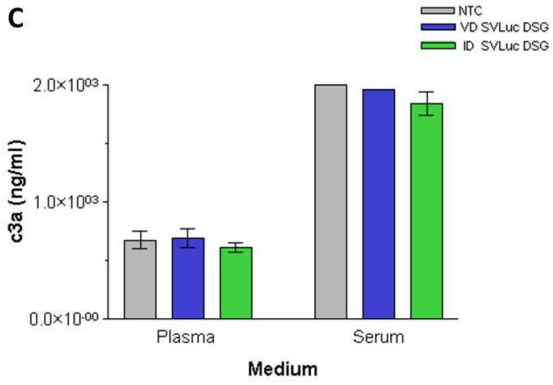
C
NTC
VD SVLuc DSG
ID SVLuc DSG
c3a (ng/ml)
2.0×10⁰³
1.0×10⁰³
0.0×10⁰⁰
Plasma
Serum
Medium

Figure 5.17: VD and ID SV are Resistant to Human Blood and Do Not Activate Complement– A) A simplified overview of the complement cascade illustrating the production of C3a by both the classical and alternative pathway. NA-Ig = Neutralising antibody-immunoglobulin. Adapted, with permission, from (Ratajczak and Kim 2011). **B)** VD and ID SVLuc DSG were incubated with DMEM, whole blood or plasma (from donor "L") for 15 minutes at 37 °C before infection of BHK cells. Infection of BHK cells, analysis of luciferase expression and protein content 16 h PI was carried out as described in Figure 5.1. Error bars show ± SD (n = 3). Statistical analysis was performed using two-way ANOVA with a Bonferroni post-test. Transgene expression of ID SVLuc DSG was significantly lower than VD SVLuc DSG ($P = 0.0102$) whilst incubation with blood components gave rise to no significant difference ($P = 0.1359$). Transgene expression following incubation with DMEM was significantly different (* = $P < 0.05$). **C)** 10^7 VP of VD and ID SVLuc DSG were incubated in plasma or serum for 30 minutes, complement activation was terminated by addition of 10 mM EDTA then C3a-desArg was determined by sandwich ELISA as described (Chapter 2.24). Serum was collected as standard. For plasma, blood was collected in a glass vacutainer and 50 μg/ml hirudin added immediately to prevent coagulation, then treated as standard. Statistical analysis was performed using one-way ANOVAs and Tukey's multiple comparison post-tests. The mean values of C3a in plasma and serum were not significantly different ($P = 0.5301$ and $P = 0.0941$ respectively).

5.2.13 The In Vivo Pharmacokinetics of VD and ID SV in Mice are Similar

The stability in blood of ID and VD SV was shown to be similar but the infectivity of mammalian cells as measured by transgene expression in cell lines *in vitro* was lower for ID SV. It is feasible that reduction in infectivity of ID SV is a compromise for either more favourable *in vivo* PK or biodistribution that would aid the establishment of a productive infection; for example reducing sequestration by the reticuloendothelial system (RES). In order to test this hypothesis, the PK of each was analysed by delivering VD or ID SVLuc DSG intravenously to subcutaneous B16 tumour bearing C57BL/6 mice, and blood samples collected over the course of an hour. The biodistribution of each virus was analysed by harvesting organs 1 hour after IV delivery of SV and detecting viral genomes present by RTQPCR. Results show that SV produced in invertebrate cells has equivalent PK and biodistribution to SV produced in vertebrate cells (Figure 5.18 A and B).

SV was rapidly cleared from the circulation. Based on the determined average weight of mice, 20.3 g, and estimated blood volume as 70 ml/kg, the average blood volume was taken as 1.42 ml per mouse (Diehl, Hull et al. 2001). Calculated SV titres were reconfirmed by RNA extraction and RTQPCR of an input dose and the number of SV particles measured in 10 µl blood samples were expressed as percentages of the input dose in the total circulation. For both VD and ID SV, about 20 % of the input virus dose was in the circulation after 2 minutes and only 1 % remained after 5 minutes (Figure 5.18 A).

The average mass of a C57BL/6 mouse liver is about 5 % of its body weight (Duval, Thissen et al.). Based on this value, measurements show about 15 % of input SV was present in the liver after 1 hour (Figure 5.18 B). Clearance of SV from the circulation is likely due to uptake of virus particles by Kupffer cells in the liver and marginal zone and red pulp macrophages of the spleen based on their size.

As VD and ID virus demonstrated equivalent circulation kinetics and tumour accumulation, further anti-tumour efficacy studies were performed with VD virus due to its raised transgene expression activity in cells *in vitro* (Figure 5.16).

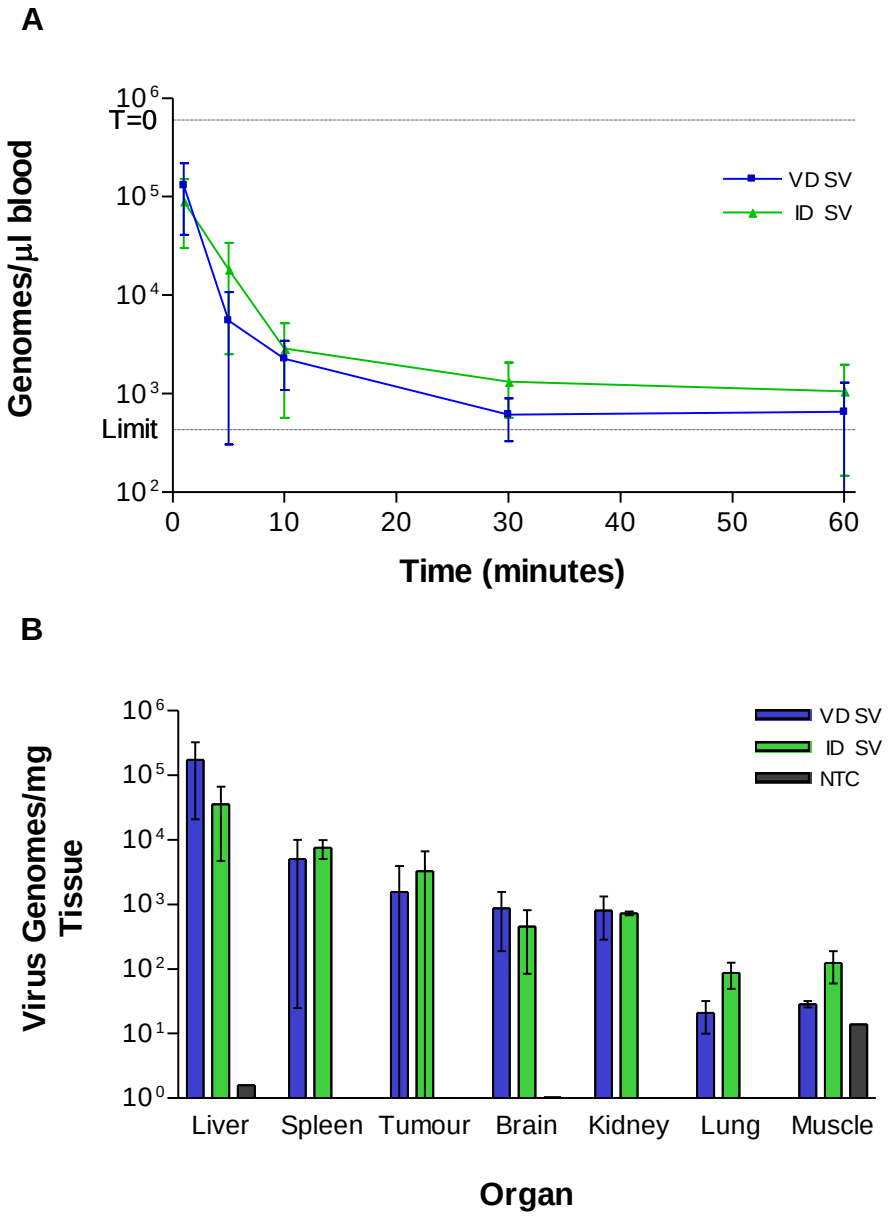
A
Genomes/µl blood
10^6
T=0
10^5
10^4
10^3
Limit
10^2
VD SV
ID SV
0
10
20
30
40
50
60
Time (minutes)
B
Virus Genomes/mg Tissue
10^6
10^5
10^4
10^3
10^2
10^1
10^0
VD SV
ID SV
NTC
Liver
Spleen
Tumour
Brain
Kidney
Lung
Muscle
Organ

Figure 5.18: Pharmacokinetics and biodistribution of VD and ID SV – A) 6 week old C57BL/6 mice bearing subcutaneous B16 tumours were injected with 8.5 x 10^8 VP of VD or ID using 25 gauge needles. Following injection blood samples were collected in Eppendorf tubes over the course of an hour by tail bleeds. Blood samples were immediately snap frozen using liquid nitrogen. RNA was extracted from whole blood samples, as well as an additional dose of neat input virus from a loaded syringe, using the QIAamp Viral RNA Mini Kit. The number of SV genomes in each RNA extract was determined by RTQPCR. Error bars show ± SD (n = 3). Statistical analysis was performed using two-way ANOVA which showed the rate of clearance of VD and ID SV from the blood was not significantly different (P = 0.6857). Dotted line represents input dose. **B)** Mice that had received PBS, VD SV or ID SV were sacrificed 1 hour post injection. Organs were harvested and soaked in RNA later and stored at 4 °C overnight then snap frozen using liquid nitrogen and stored at -80 °C until RNA extraction. RNA was extracted from tissue samples using the RNAqueous Kit. Standard curves for virus genomes in each tissue were created by spiking control tissue homogenates with known amounts of SV RNA after the addition of lysis buffer (RNA was produced by *in vitro* transcription and quantified using a Nanodrop) see Chapter 2.16. The number of virus genomes in each sample was determined by RTQPCR. Error bars show ± SD (n = 3). Statistical analysis was performed using two-way ANOVA which showed no significant difference in the accumulation of VD and ID SV in tissues collected (P = 0.1742).

5.2.14 Effect of Clodronate Liposomes on Pharmacokinetics of SV

Upon systemic use of SV as an anticancer agent, rapid clearance of virus particles from the circulation will diminish the effective dose reaching disseminated metastatic target tumour cells. Clodronate liposomes are toxic to Kupffer cells and studies with adenovirus have shown that administration 24 h before delivery of virus IV can considerably extend circulation kinetics (Green NK 2012).

In an attempt to reduce the accumulation of SV in the liver and spleen and therefore extend the circulation kinetics of SV, clodronate liposomes were used. Pre-treatment of mice with clodronate liposomes significantly lowered the accumulation of SV in the liver (2.92 fold, $P < 0.001$) following IV delivery in C57BL/6 mice (Figure 5.19 B). Reduced accumulation of SV in the liver, however, was not associated with enhanced circulation kinetics, and most importantly, did not lead to increased accumulation of SV in tumours (Figure 5.19 A). It is possible that upon depletion of Kupffer cells, splenic macrophages become more prominent in clearing SV from the circulation. Reduction of liver accumulation, however, was not associated with a statistically significant increase in accumulation of SV in the spleen.

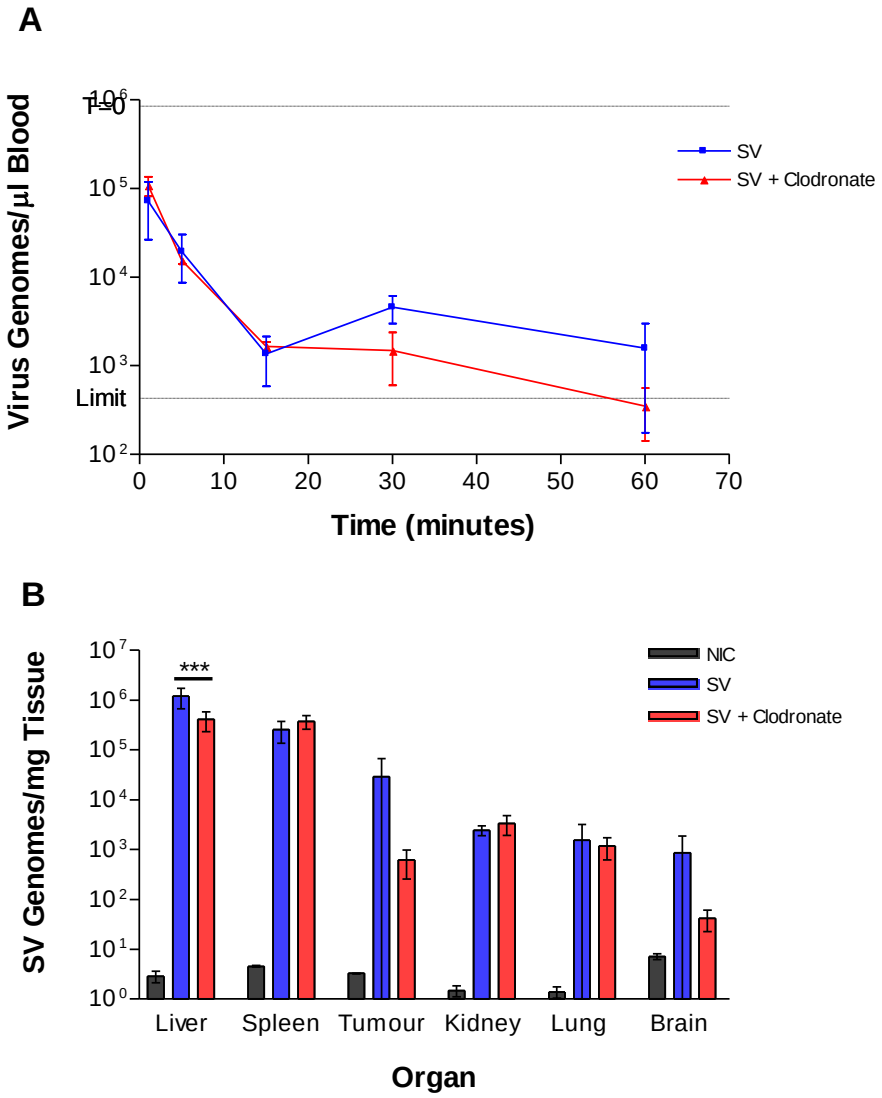
A
Virus Genomes/µl Blood
T=0
Limit
SV
SV + Clodronate
Time (minutes)
B
SV Genomes/mg Tissue
***
NIC
SV
SV + Clodronate
Liver
Spleen
Tumour
Kidney
Lung
Brain
Organ

Figure 5.19 SV Pharmacokinetics and Biodistribution after Treatment with Clodronate Liposomes – A) Tumour bearing, 6 week old C57BL/6 mice were injected with either 200 µl of clodronate liposomes 24 h before they received 1.2 x 10^9 VP of SV using 25 gauge needles. Following SV injection blood samples were collected in Eppendorf tubes over the course of an hour by tail bleeds. Blood samples were immediately snap frozen using liquid nitrogen. RNA was extracted from whole blood samples, as well as an additional dose of neat input virus from a loaded syringe, using the QIAamp Viral RNA Mini Kit. The number of SV genomes in each RNA extract was determined by RTQPCR. Error bars show ± SD (n = 3). Statistical analysis was performed using two-way ANOVA and clodronate liposome pre-treatment had no significant effect on the rate of SV blood clearance (P = 0.3700). **B)** Mice that had received SV following PBS or clodronate liposome pre-treatment were sacrificed 1 hour post IV injection of SV. Organs were harvested and soaked in RNA Later (Applied Biosystems, UK) and stored at 4 °C overnight then snap frozen using liquid nitrogen and stored at -80 °C until RNA extraction. RNA was extracted from tissue samples using the RNAqueous Kit. Standard curves for virus genomes in each tissue were created by spiking control tissue homogenates with known amounts of SV RNA after the addition of lysis buffer (RNA was produced by *in vitro* transcription and quantified using a Nanodrop). The number of virus genomes in each sample was determined by RTQPCR. Error bars show ± SD (n = 3). Statistical analysis was performed using two-way ANOVA which showed SV accumulation in tissues was significantly lower in clodronate pre-treated mice (P = 0.0492). A Bonferroni post-test showed that the accumulation of SV in the liver of clodronate pre-treated mice 1 hour after inoculation was significantly lower (P < 0.001).

5.2.15 Anticancer Efficacy of SV

The PK and biodistribution of SV could not be enhanced by utilizing invertebrate producer cells or clodronate pre-treatment. *In vitro* studies, however, show resistance of SV to neutralization by human and mouse blood. This suggests that although SV is cleared from mouse blood rapidly, time in the circulation may be sufficient for a therapeutic dose to reach disseminated metastases following IV delivery.

SV in a therapeutic setting would be required to infect and destroy disseminated tumour metastases either too small to detect or in sites inaccessible for surgical resection. Most previous studies showing anticancer efficacy of SV have been in immune deficient hosts which are inadequate models, firstly because tumours that develop in the absence of immune system interactions do not reflect those in the clinical setting (Dunn, Bruce et al. 2002), and secondly because the development of an adaptive immune response can impact on viral spread through tumours and prevent efficient delivery of multiple viral doses (Ikeda, Ichikawa et al. 1999).

Immune competent animals cannot be used in xenograft tumour models as the immune system rejects foreign antigens. The B16 mouse melanoma cell line was isolated from a C57BL/6 mouse, hence can successfully establish tumours in this immune competent mouse strain. Cells injected IV in mice accumulate in the lungs due to the narrow capillaries feeding them with a rich blood supply. This has been used previously to generate a model for cancer metastasis to the lungs (Craft, Bruhn et al. 2005; Stanford, Shaban et al. 2008). As the implanted B16 cells are derived from melanocytes they express the enzyme tyrosinase which plays a key role in the synthesis of melanin. This is absent from lung tissue, therefore measurement of tyrosinase levels can be used to

quantify the number of tumour cells in the lung if used in conjunction with a standard curve with known numbers of B16 cells.

Using B16 cells as a syngeneic model of metastatic cancer, 7 week old C57BL/6 mice were injected IV to create metastatic lung cancer. SV was then delivered IV to test its anti-tumour efficacy following such delivery. A total of 18 mice received tumour implantations and were randomly assigned to one of 3 groups; treatment, control or satellite. Mice were implanted with tumours on day 0 and those in the treatment group received 10^8 PFU of SV or PBS on days 3, 7 and 9, whereas those in the control group received PBS. Mice in the satellite group received no IV injections and were sequentially euthanised so that lungs could be resected and tumour burden analysed. This was performed so that experimentation could be terminated before any adverse symptoms arose in mice. On day 11 all mice were euthanised and their lungs removed for analysis of tumour burden.

Melanoma metastases on the surface of lungs are visible as they appear brown/black due to their synthesis of melanin. Images taken of the lungs of mice in the control and treatment groups had a considerable variation in the number of surface metastases, however, the number in the group treated with SVLuc DSG appeared reduced (Figure 5.20 A and B).

In the data shown, all three constituent lobes of the left lung of each mouse were analysed for tyrosinase content. This was related to tyrosinase levels from known numbers of B16 cells by a standard curve (Figure 5.20 C). Results show that systemic delivery of SV significantly ($P < 0.05$) reduced tumour burden from an average of 6.98×10^4 to 3.51×10^4 B16 cells/mg lung tissue by intravenous SVLuc DSG treatment; a

reduction of 1.99 fold (Figure 5.20 D). To our knowledge, this is the first time SV has shown anticancer efficacy in an immune competent model via IV delivery. The anterior lobe of the right lung of each mouse was analysed for luciferase transgene activity, however, none was detected (data not shown). In addition, RNA was extracted from the posterior lobe of the right lung of each mouse and RTQPCR for the presence of SV genomes performed. No SV RNA was detected in any of the PBS treated mice. The only mouse which was positive for SVRNA (only slightly above the limit of detection) in the SVLuc DSG treated group also had the highest tumour burden (data not shown).

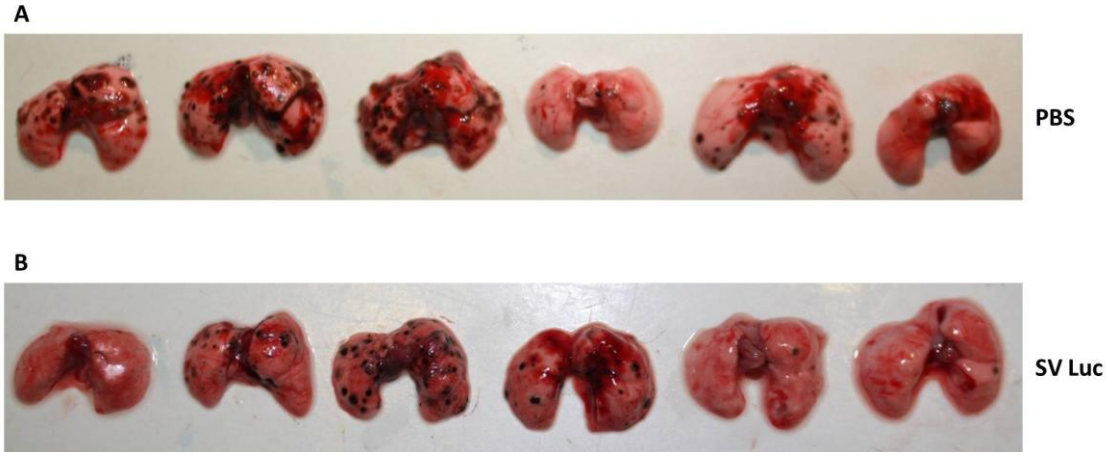
A
PBS
B
SV Luc

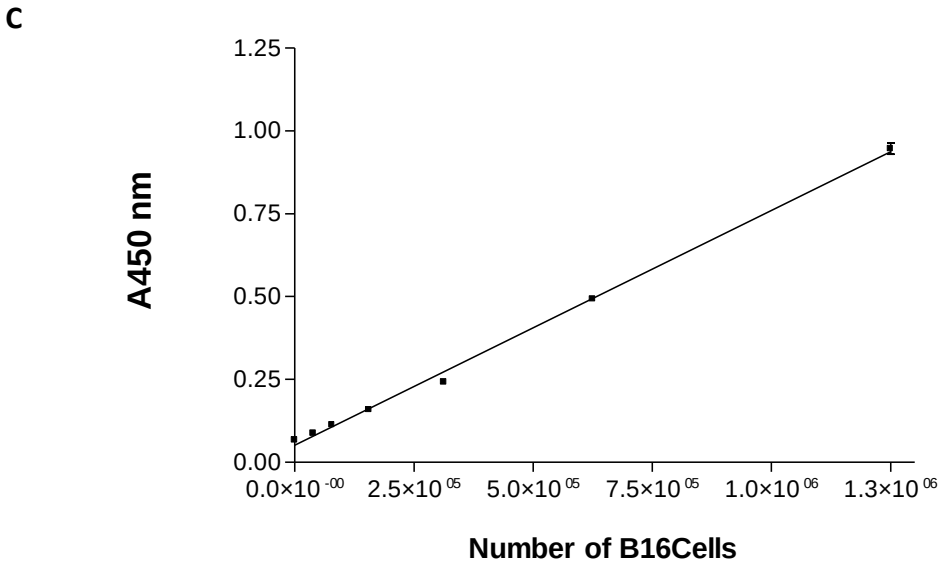
C
A450 nm
1.25
1.00
0.75
0.50
0.25
0.00
0.0×10 -00
2.5×10 05
5.0×10 05
7.5×10 05
1.0×10 06
1.3×10 06
Number of B16Cells

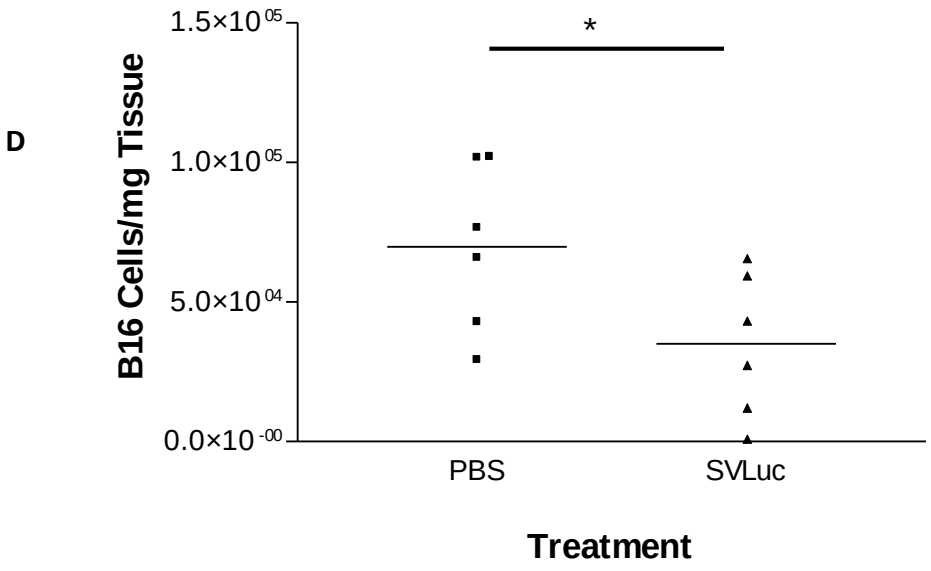
D
B16 Cells/mg Tissue
1.5×10 05
1.0×10 05
5.0×10 04
0.0×10 -00
*
PBS
SVLuc
Treatment

Figure 5.20: Antitumor Efficacy of Systemically Delivered SV – Female, 6 week old C57BL/6 mice were inoculated with 10^5 B16 cells using 29 gauge G needles via tail vain injections. Cells for implantation were trypsinised and washed 3 times with PBS and kept on ice until injection on day 0. Mice were randomly assigned to one of 3 groups, the first received no further injections but were sequentially euthanised every 48 hours starting at day 3 and lungs used as an indicator of tumour burden of non-treated control (NTC) mice. The second and third group received 100 µl volumes of PBS or SVLuc DSG (10^8 PFU/mL) respectively on days 3, 7 and 9 via tail vain injections using 29 G needles. A) and B) Lungs of PBS or SVLuc DSG treated mice were removed on day 11 and photographed using a Canon EOS 450D camera fitted with an EFS 18-55mm lens. C) Varying numbers of B16 cells were lysed analysed for their tyrosinase activity as described in Chapter 2.25. D) The left lobes of each lung were immediately frozen in liquid nitrogen and stored at -80 °C until analysis of tyrosinase activity as described in Chapter 2.25. Absorbance units were correlated to C) to determine the number of B16 cells present in each sample. Each point represents the mean of triplicates of homogenised samples and horizontal lines represent the mean value for each treatment group. Statistical analysis was performed using a T test (two tailed). * = $P < 0.05$.

5.3 Concluding Discussion

Human serum, but not whole blood, can inhibit the infectivity of SV, perhaps suggesting that a product of the clotting cascade inhibits SV infectivity. SV infectivity could be restored by the addition of lithium heparin but not ACD to serum before incubation with virus. Lithium heparin inactivates several activated clotting factors by catalysing the formation of anti-thrombin III-activated coagulation factor complexes whilst ACD does not (Figure 5.5). This might suggest that SV inhibition by serum is exerted by an activated coagulation factor. However, whole blood collected using ACD or hirudin as anticoagulants, in which activated clotting factors are present (Figure 5.5), does not significantly decrease SV infectivity. This might suggest there is an additional factor in whole blood, but absent from serum, that prevents inhibition by an activated clotting factor, or negates its effect through enhancement of SV infectivity by a separate mechanism.

It was also observed that human plasma enhances the infectivity of SV compared to whole blood. The different activity of blood and plasma is hard to explain, as these samples differ from each other only in the presence of blood cells. Though data obtained was not conclusive, it is also possible that SV binds erythrocytes, which could reduce its infectivity through sequestration away from target cell receptors. Also, since blood is approximately 50% cells (by volume), the amount of any potentially-enhancing soluble factor added to virus will be greater in plasma samples than it is in equal volumes of blood samples. Hence, if enhancement is concentration-dependent, it is conceivable that the enhancement of SV infection by plasma reflects the presence of greater amounts of a soluble stimulating factor.

Inhibition of SV by human serum and enhancement by human plasma may be due to factors that counteract one another in whole blood. However, as whole blood does not significantly inhibit SV infectivity, the effects of plasma and serum *in vitro* are probably not relevant when considering IV delivery of SV.

Experimental evidence suggests SV does not activate complement; this is not surprising as during infection of mammals through mosquito bites, virus particles are exposed to blood, providing a strong evolutionary pressure to resist complement fixation. SV complement resistance has been attributed to the presence of sialic acid glycosylations on virus surface proteins, which are acquired through the host cell glycosylation machinery (Boehme, Williams et al. 2000). These carbohydrate modifications are absent, or at least significantly reduced in complexity on SV particles produced in insect cells (Hirsch, Griffin et al. 1981). A previous report suggested that mosquito cell derived SV significantly activates complement and also is cleared from the circulation of mice more rapidly than SV produced in BHK cells (Hirsch, Griffin et al. 1981). Data presented here are contradictory to this as no complement activation or difference in blood clearance rates was observed (Chapter 5.2.13). A possible explanation for this is differences in assays used to measure complement activation; here, the extent of complement activation was measured directly by ELISA for activated C3a whereas studies showing ID SV activation of complement used haemolysis assays. Also, here, SV was incubated with neat plasma and serum at a concentration of virus particles analogous to in mice *in vivo* following IV delivery of SV for 15 minutes before termination of complement activation with EDTA. This is in contrast to incubation with human or pig serum diluted 1/10 with veronal buffered saline containing gelatin for 30 minutes. It is not clear from the above study whether in-tact virus particles were used in

complement activation studies, nor which Aedes albopictus cell line was used to produce SV (this could possibly be C6/36 cells), also Balb/c mice were used compared to C57BL/6 mice in these studies. It is hence difficult to consolidate differences in observations. It may be worth noting that SV used in said study was purified using centrifugation with sucrose cushions; sucrose can be a source of lipopolysaccharide contamination, which activates complement (Mergenhagen, Snyderman et al. 1973; Perlik, Li et al. 2005). In addition, data in Chapter 3 shows this purification method can compromise SV particle integrity, and virus proteins which are not normally exposed to blood components may activate complement. Differences in purification techniques, however, do not explain the shared observation of the inability of SV produced in BHK cells to activate complement.

The stability of SV in whole human blood is remarkable when compared to that of other viruses in development as oncolytic agents. Incubation with human serum diluted 1/5 caused an increase in the virus dose required to kill 50% of cells (IC_{50}) of HSV-1 (~ 10^6 fold), vaccinia virus (~10^3 fold) and Ad5 (10^3 fold) (unpublished data, Ying Di, University of Oxford). Data presented here shows that neat human serum inhibits SV infectivity 3-5 fold and neat whole human blood does not significantly inhibit infectivity.

Though SV is stable in human and mouse blood it is rapidly cleared from the circulation, and shows considerable accumulation in the liver. The hypothesis that the production of SV in invertebrate cells could impact on cell tropism was disproved by analysing infectivity of a panel of cell lines *in vitro*. The PK and biodistribution are also not enhanced in the C57BL/6 mouse model used here. To our knowledge, this is the first

analysis PK utilising RTQPCR rather than plaque based assays and the first showing biodistribution of SV following IV delivery.

The diameter of liver fenestrae determined by transmission electron microscopy (TEM) in healthy C57BL/6 mice and humans has been reported as 141 ± 5.4 nm and 107 ± 1.5 nm respectively (Wisse, Jacobs et al. 2008). As SV particles have been measured as ~70nm in diameter (Ferreira, Hernandez et al. 2003), it is likely that the rapid circulation clearance and concurrent accumulation in the liver following IV delivery to C57BL/6 mice is a scenario that would be mirrored in humans. Rapid clearance of SV from the circulation, rather than neutralization by blood components, may, therefore represent a significant barrier to the development of SV as an oncolytic agent.

Clodronate liposome pre-treatment of mice to deplete Kupffer cells did not enhance SV circulation despite causing a significant fall in liver capture. This indicates that other sequestration mechanisms/organs may compensate for the loss of Kupffer cells. However, although there appeared to be a compensatory increase in SV particle accumulation in the spleen, this was not statistically significant. It has been seen that the improvement in circulation kinetics observed with Ad5 upon clodronate pre-treatment of mice is dose-dependent, and only observed at doses exceeding 10^{10} virus particles per mouse (Green NK 2012). This suggests that in order to significantly extend SV circulation kinetics, input doses may be required to saturate remaining Kupffer cells, and possibly splenic macrophages. Administration of increased doses of SV might therefore lead to similar PK enhancement as seen with Ad5 (Green NK 2012).

Despite rapid clearance from the circulation, SV delivered IV was able to inhibit the growth of melanoma lung metastases in immune competent mice. Lack of detection of

transgene in the lungs of treated mice and the detection of SV genomic RNA in only 1 mouse in the treated group makes it unclear whether reduced tumour burden was due to the oncolytic activity of SV or the induction of an anti-tumour immune response. Given that it takes about 14 days from vaccination to peak adaptive immune response in C57BL/6 mice, and that the time from the first SVLuc DSG dose to experiment termination was 9 days, it is unlikely in this case, that the immune system played a major role in reduction of tumour burden.

Although SV treatment reduced tumour burden it was not curative in any mouse. Improving the circulation kinetics of SV could drastically increase the virus dose reaching tumour metastases and could hence significantly enhance therapeutic outcome. Improving virus production protocols to allow the use of higher virus titres in combination with clodronate liposome pre-treatment of mice may provide means by which to achieve this.

6 Discussion

6.1 Overview of the Main Findings of this Thesis

Using SV as an Oncolytic Agent

During this thesis, a strain of SV has been characterised with a view to its use as a systemically delivered oncolytic agent. The main pieces of work undertaken here are aimed at addressing key limitations of SV for this purpose. Efforts were made to characterise and improve its genetic stability, safety profile and pharmacokinetics following IV delivery.

Genetic Stability of SV

Loss of transgene expression by SV reporter viruses was observed to be far quicker than can be explained by point mutations expected to be introduced due to the infidelity of the SV RdRp. RTPCR showed that transgenes were deleted entirely from SVLuc DSG and SVGFP DSG. This was confirmed by RTQPCR and sequence analysis of genomes of serially passaged SVLuc DSG, SVGFP DSG and SVGFP 2A. The rate of reversion of eGFP-expressing variants was less rapid than those encoding luciferase, perhaps as the greater length of the luciferase gene imposes an increased selective pressure for its loss, due to a bigger decrease in replication time and metabolic burden. The rates of loss of the eGFP gene from SVGFP DSG and SVGFP 2A were similar, suggesting that the position of transgene insertion had no effect on genetic stability of reporter SV. The most likely mechanism for transgene loss probably involves SV RdRp “skipping” past transgene-encoding regions. This has been implicated as the cause of small deletions in the SV 3'UTR and rescue of viable SV from separate replication deficient RNAs

encoding separate genome fragments (Weiss and Schlesinger 1991; Raju, Subramaniam et al. 1995; Hajjou, Hill et al. 1996; Hill, Hajjou et al. 1997). The mechanism of RdRp "skipping" is likely to be dependent on the formation of hairpin loop structures within genomic RNA molecules or interactions between separate genomic RNA molecules (Raju, Subramaniam et al. 1995).

Tissue Specific Attenuation of SV

There are limited data on the tissue tropism of SV in humans. So far SV RNA has only successfully been detected in one study, where it was present in 4/23 skin biopsies and 1/73 whole blood samples of patients with acute SV infection (Kurkela, Manni et al. 2004). The inability to directly detect SV in clinical isolates may be a consequence of the presence of high levels of RNase, which can degrade SV RNA during extraction procedures (Tan and Yiap 2009), combined with low starting numbers of SV particles. As well as difficulties in detecting SV genomes in clinical samples, it may be that replication within any given tissue occurs only for a short time period and may not be concurrent with the experience of inflammatory symptoms. This would mean that the majority of patients analysed so far may only have low levels of SV present in tissue biopsies, making it difficult to detect.

Despite the lack of direct evidence for the tropism of SV in humans, it was hypothesised, based on clinical observations of pathogenesis, that replication in liver, neuronal, muscle and haematopoietic tissues may contribute to pathological symptoms

upon intravenous delivery of large doses. Furthermore, inhibition of replication in these tissues may ablate such unwanted symptoms and improve the usefulness of therapeutic SV for human use.

It is shown here, that through the introduction of MREs into either the 3'UTR or the structural polyprotein encoding region of the SV genomic and subgenomic RNAs, SV protein expression and replication can be inhibited. MREs introduced in the SV structural polyprotein-encoding region of the SV genome were associated with ~5 fold more miR-specific attenuation than the same MREs introduced into the 3'UTR. This may be due to stearic hindrance of SV 3'UTR RNA-RISC interactions by other proteins binding the 3'UTR, such as the SV negative strand RNA synthase complex (Strauss and Strauss 1994; Frolov, Hardy et al. 2001).

The use of MREs complementary to tissue specific miRs can hence potentially be used to ablate unwanted side effects which may be related to SV replication in non-target tissues, without affecting its anti-cancer potency.

Cell lines were used as representatives for different tissues based on their expression of tissue specific miRs complementary to SVmiR-Ts. RTQPCR showed that endogenously expressed miRs were present at variable levels compared to 293 cells. The levels of miR present in each cell type did not correlate with the degree of SV attenuation observed, for example, miR142-3p displays ~200 fold greater attenuation of SV bearing complementary MREs compared to miR122, despite being present at ~1.3 x 10^4 fold lower levels (compared to 293 cells). A possible explanation for this is differences in the proportion of free miRs available for binding to SV RNA and therefore inhibition through MREs. A second explanation could be that individual miRs have different

preferences as to which argonaute subunit is incorporated into the RISC complex. As only Ago2 has RNase H activity, incorporation of any of the other 3 argonaute proteins would only allow miR mediated translational repression rather than cleavage of SV RNA. It is likely that this would be less efficient at attenuating SV replication than direct RNA cleavage, as it would presumably lead to sequestration of MRE-complementary, miR-loaded RISC in P-bodies, depleting the cytosol of RISC capable of inhibiting SV RNA translation.

SV as a Systemically Delivered Oncolytic Agent

The vast majority of cancer related mortalities are attributed to metastatic disease. Large numbers of metastases in any essential organ can lead to interruption of its function and hence ultimately lead to death. Surgical intervention is often incapable of complete removal of metastatic disease due to the presence of micro-metastases that cannot be removed during surgery.

As many virus species have evolved separately, mechanisms by which they induce cell death can vary greatly from one another. Oncolytic agents have proved effective in patients bearing metastatic cancer resistant to chemotherapy agents (Reid, Freeman et al. 2005). This supports the hypothesis that they have the ability to kill cancer cells by mechanisms that are distinct from those employed by conventional chemotherapy drugs. Delivery of oncolytic viruses via the bloodstream hence offers the possibility of infection and eradication of metastases, and also micro-metastases that are resistant to conventional chemotherapy.

The immune system, as result of millions of years of selective pressure to eradicate pathogens from the bloodstream, is a significant barrier to the systemic delivery of oncolytic viruses. Efficient clearance and neutralisation of input viruses has a dramatic effect on the bioavailable dose reaching target tumour masses. For example, when serotype 5 adenovirus, the only clinically approved oncolytic virus, is exposed to naïve human blood for 15 minutes its infectivity is reduced to 1% due to interactions with erythrocytes (Lyons, Onion et al. 2006) . This inactivation, along with complement activation, the pre-existence of high levels of neutralising antibodies in 30-70% of the population (Jiang, Wang et al. 2004), and rapid clearance from the circulation of mice by Kupffer cells (Alemany, Suzuki et al. 2000), present major limitations on the bioavailable dose reaching tumours upon IV delivery. SV, however, has evolved in the presence of selective pressure of blood neutralisation and clearance mechanisms.

A major finding of this thesis is that SV is stable in naïve whole human and mouse blood, a characteristic lacking in other viruses in development as oncolytic agents (Chapter 5.3). Despite this stability, upon *in vivo* administration, SV particles were rapidly cleared from the circulation of immune competent mice. Blood clearance was associated with a large amount of virus accumulation in the liver, presumably due to phagocytosis by Kupffer cells, liver resident macrophages. This indicates that although circulating SV particles are probably viable, rapid clearance from the bloodstream might prevent therapeutic doses reaching and infecting target tumour cells.

SV particles in the wild that come into contact with mammalian blood are derived from mosquito cells. As naturally occurring infections are successful in the presence of human blood we hypothesised that particles produced in mosquito cells may possess properties that reduce the rate of clearance and enhance biodistribution upon IV delivery

to mice. To assess this, the C6/36 mosquito cell line was utilised to produce SV particles. SV particles produced in vertebrate and invertebrate cells, however, had indistinguishable circulation kinetics and biodistribution profiles.

In an attempt to slow the rate of virus clearance from the bloodstream, Kupffer cells were depleted using clodronate liposomes. Although this led to a measureable reduction in liver accumulation of SV particles after 1 hour, its clearance kinetics were unchanged. It is possible that although significant reduction in liver uptake was observed, greater reduction is required in order to achieve extended SV circulation kinetics. Alternatively it could mean that Kupffer cells do not play a major role in the blood clearance of SV.

Despite rapid clearance of SV from the circulation, IV administration was still able to significantly reduce the tumour burden of C57BL/6 mice bearing lung metastatic melanomas. This suggests that a large proportion of SV particles reaching metastatic tumour masses are viable as a consequence of its stability in blood and that tumour access can be achieved in a short time scale (< 10 minutes).

6.2 Future Directions

Genetic Stability of SV

Whilst SV possesses natural anticancer activity, it is likely that this could be enhanced through introduction of a transgene that either augments its oncolytic activity or induces an anti-tumour immune response against the tumour that may persevere after immune mediated eradication of SV.

SV expressing the gibbon ape leukaemia virus fusion protein (GALV.fus) has been shown to form syncytia on glioma cell lines *in vitro* and have increased cytotoxicity compared to a β-galactosidase expressing counterpart (Zhang, Frolov et al. 2004). This virus may have improved anticancer activity *in vivo* by virtue of an additional cell-cell spread mechanism, however, has not yet been tested.

As SV shows sensitivity to IFN pre-treatment of cells *in vitro* and is thought to be a protecting factor for adult mice *in vivo* (Ryman, Klimstra et al. 2000), it is possible that IFN signalling may contribute to incomplete spread of SV through tumours. Encoding proteins that inhibit IFN signalling, such as the measles virus N protein that blocks nuclear import of activated signal transducer and transactivator of transcription (STAT) dimers (Takayama, Sato et al. 2012), might therefore enhance the anticancer efficacy of SV.

A recent study showed that oncolytic SV encoding immune stimulatory IL-12 had improved anticancer activity in SCID mice through NK cell dependent anti-cancer responses (Granot and Meruelo 2012). The relevance of this study is unclear as immune competent mice were not used. However, immune stimulatory molecules, such as IL-12

and GM-CSF might lead to the induction of innate immune mediated anti-cancer activity in immune competent hosts that may prime long lasting adaptive responses.

SV encoded transgenes are lost rapidly, perhaps between consecutive virus generations, this could severely limit therapeutic potential of the virus both during manufacture and also following administration to the body. Furthermore, based on evidence presented showing rapid transgene loss from isolated clonal SV populations, it is unlikely that utilising plasmid DNA encoding SV in virus production or treatment could significantly extend transgene expression.

In some settings it is nevertheless conceivable that SV expressing transgenes may be of therapeutic value, this is most likely to occur where transgene levels produced by the intact virus far exceed the threshold required to perform their intended function. In this case, transgene loss on increased numbers of replication cycles may be insignificant within the required time frame. *In vivo* studies are therefore required in order to validate the activity of any transgene-encoding SV, whilst an increased understanding of the mechanism of transgene deletion may reveal ways in which it could be prevented or delayed.

Tissue Specific Attenuation of SV

Given that it is possible to specifically attenuate SV in liver, neuronal, muscle and haematopoietic tissues, it is probably possible to attenuate SV in a tissue-specific manner for most, if not all tissues through the use of miR-T sites complementary to tissue specific MREs.

It is also probable that having multiple miR binding sites at multiple parts of the SV genome will confer higher levels of miR mediated attenuation. Repeated sequence elements at different points in the genome, however, may increase the chances of the formation of secondary structures in genomic RNA, which may interfere with replication.

During the course of this thesis it was not possible to test the *in vivo* relevance of tissue specific SV attenuation as available mouse models do not reflect the pathogenesis observed in humans. Adult mice did not display any pathological symptoms when infected with SV, in addition replication or transgene expression was not detected in any tissue other than tumour. A feasible model in which to test SV does exist in mice, as IC inoculation of immature mice leads to encephalitis and death; hence, neuronal-specific SV attenuation would presumably alleviate or ablate this pathogenesis, but these procedures could not be carried out under the current Home Office animal licence.

A foreseeable problem for miR controlled viruses is that data on tissue specific miR expression comes from the analysis of lysates of whole tissue samples rather than purifying the cell types that make up a tissue and analysing their miR expression profiles separately. It is likely that the heterogeneous populations of cells that make up a given tissue have different expression statuses of tissue specific miRs and hence may

have varying abilities to attenuate SVmiR-T replication. If so, permissive cells may provide high local concentrations of SV which could induce inflammation sufficient to cause pathological symptoms, defeating the object of tissue specific attenuation. A second concern for the use of miR-T sites in oncolytic SV is that there is no selective pressure for replicating virus to retain miR-T sites. If replication of SV in malignant tissue is associated with reversion to a wild-type phenotype, then shedding of reverted virus from tumours to the circulation could potentially allow infection of tissues contributing to pathological symptoms, again, defeating the object of tissue specific attenuation. The significance of concerns highlighted can only be found through *in vivo* testing where pathological symptoms can be measured.

SV as a Systemically Delivered Oncolytic Agent

As SV has shown it is stable in blood, decreasing its clearance from the circulation could drastically improve the dose of viable virus particles reaching tumour cells. Based on the majority of recovered virus after 1 hour being present in mouse livers after IV delivery, without transgene expression, it is likely that phagocytosis by Kupffer cells plays a major role in the clearance of SV particles from the circulation. Although clodronate liposome pre-treatment of mice successfully reduced virus particle accumulation in the liver, circulation kinetics were not improved. This could be a consequence of insufficient depletion of Kupffer cells and/or increased capture by extra-hepatic phagocytes. If this is the case, optimising the pre-dosing of clodronate liposomes or utilising other agents such as gadolinium chloride may allow more efficient inhibition of phagocytic capture, and hence increased SV circulation kinetics.

It is also possible, however, that the accumulation of SV particles in the liver may be a consequence of virus particle size, and the increased space between the sinusoids of the epithelium in the liver and spleen compared to other tissues could lead to an extracellular trapping event. This may mean that liver accumulation of SV following IV delivery is unavoidable. It may be possible, however, to clamp blood flow to the liver during a delivery period, to increase circulation kinetics, and therefore doses reaching tumour metastases (Koska, Kramer et al. 1981).

SV has shown anticancer efficacy in several mouse models (Tseng, Levin et al. 2002; Tseng, Hurtado et al. 2004; Tseng, Levin et al. 2004). In this study it significantly reduced the tumour burden in immune competent mice following IV delivery, despite rapid clearance from the circulation. It is likely that increased doses of SV would lead to greater anticancer efficacy and possibly complete remission. In order to investigate this, however, methods of SV production must be modified in order to produce stocks of higher titre.

It has been noted that adult mice show no symptoms of pathology when infected peripherally with SV (Heise, Simpson et al. 2000); doses utilised so far, however, may all lie below a threshold above which symptoms may appear. If input doses can successfully be increased, and if circulation kinetics can be improved, it is conceivable that pathological symptoms may manifest alongside improved efficacy. If this is the case, attenuation of side effects may be crucial in allowing administration of high enough doses of SV to be curative. In such a case, miR mediated regulation of SV may provide a resolution.

During this thesis, SV particles were produced in monolayers of cells, where the achievable virus concentration is limited by the large volume of supernatant required to cover cell monolayers. In cell lines that can be cultured in suspension, the number of cells per ml cell culture supernatant can be greatly increased. Production of SV in suspension cells may therefore yield increased titres, which may be crucial in development of SV as an oncolytic agent.

Under the terms of the 2003 clinical trial directive, any virus to be tested clinically must be produced to GMP standards. This requires a clear definition of starting materials and evidence at each manufacturing stage that there is no significant deviation from the initial product. As shown in this thesis, utilising multi-generation SV replication during the amplification of virus stocks may lead to considerable deviation in genomic sequence and/or phenotype from input virus and therefore may not conform to current GMP standards.

It may be possible to produce high titre SV stocks without significant multi-generation replication by transfection of a large number of cells with RNA or DNA encoding the virus and harvesting virus after a single generation of replication. Whilst the instability and high cost of production of RNA might make this approach unattractive, the costs associated with producing large quantities of plasmid DNA are relatively low. It has, in fact, recently been shown that transfection of mammalian cells with an SV-encoding plasmid with a CMV RNA polymerase II promoter resulted in SV rescue (Steel, Henderson et al. 2011). Virus titres attained, however, were about 10 fold lower than those attained with RNA transfection (~10^8 PFU/ml) suggesting transfection efficiency may be a limiting factor in this system.

An alternative method may be to encode SV in the genome of a DNA virus so that the error prone SV RdRp is not responsible for genome amplification and SV RNA species are not produced and therefore cannot recombine during amplification steps. This “virus within a virus” approach has proved feasible using a baculovirus expression system with an insert of ~38Kb for the production of replication deficient Ad5 (Cheshenko, Krougliak et al. 2001) and has been successful in the large scale production of replication competent AAV (Galibert and Merten 2011).

Overall the data in this thesis suggest Sindbis virus has the potential for use as a systemically delivered anti-cancer agent in a clinical setting.

7 References

Abril, E., R. E. Mendez, A. Garcia, A. Serrano, T. Cabrera, F. Garrido and F. RuizCabello (1996). "Characterization of a gastric tumor cell line defective in MHC class I inducibility by both alpha- and gamma-interferon." Tissue Antigens **47**(5): 391-398.

Albert, M. L., B. Sauter and N. Bhardwaj (1998). "Dendritic cells acquire antigen from apoptotic cells and induce class I-restricted CTLs." Nature **392**(6671): 86-89.

Alemany, R., K. Suzuki and D. T. Curiel (2000). "Blood clearance rates of adenovirus type 5 in mice." Journal of General Virology **81**: 2605-2609.

Alshaker, H. and K. Matalka (2011). "IFN-gamma, IL-17 and TGF-beta involvement in shaping the tumor microenvironment: The significance of modulating such cytokines in treating malignant solid tumors." Cancer Cell International **11**(1): 33.

Alvarez-Breckenridge, C. A., J. Yu, R. Price, M. Wei, Y. Wang, M. O. Nowicki, Y. P. Ha, S. Bergin, C. Hwang, S. A. Fernandez, B. Kaur, M. A. Caligiuri and E. A. Chiocca (2012). "The Histone Deacetylase Inhibitor Valproic Acid Lessens NK Cell Action against Oncolytic Virus-Infected Glioblastoma Cells by Inhibition of STAT5/T-BET Signaling and Generation of Gamma Interferon." Journal of Virology **86**(8): 4566-4577.

Ambion, U. (2012). "Total RNA Purification from Whole Blood." http://tools.invitrogen.com/content/sfs/brochures/cms_039875.pdf.

Ambros, V. (1989). "A hierarchy of regulatory genes controls a larva-to-adult developmental switch in C. elegans." Cell **57**(1): 49-57.

Ambros, V. and H. R. Horvitz (1984). "Heterochronic mutants of the nematode Caenorhabditis elegans." Science **226**(4673): 409-416.

Antonio Chiocca, E. (2002). "Oncolytic viruses." Nat Rev Cancer **2**(12): 938-950.

Arbuthnot, P. and L. J. Thompson (2008). "Harnessing the RNA interference pathway to advance treatment and prevention of hepatocellular carcinoma." World Journal of Gastroenterology **14**(11): 1670-1681.

Asada, T. (1974). "Treatment of human cancer with mumps virus." Cancer **34**(6): 1907-1928.

Atkins, G. J. and C. L. Lancashire (1976). "Induction of interferon by temperature-sensitive mutants of Sindbis virus - its relationship to double-stranded-RNA synthesis and cytopathic effect." Journal of General Virology **30**(FEB): 157-165.

Baguley, B. C., E. S. Marshall, J. R. Whittaker, M. C. Dotchin, J. Nixon, M. R. McCrystal, G. J. Finlay, J. H. L. Matthews, K. M. Holdaway and P. Vanzijl (1995). "Resistance mechanisms determining the in-vitro sensitivity to paclitaxel of tumor-cells cultured from patients with ovarian-cancer." European Journal of Cancer **31A**(2): 230-237.

Balachandran, S. and G. N. Barber (2004). "Defective translational control facilitates vesicular stomatitis virus oncolysis." Cancer Cell **5**(1): 51-65.

Baldwin, R. W. (1977). "Immune surveillance revisited." Nature **270**(5638): 557-557.

Barber, G. N. (2005). "VSV-tumor selective replication and protein translation." Oncogene **24**(52): 7710-7719.

Barnes, D., M. Kunitomi, M. Vignuzzi, K. Saksela and R. Andino (2008). "Harnessing Endogenous miRNAs to Control Virus Tissue Tropism as a Strategy for Developing Attenuated Virus Vaccines." Cell Host & Microbe **4**(3): 239-248.

Beljanski, V. and J. Hiscott (2012). "The use of oncolytic viruses to overcome lung cancer drug resistance." Current Opinion in Virology(0).

Belousova, N., G. Mikheeva, J. Gelovani and V. Krasnykh (2008). "Modification of adenovirus capsid with a designed protein ligand yields a gene vector targeted to a major molecular marker of cancer." Journal of Virology **82**(2): 630-637.

Bexborn, F., A. E. Engberg, K. Sandholm, T. E. Mollnes, J. Hong and K. N. Ekdahl (2009). "Hirudin versus heparin for use in whole blood in vitro biocompatibility models." Journal of Biomedical Materials Research Part A **89A**(4): 951-959.

Boehme, K. W., J. C. Williams, R. E. Johnston and H. W. Heidner (2000). "Linkage of an alphavirus host-range restriction to the carbohydrate-processing phenotypes of the host cell." Journal of General Virology **81**: 161-170.

Bolovan, C. A., N. M. Sawtell and R. L. Thompson (1994). "ICP34.5 mutants of herpes simplex virus type 1 strain 17syn+ are attenuated for neurovirulence in mice and for replication in confluent primary mouse embryo cell cultures." Journal of Virology **68**(1): 48-55.

Boone, C. W. (1974). Augmented immunogenicity of tumor cell homogenates infected with influenza virus.

Bradish, C. J., K. Allner and H. B. Maber (1971). "The virulence of original and derived strains of Semliki-forest virus for mice guinea-pigs and rabbits." Journal of General Virology **12**(2): 141-160.

Brazil, D. P., Z. Z. Yang and B. A. Hemmings (2004). "Advances in protein kinase B signalling: AKTion on multiple fronts." Trends in Biochemical Sciences **29**(5): 233-242.

Brown, B. D., M. A. Venneri, A. Zingale, L. S. Sergi and L. Naldini (2006). "Endogenous microRNA regulation suppresses transgene expression in hematopoietic lineages and enables stable gene transfer." Nat Med **12**(5): 585-591.

Brown, J. D., M. D. Ryan, J. F. Atkins and R. F. Gesteland (2010). Ribosome “Skipping”: “Stop-Carry On” or “StopGo” Translation

Recoding: Expansion of Decoding Rules Enriches Gene Expression. J. M. Bujnicki, Springer New York. **24:** 101-121.

Byrnes, A. P. and D. E. Griffin (2000). "Large-plaque mutants of sindbis virus show reduced binding to heparan sulfate, heightened viremia, and slower clearance from the circulation." Journal of Virology **74**(2): 644-651.

Campbell, C. L., K. M. Keene, D. E. Brackney, K. E. Olson, C. D. Blair, J. Wilusz and B. D. Foy (2008). "Aedes aegypti uses RNA interference in defense against Sindbis virus infection." Bmc Microbiology **8**.

Carlisle, R. C., Y. Di, A. M. Cerny, A. F. P. Sonnen, R. B. Sim, N. K. Green, V. Subr, K. Ulbrich, R. J. C. Gilbert, K. D. Fisher, R. W. Finberg and L. W. Seymour (2009). "Human erythrocytes bind and inactivate type 5 adenovirus by presenting Coxsackie virus-adenovirus receptor and complement receptor 1." Blood **113**(9): 1909-1918.

Carnero, E., J. D. Sutherland and P. Fortes (2011). "Adenovirus and miRNAs." Biochimica et Biophysica Acta (BBA) - Gene Regulatory Mechanisms **1809**(11-12): 660-667.

Carson, J., D. Haddad, M. Bressman and Y. Fong (2010). "Oncolytic herpes simplex virus 1 (hsv-1) vectors: increasing treatment efficacy and range through strategic virus design." Drugs of the Future **35**(3): 183-195.

Cassetti, M. C., S. P. McElhiney, V. Shahabi, J. K. Pullen, I. C. Le Poole, G. L. Eiben, L. R. Smith and W. M. Kast (2004). "Antitumor efficacy of Venezuelan equine encephalitis virus

replicon particles encoding mutated HPV16 E6 and E7 genes." Vaccine **22**(3â€“4): 520-527.

Cavalieri, S., M. Rotoli, C. Feliciani and P. Amerio (2005). "Expression of the high-affinity laminin receptor (67 kda) in normal human skin and appendages." International Journal of Immunopathology and Pharmacology **18**(2): 223-231.

Cawood, R., H. H. Chen, F. Carroll, M. Bazan-Peregrino, N. van Rooijen and L. W. Seymour (2009). "Use of Tissue-Specific MicroRNA to Control Pathology of Wild-Type Adenovirus without Attenuation of Its Ability to Kill Cancer Cells." Plos Pathogens **5**(5).

Cawood, R., S.-L. Wong, Y. Di, D. F. Baban and L. W. Seymour (2011). "MicroRNA Controlled Adenovirus Mediates Anti-Cancer Efficacy without Affecting Endogenous MicroRNA Activity." PLoS ONE **6**(1): e16152.

Chalfie, M., H. R. Horvitz and J. E. Sulston (1981). "Mutations that lead to reiterations in the cell lineages of C. elegans." Cell **24**(1): 59-69.

Chalikonda, S., M. H. Kivlen, M. E. O'Malley, X. D. Dong, J. A. McCart, M. C. Gorry, X. Y. Yin, C. K. Brown, H. J. Zeh, III, Z. S. Guo and D. L. Bartlett (2008). "Oncolytic virotherapy for ovarian carcinomatosis using a replication-selective vaccinia virus armed with a yeast cytosine deaminase gene." Cancer Gene Therapy **15**(2): 115-125.

Chen, H. H., R. Cawood, Y. El-Sherbini, L. Purdie, M. Bazan-Peregrino, L. W. Seymour and R. C. Carlisle (2010). "Active Adenoviral Vascular Penetration by Targeted Formation of Heterocellular Endothelial-epithelial Syncytia." Mol Ther **19**(1): 67-75.

Chendrimada, T. P., R. I. Gregory, E. Kumaraswamy, J. Norman, N. Cooch, K. Nishikura and R. Shiekhattar (2005). "TRBP recruits the Dicer complex to Ago2 for microRNA processing and gene silencing." Nature **436**(7051): 740-744.

Cheshenko, N., N. Krougliak, R. C. Eisensmith and V. A. Krougliak (2001). "A novel system for the production of fully deleted adenovirus vectors that does not require helper adenovirus." Gene Therapy **8**(11): 846-854.

Chikkanna-Gowda, C. P., B. J. Sheahan, M. N. Fleeton and G. J. Atkins (2005). "Regression of mouse tumours and inhibition of metastases following administration of a Semliki Forest virus vector with enhanced expression of IL-12." Gene Therapy **12**(16): 1253-1263.

Condit, R. C. (2010). "Surf and Turf: Mechanism of Enhanced Virus Spread During Poxvirus Infection." Viruses **2**(5): 1050-1054.

Coukos, G., A. Makrigiannakis, E. H. Kang, S. C. Rubin, S. M. Albelda and K. L. Molnar-Kimber (2000). "Oncolytic Herpes Simplex Virus-1 Lacking ICP34.5 Induces p53-independent Death and Is Efficacious against Chemotherapy-resistant Ovarian Cancer." Clinical Cancer Research **6**(8): 3342-3353.

Craft, N., K. W. Bruhn, B. D. Nguyen, R. Prins, L. M. Liau, E. A. Collisson, A. De, M. S. Kolodney, S. S. Gambhir and J. F. Miller (2005). "Bioluminescent imaging of melanoma in live mice." Journal of Investigative Dermatology **125**(1): 159-165.

Cross, R. K. and P. J. Gomatos (1981). "Concomitant methylation and synthesis invitro of Semliki forest virus (SFV) ss rnas by a fraction from infected-cells." Virology **114**(2): 542-554.

Csatary, L. K., S. Eckhardt, I. Bukosza, F. Czegledi, C. Fenyvesi, P. Gergely, B. Bodey and C. M. Csatary (1993). "Attenuated veterinary virus-vaccine for the treatment of cancer." Cancer Detection and Prevention **17**(6): 619-627.

Cullen, B. R. (2004). "Transcription and Processing of Human microRNA Precursors." Molecular Cell **16**(6): 861-865.

Dar, A. C., T. E. Dever and F. Sicheri (2005). "Higher-order substrate recognition of eIF2 alpha by the RNA-dependent protein kinase PKR." Cell **122**(6): 887-900.

Davis, N. L., F. J. Fuller, W. G. Dougherty, R. A. Olmsted and R. E. Johnston (1986). "A single nucleotide change in the E2-glycoprotein gene of sindbis virus affects penetration rate in cell-culture and virulence in neonatal mice." Proceedings of the National Academy of Sciences of the United States of America **83**(18): 6771-6775.

Davoren, P., R. McNeill, A. Lowery, M. Kerin and N. Miller (2008). "Identification of suitable endogenous control genes for microRNA gene expression analysis in human breast cancer." BMC Molecular Biology **9**(1): 76.

Demers, G. W., D. E. Johnson, V. Tsai, S.-F. Wen, E. Quijano, T. Machemer, J. Philopena, M. Ramachandra, J. A. Howe, P. Shabram, R. Ralston and H. Engler (2003). "Pharmacologic Indicators of Antitumor Efficacy for Oncolytic Virotherapy." Cancer Research **63**(14): 4003-4008.

DeWeese, T. L., H. van der Poel, S. Li, B. Mikhak, R. Drew, M. Goemann, U. Hamper, R. DeJong, N. Detorie, R. Rodriguez, T. Haulk, A. M. DeMarzo, S. Piantadosi, D. C. Yu, Y. Chen, D. R. Henderson, M. A. Carducci, W. G. Nelson and J. W. Simons (2001). "A Phase I Trial of CV706, a Replication-competent, PSA Selective Oncolytic Adenovirus, for the Treatment of Locally Recurrent Prostate Cancer following Radiation Therapy." Cancer Research **61**(20): 7464-7472.

Diehl, K. H., R. Hull, D. Morton, R. Pfister, Y. Rabemampianina, D. Smith, J. M. Vidal and C. van de Vorstenbosch (2001). "A good practice guide to the administration of substances and removal of blood, including routes and volumes." Journal of Applied Toxicology **21**(1): 15-23.

Dmitrieva, N., L. Yu, M. Viapiano, T. P. Cripe, E. A. Chiocca, J. C. Glorioso and B. Kaur (2011). "Chondroitinase ABC I-Mediated Enhancement of Oncolytic Virus Spread and Antitumor Efficacy." Clinical Cancer Research **17**(6): 1362-1372.

Donnelly, M. L. L., G. Luke, A. Mehrotra, X. J. Li, L. E. Hughes, D. Gani and M. D. Ryan (2001). "Analysis of the aphthovirus 2A/2B polyprotein 'cleavage' mechanism indicates not a proteolytic reaction, but a novel translational effect: a putative ribosomal 'skip'." Journal of General Virology **82**: 1013-1025.

Doronina, V. A., P. de Felipe, C. Wu, P. Sharma, M. S. Sachs, M. D. Ryan and J. D. Brown (2008). "Dissection of a co-translational nascent chain separation event." Biochemical Society Transactions **36**: 712-716.

Dunn, G. P., A. T. Bruce, H. Ikeda, L. J. Old and R. D. Schreiber (2002). "Cancer immunoediting: from immunosurveillance to tumor escape." Nature Immunology **3**(11): 991-998.

Dunn, G. P., C. M. Koebel and R. D. Schreiber (2006). "Interferons, immunity and cancer immunoediting." Nature Reviews Immunology **6**(11): 836-848.

Durbin, R. K. and V. Stollar (1986). "Sequence-analysis of the E2 gene of a hyperglycosylated, host restricted mutant of sindbis virus and estimation of mutation-rate from frequency of revertants

" Virology **154**(1): 135-143.

Durupt, F., D. Koppers-Lalic, B. Balme, L. Budel, O. Terrier, B. Lina, L. Thomas, R. C. Hoeben and M. Rosa-Calatrava (2011). "The chicken chorioallantoic membrane tumor assay as model for qualitative testing of oncolytic adenoviruses." Cancer Gene Ther **19**(1): 58-68.

Duval, C., U. Thissen, S. Keshtkar, B. Accart, R. Stienstra, M. V. Boekschoten, T. Roskams, S. Kersten and M. Muller (2010). "Adipose Tissue Dysfunction Signals Progression of Hepatic Steatosis Towards Nonalcoholic Steatohepatitis in C57Bl/6 Mice." Diabetes **59**(12): 3181-3191.

Edens, R. E. L., R.J. Weiler, J.M. Cruse, J.M. Lewis, R.E. (1993). "Heparin is not just an anticoagulant anymore: six and one-half decades of studies on the ability of heparin to regulate complement activity. ." Complement Today: 96-120.

Edge, R. E., T. J. Falls, C. W. Brown, B. D. Lichty, H. Atkins and J. C. Bell (2008). "A let-7 microRNA-sensitive vesicular stomatitis virus demonstrates tumor-specific replication." Molecular Therapy **16**(8): 1437-1443.

Efrat, S., D. Serreze, A. Svetlanov, C. M. Post, E. A. Johnson, K. Herold and M. Horwitz (2001). "Adenovirus Early Region 3 (E3) Immunomodulatory Genes Decrease the Incidence of Autoimmune Diabetes in NOD Mice." Diabetes **50**(5): 980-984.

Esquela-Kerscher, A. and F. J. Slack (2006). "Oncomirs [mdash] microRNAs with a role in cancer." Nat Rev Cancer **6**(4): 259-269.

Fabian, M. R. and N. Sonenberg (2012). "The mechanics of miRNA-mediated gene silencing: a look under the hood of miRISC." Nat Struct Mol Biol **19**(6): 586-593.

Ferreira, D., R. Hernandez, M. Horton and D. T. Brown (2003). "Morphological variants of sindbis virus produced by a mutation in the capsid protein." Virology **307**(1): 54-66.

Filipowicz, W., S. N. Bhattacharyya and N. Sonenberg (2008). "Mechanisms of post-transcriptional regulation by microRNAs: are the answers in sight?" Nat Rev Genet **9**(2): 102-114.

Freeman, A. I., J. M. Gomori, E. Linetsky, Z. Zakay-Rones, A. Panet, E. Libson, C. S. Irving, E. Galun and T. Siegal (2004). "Phase I/II trial of intravenous OV001 oncolytic virus in resistant glioblastoma multiforme (GBM)." Journal of Clinical Oncology **22**(14): 110S-110S.

Freytag, S. O., M. Khil, H. Stricker, J. Peabody, M. Menon, M. DePeralta-Venturina, D. Nafziger, J. Pegg, D. Paielli, S. Brown, K. Barton, M. Lu, E. Aguilar-Cordova and J. H. Kim (2002). "Phase I Study of Replication-competent Adenovirus-mediated Double Suicide Gene Therapy for the Treatment of Locally Recurrent Prostate Cancer." Cancer Research **62**(17): 4968-4976.

Freytag, S. O., H. Stricker, J. Pegg, D. Paielli, D. G. Pradhan, J. Peabody, M. DePeralta-Venturina, X. Xia, S. Brown, M. Lu and J. H. Kim (2003). "Phase I Study of Replication-Competent Adenovirus-Mediated Double-Suicide Gene Therapy in Combination with Conventional-Dose Three-Dimensional Conformal Radiation Therapy for the

Treatment of Newly Diagnosed, Intermediate- to High-Risk Prostate Cancer." Cancer Research **63**(21): 7497-7506.

Frolov, I., R. Hardy and C. M. Rice (2001). "Cis-acting RNA elements at the 5' end of Sindbis virus genome RNA regulate minus- and plus-strand RNA synthesis." RNA **7**(11): 1638-1651.

Fu, X., A. Rivera, L. Tao and X. Zhang (2012). "Incorporation of the B18R Gene of Vaccinia Virus Into an Oncolytic Herpes Simplex Virus Improves Antitumor Activity." Mol Ther.

Fu, X. and X. Zhang (2001). "Delivery of Herpes Simplex Virus Vectors through Liposome Formulation." Mol Ther **4**(5): 447-453.

Gaedigknitschko, K., M. X. Ding, M. A. Levy and M. J. Schlesinger (1990). "Site-directed mutations in the sindbis virus-6k protein reveal sites for fatty acylation and the underacylated protein affects virus release and virion structure

" Virology **175**(1): 282-291.

Gaedigknitschko, K. and M. J. Schlesinger (1991). "SIte-directed mutations in sindbis virus-E2 glycoproteins cytoplasmic domain and the 6k protein lead to similar defects in virus assembly and budding." Virology **183**(1): 206-214.

Galanis, E., L. C. Hartmann, W. A. Cliby, H. J. Long, P. P. Peethambaram, B. A. Barrette, J. S. Kaur, P. J. Haluska, Jr., I. Aderca, P. J. Zman, J. A. Sloan, G. Keeney, P. J. Atherton, K. C. Podratz, S. C. Dowdy, C. R. Stanhope, T. O. Wilson, M. J. Federspiel, K.-W. Peng and S. J. Russell (2010). "Phase I Trial of Intraperitoneal Administration of an Oncolytic Measles Virus Strain Engineered to Express Carcinoembryonic Antigen for Recurrent Ovarian Cancer." Cancer Research **70**(3): 875-882.

Galibert, L. and O.-W. Merten (2011). "Latest developments in the large-scale production of adeno-associated virus vectors in insect cells toward the treatment of neuromuscular diseases." Journal of Invertebrate Pathology **107**: S80-S93.

Garcia-Hernandez, M. d. l. L., A. Gray, B. Hubby and W. M. Kast (2007). "In vivo Effects of Vaccination with Six-Transmembrane Epithelial Antigen of the Prostate: A Candidate Antigen for Treating Prostate Cancer." Cancer Research **67**(3): 1344-1351.

Garcia-Hernandez, M. D. L. L., A. Gray, B. Hubby, O. J. Klinger and W. M. Kast (2008). "Prostate stem cell antigen vaccination induces a long-term protective immune response against prostate cancer in the absence of autoimmunity." Cancer Research **68**(3): 861-869.

Garmashova, N., R. Gorchakov, E. Frolova and I. Frolov (2006). "Sindbis virus nonstructural protein nsP2 is cytotoxic and inhibits cellular transcription." Journal of Virology **80**(12): 5686-5696.

Geevarghese, S. K., D. A. Geller, H. A. de Haan, M. Hoerer, A. E. Knoll, A. Mescheder, J. Nemunaitis, T. R. Reid, D. Y. Sze, K. K. Tanabe and H. Tawfik (2010). "Phase I/II Study of Oncolytic Herpes Simplex Virus NV1020 in Patients with Extensively Pretreated Refractory Colorectal Cancer Metastatic to the Liver." Human Gene Therapy **21**(9): 1119-1128.

Giraldez, A. J., Y. Mishima, J. Rihel, R. J. Grocock, S. Van Dongen, K. Inoue, A. J. Enright and A. F. Schier (2006). "Zebrafish MiR-430 Promotes Deadenylation and Clearance of Maternal mRNAs." Science **312**(5770): 75-79.

Girod, A., M. Ried, C. Wobus, H. Lahm, K. Leike, J. Kleinschmidt, G. Deleage and M. Hallek (1999). "Genetic capsid modifications allow efficient re-targeting of adeno-associated virus type 2." Nature Medicine **5**(9): 1052-1056.

Goldberg, S. M., S. M. Bartido, J. P. Gardner, J. Guevara-Patino, S. C. Montgomery, M.-A. Perales, M. F. Maughan, J. Dempsey, G. P. Donovan, W. C. Olson, A. N. Houghton and J. D. Wolchok (2005). "Comparison of Two Cancer Vaccines Targeting Tyrosinase: Plasmid DNA and Recombinant Alphavirus Replicon Particles." Clinical Cancer Research **11**(22): 8114-8121.

Graham, A., R. Walker, P. Baird, C. N. Hahn and J. K. Fazakerley (2006). "CNS gene therapy applications of the Semliki Forest virus 1 vector are limited by neurotoxicity." Molecular Therapy **13**(3): 631-635.

Granot, T. and D. Meruelo (2012). "The role of natural killer cells in combinatorial anti-cancer therapy using Sindbis viral vectors and irinotecan." Cancer Gene Therapy **19**(8): 588-591.

Green NK, H. A., Cawood R, Illingworth S, Herbert C, Hermiston T, Subr V, Ulbrich K, van Rooijen N, Seymour LW, Fisher KD. (2012). "Tropism ablation and stealthing of oncolytic adenovirus enhances systemic delivery to tumors and improves virotherapy of cancer." Nanomedicine **0**: 1-13.

Green, N. K., A. Hale, R. Cawood, S. Illingworth, C. Herbert, T. Hermiston, V. Subr, K. Ulbrich, N. van Rooijen, L. W. Seymour and K. D. Fisher (2012). "Tropism ablation and stealthing of oncolytic adenovirus enhances systemic delivery to tumors and improves virotherapy of cancer." Nanomedicine (Lond).

Griffith, I. P., N. E. Crook and D. O. White (1975). "Protection of mice against cancer by immunization with membranes but not purified virions from virus-infected cancer-cells

" British Journal of Cancer **31**(6): 603-613.

Guo, H. S., Q. Xie, J. F. Fei and N. H. Chua (2005). "MicroRNA directs mRNA cleavage of the transcription factor NAC1 to downregulate auxin signals for Arabidopsis lateral root development." Plant Cell **17**(5): 1376-1386.

Hadac, E. M., E. J. Kelly and S. J. Russell (2011). "Myeloma Xenograft Destruction by a Nonviral Vector Delivering Oncolytic Infectious Nucleic Acid." Mol Ther **19**(6): 1041-1047.

Hajjou, M., K. R. Hill, S. V. Subramaniam, J. Y. Hu and R. Raju (1996). "Nonhomologous RNA-RNA recombination events at the 3' nontranslated region of the Sindbis virus genome: hot spots and utilization of nonviral sequences." Journal of Virology **70**(8): 5153-64.

Hammill, A. M., J. Conner and T. P. Cripe (2010). "Oncolytic virotherapy reaches adolescence." Pediatric Blood & Cancer **55**(7): 1253-1263.

Hardy, W. R. and J. H. Strauss (1989). "Processing the nonstructural polyproteins of sindbis virus: nonstructural proteinase is in the C-terminal half of nsP2 and functions both in cis and in trans." Journal of Virology **63**(11): 4653-4664.

He, B., J. Chou, R. Brandimarti, I. Mohr, Y. Gluzman and B. Roizman (1997). "Suppression of the phenotype of gamma(1)34.5- herpes simplex virus 1: failure of activated RNA-dependent protein kinase to shut off protein synthesis is associated with a deletion in the domain of the alpha47 gene." Journal of Virology **71**(8): 6049-54.

He, L. and G. J. Hannon (2004). "MicroRNAs: small RNAs with a big role in gene regulation." Nat Rev Genet **5**(7): 522-531.

He, L., A. Piper, F. Meilleur, D. A. A. Myles, R. Hernandez, D. T. Brown and W. T. Heller (2010). "The Structure of Sindbis Virus Produced from Vertebrate and Invertebrate Hosts as Determined by Small-Angle Neutron Scattering." Journal of Virology **84**(10): 5270-5276.

Heikkilä, J. E., M. J. V. Vaha-Koskela, J. J. Ruotsalainen, M. W. Martikainen, M. M. Stanford, J. A. McCart, J. C. Bell and A. E. Hinkkanen (2010). "Intravenously Administered Alphavirus Vector VA7 Eradicates Orthotopic Human Glioma Xenografts in Nude Mice." PLoS ONE **5**(1): e8603.

Heise, M. T., D. A. Simpson and R. E. Johnston (2000). "Sindbis-group alphavirus replication in periosteum and endosteum of long bones in adult mice." Journal of Virology **74**(19): 9294-9299.

Helenius, A., M. Kielian, J. Wellsteed, I. Mellman and G. Rudnick (1985). "Effects of mono-valent cations on semliki forest virus entry into BHK-21-cells

" Journal of Biological Chemistry **260**(9): 5691-5697.

Heo, J., Breitbach, C, Cho, M, Hwang, T, Kim, C.W, Jeon, U.B, Woo, H.Y, Yoon, K.T, Lee, J.W, Burke, J, Hickman, T, DuBois, K.S, Longpre, L, Patt, R.H, Kirn, D.H. (2012). "A phase II trial of JX-594, a targeted multimechanistic oncolytic vaccinia virus, followed by sorafenib in patients with advanced hepatocellular carcinoma (HCC)." Journal of Clinical Oncology **30**: suppl; abstract e14566.

Hernandez, R., C. Sinodis and D. T. Brown (2010). "Sindbis virus: propagation, quantification, and storage." Current protocols in microbiology **Chapter 15**.

Hesketh, P. J. (2008). "Drug therapy: Chemotherapy-induced nausea and vomiting." New England Journal of Medicine **358**(23): 2482-2494.

Hill, K. R., M. Hajjou, J. Y. Hu and R. Raju (1997). "RNA-RNA recombination in Sindbis virus: roles of the 3' conserved motif, poly(A) tail, and nonviral sequences of template RNAs in polymerase recognition and template switching." Journal of Virology **71**(4): 2693-704.

Hirsch, R. L., D. E. Griffin and J. A. Winkelstein (1981). "Host modification of sindbis virus sialic-acid content influences alternative complement pathway activation and virus clearance." Journal of Immunology **127**(5): 1740-1743.

Huang, P.-Y., J.-H. Guo and L.-H. Hwang (2011). "Oncolytic Sindbis Virus Targets Tumors Defective in the Interferon Response and Induces Significant Bystander Antitumor Immunity In Vivo." Molecular Therapy **20**(2): 298-305.

Hutvágner, G. and P. D. Zamore (2002). "A microRNA in a Multiple-Turnover RNAi Enzyme Complex." Science **297**(5589): 2056-2060.

Ignowski, J. M. and D. V. Schaffer (2004). "Kinetic analysis and modeling of firefly luciferase as a quantitative reporter gene in live mammalian cells." Biotechnology and Bioengineering **86**(7): 827-834.

Ikeda, K., T. Ichikawa, H. Wakimoto, J. S. Silver, T. S. Deisboeck, D. Finkelstein, G. R. Harsh, D. N. Louis, R. T. Bartus, F. H. Hochberg and E. A. Chiocca (1999). "Oncolytic virus therapy of multiple tumors in the brain requires suppression of innate and elicited antiviral responses." Nature Medicine **5**(8): 881-887.

Jarnicki, A. G., J. Lysaght, S. Todryk and K. H. G. Mills (2006). "Suppression of Antitumor Immunity by IL-10 and TGF-Î²-Producing T Cells Infiltrating the Growing Tumor: Influence of Tumor Environment on the Induction of CD4+ and CD8+ Regulatory T Cells." The Journal of Immunology **177**(2): 896-904.

Jeang, K.-T. (2012). "RNAi in the regulation of mammalian viral infections." Bmc Biology **10**.

Jiang, H., Z. Wang, D. Serra, M. M. Frank and A. Amalfitano (2004). "Recombinant Adenovirus Vectors Activate the Alternative Complement Pathway, Leading to the Binding of Human Complement Protein C3 Independent of Anti-Ad Antibodies." Mol Ther **10**(6): 1140-1142.

Kadar, J. G., M. Parusel and H. Borberg (1992). "Anticoagulation-dependent inhibition of invitro complement activation by anti-apo-B sepharose-4B-CL." Infusionstherapie Und Transfusionsmedizin **19**(5): 237-240.

Kamer, G. and P. Argos (1984). "Primary structural comparison of rna-dependent polymerases from plant, animal and bacterial-viruses." Nucleic Acids Research **12**(18): 7269-7282.

Kandel, E. S., J. Skeen, N. Majewski, A. Di Cristofano, P. P. Pandolfi, C. S. Feliciano, A. Gartel and N. Hay (2002). "Activation of Akt/protein kinase B overcomes a G(2)/M cell cycle checkpoint induced by DNA damage." Molecular and Cellular Biology **22**(22): 7831-7841.

Kelly, E. and S. J. Russell (2007). "History of oncolytic viruses: Genesis to genetic engineering." Molecular Therapy **15**(4): 651-659.

Kelly, E. J., E. M. Hadac, S. Greiner and S. J. Russell (2008). "Engineering microRNA responsiveness to decrease virus pathogenicity." Nat Med **14**(11): 1278-1283.

Kelly, E. J., R. Nace, G. N. Barber and S. J. Russell (2010). "Attenuation of Vesicular Stomatitis Virus Encephalitis through MicroRNA Targeting." Journal of Virology **84**(3): 1550-1562.

Kelly, E. J. and S. J. Russell (2009). "MicroRNAs and the Regulation of Vector Tropism." Molecular Therapy **17**(3): 409-416.

Khuri, F. R., J. Nemunaitis, I. Ganly, J. Arseneau, I. F. Tannock, L. Romel, M. Gore, J. Ironside, R. H. MacDougall, C. Heise, B. Randlev, A. M. Gillenwater, P. Bruso, S. B. Kaye, W. K. Hong and D. H. Kirn (2000). "A controlled trial of intratumoral ONYX-015, a selectively-replicating adenovirus, in combination with cisplatin and 5-fluorouracil in patients with recurrent head and neck cancer." Nature Medicine **6**(8): 879-885.

Kim, J., P.-H. Kim, H. Y. Nam, J.-S. Lee, C.-O. Yun and S. W. Kim (2012). "Linearized oncolytic adenoviral plasmid DNA delivered by bioreducible polymers." Journal of Controlled Release **158**(3): 451-460.

Kirn, D. (2000). "Replication-selective oncolytic adenoviruses: virotherapy aimed at genetic targets in cancer." Oncogene **19**(56): 6660-6669.

Kirn, D. (2001). "Clinical research results with dl1520 (Onyx-015), a replication-selective adenovirus for the treatment of cancer: what have we learned?" Gene Therapy **8**(2): 89-98.

Klimp, A. H., E. van der Vaart, P. O. Lansink, S. Withoff, E. G. E. de Vries, G. L. Scherphof, J. Wilschut and T. Daemen (2001). "Activation of peritoneal cells upon in vivo transfection with a recombinant alphavirus expressing GM-CSF." Gene Therapy **8**(4): 300-307.

Kondorkoch, C., B. Burke and H. Garoff (1983). "Expression of semliki forest virus proteins from cloned complementary-DNA .1. the fusion activity of the spike glycoprotein." Journal of Cell Biology **97**(3): 644-651.

Koska, A. J., W. G. Kramer, A. Romagnoli, A. S. Keats and P. B. Sabawala (1981). "Pharmacokinetics of Highâ€Dose Meperidine in Surgical Patients." Anesthesia & Analgesia **60**(1): 8-11.

Kosova, J., Bowers, D. F (2003). "Longevity Studies of Sindbis Virus Infected Aedes Albopictus." Osprey Journal of Ideas and Inquiry **Volume III**: Paper 94.

Kueberuwa, G., R. Cawood and L. W. Seymour (2010). "Blood compatibility of enveloped viruses." Current Opinion in Molecular Therapeutics **12**(4): 412-420.

Kundig, T. M., C. P. Kalberer, H. Hengartner and R. M. Zinkernagel (1993). "Vaccination with 2 different vaccinia recombinant viruses - long-term inhibition of secondary vaccination

" Vaccine **11**(11): 1154-1158.

Kurkela, S., T. Manni, J. Myllynen, A. Vaheri and O. Vapalahti (2005). "Clinical and laboratory manifestations of Sindbis virus infection: Prospective study, Finland, 2002-2003." Journal of Infectious Diseases **191**(11): 1820-1829.

Kurkela, S., T. Manni, A. Vaheri and O. Vapalahti (2004). "Causative agent of pogosta disease isolated from blood and skin lesions." Emerging Infectious Diseases **10**(5): 889-894.

Kwon, O.-J., E. Kang, S. Kim and C.-O. Yun (2011). "Viral genome DNA/lipoplexes elicit in situ oncolytic viral replication and potent antitumor efficacy via systemic delivery." Journal of Controlled Release **155**(2): 317-325.

Lachman, L. B., X. M. Rao, R. H. Kremer, B. Ozpolat, G. Kiriakova and J. E. Price (2001). "DNA vaccination against neu reduces breast cancer incidence and metastasis in mice." Cancer Gene Therapy **8**(4): 259-268.

Laine, M., R. Luukainen, J. Jalava, J. Ilonen, P. Kuusisto and A. Toivanen (2000). "Prolonged arthritis associated with Sindbis-related (Pogosta) virus infection." Rheumatology **39**(11): 1272-1274.

Lammerts, E., P. Roswall, C. Sundberg, P. J. Gotwals, V. E. Koteliansky, R. K. Reed, N.-E. Heldin and K. Rubin (2002). "Interference with TGF-β1 and -β3 in tumor stroma lowers tumor interstitial fluid pressure independently of growth in experimental carcinoma." International Journal of Cancer **102**(5): 453-462.

Landgraf, P., M. Rusu, R. Sheridan, A. Sewer, N. Iovino, A. Aravin, S. Pfeffer, A. Rice, A. O. Kamphorst, M. Landthaler, C. Lin, N. D. Socci, L. Hermida, V. Fulci, S. Chiaretti, R. Foa, J. Schliwka, U. Fuchs, A. Novosel, R. U. Muller, B. Schermer, U. Bissels, J. Inman, Q. Phan, M. C. Chien, D. B. Weir, R. Choksi, G. De Vita, D. Frezzetti, H. I. Trompeter, V. Hornung, G. Teng, G. Hartmann, M. Palkovits, R. Di Lauro, P. Wernet, G. Macino, C. E. Rogler, J. W. Nagle, J. Y. Ju, F. N. Papavasiliou, T. Benzing, P. Lichter, W. Tam, M. J. Brownstein, A. Bosio, A. Borkhardt, J. J. Russo, C. Sander, M. Zavolan and T. Tuschl (2007). "A mammalian microRNA expression atlas based on small RNA library sequencing." Cell **129**(7): 1401-1414.

Lappegard, K. T., M. Fung, G. Bergseth, J. Riesenfeld, J. D. Lambris, V. Videm and T. E. Mollnes (2004). "Effect of complement inhibition and heparin coating on artificial surface-induced leukocyte and platelet activation." Ann Thorac Surg **77**(3): 932-941.

Lee, C. Y. F., P. S. Rennie and W. W. G. Jia (2009). "MicroRNA Regulation of Oncolytic Herpes Simplex Virus-1 for Selective Killing of Prostate Cancer Cells." Clinical Cancer Research **15**(16): 5126-5135.

Lee, P. Y., R. Knight, J. M. Smit, J. Wilschut and D. E. Griffin (2002). "A single mutation in the E2 glycoprotein important for neurovirulence influences binding of Sindbis virus to neuroblastoma cells." Journal of Virology **76**(12): 6302-6310.

Lee, R. C., R. L. Feinbaum and V. Ambros (1993). "The C. elegans heterochronic gene lin-4 encodes small RNAs with antisense complementarity to lin-14." Cell **75**(5): 843-854.

Lee, Y., C. Ahn, J. Han, H. Choi, J. Kim, J. Yim, J. Lee, P. Provost, O. Radmark, S. Kim and V. N. Kim (2003). "The nuclear RNase III Drosha initiates microRNA processing." Nature **425**(6956): 415-419.

Leitner, W. W., L. N. Hwang, M. J. deVeer, A. Zhou, R. H. Silverman, B. R. G. Williams, T. W. Dubensky, H. Ying and N. P. Restifo (2003). "Alphavirus-based DNA vaccine breaks immunological tolerance by activating innate antiviral pathways." Nat Med **9**(1): 33-39.

Leitner, W. W., H. Ying, D. A. Driver, T. W. Dubensky and N. P. Restifo (2000). "Enhancement of Tumor-specific Immune Response with Plasmid DNA Replicon Vectors." Cancer Research **60**(1): 51-55.

Leja, J., B. Nilsson, D. Yu, E. Gustafson, G. Akerstrom, K. Oberg, V. Giandomenico and M. Essand (2010). "Double-Detargeted Oncolytic Adenovirus Shows Replication Arrest in Liver Cells and Retains Neuroendocrine Cell Killing Ability." PLoS ONE **5**(1): e8916.

Lemaire, P. A., E. Anderson, J. Lary and J. L. Cole (2008). "Mechanism of PKR activation by dsRNA." Journal of Molecular Biology **381**(2): 351-360.

Leslie, M. C., Y. J. Zhao, L. B. Lachman, P. Hwu and M. Bar-Eli (2006). "Immunization against MUC18//MCAM, a novel antigen that drives melanoma invasion and metastasis." Gene Ther **14**(4): 316-323.

Levine, B., J. M. Hardwick and D. E. Griffin (1994). "Persistence of alphaviruses in vertebrate hosts." Trends in Microbiology **2**(1): 25-28.

Li, G. and C. M. Rice (1993). "The signal for translational readthrough of a UGA codon in Sindbis virus RNA involves a single cytidine residue immediately downstream of the termination codon." Journal of Virology **67**(8): 5062-5067.

Li, G. P., M. W. Lastarza, W. R. Hardy, J. H. Strauss and C. M. Rice (1990). "Phosphorylation of sindbis virus nsp3 invivo and invitro." Virology **179**(1): 416-427.

Li, L., J. Jose, Y. Xiang, R. J. Kuhn and M. G. Rossmann (2010). "Structural changes of envelope proteins during alphavirus fusion." Nature **468**(7324): 705-708.

Lin, Y., P. Cheung, J. C. Roth, D. L. Wilson and S. L. Gerson (2011). "Imaging Stem Cell-derived Persistent Foci After In Vivo Selection of Lentiviral MGMT-P140K Transduced Murine Bone Marrow Cells." Molecular Therapy **19**(7): 1342-1352.

Liu, J., M. A. Carmell, F. V. Rivas, C. G. Marsden, J. M. Thomson, J.-J. Song, S. M. Hammond, L. Joshua-Tor and G. J. Hannon (2004). "Argonaute2 Is the Catalytic Engine of Mammalian RNAi." Science **305**(5689): 1437-1441.

Liu, T.-C., E. Galanis and D. Kirn (2007). "Clinical trial results with oncolytic virotherapy: a century of promise, a decade of progress." Nature Clinical Practice Oncology **4**(2): 101-117.

Lober, C., C. Lenz-Stoppler and M. Dobbelstein (2002). "Adenovirus E1-transformed cells grow despite the continuous presence of transcriptionally active p53." Journal of General Virology **83**: 2047-2057.

Lundstrom, K. (2012). "Purification and Concentration of Alphavirus." Cold Spring Harbor Protocols **2012**(7): pdb.prot070169.

Luukkainen, R., M. Laine and J. Nirhamo (2000). "Chronic arthritis after Sindbis-related (Pogosta) virus infection." Scandinavian Journal of Rheumatology **29**(6): 399-400.

Lyons, M., D. Onion, N. K. Green, K. Aslan, R. Rajaratnam, M. Bazan-Peregrino, S. Phipps, S. Hale, V. Mautner, L. W. Seymour and K. D. Fisher (2006). "Adenovirus type 5 interactions with human blood cells may compromise systemic delivery." Molecular Therapy **14**(1): 118-128.

Mallory, A. C., B. J. Reinhart, M. W. Jones-Rhoades, G. L. Tang, P. D. Zamore, M. K. Barton and D. P. Bartel (2004). "MicroRNA control of PHABULOSA in leaf development: importance of pairing to the microRNA 5 ' region." Embo Journal **23**(16): 3356-3364.

Maniataki, E. and Z. Mourelatos (2005). "A human, ATP-independent, RISC assembly machine fueled by pre-miRNA." Genes & Development **19**(24): 2979-2990.

Manservigi, R., R. Argnani and P. Marconi (2010). "HSV Recombinant Vectors for Gene Therapy." The open virology journal **4**: 123-56.

Mansour, M., P. Palese and D. Zamarin (2011). "Oncolytic Specificity of Newcastle Disease Virus Is Mediated by Selectivity for Apoptosis-Resistant Cells." Journal of Virology **85**(12): 6015-6023.

Marie H, M. R. (2006). "Acute In Vivo Expression of Recombinant Proteins in Rat Brain Using Sindbis Virus." Dynamic Synapse: Molecular Methods in Ionotropic Receptor Biology **Chapter 12**.

Markert, J. M., M. D. Medlock, S. D. Rabkin, G. Y. Gillespie, T. Todo, W. D. Hunter, C. A. Palmer, F. Feigenbaum, C. Tornatore, F. Tufaro and R. L. Martuza (2000). "Conditionally replicating herpes simplex virus mutant, G207 for the treatment of malignant glioma: results of a phase I trial." Gene Therapy **7**(10): 867-874.

Marusyk, A., V. Almendro and K. Polyak (2012). "Intra-tumour heterogeneity: a looking glass for cancer?" Nat Rev Cancer **12**(5): 323-334.

Mastrangelo, M. J., H. C. Maguire, L. C. Eisenlohr, C. E. Laughlin, C. E. Monken, P. A. McCue, A. J. Kovatich and E. C. Lattime (1999). "Intratumoral recombinant GM-CSF-encoding virus as gene therapy in patients with cutaneous melanoma." Cancer Gene Therapy **6**(5): 409-422.

Mathonnet, G. r., M. R. Fabian, Y. V. Svitkin, A. Parsyan, L. Huck, T. Murata, S. Biffo, W. C. Merrick, E. Darzynkiewicz, R. S. Pillai, W. Filipowicz, T. F. Duchaine and N. Sonenberg (2007). "MicroRNA Inhibition of Translation Initiation in Vitro by Targeting the Cap-Binding Complex eIF4F." Science **317**(5845): 1764-1767.

McCormick, F. (2000). "ONYX-015 selectivity and the p14ARF pathway." Oncogene **19**(56): 6670-6672.

Mergenhagen, S. E., R. Snyderman and J. K. Phillips (1973). "Activation of Complement by Endotoxin." The Journal of Infectious Diseases **128**: S86-S90.

miRBase. (2012). "http://www.mirbase.org/cgi-bin/browse.pl?org=hsa." Retrieved 31/07/2012.

Mitchison, T. J. (2011). "The proliferation rate paradox in antimitotic chemotherapy." Molecular Biology of the Cell **23**(1): 1-6.

Moini, J., Jones & Bartlett (2012). "Phlebotomy: Principles and Practice Book Only."

Morris, D. G., Forsyth, P.A, Paterson, A.H, Fonseca, K, Difrancesco, L.M, Thompson, B.G, Coffey, M.C (2002). "A phase I clinical trial evaluating intralesional Reolysin (reovirus) in histologically confirmed malignancies." Proceedings of the Annual Meeting of the American Society for Clinical Oncology(21): a24.

Morrison, J., S. S. Briggs, N. K. Green, C. Thoma, K. D. Fisher, S. Kehoe and L. W. Seymour (2009). "Cetuximab Retargeting of Adenovirus via the Epidermal Growth Factor Receptor for Treatment of Intraperitoneal Ovarian Cancer." Human Gene Therapy **20**(3): 239-251.

Morse, M. A., A. C. Hobeika, T. Osada, P. Berglund, B. Hubby, S. Negri, D. Niedzwiecki, G. R. Devi, B. K. Burnett, T. M. Clay, J. Smith and H. K. Lyerly (2010). "An alphavirus vector overcomes the presence of neutralizing antibodies and elevated numbers of Tregs to induce immune responses in humans with advanced cancer." Journal of Clinical Investigation **120**(9): 3234-3241.

Mukhopadhyay, S., W. Zhang, S. Gabler, P. R. Chipman, E. G. Strauss, J. H. Strauss, T. S. Baker, R. J. Kuhn and M. G. Rossmann (2006). "Mapping the structure and function of the E1 and E2 glycoproteins in alphaviruses." Structure **14**(1): 63-73.

Nakamura, T. and S. J. Russell (2004). "Oncolytic measles viruses for cancer therapy." Expert Opinion on Biological Therapy **4**(10): 1685-1692.

Näslund, T. I., C. Uyttenhove, E. K. L. NordstrÃ¶m, D. Colau, G. Warnier, M. Jondal, B. Ì. t. J. Van den Eynde and P. LiljestrÃ¶m (2007). "Comparative prime-boost vaccinations using Semliki forest virus, adenovirus, and alvac vectors demonstrate differences in the generation of a protective central memory CTL response against the P815 tumor." The Journal of Immunology **178**(11): 6761-6769.

Nemunaitis, J., A. W. Tong, M. Nemunaitis, N. Senzer, A. P. Phadke, C. Bedell, N. Adams, Y.-A. Zhang, P. B. Maples, S. Chen, B. Pappen, J. Burke, D. Ichimaru, Y. Urata and T. Fujiwara (2009). "A phase I study of telomerase-specific replication competent oncolytic adenovirus (telomelysin) for various solid tumors." Mol Ther **18**(2): 429-434.

Ni, B., Z. Lin, L. Zhou, L. Wang, Z. Jia, W. Zhou, D. P. DiCiommo, J. Zhao, R. Bremner and Y. Wu (2004). "Induction of P815 tumor immunity by DNA-based recombinant Semliki Forest virus or replicon DNA expressing the P1A gene." Cancer Detection and Prevention **28**(6): 418-425.

Ohno, K., K. Sawai, Y. Iijima, B. Levin and D. Meruelo (1997). "Cell-specific targeting of Sindbis virus vectors displaying IgG-binding domains of protein A." Nature Biotechnology **15**(8): 763-767.

Pandha, H., A. Melcher, K. Harrington and R. Vile (2009). "Oncolytic viruses: time to compare, contrast, and combine?" Mol Ther **17**(6): 934-935.

Parato, K. A., C. J. Breitbach, F. Le Boeuf, J. Wang, C. Storbeck, C. Ilkow, J.-S. Diallo, T. Falls, J. Burns, V. Garcia, F. Kanji, L. Evgin, K. Hu, F. Paradis, S. Knowles, T.-H. Hwang, B. C. Vanderhyden, R. Auer, D. H. Kirn and J. C. Bell (2012). "The oncolytic poxvirus JX-594 selectively replicates in and destroys cancer cells driven by genetic pathways commonly activated in cancers." Molecular Therapy **20**(4): 749-758.

Pecora, A. L., N. Rizvi, G. I. Cohen, N. J. Meropol, D. Sterman, J. L. Marshall, S. Goldberg, P. Gross, J. D. O'Neil, W. S. Groene, M. S. Roberts, H. Rabin, M. K. Bamat and R. M. Lorence (2002). "Phase I trial of intravenous administration of PV701, an oncolytic virus, in patients with advanced solid cancers." Journal of Clinical Oncology **20**(9): 2251-2266.

Peng, K. W., R. Myers, A. Greenslade, E. Mader, S. Greiner, M. J. Federspiel, A. Dispenzieri and S. J. Russell (2012). "Using clinically approved cyclophosphamide regimens to control the humoral immune response to oncolytic viruses." Gene Ther.

Perez, J. T., A. M. Pham, M. H. Lorini, M. A. Chua, J. Steel and B. R. tenOever (2009). "MicroRNA-mediated species-specific attenuation of influenza A virus." Nat Biotech **27**(6): 572-576.

Perlik, V., Z. Li, S. Goorha, L. R. Ballou and C. M. Blatteis (2005). "LPS-activated complement, not LPS per se, triggers the early release of PGE2 by Kupffer cells." American Journal of Physiology - Regulatory, Integrative and Comparative Physiology **289**(2): R332-R339.

Petersen, C. P., M.-E. Bordeleau, J. Pelletier and P. A. Sharp (2006). "Short RNAs repress translation after initiation in mammalian cells." Molecular Cell **21**(4): 533-542.

Poulin, K. L., R. M. Lanthier, A. C. Smith, C. Christou, M. R. Quiroz, K. L. Powell, R. W. O'Meara, R. Kothary, I. A. Lorimer and R. J. Parks (2010). "Retargeting of adenovirus vectors through genetic fusion of a single-chain or single-domain antibody to capsid protein IX." Journal of Virology **84**(19): 10074-10086.

Power, A. T. and J. C. Bell (2008). "Taming the Trojan horse: optimizing dynamic carrier cell/oncolytic virus systems for cancer biotherapy." Gene Therapy **15**(10): 772-779.

Prestwich, R. J., F. Errington, K. J. Harrington, H. S. Pandha, P. Selby and A. Melcher (2008). "Oncolytic viruses: do they have a role in anti-cancer therapy?" Clinical medicine. Oncology **2**: 83-96.

Raju, R., S. V. Subramaniam and M. Hajjou (1995). "Genesis of sindbis virus by in-vivo recombination of nonreplicative rna precursors." Journal of Virology **69**(12): 7391-7401.

Ratajczak, M. and C. Kim (2011). "Bioactive Sphingolipids and Complement Cascade as New Emerging Regulators of Stem Cell Mobilization and Homing." Journal of Stem Cell Research & Therapy.

Reddy, P. S., K. D. Burroughs, L. M. Hales, S. Ganesh, B. H. Jones, N. Idamakanti, C. Hay, S. S. Li, K. L. Skele, A.-J. Vasko, J. Yang, D. N. Watkins, C. M. Rudin and P. L. Hallenbeck (2007). "Seneca valley virus, a systemically deliverable oncolytic picornavirus, and the treatment of neuroendocrine cancers." Journal of the National Cancer Institute **99**(21): 1623-1633.

Rehwinkel, J. A. N., I. Behm-Ansmant, D. Gatfield and E. Izaurralde (2005). "A crucial role for GW182 and the DCP1:DCP2 decapping complex in miRNA-mediated gene silencing." RNA **11**(11): 1640-1647.

Reid, T. R., S. Freeman, L. Post, F. McCormick and D. Y. Sze (2005). "Effects of Onyx-015 among metastatic colorectal cancer patients that have failed prior treatment with 5-FU//leucovorin." Cancer Gene Ther **12**(8): 673-681.

Ren, H., T. Boulikas, A. Soling, P. C. Warnke and N. G. Rainov (2003). "Immunogene therapy of recurrent glioblastoma multiforme with a liposomally encapsulated replication-

incompetent Semliki forest virus vector carrying the human interleukin-12 gene - a phase I/II clinical protocol." Journal of Neuro-Oncology **64**(1): 147-154.

Rodriguez-Madoz, J. R., J. Prieto and C. Smerdou (2005). "Semliki forest virus vectors engineered to express higher IL-12 levels induce efficient elimination of murine colon adenocarcinomas." Molecular Therapy **12**(1): 153-163.

Roenigk, H. H., S. Deodhar, Stjacque.R and K. Burdick (1974). "Immunotherapy of malignant-melanoma with vaccinia virus." Archives of Dermatology **109**(5): 668-673.

Ruby, J. G., C. H. Jan and D. P. Bartel (2007). "Intronic microRNA precursors that bypass Drosha processing." Nature **448**(7149): 83-86.

Rudin, C. M., Senzer, N, Stephenson, J, Loesch, D Burroughs, K, Police, S.R, Hallenbeck, P (2009). "Phase I study of intravenous Seneca Valley virus (NTX-010), a replication competent oncolytic virus, in patients with neuroendocrine (NE) cancers." Journal of Clinical Oncology **27**(15s): supplimentary abstract 4629.

Ryman, K. D., W. B. Klimstra, K. B. Nguyen, C. A. Biron and R. E. Johnston (2000). "Alpha/beta interferon protects adult mice from fatal Sindbis virus infection and is an important determinant of cell and tissue tropism." Journal of Virology **74**(7): 3366-3378.

Ryman, K. D., K. C. Meier, E. M. Nangle, S. L. Ragsdale, N. L. Korneeva, R. E. Rhoads, M. R. MacDonald and W. B. Klimstra (2005). "Sindbis virus translation is inhibited by a PKR/RNase L-independent effector induced by alpha/beta interferon priming of dendritic cells." Journal of Virology **79**(3): 1487-1499.

Sanz, M., A. Castello, I. Ventoso, J. Berlanga and L. Carrasco (2009). "Dual Mechanism for the Translation of Subgenomic mRNA from Sindbis Virus in Infected and Uninfected Cells." PLoS ONE **4**(3): e4772.

Saraste, A. and K. Pulkki (2000). "Morphologic and biochemical hallmarks of apoptosis." Cardiovascular Research **45**(3): 528-537.

Schaefer, S., S. Weibel, U. Donat, Q. Zhang, R. Aguilar, N. Chen and A. Szalay (2012). "Vaccinia virus-mediated intra-tumoral expression of matrix metalloproteinase 9 enhances oncolysis of PC-3 xenograft tumors." BMC Cancer **12**(1): 366.

Schroder, K., P. J. Hertzog, T. Ravasi and D. A. Hume (2004). "Interferon-gamma: an overview of signals, mechanisms and functions." Journal of Leukocyte Biology **75**(2): 163-189.

Senzer, N. N., H. L. Kaufman, T. Amatruda, M. Nemunaitis, T. Reid, G. Daniels, R. Gonzalez, J. Glaspy, E. Whitman, K. Harrington, H. Goldsweig, T. Marshall, C. Love, R. Coffin and J. J. Nemunaitis (2009). "Phase II Clinical Trial of a Granulocyte-Macrophage Colony-Stimulating Factor-Encoding, Second-Generation Oncolytic Herpesvirus in Patients With Unresectable Metastatic Melanoma." Journal of Clinical Oncology **27**(34): 5763-5771.

Shapiro, J. S., A. Varble, A. M. Pham and B. R. tenOever (2010). "Noncanonical cytoplasmic processing of viral microRNAs." RNA **16**(11): 2068-2074.

Shaw, G., S. Morse, M. Ararat and F. L. Graham (2002). "Preferential transformation of human neuronal cells by human adenoviruses and the origin of HEK 293 cells." The FASEB Journal **16**(8): 869-871.

Shimada, A., G. Shiota, H. Miyata, T. Kamahora, H. Kawasaki, K. Shiraki, S. Hino and T. Terada (1998). "Aberrant expression of double-stranded RNA-dependent protein kinase in

hepatocytes of chronic hepatitis and differentiated hepatocellular carcinoma." Cancer Research **58**(19): 4434-4438.

Shimakami, T., D. Yamane, C. Welsch, L. Hensley, R. K. Jangra and S. M. Lemon (2012). "Base Pairing between Hepatitis C Virus RNA and MicroRNA 122 3' of Its Seed Sequence Is Essential for Genome Stabilization and Production of Infectious Virus." Journal of Virology **86**(13): 7372-7383.

Shirako, Y. and J. H. Strauss (1994). "Regulation of Sindbis virus RNA replication: uncleaved P123 and nsP4 function in minus-strand RNA synthesis, whereas cleaved products from P123 are required for efficient plus-strand RNA synthesis." Journal of Virology **68**(3): 1874-1885.

Small, E. J., M. A. Carducci, J. M. Burke, R. Rodriguez, L. Fong, L. van Ummersen, D. C. Yu, J. Aimi, D. Ando, P. Working, D. Kirn and G. Wilding (2006). "A phase I trial of intravenous CG7870, a replication-selective, prostate-specific antigen-targeted oncolytic adenovirus, for the treatment of hormone-refractory, metastatic prostate cancer." Molecular Therapy **14**(1): 107-117.

Smith, K. D., J. J. Mezhir, K. Bickenbach, J. Veerapong, J. Charron, M. C. Posner, B. Roizman and R. R. Weichselbaum (2006). "Activated MEK suppresses activation of PKR and enables efficient replication and in vivo oncolysis by Delta gamma(1)34.5 mutants of herpes simplex virus 1." Journal of Virology **80**(3): 1110-1120.

Smith, R. R., R. J. Huebner, W. P. Rowe, W. E. Schatten and L. B. Thomas (1956). "Studies on the use of viruses in the treatment of carcinoma of the cervix." Cancer **9**(6): 1211-1218.

Sonenberg, N. and A. G. Hinnebusch (2009). "Regulation of Translation Initiation in Eukaryotes: Mechanisms and Biological Targets." Cell **136**(4): 731-745.

Soussi, T. and K. G. Wiman (2007). "Shaping genetic alterations in human cancer: The p53 mutation paradigm." Cancer Cell **12**(4): 303-312.

Southam, C. M. and A. E. Moore (1952). "Clinical studies of viruses as antineoplastic agents, with particular reference to Egypt 101 virus." Cancer **5**(5): 1025-1034.

Stanford, M. M., J. W. Barrett, S. H. Nazarian, S. Werden and G. McFadden (2007). "Oncolytic virotherapy synergism with signaling inhibitors: Rapamycin increases myxoma virus tropism for human tumor cells." Journal of Virology **81**(3): 1251-1260.

Stanford, M. M., J. C. Bell and M. J. V. Vähä-Koskela (2010). "Novel oncolytic viruses: Riding high on the next wave?" Cytokine & Growth Factor Reviews **21**(23): 177-183.

Stanford, M. M., M. Shaban, J. W. Barrett, S. J. Werden, P.-A. Gilbert, J. Bondy-Denomy, L. MacKenzie, K. C. Graham, A. F. Chambers and G. McFadden (2008). "Myxoma virus oncolysis of primary and metastatic B16F10 mouse tumors in vivo." Molecular Therapy **16**(1): 52-59.

Steel, J. J., B. R. Henderson, S. B. C. Lama, K. E. Olson and B. J. Geiss (2011). "Infectious alphavirus production from a simple plasmid transfection." Virology Journal **8**.

Stoff-Khalili, M. A., A. A. Rivera, A. Stoff, J. M. Mathis, R. P. Rocconi, Q. L. Matthews, M. T. Numnum, I. Herrmann, P. Dall, D. E. Eckhoff, J. T. Douglas, G. P. Siegal, Z. B. Zhu and D. T. Curiel (2007). "Combining high selectivity of replication via CXCR4 promoter with fiber chimerism for effective adenoviral oncolysis in breast cancer." International Journal of Cancer **120**(4): 935-941.

Stojdl, D. F., B. Lichty, S. Knowles, R. Marius, H. Atkins, N. Sonenberg and J. C. Bell (2000). "Exploiting tumor-specific defects in the interferon pathway with a previously unknown oncolytic virus." Nature Medicine **6**(7): 821-825.

Strauss, J. H. and E. G. Strauss (1994). "The alphaviruses - gene-expression, replication, and evolution." Microbiological Reviews **58**(3): 491-562.

Sullivan, C. S., A. T. Grundhoff, S. Tevethia, J. M. Pipas and D. Ganem (2005). "SV40-encoded microRNAs regulate viral gene expression and reduce susceptibility to cytotoxic T cells." Nature **435**(7042): 682-686.

Sumida, S. M., D. M. Truitt, A. A. C. Lemckert, R. Vogels, J. H. H. V. Custers, M. M. Addo, S. Lockman, T. Peter, F. W. Peyerl, M. G. Kishko, S. S. Jackson, D. A. Gorgone, M. A. Lifton, M. Essex, B. D. Walker, J. Goudsmit, M. J. E. Havenga and D. H. Barouch (2005). "Neutralizing Antibodies to Adenovirus Serotype 5 Vaccine Vectors Are Directed Primarily against the Adenovirus Hexon Protein." The Journal of Immunology **174**(11): 7179-7185.

Suzuki, T., F. Sakurai, S.-i. Nakamura, E. Kouyama, K. Kawabata, M. Kondoh, K. Yagi and H. Mizuguchi (2008). "miR-122a-Regulated Expression of a Suicide Gene Prevents Hepatotoxicity Without Altering Antitumor Effects in Suicide Gene Therapy." Mol Ther **16**(10): 1719-1726.

Taha, T. A., T. D. Mullen and L. M. Obeid (2006). "A house divided: Ceramide, sphingosine, and sphingosine-1-phosphate in programmed cell death." Biochimica et Biophysica Acta (BBA) - Biomembranes **1758**(12): 2027-2036.

Takakura, M., S. Kyo, T. Kanaya, H. Hirano, J. Takeda, M. Yutsudo and M. Inoue (1999). "Cloning of human telomerase catalytic subunit (hTERT) gene promoter and identification of proximal core promoter sequences essential for transcriptional activation in immortalized and cancer cells." Cancer Research **59**(3): 551-557.

Takayama, I., H. Sato, A. Watanabe, M. Omi-Furutani, A. Sugai, K. Kanki, M. Yoneda and C. Kai (2012). "The nucleocapsid protein of measles virus blocks host interferon response." Virology **424**(1): 45-55.

Tan, S. C. and B. C. Yiap (2009). "DNA, RNA, and Protein Extraction: The Past and The Present." Journal of Biomedicine and Biotechnology.

Tang, J., J. Jose, P. Chipman, W. Zhang, R. J. Kuhn and T. S. Baker (2011). "Molecular Links between the E2 Envelope Glycoprotein and Nucleocapsid Core in Sindbis Virus." Journal of Molecular Biology **414**(3): 442-459.

Tesh, R. B. (1982). "Arthritides caused by mosquito-borne viruses." Annual Review of Medicine **33**: 31-40.

Testa, J. R. and A. Bellacosa (2001). "Commentary - AKT plays a central role in tumorigenesis." Proceedings of the National Academy of Sciences of the United States of America **98**(20): 10983-10985.

Thomas, J. M., W. B. Klimstra, K. D. Ryman and H. W. Heidner (2003). "Sindbis virus vectors designed to express a foreign protein as a cleavable component of the viral structural polyprotein." Journal of Virology **77**(10): 5598-5606.

Thorne, S. H. (2009). Design and Testing of Novel Oncolytic Vaccinia Strains. Methods in Molecular Biology. W. S. U. S. Walther. **542:** 635-647.

Tseng, J. C., A. Hurtado, H. Yee, B. Levin, C. Boivin, M. Benet, S. V. Blank, A. Pellicer and D. Meruelo (2004). "Using Sindbis viral vectors for specific detection and suppression of advanced ovarian cancer in animal models." Cancer Research **64**(18): 6684-6692.

Tseng, J. C., B. Levin, T. Hirano, H. Yee, C. Pampeno and D. Meruelo (2002). "In vivo antitumor activity of Sindbis viral vectors." Journal of the National Cancer Institute **94**(23): 1790-1802.

Tseng, J. C., B. Levin, A. Hurtado, H. Yee, I. Perez de Castro, M. Jimenez, P. Shamamian, R. Z. Jin, R. P. Novick, A. Pellicer and D. Meruelo (2004). "Systemic tumor targeting and killing by Sindbis viral vectors." Nature Biotechnology **22**(1): 70-77.

Turell, M. J., J. O. Lundstrom and B. Niklasson (1990). "Transmission of Ockelbo virus by Aedes-Cinereus, Ae-Communis, and Ae-Excrucians (Diptera, Culicidae) collected in an enzootic area in central Sweden." Journal of Medical Entomology **27**(3): 266-268.

Ulmanen, I., H. Soderlund and L. Kaariainen (1979). "Role of protein-synthesis in the assembly of Semliki forest virus nucleocapsid." Virology **99**(2): 265-276.

Vähä-Koskela, M. J. V., J. P. Kallio, L. C. Jansson, J. E. HeikkilÃ¤, V. A. Zakhartchenko, M. A. Kallajoki, V.-M. KÃ¤hÃ¤ri and A. E. Hinkkanen (2006). "Oncolytic Capacity of Attenuated Replicative Semliki Forest Virus in Human Melanoma Xenografts in Severe Combined Immunodeficient Mice." Cancer Research **66**(14): 7185-7194.

Valencia-Sanchez, M. A., J. D. Liu, G. J. Hannon and R. Parker (2006). "Control of translation and mRNA degradation by miRNAs and siRNAs." Genes & Development **20**(5): 515-524.

Varghese, S. and S. D. Rabkin (2002). "Oncolytic herpes simplex virus vectors for cancer virotherapy." Cancer Gene Ther **9**(12): 967-978.

Ventoso, I. n. (2012). "Adaptive Changes in Alphavirus mRNA Translation Allowed Colonization of Vertebrate Hosts." Journal of Virology **86**(17): 9484-9494.

Verheije, M. H. and P. J. M. Rottier (2012). "Retargeting of viruses to generate oncolytic agents." Advances in virology **2012**: 798526.

Wang, G., J. W. Barrett, M. Stanford, S. J. Werden, J. B. Johnston, X. J. Gao, M. Sun, J. Q. Cheng and G. McFadden (2006). "Infection of human cancer cells with myxoma virus requires Akt activation via interaction with a viral ankyrin-repeat host range factor." Proceedings of the National Academy of Sciences of the United States of America **103**(12): 4640-4645.

Wang, K. S., R. J. Kuhn, E. G. Strauss, S. Ou and J. H. Strauss (1992). "High-affinity laminin receptor is a receptor for Sindbis virus in mammalian cells." Journal of Virology **66**(8): 4992-5001.

Wang, X. Y., J. P. Wang, M. F. Maughan and L. B. Lachman (2005). "Alphavirus replicon particles containing the gene for HER2/neu inhibit breast cancer growth and tumorigenesis." Breast Cancer Research **7**(1): R145-R155.

Wang, Y., G. Hallden, R. Hill, A. Anand, T.-C. Liu, J. Francis, G. Brooks, N. Lemoine and D. Kirn (2003). "E3 gene manipulations affect oncolytic adenovirus activity in immunocompetent tumor models." Nat Biotech **21**(11): 1328-1335.

Weiler, J. M., R. W. Yurt, D. T. Fearon and K. F. Austen (1978). "Modulation of formation of amplification convertase of complement, c3b,bb, by native and commercial heparin

" Journal of Experimental Medicine **147**(2): 409-421.

Weiss, B., H. Nitschko, I. Ghattas, R. Wright and S. Schlesinger (1989). "Evidence for specificity in the encapsidation of Sindbis virus RNAs

" Journal of Virology **63**(12): 5310-5318.

Weiss, B., H. Nitschko, I. Ghattas, R. Wright and S. Schlesinger (1989). "Evidence for specificity in the encapsidation of Sindbis virus RNAs." Journal of Virology **63**(12): 5310-5318.

Weiss, B. G. and S. Schlesinger (1991). "Recombination between Sindbis virus RNAs." Journal of Virology **65**(8): 4017-4025.

Wheelock, E. F. and J. H. Dingle (1964). "Observations on repeated administration of viruses to patient with acute leukemia - preliminary report

" New England Journal of Medicine **271**(13): 645-&.

Wilson, E. B., J. J. El-Jawhari, A. L. Neilson, G. D. Hall, A. A. Melcher, J. L. Meade and G. P. Cook (2011). "Human tumour immune evasion via TGF-β blocks nk cell activation but not survival allowing therapeutic restoration of anti-tumour activity." PLoS ONE **6**(9): e22842.

Wisse, E., F. Jacobs, B. Topal, P. Frederik and B. De Geest (2008). "The size of endothelial fenestrae in human liver sinusoids: implications for hepatocyte-directed gene transfer." Gene Ther **15**(17): 1193-1199.

Wong, L. H., K. G. Krauer, I. Hatzinisiriou, M. J. Estcourt, P. Hersey, N. D. Tam, S. Edmondson, R. J. Devenish and S. J. Ralph (1997). "Interferon-resistant human melanoma cells are deficient in ISGF3 components, STAT1, STAT2, and p48-ISGF3 gamma." Journal of Biological Chemistry **272**(45): 28779-28785.

Xia, Z.-J., J.-H. Chang, L. Zhang, W.-Q. Jiang, Z.-Z. Guan, J.-W. Liu, Y. Zhang, X.-H. Hu, G.-H. Wu, H.-Q. Wang, Z.-C. Chen, J.-C. Chen, Q.-H. Zhou, J.-W. Lu, Q.-X. Fan, J.-J. Huang and X. Zheng (2004). "[Phase III randomized clinical trial of intratumoral injection of E1B gene-deleted adenovirus (H101) combined with cisplatin-based chemotherapy in treating squamous cell cancer of head and neck or esophagus]." Chinese journal of cancer **23**(12): 1666-70.

Yamanaka, R. and K. G. Xanthopoulos (2005). "Induction of antigen-specific immune responses against malignant brain tumors by intramuscular injection of Sindbis DNA encoding Gp100 and IL-18." DNA and Cell Biology **24**(5): 317-324.

Yap, T. A., A. Brunetto, H. Pandha, K. Harrington and J. S. de Bono (2008). "Reovirus therapy in cancer: has the orphan virus found a home?" Expert Opinion on Investigational Drugs **17**(12): 1925-1935.

Yekta, S., I. H. Shih and D. P. Bartel (2004). "MicroRNA-directed cleavage of HOXB8 mRNA." Science **304**(5670): 594-596.

Yi, R., Y. Qin, I. G. Macara and B. R. Cullen (2003). "Exportin-5 mediates the nuclear export of pre-microRNAs and short hairpin RNAs." Genes & Development **17**(24): 3011-3016.

Ying, H., T. Z. Zaks, R.-F. Wang, K. R. Irvine, U. S. Kammula, F. M. Marincola, W. W. Leitner and N. P. Restifo (1999). "Cancer therapy using a self-replicating RNA vaccine." Nat Med **5**(7): 823-827.

Zeng, Y. and B. R. Cullen (2004). "Structural requirements for pre-microRNA binding and nuclear export by Exportin 5." Nucleic Acids Research **32**(16): 4776-4785.

Zhang, J., I. Frolov and S. J. Russell (2004). "Gene therapy for matignant glioma using Sindbis vectors expressing a fusogenic membrane glycoprotein." Journal of Gene Medicine **6**(10): 1082-1091.

Zhang, Y.-Q., Y.-C. Tsai, A. Monie, T. C. Wu and C.-F. Hung (2010). "Enhancing the Therapeutic Effect Against Ovarian Cancer Through a Combination of Viral Oncolysis and Antigen-specific Immunotherapy." Molecular Therapy **18**(4): 692-699.